



ESAO 2025 Innovations in (bio)artificial organs and organ models

The International Journal of Artificial Organs 2025, Vol. 48(7) 439–544 © The Author(s) 2025 Article reuse guidelines: sagepub.com/journals-permissions DOI: 10.1177/03913988251342624 journals.sagepub.com/home/jao



PLENARY LECTURES

MEDICAL DEVICE DEVELOPMENT; FROM FRUSTRATION TO FAILURE TO SUCCESS

Stephen R. Ash

HemoCleanse Technologies LLC, Lafayette, Indiana USA

Everyone knows that *necessity* is the mother of invention. The question is, who is the father? From personal experience I can tell you that it is *frustration*. That is, frustration with devices and medications that fail to help an ailing patient. We feel extreme disappointment when our tools and methods fail the patient. Frustration turns to despair and grief when treatments fail to halt progression of organ failure.

Many physicians abandon the technology or stop treating patients at this time. Fortunately, some physicians use their medical knowledge and experience, and collaboration with engineers and scientists, to find or invent new and novel approaches. When the new approach causes problems or fails to help the patient, those physicians keep looking for modifications or new components to fix it. That process may take years or even decades of effort.

Willem Kolff was one of these pioneers. He realized that it is the early adopters who convert an invention to an innovation. He encouraged physicians and scientists such as John Merrill, Belding Scribner, Wayne Quinton and Chris Blagg to prove that dialysis could be workable as long-term therapy for kidney failure. They contributed new inventions and dialysis schedules to make dialysis more practical, therapeutic, and workable in the home environment.

When I graduated from Fellowship in Nephrology in 1975 it was obvious that dialysis worked to sustain life in patients with kidney failure. But 3-per-week sessions of dialysis caused adverse symptoms, and the new equipment was even more difficult to implement in the home. I committed my research career to finding ways to make dialysis simpler, safer, and more suited for the home environment. I went to the University of Utah as a temporary staff member that summer to work with the Nephrology Department and Dr. Kolff in development of his Wearable Artificial Kidney (WAK).

In the following decades while in Lafayette, Indiana I led a research team to find new technology and invent new devices to improve dialysis therapy. Twelve projects were dedicated to hemodialysis, and these are described in Editorials in the Artificial Organs journal and in a book. ^{1, 2} Two of the projects were highly successful, resulting in widescale changes in nephrology practice (the Ash Split Catheter and oral zirconium cyclosilicate for potassium control). Ohers were technically successful but did not change medical practice widely. I will discuss these projects and reasons for success or failure in my presentation at ESAO 2025. Along the way I came up with 10 suggestions on how to develop new medical technologies:³

- 1. Know the problem
- 2. Know but doubt the paradigm
- 3. Train with the best in scientific method
- 4. Use the newest tools, model all you can

- 5. Focus
- 6. Collaborate
- 7. Communicate, Publish
- 8. Be patient
- 9. Be careful
- Keep balance in your life, strong family ties and faith, but maintain humility.

References

- 1. Ash SR, Artificial Organs 2022, Editorials Jan-Dec
- Ash SR, "Success is Just Running Out of Mistakes", Moon Shard Media. 2024
- 3. Ash SR, ASAIO J. 2006 Nov- Dec;52(6):e3-9

ORGANS-ON-CHIPS: FROM PLATFORM TECHNOLOGY TO APPLICATIONS IN DRUG DEVELOPMENT

Andries van der Meer^{1,2,3}

¹Department of Bioengineering Technologies, University of Twente, The Netherlands; ²Organ-on-Chip Centre Twente, University of Twente, The Netherlands; ³Bio/MicroSystems Centre, University of Twente/TNO, The Netherlands

Introduction: Organs-on-chips are advanced tissue culture models that can mimic organ-level functionality in a controlled, dynamic microsystem. They differ from other cell culture models in that they use microenvironment engineering to capture increasingly complex physiological functions. In the past years it has been shown that organs-on-chips can provide accurate and relevant data for preclinical studies, thereby potentially reducing the time and cost of drug development and clinical trials. Moreover, with their unique combination of person-specific human cells and high-level tissue function, organs-on-chips challenge the strong reliance on animal models in

Open technology platforms: Functional organs-on-chips rely on integrated systems that combine microfluidic devices, biological materials, and engineering techniques, which are collectively known as 'technology platforms'. Recently, there has been a push to make organ-on-chip technology platforms more 'open', aiming to enhance accessibility, interoperability, and implementation by many stakeholders in the field [1]. We have performed pioneering work in developing an open platform for organ-on-chip, known as the 'Translational Organ- on-Chip Platform', or TOP [1].

Standardization: Standards are central in the development and implementation of open technology platforms for organ-on-chip as they facilitate interoperability and benchmarking. Even beyond mere technological innovation, standardization also supports future regulatory compliance and qualification, providing a framework for evaluating whether an organ-on-chip models is fit-for-purpose within a specific context of use. We have spearheaded efforts in Europe to establish a roadmap for standardization for organ-on-chip, in the form of a CEN

CENELEC Focus Group supported by the Dutch Standardization Institute, NEN [2].

Preclinical drug development: In multiple studies, we have demonstrated how to apply organ-on-chip models in the identification of potential therapeutic targets, as well as in the evaluation of the safety and efficacy of drug candidates. For example, we used vessel-on-chip models to understand how severe COVID-19 leads to pulmonary microthrombosis, or how treatment of tumors with immune cell therapy can lead to systemic intravascular coagulation.

Outlook: Developments in organ-on-chip technology and artificial organs are currently mostly parallel, even though both fields essentially aim to achieve the same goal: to technologically replicate human organ functions. Lessons learned from the development of organs-onchips, such as the importance of open platforms, standardization, and interoperability, can be applied to enhance the development of artificial organs. Moreover, organ- on-chip models can potentially be used to evaluate the safety and efficacy of components of artificial organ systems. Looking ahead, we could even envision further integration of technological innovations from both fields. For example, artificial organ technologies could enhance the functionality of organ-on-chip systems in maintaining higher level, multi-organ or even organismlevel functions. Alternatively, organs-on-chips could become clinical 'mini-artificial organs' that support real-time monitoring of bodily functions. Overall, cross-pollination between the two respective fields will likely have a strong future impact on personalized medicine and improved patient care.

References

- 1. Vollertsen, et al. Biomicrofluidics, 15:051301, 2021.
- CEN/CENELEC FGOOC, & Secretariat: NEN. https://doi.org/10.5281/ zenodo.13927792, 2024

(BIO) ARTIFICIAL SOLUTIONS FOR HEART REPLACEMENT THERAPY

Cristiano Amarelli¹

¹Monaldi, Azienda Ospedaliera dei Colli, Naples, ITALY

Introduction: There is a growing number of patients needing heart replacement or hemodynamic support. Medical therapy, interventional procedures, and surgery are insufficient to answer the impressive number of patients requiring more flow. The improved outcomes of medical treatment have shifted the clinical settings of patients from isolated left ventricular dysfunction toward biventricular failure.

Methods: The lecture will deal with the clinical features of patients requiring heart replacement or hemodynamic support. The growing number of patients with biventricular impairment relaunched solutions to replace both ventricles:

- DBD Heart Transplantation
- DCD Heart Transplantation
- BiVADs
- TAHs
- Xenotransplantation

The lecture will focus on each current surgical solution's comparative benefits and limitations for end-stage organ dysfunction.

Results: DBD and DCD heart transplantation merged with new technologies for myocardial preservation based on machine perfusion of the heart remain the most effective solution for patients affected by endstage heart failure.

BiVAD remains a suboptimal solution in terms of QoL and incidence of complications. TAHs have recently come back as a potential solution, allowing for end-organ recovery and reestablishing transplant candidacy for potential candidates whose clinical status slides toward overt biventricular failure, compromising end-organ failure.

Xenotransplantation has demonstrated the possibility of genetically modifying the organs to overcome the innate barriers against xenotransplantation. Despite the demonstration of its feasibility, it remains a surgical holy grail promising to scale up the possibility of saving lives without organ shortage, but the preliminary results are still poor.

Discussion: Clinicians and surgeons have a broad armamentarium to fight the heart failure pandemic. LVADs have significantly improved their outcomes, improving hemocompatibility, but the dependence on a driveline causes many infections and adverse events that still impact the QoL of candidates, limiting the clinical implementation of this technology to a broader population. Merging machine perfusion technologies with gene therapy and organ modification strategies promises to reduce the hazard of primary graft failure in the immediate postoperative phase and to modify the allocation rules to improve the long-term outcomes of heart transplantation. Despite its attractiveness, Xenotransplantation remains far from adoption in the clinical arena.

Conclusions: LVADs warrant optimal outcomes with low incidence of adverse and hemocompatibility- related events in patients with isolated left ventricular failure having urgent need of transplantation. Heart transplantation remains the best solution to warrant optimal long-term outcomes for patients needing heart replacement therapy. Tailoring the right surgical solution to the patients by selecting TAHs or BIVADs may lead unstable patients to become elective heart transplantation candidates. DCD represents a potential solution to enlarge the donor pool significantly.

References

- Joshi Y, Wang K, MacLean C, et al. The Rapidly Evolving Landscape of DCD Heart Transplantation. Curr Cardiol Rep. 2024 Dec;26(12):1499-1507. doi: 10.1007/s11886-024-02148-w. Epub 2024 Oct 9. PMID: 39382782; PMCID: PMC11668896.
- Bowles DE, Karimov JH, Amarelli C. Editorial: Graft preservation. Front Cardiovasc Med. 2024 Oct 25;11:1478730. doi: 10.3389/fcvm.2024.1478730. PMID: 39526188; PMCID: PMC11544373.

1A: PAEDIATRIC MECHANICAL CIRCULATORY SUPPORT: MECHANICAL CIRCULATORY SUPPORT FOR PAEDIATRIC PATIENTS

TOWARDS OPTIMISATION OF A PAEDIATRIC AXIAL BLOOD PUMP WITH VARIABLE BLADE THICKNESS

Nathaniel S. Kelly¹, Lee Nissim¹, Preston Peak², Nobuyuki Kurita³, O. H. Frazier², Yaxin Wang², Katharine H. Fraser¹

¹University of Bath, Bath, UK; 2. Texas Heart Institute, Houston, United States of America; 3. Baylor College of Medicine, Houston, United States of America

Introduction: The NeoVAD is a prototype axial flow pump designed for neonates with left ventricular failure. Past investigations used machine-learning to optimize constant-thickness, circular-arc blade shapes [1]. To improve the device further, we have developed a baseline pump with blades varying in thickness along their length, to reduce pressure losses and improve efficiency. This work aimed to generate a training dataset and compare a single pump design with the new baseline design to examine the potential for future optimisation.

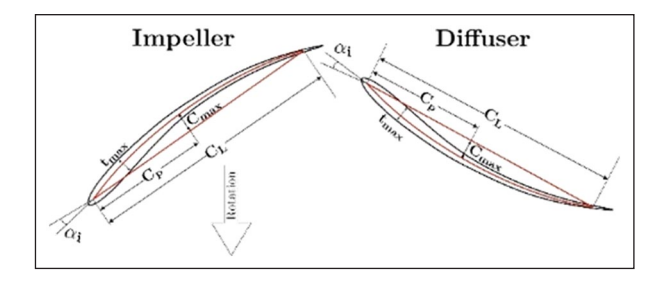


Figure 1. Impeller and diffuser blade parameterisation.

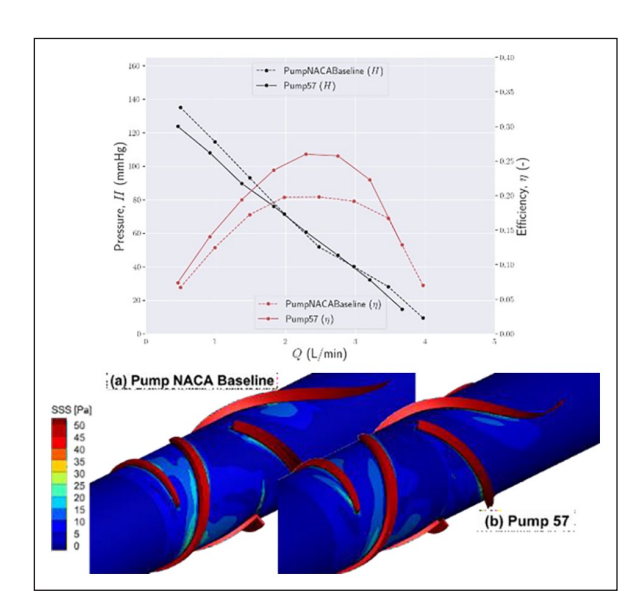


Figure 2. HQ and ηQ curves for Pump NACA Baseline and Pump 57 (top) and Scalar shear stress distribution around blades for (a) Pump NACA Baseline (b) Pump 57.

Methods: The impeller and diffuser blades each used 5 parameters based on the 4-digit NACA (National Advisory Committee for Aeronautics) airfoil series: the chord length, max camber, point of max camber, max thickness and angle of incidence. Figure 1 shows the new blade shapes based on these parameters.

An Optimised Latin Hypercube Sampling (OLHS) generated 64 pump designs based on these 10 parameters. These samples formed the training dataset for machine-learning optimisation. From this dataset, a random pump (Pump 57) was selected for comparison with the baseline design (Pump NACA Baseline). Blade profiles were created using ANSYS BladeGen and meshed with a 6 million hexahedral mesh using TurboGrid. Computational fluid dynamic (CFD) simulations were performed using OpenFOAM v9, using a Multiple Reference Frame to simulate mesh motion. The $k\text{-}\omega$ SST model was used to close the Reynolds averaged Navier-Stokes equations.

Results: Figure 2 compares the pressure-flow (HQ) and efficiency-flow (η Q) curves between Pump NACA Baseline and Pump 57. Although the pressure head is similar between the pumps, Pump 57 has an improved efficiency of 18% at 2 L/min.

Figure 2 also shows scalar shear stress (SSS) distribution in a cylindrical cross-section of both pumps at 2 L/min. The average Modified Index of Haemolysis (MIH) shows that Pump 57 is slightly less damaging to blood cells, with a difference of 2.13% and a reduction of high SSS around the blades.

Discussion: The results indicate that samples produced using OLHS could yield pumps with improved efficiency and lower haemolysis. Initial findings suggest that a variable thickness design enhances efficiency, with the NACA shape contributing to a more effective pump. Our ongoing and future work will focus on performing Computational Fluid Dynamics (CFD) on the training dataset and applying CFD-based machine learning optimisation. This will aim to further enhance efficiency and reduce hemolysis through multi- objective optimisation.

References

1. Nissim, L et al. Scientific Reports, 13(1), 2023

Acknowledgements

Research supported by the National Heart, Lung, and Blood Institute of the National Institute of Health under Award Number 1R01HL153538-04. The authors gratefully acknowledge the University of Bath's Research Computing Group (doi.org/10.15125/b6cd- s854) for their support in this work.

1B: NEW APPROACHES FOR IMPROVED BLOOD PURIFICATION

POLYELECTROLYTE-COATED SILICON-RICH SILICON NITRIDE SUBSTRATES FOR HIGH-CLEARANCE SELECTIVE MEMBRANES FOR AN IMPLANTABLE ARTIFICIAL KIDNEY

Tadeo Alcerreca^{1,2}, Tugrul Irmak¹, Iske Achterhuis², Wiebe de Vos², Mathieu Odijk², Karin Gerritsen¹, Jeroen Vollenbroek^{1,2,3}

¹Department of Nephrology and Hypertension, University Medical Centre Utrecht, Utrecht, NL; ²BIOS Lab on a Chip Group, MESA + Institute, Twente Membranes, University of Twente, Hallenweg 15, 7522 NH Enschede, NL; ³IMEC, Holst Centre, 5656 AE Eindhoven, NL

Introduction: An implantable artificial kidney will considerably lower the burden of hemodialysis. For this purpose, a miniaturized membrane that can mimic the glomerular filter in both clearance and selectivity is required. Pore size uniformity, surface charge, thickness, and effective porous area of the membrane are directly linked to permeability and selectivity by determining the hydraulic resistance to overcome. Nanofabrication processes, such as the ones extensively used in the semiconductor industry, allow the development of silicon-based membranes that could potentially mimic the glomerulus. The work done by the UCLA's Kidney Project Initiative has shown potential of 450nm thick Si- based membranes but their design requires extensive support areas due to the brittleness of pure Si, reducing permeability [1]. In this work, we tested large area (1.5 - 9 mm²) ultrathin free-hanging 75nm thick Silicon-rich Silicon Nitride (SiRN) sheets as a substrate material and tested its mechanical integrity under hydrostatic pressure. In addition, we tested the viability of polyelectrolyte multilayer (PEM) coatings on SiRN substrates for future surface charge and pore size modification of porous structures to increase selectivity and biocompatibility.

Methods: SiRN membranes made with cleanroom fabrication processes were tested for mechanical strength by flushing DI water over the membrane with increasing transmembrane pressure. SiRN substrates were coated with branched Polyethylenimine (PEI) as an initial layer, and proceeded with Poly(styrene sulfonate) sodium (PSS) and Poly(diallyl dimethylammonium) chloride (PDADMAC), being PEI and PDADMAC positively charged and PSS negatively charged. The thickness of the coating on the SiRN substrate was measured via ellipsometry. Fig. 1 shows a schematic of the flow cell in which the SiRN were tested.

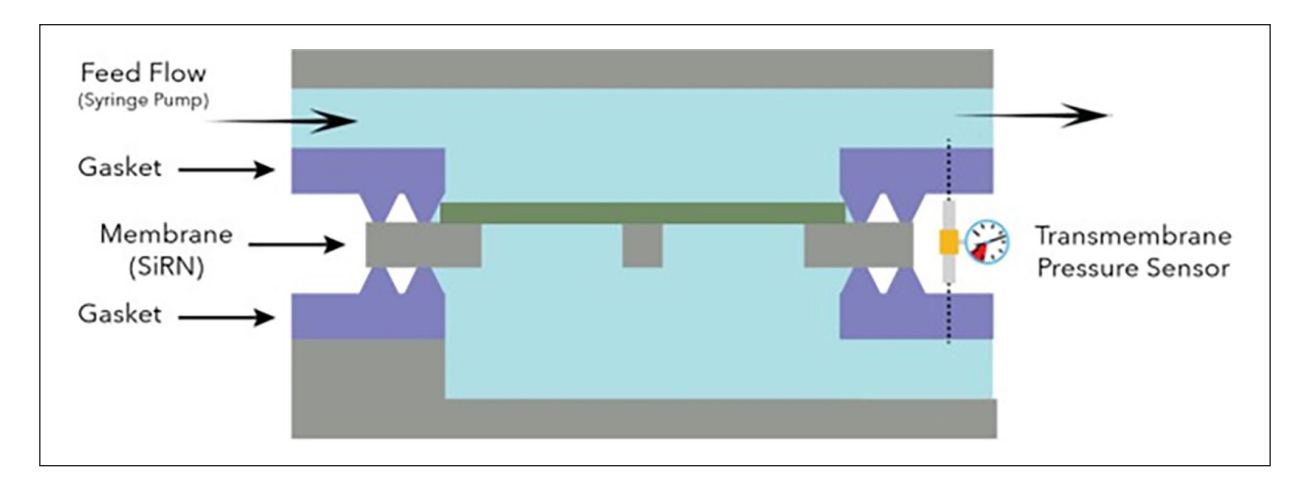


Figure 1. Flow Cell Schematic.

Results

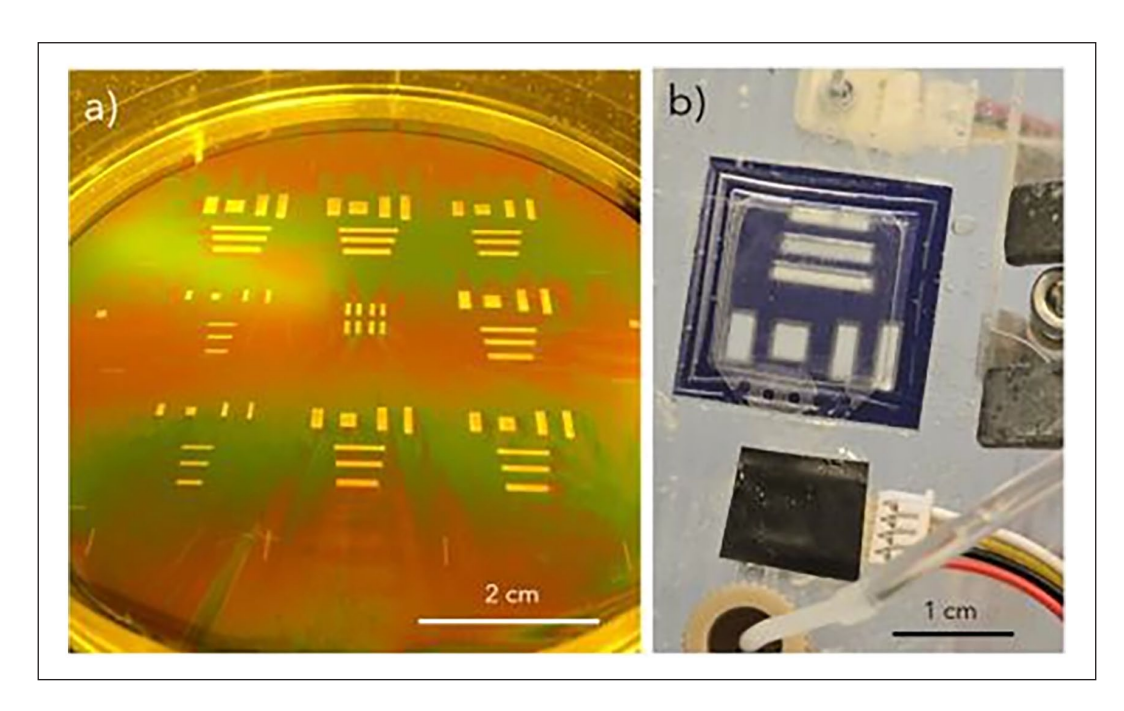


Figure 2. SiRN membrane wafer, a) full wafer, b) chip during testing. Free-hanging membranes withstood hydrostatic pressure tests beyond 275 mbar.

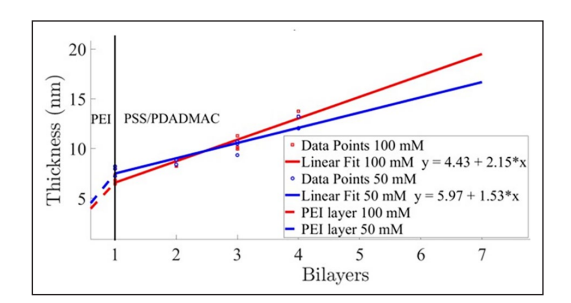


Figure 3. PEM thickness to bilayer number on SiRN under different ionic strength at R.H. 50% with a $0.1 \, \text{g/L}$ PE concentration, being $1.5 - 2.1 \, \text{nm}$ per bilayer.

Discussion: 75-nm thick SiRN sheets of different aspect ratios kept mechanical integrity while being subjected to hydrostatic pressures higher than physiological blood pressure[1,2]. The largest membrane window area tested was 6 times larger than previous work, indicating the potential of the material for hemodialysis and hemofiltration. PE coatings showed that the pore size can be tuned with nanometer (~2nm) precision, leaving open the possibility of using large scale photolithographic processes and modify the pore size using coatings. More research needs to be done regarding pore transfer onto SiRN and biocompatibility.

References

- 1. S. Kim et al., PLOS ONE, 11:1-12, 2016.
- 2. J. P. Desormeaux et al., Nanoscale, 6:10798-10805.

Acknowledgements

We thank the MESA+ institute for use of their cleanroom facilities. This project was funded by KIDNEW (HORIZON- EIC-2022 Pathfinder GA 101099092), MICROMERULUS (OCENW.XS24.1.159 from NWO), ACX Grant and Dutch Growth Fund (NXTGEN HighTech, Biomed04 'Artificial Organs').

OPTIMIZING USABILITY IN EXTRACORPOREAL ALBUMIN DIALYSIS

Stine Koball^{1,2,3}, Adrian Dominik¹, Sebastian Koball¹, Jan Stange^{1,2}

¹University of Rostock, Nephrology Department, Germany; ²Albutec GmbH, Germany; ³ProMedTec Germany GmbH, Germany

Introduction: Acute and chronic liver failure are frequently associated with systemic inflammation and the accumulation of both water-soluble and albumin- bound toxins, contributing to multi-organ dysfunction. Extracorporeal liver support systems facilitate detoxification and may help mitigate secondary organ failure. Extracorporeal albumin dialysis utilizes asymmetric semipermeable membranes and ultrapure, albumin-enriched dialysate recycled through adsorbents to optimize toxin clearance. Efficient removal of albumin-bound toxins is crucial for enhancing recovery.

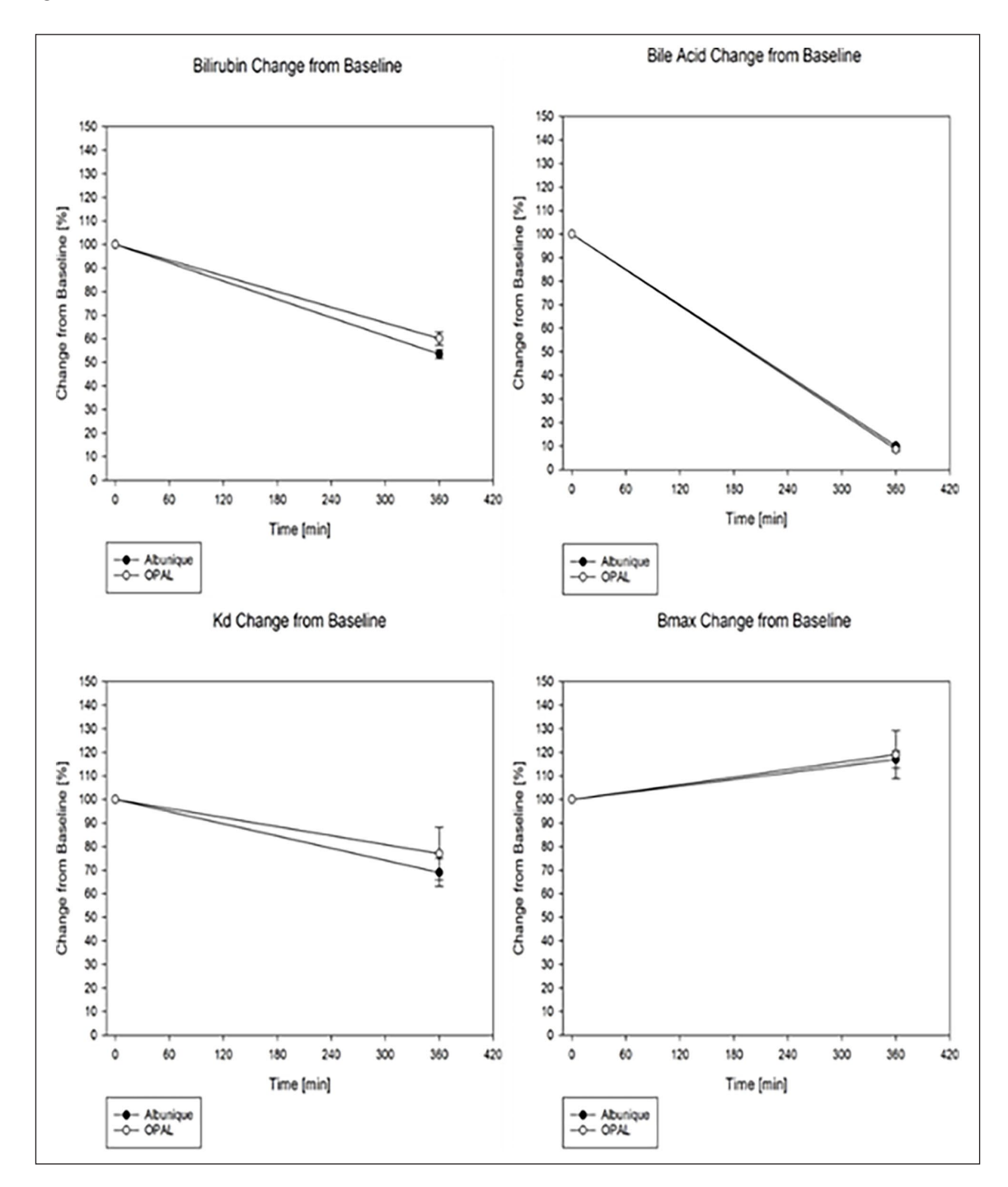


Figure 1. Reduction of Bile Acids and Bilirubin, and Enhancement of Albumin Binding Properties Over Six Hours of Treatment with Albunique™ and OPAL™.

To ensure both patient and staff safety, a rapid and straightforward setup is essential, as well as the ability to integrate multiple organ support therapies into a single device. This study compares two liver support systems: Albunique™ (Albutec GmbH) and OPAL™ (Hepanet GmbH). While OPAL utilized an extra monitor, enabling high albumin dialysate flow rates, Albunique runs on common CRRT platforms.

Methods: A two-compartment model [1] was used to simulate liver failure, characterized by high concentrations of liver failure toxins.

Both systems employed identical high-flux and low- flux filters, as well as a MaxiCycler7TM (Albutec GmbH), an activated carbon adsorber was utilized for toxin removal.

Samples were collected over a six-hour period and analyzed via standard assays using a Cobas Mira Plus analyzer. Additionally, titration with increasing concentrations of dansylsarcosine was performed to assess the impact of both treatments on albumin's toxin-binding capacity.

Results:

Toxin Removal

Bile acid levels were reduced to below 11% of baseline within six hours, with no significant difference between the two treatments.

Bilirubin concentrations decreased to below 63% of baseline within six hours, with no notable differences between treatments.

Albumin Binding Site Sudlow II – Dansylsarcosine Titration

Both treatments resulted in a mean Bmax increase of 18% and a Kd reduction of 27% over six hours, with no significant differences between the two systems.

Discussion: Both liver support treatments equally effectively reduce albumin bound toxins and improve albumin's binding capacity, demonstrating substantial equivalence.

References

 Stiffel M, Dammeier N, Schmidt S, Szyszkowitz T, Sikole M, Sieveking C, Stange J. 24-hour performance of albumin dialysis assessed by a new two-compartment in vitro model. Ther Apher Dial. 2014 Feb;18(1):79-86. doi: 10.1111/1744-9987.12025. Epub 2013 Apr 12. PMID: 24499088.

Acknowledgements

We thank Helga Weiss-Reining for her help in the experiments.

DRUG-TOXIN INTERACTIONS AT ORGANIC ANIONIC TRANSPORTER 1: IMPLICATIONS FOR BIOARTIFICIAL KIDNEY DEVELOPMENT

Silvia M. Mihăilă¹, Jasia King², João F. Faria¹, Nargis Khoso ¹, Sabbir Ahmed¹, Leyla Sharafutdinova¹, Leyla, Noroozbabaee¹, Dimitrios Stamatialis³, Karin GF Gerritsen⁴, Aurélie Carlier², Rosalinde Masereeuw ¹

¹Division of Pharmacology, Utrecht Institute for Pharmaceutical Sciences, Utrecht University, 3584 CG Utrecht, The Netherlands;
²MERLN Institute for Technology-Inspired Regenerative Medicine, Maastricht University, 6229 ER Maastricht, The Netherlands;
³Advanced Organ Bioengineering and Therapeutics, Faculty of Science and Technology, Technical Medical Centre, University of Twente, 7522 NB Enschede, The Netherlands; ⁴Department of Nephrology and Hypertension, University Medical Center, 3508 GA Utrecht, The Netherlands

Introduction: The bioartificial kidney (BAK) aims to enhance uremic toxin clearance by utilizing proximal tubule epithelial cells (PTECs) with active transporter function. Organic anion transporter 1 (OAT1) plays a key role in protein-bound uremic toxin (PBUT) uptake from the blood, while efflux pumps facilitate their removal into the dialysate. However, chronic kidney disease (CKD) blood contains high levels of PBUTs and

pharmaceuticals, such as statins, diuretics, ACE inhibitors (ACEIs), and angiotensin receptor blockers (ARBs), due to polypharmacy. These compounds may compete at OAT1, potentially hampering PBUT excretion and BAK efficiency. This study investigates drug-toxin interactions at OAT1 using computational and experimental approaches to provide insights for BAK development and optimize drug treatment in CKD.

Methods: We used proximal tubule cells with confirmed OAT1 activity to study the competitive uptake of PBUTs and CKD-associated drugs. A fluorescein- based assay assessed OAT1-mediated transport inhibition by selected pharmaceuticals (ACEIs, ARBs, statins, and diuretics). Additionally, we tested functional BAK hollow fiber membranes decorated with PTECs using LC-MS to quantify toxin clearance in single and multi-toxin conditions. A computational model was developed to simulate indoxyl sulfate (IS), a prototypical PBUT, transport dynamics, incorporating transporter density, albumin-binding kinetics, and toxin dissociation rates to predict clearance efficiency under physiological and uremic conditions.

Results: Experiments with the BAK functional unit confirmed effective PBUT removal, but toxin-toxin interactions led to variable clearance rates, underscoring the need to understand their impact on function (1). Anticipating this effect, we examined drug-toxin and toxin-toxin interactions at OAT1. Our findings show that CKD-associated drugs compete with PBUTs for OAT1-mediated uptake, with ARBs and furosemide significantly inhibiting fluorescein uptake at clinically relevant concentrations, a trend exacerbated by PBUTs (2). Computational modeling revealed that transporter density and PBUT dissociation rates are key determinants of clearance efficiency. Experimental data also indicated that albumin enhances PBUT removal (2). However, computational simulations suggested that albumin conformational changes in uremic conditions may reduce PBUT dissociation rates, limiting their availability for clearance (3).

Discussion: This study provides key insights into toxin- transporter interactions, emphasizing drug-toxin competition in BAK system design. By integrating computational modeling with in vitro validation, we offer a framework to optimize transporter function in BAK. Additionally, we are investigating multi- toxin and drug-toxin interactions by measuring intracellular concentrations and develop a computational framework to predict these interactions, allowing for better-informed strategies in BAK design. Future studies should refine transporter expression strategies and mitigate drug-induced inhibition to enhance BAK efficacy.

References

- 1. Faria J, et al, Int J Mol Sci.24(15):12435, 2023
- 2. Mihaila, SM, et al, Toxins, 12(6), 391, 2020
- 3. King, J, et al,. Toxins, 13(10), 674, 2021

Acknowledgements

This work was supported by DETOX from Dutch Kidney Foundation (22OK1019), EUTox working group of ESAO, the MSCA- doctoral network (RenalToolBox, 813839), and NWO OTP BAKTOTHE FUTURE (Grant nr 20775)

SILICA MEMBRANES FOR A BIO-ARTIFICIAL KIDNEY

Ronald van Gaal¹, Cian Cummins², Tugrul Irmak³, Karin Gerritsen³, Silvia Mihaila¹, Roos Masereeuw¹

¹Experimental Pharmacology, Utrecht University, the Netherlands; ²Interuniversitair Micro-Electronica Centrum (imec), Belgium; ³Nephrology, University Medical Centre Utrecht, the Netherlands

Introduction: Solid state technologies enable the creation of highly defined porous Si-membranes. Here, we integrated renal cells to create prospective living membranes, which can be used in a bio-artificial

kidney. A bio- artificial kidney is a device coupled to hemodialysis where it is proposed to clear protein bound toxins (PBUTs) from the blood via its cellular components grown on the membrane. Currently, PBUTS cannot effectively be cleared by dialysis and lead to secondary health issues such as cardiovascular disease in kidney patients.

Methods: Conditionally immortalized proximal tubule epithelial cells (ciPTECs) were cultured on Si-waiver cut to 1x1 cm. Si-waivers were left blank or were etched to included pores with a diameter of $1.5-10~\mu m$ or concave structures with a 400 μm diameter. The surface was either Si-oxide or bare Si. Materials were left uncoated or coated with L-DOPA, or L-DOPA and Collagen IV. ciPTECs were seeded at various cell densities in media supplement +/- FBS. ciPTECs were allowed to proliferate at 33° C for 1-7d post seeding before switching to 37° C. Cell coverage was quantified using fluorescent staining.

Results: ciPTECs were able to form monolayers on Si-oxide waivers either by coating with L-DOPA/Collagen IV in serum rich conditions or on pristine is serum low conditions. By either increasing the cell density or proliferation time a monolayer could be created on the material. No cell debris could be found in pores below 2 um. Bare Si waivers were not preferred by the cells under any coating condition, expect at porous regions.

Discussion: We here show that proximal tubule cells are compatible with silica waivers opening up the possibility to create living membranes on Si-membranes for a bioartificial kidney. Future work will focus on producing highly porous membranes with pores below 2 um. The living membranes will also be integrated in on-chip technology to investigate active toxin clearing and nutrient resorption under flow.

References

- 1. Feinberg, B. J. et al. J Colloid Interface Sci 517, 176–181 (2018).
- 2. 2. Jansen, J. et al. Biotechnol Adv 32, 1317–1327 (2014).

1C: IN-VITRO AND IN-SILICO INNOVATIONS IN HEMODYNAMICS

A NOVEL HAEMOLYSIS TEST CASE: PROGRESS FROM THE "BLOOD DAMAGE WORKSHOP GROUP":

Christopher Blum⁵, Johanna C. Clauser⁵, Nico Dirkes⁸, Kira Fechner², Katharine Fraser⁴, Vera Froese⁹, Fei-Hong Gao³, Michael Lommel⁹, Michael Neidlin⁵, Lee Nissim⁴, Maxime Renault¹⁰, Benjamin Torner*^{1,2}, Christian Wagner^{6,7}, Calvin Wolfgramm², Peng Wu³, Frank-Hendrik Wurm ²

¹Medical University of Vienna, Austria; ²University of Rostock, Germany; ³Southeast University; China University of Bath, UK; ⁵CVE RWTH Aachen University, Germany; ⁶Saarland University, Saarbruecken, Germany; ⁷: University of Luxembourg, Luxembourg; ⁸CATS RWTH Aachen University, Germany; ⁹ICM Charité - Universitaetsmedizin Berlin; ¹⁰CFL CEMEF. Mines Paris - PSL

Introduction: Mechanical medical devices, such as ventricular assist devices, extracorporeal membrane oxygenation (ECMO), and bileaflet mechanical valves, play a critical role in treating cardiovascular diseases

Achieving minimal blood damage is a central design objective for these devices, and preclinical evaluation often relies on numerical studies combining flow simulations with blood damage modelling. For these assessments to be reliable, ensuring the accuracy and validation of haemolysis models is paramount. Yet, no existing model has been universally validated for accurate haemolysis predictions.

To address this gap, an international consortium of eight laboratories — the "Blood Damage Workshop Group" was established in 2022. A novel test case with well-defined flow fields and experimental protocols was created. Here, we present the test case concept, its methodology, and the progress thus far.

Methods: We chose a plane channel flow as our haemolysis test case (see Figure 1, left), with flow conditions ranging from laminar to transitional turbulent states. The analysis covered three operating points, corresponding to Reynolds numbers of Re = 900, 1800, 2700.

Experiments with blood flow and haemolysis measurements are conducted in two laboratories, while flow simulations and numerical haemolysis modelling are carried out by six other laboratories. The experimental and numerical work has been conducted in two stages:

Stage One focuses on both experimental and numerical investigations using a single-phase fluid. The simulations are validated through experimental measurements and analytical solutions of the plane channel flow. This is shown in Figure 1.

Stage Two involves the actual haemolysis measurements and blood simulations. Each of the six laboratories will perform blood simulations and test various haemolysis models — such as Eulerian versus Lagrangian and stress-based versus strain-based approaches — to assess the accuracy of these models.

Results: The simulation results of Stage One indicate that the theoretical values are well captured by four out of six labs, with a maximum deviation of 2%. However, two labs show larger deviations, with one lab deviating by approximately 6% and another by around 20%. Further work is being done on these simulations to achieve consistent results for all labs. Stage Two is currently in progress, with initial haemolysis measurements and model comparisons underway.

Discussion: A test case for experimental and numerical assessment has been established. Numerical and experimental data correspond well for the Newtonian hydrodynamic data. Haemolysis assessment is ongoing. The test case will be made available for the scientific community after completion of stage two.

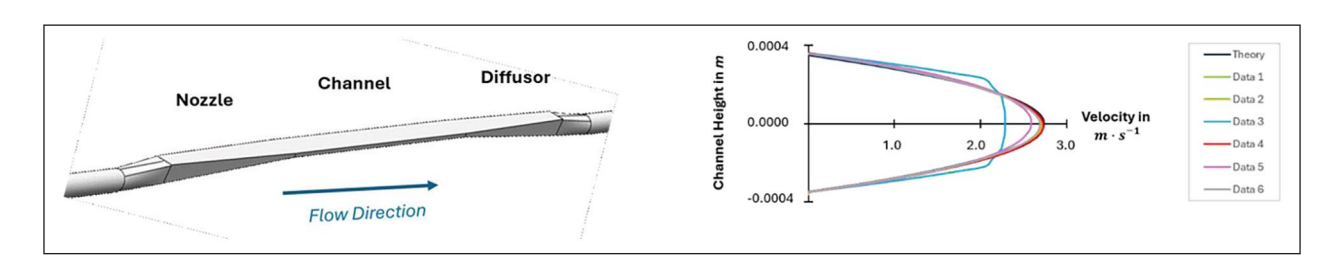


Figure 1. Geometry of the test case (left); theoretical and simulated velocity profile in the channel part of the test case (right).

QUANTIFYING EXPERIMENTAL VARIABILITY IN SHEAR-INDUCED HEMOLYSIS TO SUPPORT UNCERTAINTY-AWARE HEMOLYSIS MODELS

Christopher Blum¹, Markus Mous¹, Ulrich Steinseifer¹, Johanna C. Clauser¹, Michael Neidlin¹

¹Department of Cardiovascular Engineering, Institute of Applied Medical Engineering, Medical Faculty, RWTH Aachen University, Aachen, Germany

Introduction: Numerical hemolysis models rely on experimental data to fit parameters and predict hemolysis under various conditions. However, existing experiments often use few replicates per condition, leaving inherent variability largely unaddressed. This can lead to oversimplified models that fail to capture the true nature of hemolysis. We have recently presented a numerical hemolysis model which is able to incorporate experimental uncertainty [1]. Here, we quantify intra- and interdonor variability at a single, well-defined shear stress and exposure time, and examine how sample size affects measurement precision.

Methods: Human blood from five healthy donors was subjected to a fixed shear rate (43000 s-1) and exposure time (15 s) condition using a custom designed Couette shearing device. For each donor, 20 independent measurements (180 μL volume with a hematocrit of 25 \pm 1%), were performed to calculate a hemolysis index (HI). Intra-donor variability (variation within a single donor's measurements) and inter-donor variability (variation between donor means) were compared. Additionally, bootstrap analyses were used to explore the effect of the sample size on the confidence intervals of the mean HI.

Results: Intra-donor variability was approximately four times higher than inter-donor variability, indicating that most of the uncertainty originated from within a single donor's set of samples rather than between donors, see Figure 1.

Increasing the sample size from 2 to 20 replicates substantially narrowed the confidence intervals of the mean hemolysis estimate, suggesting that commonly used small sample sizes may underrepresent the true variability in hemolysis measurements. For instance, a hemolysis measurement under the investigated operating point with n=2 delivers HI of $^{\sim}$ 0.5 +/- 0.3%, while n=20 yields HI of $^{\sim}$ 0.5 +/- 0.1%, emphasizing the error made with small sample sizes.

Discussion: Intra-donor variability is a significant driver of uncertainty in hemolysis measurements at a fixed shear stress and exposure time condition, surpassing differences among donors. Obtaining robust and reliable hemolysis estimates requires increasing the number of replicate

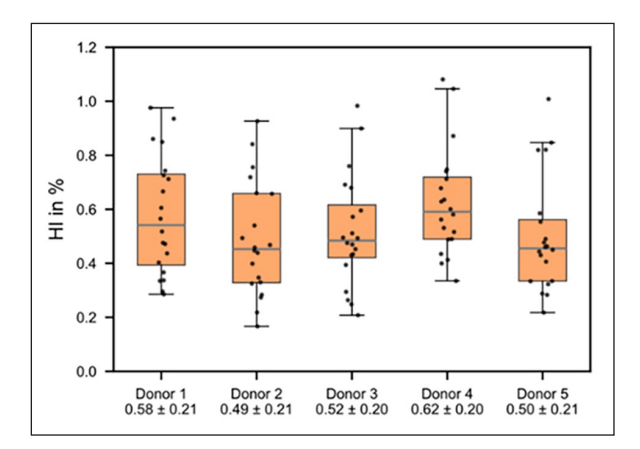


Figure 1. Hemolysis index (HI) for all donors.

Table 1. Variability of HI based on the sample size.

Sample size	Variability of HI
2 samples	±0.3%
5 samples	±0.2%
20 samples	±0.1%

measurements to reduce uncertainty. Integrating these insights into future experimental designs and uncertainty- aware hemolysis models will improve the reliability of in-silico predictions and inform safer, more effective blood-contacting medical device designs.

References

1. Blum et al. arXiv:2407.18757

Acknowledgements

Funded by the Deutsche Forschungsgemeinschaft (DFG, German Research Foundation) – project number 467133626 and the Elisabeth und Rudolf Hirsch Stiftung für medizinische Forschung.

DEVELOPMENT OF BLOOD MIMICKING FLUIDS: A COMPARATIVE STUDY OF RHEOLOGICAL AND MECHANICAL PROPERTIES

Gesine Hentschel¹, Katharina Doll-Nikutta², Marc Mueller¹, Philipp Berg^{3,4}, Birgit Glasmacher¹

¹Institute for Multiphase Processes, Leibniz University Hannover, Germany; ²Department of Prosthetic Dentistry and Biomedical Materials Science; Hannover Medical School, Germany; ³Research Campus STIMULATE, University of Magdeburg, Germany; ⁴Department of Medical Engineering, University of Magdeburg, Germany

Introduction: Blood is a highly complex fluid, and the ability to accurately reproduce it in an experimental setting has, thus far, proven to be a profound challenge [1]. Hemodynamic flow models typically rely on single-phase glycerin/water solutions as substitutes to visualize blood flow. These models are accurate only at high shear rates, limiting their applicability at lower shear rates, where non- Newtonian flow behavior dominates [2,3]. To address these limitations, we developed a multiphase blood mimicking fluid (BMF) using hydrogel microparticles (beads) made from poly- sodiumacrylate-co-acrylamide (P(SA-Am)).

Methods: Beads were produced using microfluidic systems with a rectangular channel geometry. After production, the beads were suspended in three artificial plasma solutions: 10% and 50% (v/v) glycerin/water solutions and a Dextran40/CaCl₂ solution. Rheometry was performed at room temperature using a plate-plate configuration, with shear rates ranging from 5 to 500s⁻¹. Yield stress behavior was further analyzed with shear stress ramps between 0 and 200 Pa. All rheological data was compared to data of porcine blood. Young's modulus of the beads was investigated with an atomic force microscope. Ten force spectroscopy curves were recorded per bead, with a setpoint force of 50 nN.

Results: Through confined channel geometry the production of biconcave beads could be implemented (see Figure 1). The diameters of the beads ranged from 200 to 700μm. Beads dispersed in Dextran40/CaCl₂ led to the smallest beads (220 μm), while dispersing in the glycerol solutions lead to two times higher diameters. Rheometric analysis confirmed shear thinning behavior similar to between 5 to 500s⁻¹.The Dextran40/CaCl₂ solution closely matched that behavior of porcine blood. In contrast, both glycerol solutions exhibited high viscosity and yield stress,

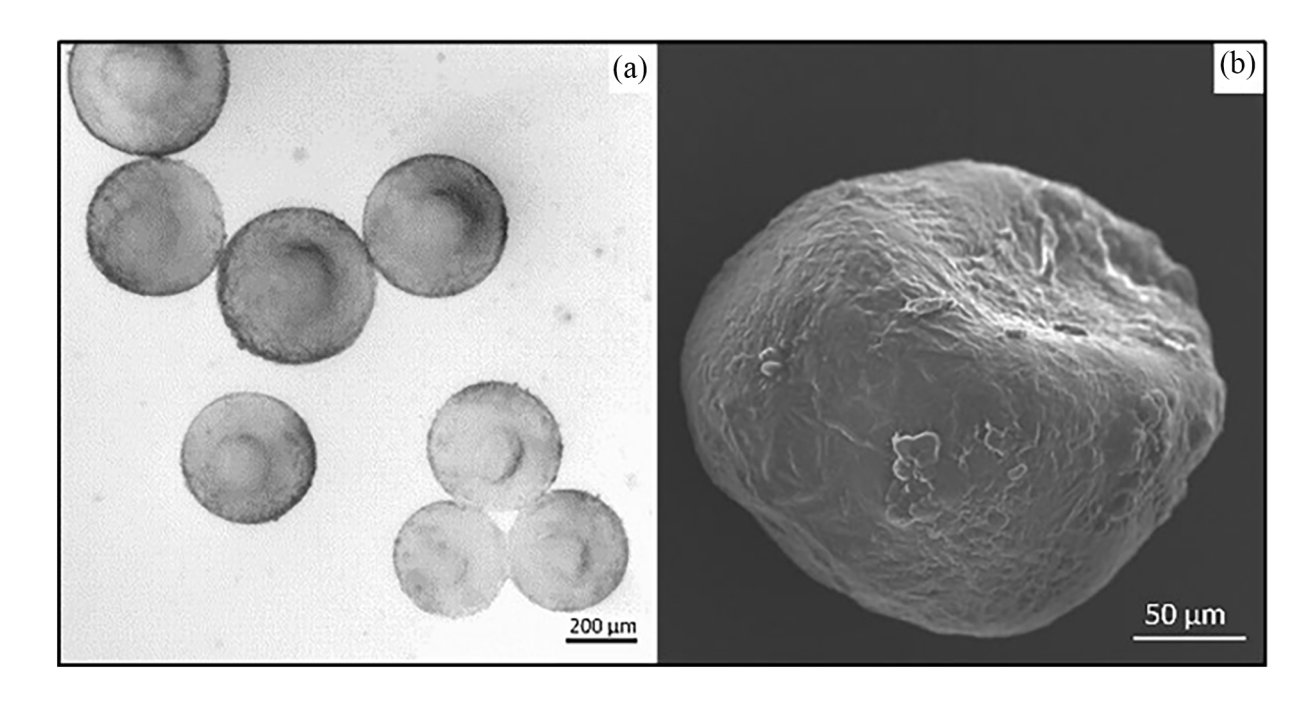


Figure 1. Light microscopic image of P(SA-Am) beads dispersed in Dextran40/CaCl₂ (a). Scanning electron microscope image of a bead, showing the biconcave shape of the particles (b).

making them unsuitable as BMF. Examination of the mechanical response showed a close match in Young's modulus of the beads dispersed in Dextran40/CaCl₂ and glycerol 10% (v/v) to porcine erythrocytes.

Discussion: We successfully characterized the rheological and mechanical behavior of novel microbead-based BMFs. The Dextran40/CaCl₂ model showed promising results with its mechanical and rheological behavior closely aligned to that of porcine blood, which supports its use in hemo-dynamic research. The greatest differences among the tested BMFs emerged in their shear rheological behavior, especially in their respective yield stress, highlighting the significant impact of the plasma phase on fluid properties. Despite the current limitations in particle size, the proposed BMF demonstrates a versatile range of well-matched parameters and is, thus, promising for further investigation.

References

- 1. Q. Chen, Soft Matter, 2023, 19, 5249–526
- 2. K. Sriram et al., Microcirculation, 2014, 21, 628–639.
- 3. S. Lynch et al., Scientific Reports, 2022.

Acknowledgements

The authors would like to thank the NETZSCH GmbH (Selb, Germany) for the provision of the rheometer.

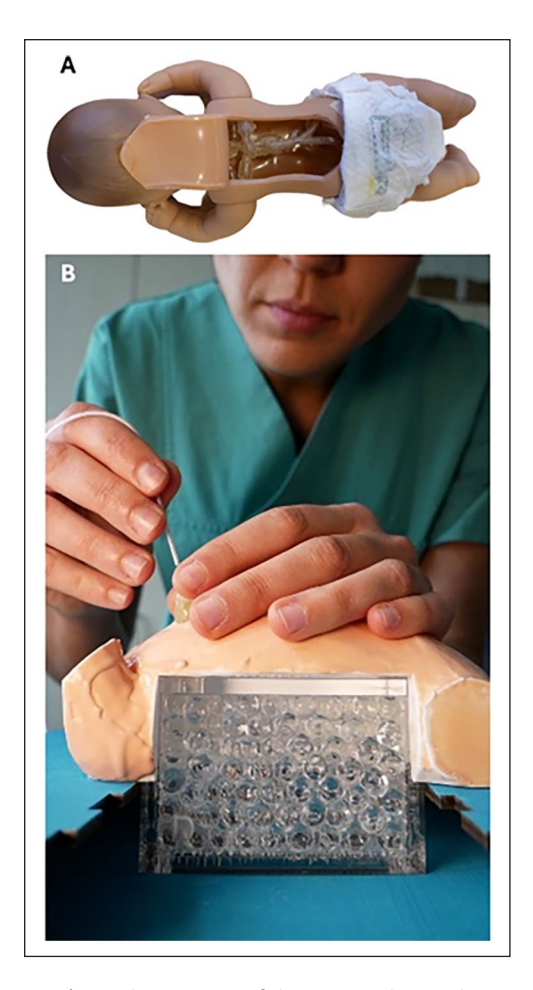


Figure 1. A) Initial prototype of the neonatal cannulation simulator featuring a 3D resin-printed venous tract incl. right heart. B) A neonatologist practicing the cannulation procedure on a neonatal cannulation simulator prototype. Water beads replicate the internal organs and allow for vessel movement.

⁵Department of Cardio-Thoracic Surgery, Thorax Centrum Twente, Medisch Spectrum Twente, Enschede, the Netherlands; ⁶HORIZON-EIC-2022-PATHFINDEROPEN- 01, Grant agreement ID: 101099596

Introduction: The ArtPlac consortium aims to develop an artificial placenta for preterm neonates for acute lung and kidney support in a single device. This device will be connected to the umbilical vessels using large cannulas. Currently, there is no simulator available to train neonatologists in the use of this novel cannulation procedure. The goal of this innovation is to develop a simulator for neonatal cannulation training based on the evaluation of neonatologists needs.

Methods: Neonatologists were contacted for current practices, regulations, and weaknesses. Training needs were discussed and used as requirements for the development of an initial neonatal cannulation simulator. Validation testing was conducted with 11 medical professionals (neonatologists or paediatricians).

Results: The initial protype of the neonatal cannulation simulator incorporated only the venous tract (Fig. 1A). Wharton's Jelly was replicated using gelatine. An outer shell with the shape of a neonate body was filled with water beads (Fig. 1B), which replicated the internal organs and allowed for movement of the vessels. User validation showed that vessel puncturing with silicone was too easy and 3D-printing resin too hard to

DEVELOPMENT OF A TRAINING SIMULATOR FOR NEONATAL CANNULATION IN ARTIFICIAL PLACENTA APPLICATIONS

D.J.M. van Galen¹, F.R. Claybrook¹, L.G. van der Woerd¹, N. Rochow^{2,3}, S. Georgiev⁴, K. Gendera⁴, F.R. Halfwerk ^{1,5}, J. Arens¹, on behalf of the ArtPlac Research Consortium ⁶

¹Engineering Organ Support Technologies, Department of Biomechanical Engineering, Faculty of Engineering Technologies, Technical Medical (TechMed) Centre, University of Twente, Enschede, the Netherlands; ²Department of Pediatrics, Paracelsus Medical University, Nuremberg, Germany; ³Department of Pediatrics, University Medicine Rostock, Rostock, Germany; ⁴Department of Paediatric Cardiology and Congenital Heart Defects, German Heart Centre Munich, Technische Universität München, Munich, Germany;

puncture. The umbilical cord tissue required a 'more slippery' and 'compliant' consistency with 64% strongly agreeing for simulating umbilical cord characteristics more closely. Similarly, realistic organ shapes are warranted to observe the effects of vascular curvature on the simulator while performing cannulation.

Furthermore, the emulation of blood flow within the simulator can serve as a model for neonatal circulation, offering insights into flow rate and pressure levels.

Discussion: Professional development for a cannulation simulator could enhance end-user needs for functional verification and requirements for procedural accuracy. In addition, future focus on the material properties of the simulated umbilical cord and umbilical vessels is necessary to develop a realistic simulator.

2A: OMICS IN PERSONALIZED MANAGEMENT OF CARDIOVASCULAR AND KIDNEY DISEASE

(PROTE)OMICS FOR SUPERIOR MANAGEMENT OF KIDNEY AND CARDIOVASCULAR DISEASE - A THOUGHT-PROVOKING IMPULSE FROM NEPHROLOGY

Joachim Beige^{1,2}, Agnieszka Latosisnka,³

¹Kuratorium for Dialysis and Transplantation, Neu-Isenburg; ² Martin-Luther- University Halle/Wittenberg; ³Mosaiques Diagnostics and Therapeutics

Abstract: Chronic kidney disease (CKD) and cardiovascular disease (CVD) are complex conditions often managed by nephrologists. This viewpoint paper advocates for a multi-omics approach, integrating clinical symptom patterns, non-invasive biomarkers, imaging, and invasive diagnostics to enhance diagnosis and treatment. Early detection of molecular changes, particularly in collagen turnover, is crucial for preventing disease progression. For instance, urinary proteomics can detect early molecular changes in diabetic kidney disease (DKD), heart failure (HF), and coronary artery disease (CAD), enabling proactive interventions and reducing the need for invasive procedures like renal biopsies. For example, urinary proteomic patterns can differentiate between glomerular and extraglomerular pathologies, aiding in the diagnosis of specific kidney diseases. Additionally, urinary peptides can predict CKD progression and HF development, offering a non-invasive alternative to traditional biomarkers like eGFR and NT-proBNP. The integration of multi-omics data with artificial intelligence (AI) holds promise for personalized treatment strategies, optimizing patient outcomes. This approach can also reduce healthcare costs by minimizing unnecessary invasive procedures and hospitalizations. In conclusion, the adoption of multi-omics and non-invasive biomarkers in nephrology and cardiology can revolutionize disease management, enabling early detection, personalized treatment, and improved patient outcomes.

CALPROTECTIN IN VASCULAR CALCIFICATION AND CARDIOVASCULAR COMPLICATIONS

Ana Amaya-Garrido¹, Julie Klein¹

¹Institut National de la Santé et de la Recherche Médicale (INSERM), U1297, Institute of Cardiovascular and Metabolic Disease, 31432 Toulouse, France

Introduction: In patients with chronic kidney disease (CKD), vascular calcification is considered a major risk factor of cardiovascular (CV) mortality. Involving osteochondrogenic differentiation of vascular smooth muscle cells (VSMCs) and abnormal deposition of minerals in the vascular wall, vascular calcification is an overly complex process and treatment options remain limited. Serum proteome analysis could help

identify novel actors and potential therapeutic targets in vascular calcification associated with CKD.

Methods: We included 453 CKD stages 3-4 or stage 5 patients with 2 to 4 years follow-up and originating from three independent cohorts. Serum proteome analysis was performed using LC-MS/MS on a subset of 66 CKD3-4 patients. Circulating calprotectin concentration was further validated in the serum or plasma from the full cohorts by ELISA. Calprotectin levels were associated with CV outcome using Kaplan-Meyer and Cox analysis. Serum calprotectin concentration was also associated with vascular calcification score. The effect of calprotectin, calprotectin inhibitor paquinimod and human uremic serum on calcification was measured in primary human VSMCs and mouse aortic rings. The anticalcific potential of paquinimod was also studied in a 5/6 subtotal nephrectomy mouse model and in aged ApoE-/- mice.

Results: Among 134 proteins with differential abundance between patients with (n=32) or without CV events (n=34), calprotectin appeared among the strongest candidates in both univariate and multivariate analyses. Using ELISA, we validated that elevated calprotectin was independently associated with severe CV outcome in 112 CKD3-4 (Hazard Ratio [95% Confidence Interval], 1.33 [1.12-1.59], P=0.0008) and 171 dialysis patients (1.24 [1.10- 1.41], P=0.0005). Calprotectin increased calcium deposition in VSMCs and mouse aortic rings. Paquinimod reduced calcification *in vitro* and *in vivo* in 5/6 nephrectomy mouse model of CKD and aged atherosclerotic ApoE-/- mice. In an independent additional cohort of 170 CKD5 patients, increased serum calprotectin correlated with increased medial vascular calcification score. Finally, paquinimod reduced calcification induced by the serum of uremic patients in VSMCs (P<0.01).

Discussion: We identified calprotectin as a key factor associated with vascular calcification, CV outcome and mortality in CKD patients. Blockade of calprotectin by paquinimod might be a promising strategy to reduce the burden of vascular calcification in CKD.

THE NEED FOR AI MODELLING IN CKD USING BIG DATA

Marta B. Lopes^{1,2}

¹Center for Mathematics and Applications (NOVA Math), NOVA School of Science and Technology (NOVA FCT), Caparica, Portugal; ²UNIDEMI, Department of Mechanical and Industrial Engineering, NOVA School of Science and Technology (NOVA FCT), Caparica, Portugal

Introduction: Chronic kidney disease (CKD) is a global health issue requiring early detection and intervention. Traditional diagnostics often fail to capture CKD's complexity. Progress in omics technologies has significantly enhanced our comprehension of the molecular mechanisms underlying diseases, facilitating the discovery of biomarkers for better disease evaluation and management. By combining artificial intelligence (AI), particularly machine learning (ML), with complex big data such as multi-omics data, there is promising potential to achieve early diagnosis of CKD, predict risks, and develop personalized treatment plans. This integrated approach provides tailored insights for patient care, improves decision-making support, and increases cost-effectiveness by enabling early detection and reducing the need for unnecessary interventions.

Methods: This review explores the distinct omics layers and the rapidly evolving role of ML in extracting meaningful insights from CKD omics datasets [1]. It provides an overview on which ML methods have been applied with the goal of transforming CKD omics data into enhanced diagnostic tools and treatment strategies, emphasizing the critical contribution of ML in advancing personalized care for CKD patients.

Results: Multiple omics data sets have been generated from a diversity of sample types across various omics studies conducted in CKD patients (Figure 1).

Figure 2 outlines the trends in the application of statistical and ML methods to CKD omics data, from unsupervised to supervised learning and network discovery methods.

Discussion: Integrating omics data with advanced ML is crucial for identifying molecular diagnostic and prognostic markers in CKD. However, beyond model validation, biological validation is essential to confirm the clinical relevance of these findings. Future directions in applying AI to CKD care should emphasize the importance of such validation.

References

 Marta B. Lopes, Roberta Coletti, Flore Duranton, Griet Glorieux, Mayra Alejandra Jaimes Campos, Julie Klein, Matthias Ley, Paul Perco, Alexia Sampri, Aviad Tur-Sinai (2024). The Omics-Driven

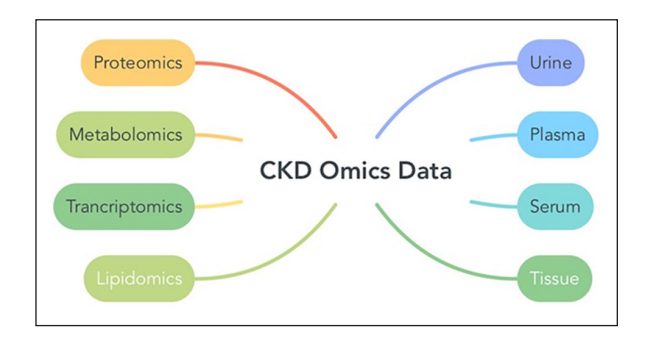


Figure 1. Omics layers and sample types used in CKD studies.

Machine Learning Path to Cost- Effective Precision Medicine in Chronic Kidney Disease. Proteomics e202400108

Acknowledgements

This work is based upon work from COST Action PerMediK, CA21165, supported by COST (European Cooperation in Science and Technology).

OMICS STUDIES IN CKD: DIAGNOSTIC OPPORTUNITIES AND THERAPEUTIC POTENTIAL

Prof.Assoc.Merita Rroji^{1,2}

¹Faculty of Medicine, University of Medicine of Tirana, Tirana; ²Department of Nephrology, University Hospital Center" Mother Tereza", Tirana, Albania

Introduction: Chronic kidney disease (CKD) is a major global health issue. Traditional diagnostics and treatments often do not capture the full molecular complexity of the disease. In recent years, multi-omics research—including genomics, transcriptomics, proteomics, and metabolomics— has revealed new disease mechanisms, improved biomarker detection, and led to better risk stratification methods. These approaches have opened new paths toward personalized therapies by linking genetic variants and molecular signatures to key kidney targets.

Methods: We conducted a review of recent multi-omics studies in chronic Over the past decade, we reviewed multi-omics studies related to chronic kidney disease (CKD). We explored literature from

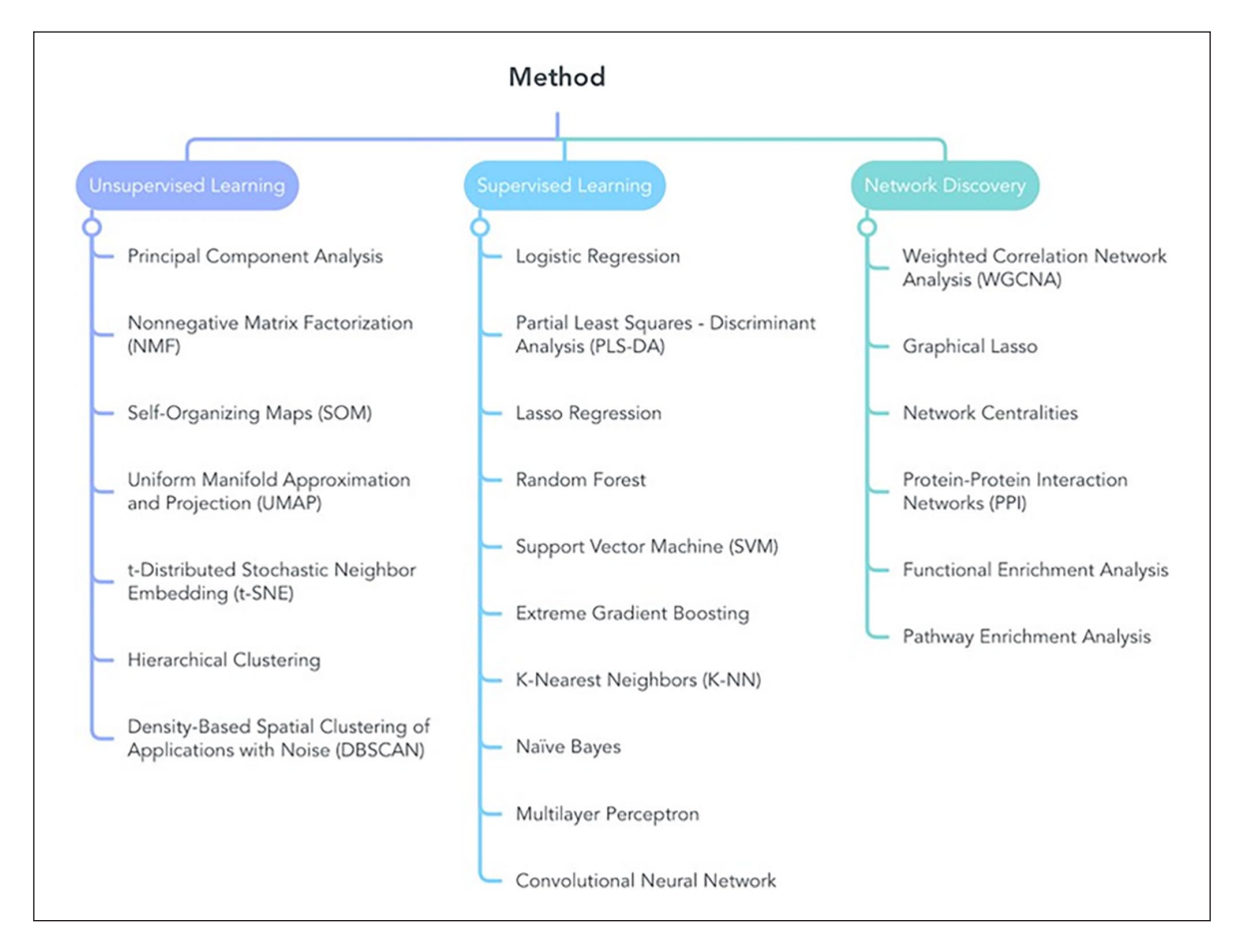


Figure 2. Summary of methods used for predicting and understanding CKD-related conditions.



Fig1. Integrating multi-omics approaches for personalized medicine: from molecular insights to clinical applications.

databases—including PubMed, Scopus, and Web of Science—that focused on proteomics, metabolomics, transcriptomics, and genomics, highlighting their roles in advancing clinical data. Additionally, we examined emerging clinical trial designs, such as biomarker-based strategies and adaptive enrichment protocols, to assess the potential of multiomics approaches in improving CKD diagnosis, risk stratification, and treatment.

Results: These multi-omics approaches have led to the identification of critical molecular pathways and actionable treatment targets. Studies have shown that linking genetic variants and molecular markers to kidney targets can improve risk prediction and refine disease classification across a wide range of kidney conditions. Enhanced biomarker detection and risk stratification methods have supported the development of more personalized therapeutic strategies, resulting in improved diagnostic accuracy and more effective interventions [1,2].

Discussion: Despite these advances, several challenges remain before multi-omics research can be routinely applied in clinical practice. Integrating diverse datasets and ensuring consistent data storage and interpretation are ongoing issues. Although urine samples have been widely used, blood-based approaches are gaining importance, particularly for patients with anuric end-stage kidney disease. Additionally, ethical considerations and data privacy must be carefully managed. Standardized protocols, external validation across diverse populations, and international collaboration are essential. In summary, combining comprehensive omics profiling, advanced computational analysis, and innovative clinical trial designs holds great promise for improving CKD management by offering more precise diagnostics, better risk prediction, and truly personalized treatment strategies [1-3].

References

 Rroji M, Spasovski G. Omics Studies in CKD: Diagnostic Opportunities and Therapeutic Potential. Proteomics.doi: 10.1002/ pmic.202400151,2024

- J. Su, L. Yang, Z. Sun, and etal, "Personalized Drug Therapy: Innovative Concept Guided With Proteoformics," Molecular & Cellular Proteomics: https://doi.org/10.1016/j.mcpro,2024
- N. Grobe, J. Scheiber, Het al "Omics and Artificial Intelligence in Kidney Diseases," Advances in Kidney Disease and Health 30: 47– 52, 2023. https://doi.org/10.1053/j.akdh.2022.11.

Note: This abstract is submitted for EUTox symposium in collaboration with PerMediK COST Action

Title: Omics in Personalized Management of Cardiovascular and Kidney Disease

COMPUTATIONAL DRUG REPOSITIONING IN CARDIORENAL DISEASE: OPPORTUNITIES, CHALLENGES, AND APPROACHES

Paul Perco^{1,2}, Matthias Ley^{1,3}, Kinga Kęska-Izworska¹, Dorota Wojenska¹, Enrico Bono^{1,3}, Samuel M. Walter¹, Lucas Fillinger ¹, Klaus Kratochwill ^{1,3}

¹Delta4 GmbH, Vienna, Austria; ²Department of Internal Medicine IV, Medical University of Innsbruck, Innsbruck, Austria; ³Comprehensive Center for Pediatrics, Department of Pediatrics and Adolescent Medicine, Division of Pediatric Nephrology and Gastroenterology, Medical University of Vienna, Vienna, Austria

Introduction: There is currently increased interest in drug repositioning programs, namely the identification of new therapeutic areas for already approved drugs, both in academia as well as in the biotech and pharmaceutical industry. Since 2012, the number of publications indexed in MEDLINE on drug repositioning or drug repurposing is exponentially increasing with a peak in the year 2021 due to the worldwide search for therapeutic options to combat the COVID-19 pandemic. Drug

repositioning, however, is not new, and pharmaceutical companies have ever since been looking for additional market opportunities for their products, in particular when patents expire and generics manufacturers enter the market of the therapeutic areas of initial approvals. Drug repositioning candidates are also tested in clinical trials in the context of cardiorenal disease.

Methods: We used Delta4's Hyper-C software platform to extract information on running Phase III clinical trials in the context of renal and cardiovascular disease (CVD) [1]. Curated phenotype and drug catalogs based on MeSH and ChEMBL were used to mine clinical trial information on ongoing Phase III clinical trials. Ongoing clinical trials included trials with one of the following statuses: "Active, not recruiting", "Recruiting", "Not yet recruiting", or "Enrolling by invitation". Only clinical trials of type "intervention" have been included, which are testing at least one drug. Renal and cardiovascular neoplasm disease entities have been removed from the analysis. Information regarding approved indications for drugs in the catalog has been extracted from FDA drug labels. Drug repositioning cases in the renal context were considered if the drug that is tested in a Phase III clinical trial for a dedicated renal disease has already been approved for at least one other indication outside the area of nephrology without any approval for any nephrological disease. The same procedure was done to list all drug repositioning cases in the cardiovascular space.

Results: We identified 18 unique drugs being tested for 11 renal diseases which are approved for diseases outside the field of nephrology. CVDs were separated into vascular diseases and heart diseases. We identified 9 unique drugs being tested for 12 heart diseases which are approved for diseases outside the field of cardiovascular. Similarly, we identified 28 unique drugs being tested for 25 vascular diseases, which are approved for diseases outside the field of CVDs.

Discussion: Almost 50 unique drugs in clinical Phase III testing for renal and CVDs are approved for indications outside the renal and cardiovascular area, respectively, highlighting that drug repositioning is a very promising approach to bring new therapeutic options to the market and thus to the patient in the end. We will discuss these drug candidates as well as different computational approaches to identify novel drug repositioning opportunities [2].

References

- 1. Perco et al, Proteomics, 0:e202400109, 2025
- 2. Gebeshuber et al, Translational Research, 259:28-34, 2023

Acknowledgements

This project has received funding from the Austrian Research Promotion Agency (FFG) under grant agreement No 911422 (Delta4Tech). Additional support was provided by the project DC-ren, that has received funding from the European Union's Horizon 2020 research and innovation programme under grant agreement No. 848011. Enrico Bono is supported by a grant from European Union's Horizon Europe Marie Skłodowska-Curie Actions Doctoral Networks (HORIZON–MSCA–2023–DN-01, grant number 101168626, PICKED).

2C: BIOMATERIALS & SURFACES

MIMICKING THE ENDOTHELIAL GLYCOCALYX: ANTIMICROBIAL PEPTIDE-COATED SURFACES FOR BIOFILM PREVENTION

Denisa Cont^{1,2}, Claudia Schildböck¹, Viktoria Weber¹, Stephan Harm¹

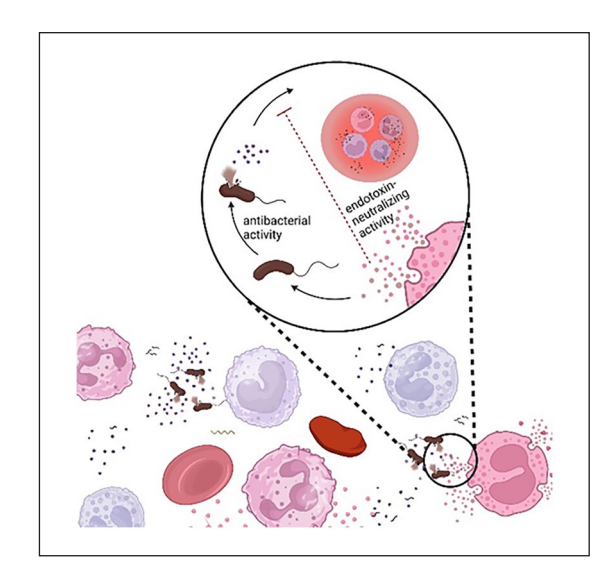


Figure 1. AMPs are naturally occurring, cationic peptides from the innate immune system with antimicrobial and immunomodulatory properties.

¹Department for Biomedical Research, University for Continuing Education Krems, Austria; ²Department of Pharmacology, Physiology, and Microbiology, Karl Landsteiner University, Austria

Introduction: The endothelial glycocalyx is a negatively charged, protective layer lining the vascular endothelium. One of its major components, heparan sulfate, shares structural similarities with heparin, a widely used anticoagulant, which has been shown to bind antimicrobial peptides (AMPs) (Figure 1) [1,2]. We hypothesized that blood-derived AMPs interact with glycosaminoglycan (GAG)-coated surfaces, potentially reducing biofilm formation.

Methods: GAG-functionalized surfaces were prepared in 96- well plates using unfractionated heparin (UFH) and chondroitin sulfate (CHS). These surfaces were incubated with fresh serum or saline solution (NaCl, control) for 4 h at 37 °C, then washed and exposed to a 104 colony forming units (CFU)/mL *Staphylococcus aureus* suspension for 48 h at 37 °C. Biofilm formation was assessed using scanning electron microscope (SEM) and fluorescence- based live/dead viability assay.

Results: Both UFH- and CHS-coated surfaces incubated with serum significantly reduced the *S. aureus* biofilm formation compared to controls. This was evidenced by lower bacterial adhesion (**Figure 2**) and reduced biofilm viability (**Figure 3**).

Discussion: These findings underscore the important role of the glycocalyx in infection control, particularly through its interaction with bloodderived AMPs to form a protective barrier at infection sites. Understanding this glycocalyx-AMP equilibrium could pave the way for innovative strategies, such as pre-coating biomedical implants with blood-derived AMPs, to enhance biocompatibility and longevity, reducing the risk of implant-associated infections.

References

- 1. Harm et al, Sci Rep, 11:4192, 2021.
- 2. Cont et al, Front Immunol, 15:1373255, 2024.

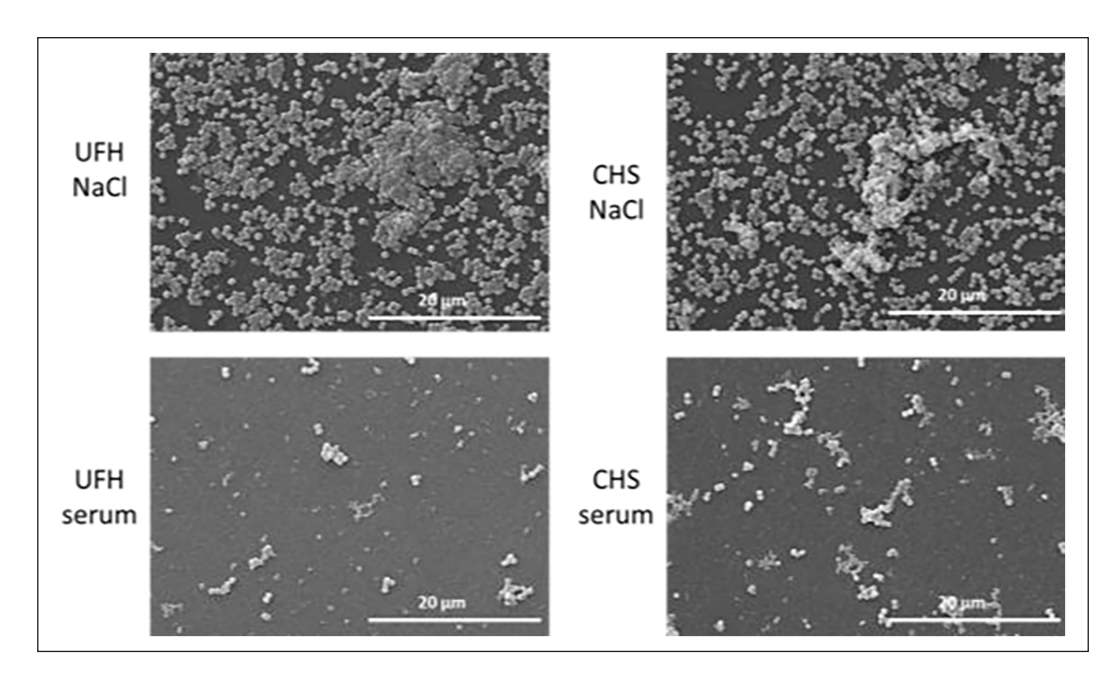


Figure 2. SEM images demonstrated reduced biofilm formation on UFH- and CHS-functionalized surfaces, as evidenced by lower bacterial adhesion in serum-treated samples compared to saline controls (n=6).

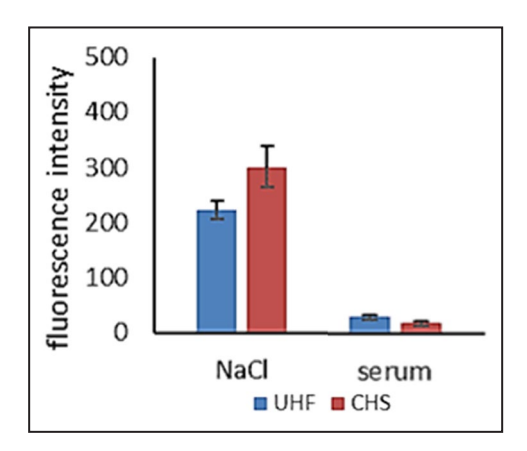


Figure 3. Fluorescence-based live/dead assays showed reduced bacterial viability on GAG-functionalized surfaces incubated with serum compared to saline controls (n=3).

COMPARISON OF PLATELET ADHESION ON DIFFERENT HARD MATERIAL COATINGS AND BONDING AGENTS FOR VENTRICULAR ASSIST DEVICES IN A FLOW CHAMBER

Isabell Esslinger^{1,2}, Henri Wolff^{1,2}, Tim Bierewirtz^{1,2}, Michael Lommel^{1,2}, Ulrich Kertzscher^{1,2}

¹Deutsches Herzzentrum der Charité, Institute of Computerassisted Cardiovascular Medicine, Biofluid Mechanics Laboratory, Augustenburger Platz 1, 13353, Berlin, Germany; ²Charité – Universitätsmedizin Berlin, corporate member of Freie Universität Berlin and Humboldt- Universität zu Berlin, Charitéplatz 1, 10117 Berlin, Germany Introduction: Ventricular assist devices (VADs) still lead to thrombus formation on blood-contacting surfaces and used materials like Ti6Al4V (titanium alloy) do not provide sufficient wear resistance in critical areas, so more durable coatings are required. Bonding agents are needed for stable coatings but can be exposed to blood if the coating is damaged. This study aimed to evaluate hard material coatings (HMCs) and bonding agents for platelet adhesion to assess their thrombogenic potential.

Methods: Three HMCs: silicon-incorporated diamond-like carbon (SiDLC), titanium nitride with droplets (TiN_D) and without droplets (TiN) and two bonding agents: chrome (Cr) and chrome nitride (CrN) were investigated. Aluminum (Alu) served as positive control and uncoated Ti6Al4V as reference. Platelet adhesion was measured with fluorescence microscopy and surface coverage quantified via digital image processing. The experimental setup (Figure 1) was tempered to 37°C. Pathologically high shear rates exceeding 5,000 s⁻¹, known to trigger platelet thrombosis, guided our choice of experimental conditions of an numerically calculated average wall shear rate of 5730.5 1/s on the evaluated area. The normalized percentage of the covered surface area (NCSA) was calculated by dividing the percentage of the covered surface area by the platelet count of each respective blood draw. P-values and Wilcoxon test effect sizes were used for statistical analysis.

Results: Figure 2 summarizes the results, with Alu showing the highest value (8.7), significantly higher than CrN and SiDLC (both 0.3, p<0.05). Alu had medium effect sizes compared to the HMCs, Ti (0.2) and CrN and a weak effect compared to Cr (3.6). Cr had significantly higher platelet adhesion than CrN and medium effects compared to CrN, Ti, TiN (0.3), and SiDLC, with weak effects relative to TiN_D (0.4) and Alu. No significant differences were observed between the HMCs, Ti, and CrN.

Discussion: The results showed that chrome possesses a high thrombosis risk and should be avoided as bonding agent, while chrome nitride demonstrated lower platelet adhesion and performed similarly to the titanium alloy Ti6Al4V. The hard material coatings exhibited hemocompatibility comparable to Ti6Al4V, supporting their suitability for VADs.

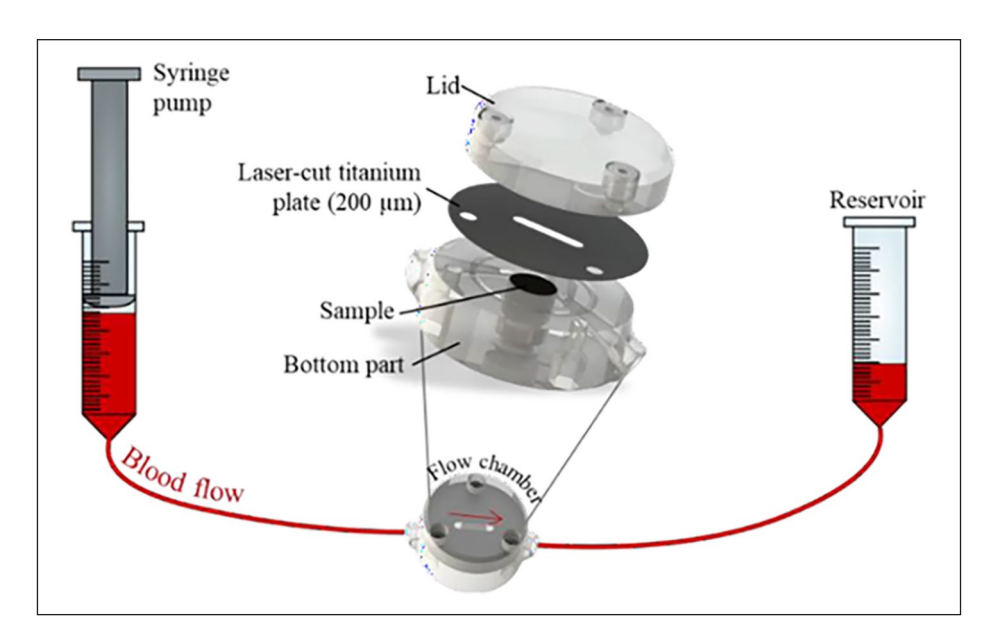


Figure 1. Experimental setup with flow chamber.

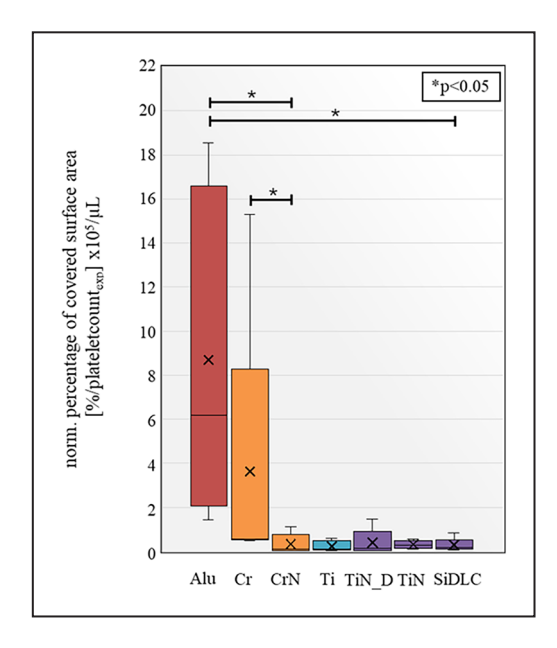


Figure 2. Normalized percentage of the covered surface area (NCSA); *N*=5.

IMPACT OF MICROSTRUCTURED ARIFICIAL SURFACE ON THE DYNAMICS OF BLOOD PLATELETS

Corentin Raveleau¹, Simon Mendez¹, Franck Nicoud^{1,2}

¹IMAG, CNRS, Université de Montpellier, Montpellier, France; ²IUF, Institut Universitaire de France, France

Introduction: Cardiovascular diseases are the leading cause of death worldwide, creating a high demand for medical devices for treatment. Given their direct blood exposure, ensuring their hemocompatibility is essential but still an issue. Artificial surface structuring in the micrometer range have been shown to influence the thrombogenicity of the surface although this effect is not well characterized and understood [1]. This abstract presents the preliminary outcomes of a computational study aiming at better understanding how the platelets adhesion, the key mechanism in thrombus initiation, can be affected by micro-structuration of the artificial surface.

Method: The numerical model is implemented in the YALES2BIO solver developed at IMAG (https://imag.umontpellier.fr/~yales2bio/) and dedicated to the simulation of blood flows [2].

The surrounding plasma movement is described by the incompressible Navier-Stokes equations:

$$\nabla \mathbf{u} = \mathbf{0} \tag{1}$$

$$\rho^{\frac{|\mathbf{u}|}{|\mathbf{f}|}} + \rho \mathbf{u} \nabla \mathbf{u} = -\nabla p + \mu \nabla^2 \mathbf{u} + \mathbf{f}(\mathbf{x}, t)$$
 (2)

$$f_{i}(\mathbf{x},t) = F_{i}\Delta(\mathbf{x} - \mathbf{Y}) + \frac{\$}{\frac{9}{6}} \varepsilon \&' \left(T\left(\frac{\partial}{\partial xj}\Delta_{d}(\mathbf{x} - \mathbf{Y})\right)\right)$$
(3)

The presence of a platelet in the flow, represented by a rigid ellipsoid, is taken into account by the force $\mathbf{f}(\mathbf{x},t)$ in equation (2) and detailed in equation (3). It relates the external forces \mathbf{F} and torques \mathbf{T} acting on the particle as well as its incompressibility to the particle dynamics and surrounding flow perturbation, via 2 Gaussian enveloppes Δ and Δ_d centered at the particle center of mass \mathbf{Y} , as prescribed by the Force Coupling Method [3].

Results: Single particle dynamics over 3 surface structures was studied: square grooves, downward sawtooth grooves and upward sawtooth grooves. The drift angle θ is measured over each of the structure for different initial particle positions x^* and constant initial altitude z^* , after a 180° rotation of the particle induced by the ambient shear flow (Figure 1). The mean drift angle is obtained by integrating over the possible values of x^* in a structure pattern period L. Table 1 shows that the square grooves

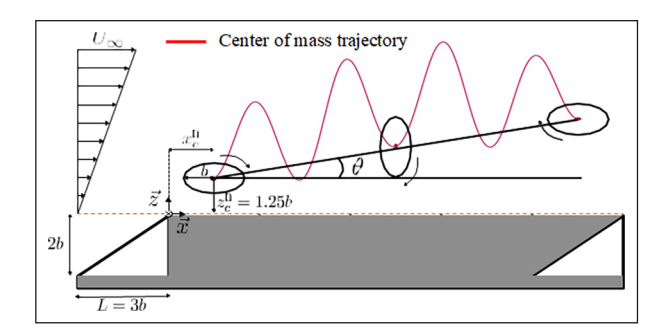


Figure 1. Drift angle θ over upward sawtooth grooves after a 180° rotation (scaled for clarity).

	Flat surface	Square	Downward Sawtooth	Upward Sawtooth
Mean drift angle	0.15	0.24	-1.23	1.38

Figure 2. Particle mean drift angle (milli-radians). $b = 1.5 \mu m$, $Re = 3.8 \times 10^{+}$.

produces a mean drift angle comparable to the one observed on a flat surface. This is caused by the small yet non-zero inertial forces inducing a lift of the particle.

However, sawtooth structures generate a mean drift which sign depends on the orientation of the sawtooth, and of greater amplitude. Indeed, the upward sawtooth structure requires the particle to flow past 15 structures (\approx 70 μm) to drift 100 nm away from the surface, the typical formation length of platelets adhesive bonds [4], compared to around 90 (\approx 400 μm) for the square grooves.

Conclusion: A numerical model of blood platelet has been used to study the effect of microstructured artificial surface on the dynamics of a single platelet. Upward sawtooth grooves seem to be of particular interest for reducing particle-surface interaction and ultimately platelet adhesion.

Acknowledgements

This work has been initiated during the Extreme CFD Workshop & Hackathon (https://ecfd.coria-cfd.fr). It is part of the THROMBOSURF project co-funded by Agence Nationale de la Recherche (ANR-21-CE45-0035-02) and DFG.

References

- 1. Kuchinka et al, Bioengineering, 8:215, 2021.
- 2. Mendez et al. Bio Flow in Lar Vessel.183-206. 2022.
- 3. Liu et al, J Comp Phys, 228:3559-3581, 2009.
- 4. Z. M. Ruggeri, Microcirculation, 16:58-83, 2009.

BIO-INSPIRED HYDROPHILIC SURFACE FOR INHIBITING THROMBUS FORMATION

Dominika Wójtowicz^{1,2}, Barbara Buśko¹, Syliwa Golba³, Justyna Jurek-Suliga³, Dominika Nguyen Ngoc⁴, Joanna Wessely-Szponder⁴, Ewa Stodolak- Zych¹

¹Department of Biomaterials and Composites, Faculty of Materials Science and Ceramics, AGH University of Krakow, al. Mickiewicza 30, 30-059 Krakow, Poland; ²Clinical Department of Anesthesiology and Intensive Care, University Hospital in Krakow, ul. Jakubowskiego 2, 30-688 Krakow, Poland; ³Institute of Materials Engineering, University of Silesia, ul. 75 Pulku Piechoty 1A, 41-500 Chorzow, Poland, ⁴Division of Pathophysiology, Department of Preclinical Veterinary Sciences, Faculty of Veterinary Medicine, University of Life Sciences in Lublin, Poland

Introduction: The physiochemical properties of the blood-contacting surface of dialysis membranes are among main factors influencing their hemocompatibility. From the literature, we know that superhydrophobic surfaces are preferable for ensuring high biocompatibility [1]. However, results from our previous study, focused mainly on improving polysulfone (PSU) biocompatibility by changing surface properties, suggest that polymer membranes modified with nanometric SiO2 show improved thrombogenicity despite their hydrophilic surface [2].

The purpose of this study was to modify the surface charge of the membrane by using core-shell nanoparticles based on silica and polypyrrole nanoparticles in order to (1) facilitate the dispersion of nanofiller in the polymer matrix, (2) increase surface free energy of the membrane surface and (3) reduce the tendency for blood clot formation on the membrane.

Methods: Commercially available polymers: polysulfone (PSU), polyvinylpyrrolidone (PVP), polypyrrole (PPy) (Sigma-Aldrich) were used to prepare membranes. The PSU/DMF membrane solution (15%wt) was modified with PVP/DMF. A weight fraction of modified SiO2-PPy nanoparticles (1-5%wt) was added during PSU/PVP/DMF homogenization. Core-shell nanoparticles based on SiO2 (NanoAmor) were obtained according to a previous paper [3]. Membranes were obtained by nonsolvent induced phase separation (NIPS) and subjected to stepwise dehydration through a series of alcohols (EtOH 50-98%). Membranes' surface and microstructure were observed using scanning electron microscopy (SEM, Apreo 2). Contact angle and surface free energy were determined with goniometer (Krüss DSA 25). Thrombogenicity was studied according to the Sabino's and Popat's protocol with whole blood without anticoagulants.

Results: The method used to obtain membranes with SiO2- PPy particles in the PSU/PVP matrix increases the total porosity of the membranes (by ~30% compared to the membrane with PSU). Presence of SiO2-PPy in the matrix increases surface free energy (from 40mm/mN to 48mm/mN). This effect is caused by a threefold decrease in the surface charge of the core-shell particles relative to pure nanosilica (from -24mV for SiO2 to -7mV for SiO2- PPy). Thus, the surface charge of the membrane changes lowering its thrombogenicity.

Discussion: Membrane surface with a balanced electrostatic charge can reduce platelet aggregation. Neutral or lightly charged surfaces are beneficial because too strong a charge can attract blood cells and promote their activation. Membranes with lower surface properties can instead increase interaction with albumin present in blood reducing subsequent platelet adherence. The use of PSU/PVP/SiO2-PPy membranes in hemodialyzers can improve blood flow maintenance without the risk of blood clotting.

Conclusion: Using nanocomposite membrane such as PSU/PVP/SiO2-PPy might be an effective way to obtain dialysis membranes with improved hemocompatibility.

References

- 1. V. Jokinen et al. A. Ras, Adv. Mater. 2018, 30, 1705104.
- 2. D. Wójtowicz et al. *IJAO* 2024, 47, 8,582 589.
- 3. Golba, S et al. *Materials* 2023, 16, 7069.

Acknowledgements

This work was supported by "Initiative of Excellence – Research University" (IDUB) grant ID 4204.

3A INTERNATIONAL KIDNEY REPLACEMENT INNOVATION ROADMAP

ABSTRACT: AMMONIUM SORBENT WITH HIGH SELECTIVITY AND CAPACITY FOR USE IN DIALYSATE REGENERATION: COATED HYDROGEN-LOADED ZIRCONIUM PHOSPHATE

Stephen Ash¹, David Carr¹, Yihan Song², Sang-Ho Ye², and Lei Li²

¹HemoCleanse Technologies LLC, Lafayette, IN, USA; ²University of Pittsburgh, Department of Chemical & Petroleum Engineering, Pittsburgh, PA, USA

Introduction: Cation exchangers are essential components of dialysate regenerating columns. Urease converts urea to NH $^+$ and bicarbonate and a cation exchanger (such as zirconium phosphate, ZP) removes NH $^+$. But cation exchangers such as zirconium phosphate (ZP) are nonselective and bind cations in proportion to concentration and charge density. In physiological solutions ZP binds Ca 2 +, Mg 2 +, and K $^+$ more than it binds NH $^+$ (only about 1 meq/gram).

We postulated that if we loaded ZP completely with H $^+$ (H-ZP) and coated it with a gas-permeable and hydrophobic membrane, we could create a sorbent that would be exclusively selective for binding NH $^+$. In solution, NH $^+$ equilibrates with NH3, which will pass through the gas-permeable membrane and attach to H $^+$ within the membrane. The coated sorbent having a low pH will act as an "acid trap", creating a pH gradient for passage of NH3 across the membrane whereas all other ions in the water solution would be excluded due to the hydrophobicity of the membrane. Without competing cations, NH $^+$ would be efficiently and selectively bound by H-ZP. $^{1.2}$

Methods: A simple thermal vapor deposition (TVD) process exposed H-ZP particles to vapor from 1 ml of TEOS for 24 hours and then 5 ml FOTS for 24 h at 80 °C. We constructed a small column containing dry, coated ZP and perfused it with a solution of 14 mm CaCl2, 14 mM at rate of one void volume per minute.

Results: Physical testing confirmed the hydrophobic nature of the coated ZP. In vitro studies with solutions containing multiple ions confirmed that at equilibrium, coated sorbent had little sorption of Ca²⁺ and maintained high capacity for binding NH ⁺ up to 4 meq/gm with high pH in solution.³ Coated H-ZP displayed characteristics of hydrophobicity, with very high water contact angle, floating in solution and adherence to container walls and air- fluid interfaces. However, kinetics were slow due to diffusion limitations in solution. In the column coated H-ZP was contained and perfused easily with solution. Reaction times were rapid, with low

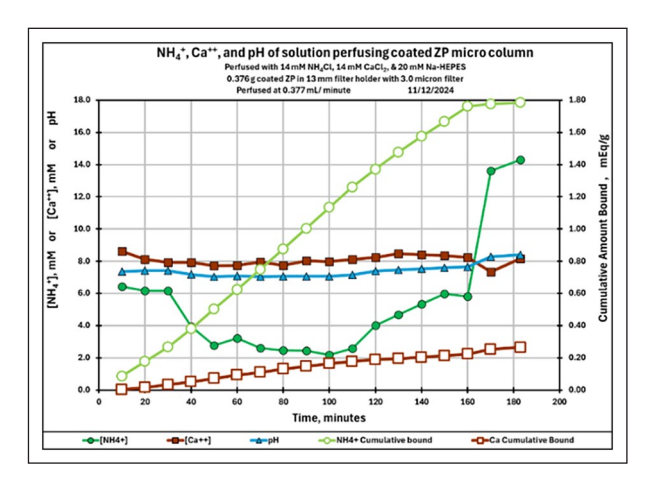


Figure 1. Inflow and outflow concentrations of NH4+ and Ca²⁺ and outflow pH of perfusate of the microcolumn.

NH ⁺ levels in outflow after one minute of residence time. (**Figure 1**). NH ⁺ levels were stable and much lower than perfusing fluid concentrations, especially after wetting of the coated H-ZP by water vapor transfer which occurred in the first 40 minutes. Binding capacity was 1.7 meq, higher than expected for H-ZP without coating and Ca²+ binding was minimal.

Discussion: Coated H-ZP is a highly effective sorbent for NH $^+$ in a column configuration. In combination with urease in a column regenerating dialysate, it could minimize the size and weight of the NH $^+$ sorbent, avoid excess removal of other cations such as Ca^2+ , Mg^2+ and K^+ , and minimize need for electrolyte reinfusion to the dialysate. This could make highly portable or wearable dialysis machines lighter, smaller, simpler and easier to use in the home.

References

- 1. Richards E et.al. Langmuir 22, 7912-21, 2023
- 2. Richards E et.al. Langmuir 28. 8677-85, 2022
- 3. Song Y et.al. Langmuir 40, 16502-10, 2024

3B: BIOENGINEERING - TISSUE REGENERATION

BIOFABRICATION TECHNOLOGIES TO INSTRUCT REGENERATION

Lorenzo Moroni¹

¹Maastricht University, MERLN Institute for Technology-Inspired Regenerative Medicine, Complex Tissue Regeneration Department, Universiteitssingel 40, 6229ER Maastricht, the Netherlands

A key factor in current approaches for tissue and organ regeneration relies on enhancing (stem) cell-material interactions to obtain the same original functionality. Different approaches include delivery of biological factors, functionalization of biological factors onto 3D scaffolds surface, engineering surface properties (e.g. via topography modifications), and controlling bulk and structural chemical and mechanical properties of the cell- laden biomaterial porous constructs that are developed for regeneration. Although these strategies have proved to augment cell activity on biomaterials, they are still characterized by limited control in space and time, which hampers the proper regeneration of complex tissues. Here, we present a few examples where integration of biofabrication platforms allowed the generation of a new library of biological constructs with tailored biological, physicochemical, and mechanical cues at the macro, micro, and nano scale. These biological constructs are characterized by tailored cell-material interactions able to influence the activity of stem cells, thereby sustaining the regeneration of complex tissues. From these examples as well as from the study of other scientists, converging technologies seems to be a powerful route towards designing of biological constructs with instructive properties able to control cell activity for the regeneration of functional tissues. Future efforts should aim at further improving technology integration to achieve a fine control on stem cell fate by biomaterial and scaffolds design at multiple scales. This will enable the regeneration of complex tissues including vasculature and innervation, which will result in enhanced in vivo integration with surrounding tissues. By doing so, the gap from tissue to organ regeneration will be reduced, bringing regenerative medicine technologies closer to the clinics.

AIMP - AUTOMIZED, AI SUPPORTED PLATFORM FOR IMPLANT DESIGN, FABRICATION AND TESTING

Erik Kornfellner¹, Laurenz Berger¹,², Lorenzo Civilla¹,², Francesco Moscato¹,²,³

¹Center for Medical Physics and Biomedical Engineering, Medical University of Vienna, Austria; ²Ludwig Boltzmann Institute for Cardiovascular Research, Austria; ³Austrian Cluster for Tissue Regeneration, Austria

Introduction: Hospitals are increasingly setting up point-of-care workshops to manufacture patient-specific implants [1]. Currently, the workflow involves manual segmentation of CT/MRI data and tedious iterative optimization of implants. The use of AI and novel automation tools can facilitate this process [2]. A comprehensive platform (AImp) that integrates existing software with new, AI-based modules has been established.

Methods: Almp's modular structure allows the execution of different workflow steps in various ways, patient- specific and user-centered. Within the toolbox, patient data is first loaded and segmented, then a generative Al automatically generates the desired implant based on preoperative planning. In the next step, the implant is optimized according to the biomechanical load cases and the implant is validated via

simulation [3]. In the final step of the process, the implant that has been optimized and the corresponding surgical guides are prepared for 3D printing. This integration ensures seamless data transfer between the modules, thereby facilitating an efficient and streamlined workflow.

Results: The Almp software has been demonstrated to enhance the efficiency of implant design by facilitating the integration of novel modules, accelerating the testing process, and validating solutions for individual workflow steps. The software utilizes biomechanical load cases to simulate implants prior to manufacturing, ensuring optimal designs. An illustration of this workflow is presented in Figure 1, showing an example of an automatically generated, topology-optimized mandibular bone plate. Beyond implant generation, Almp incorporates dedicated modules for surgical guides, preoperative planning tools, and demonstrators, automating their creation. This comprehensive approach enhances surgical precision and improves patient outcomes by addressing all critical aspects of the procedure.

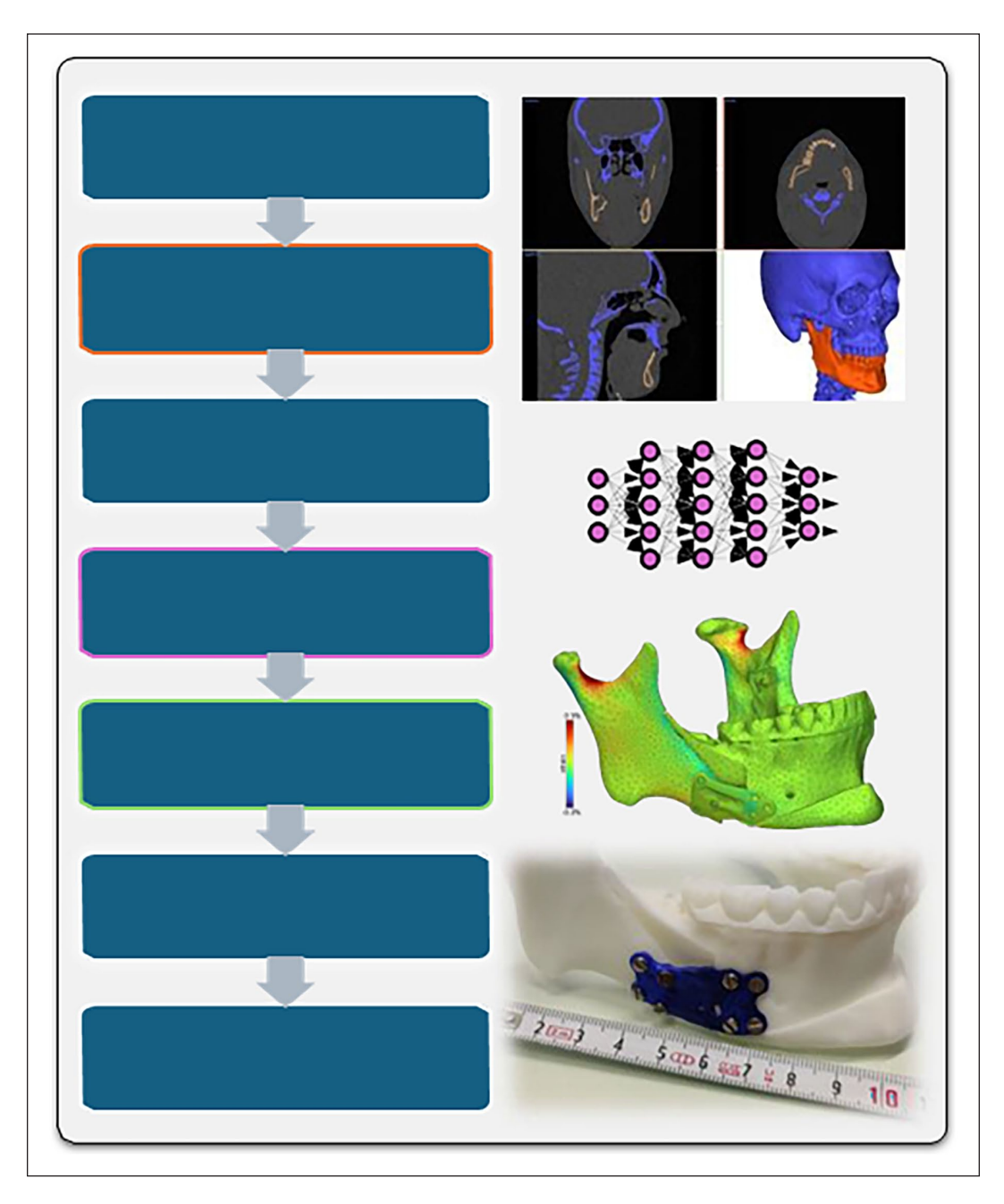


Figure 1. The workflow to create implants and accessories, completely covered by Almp.

Discussion: The integration of AI and automation in implant design, as exemplified by AImp, represents a substantial advancement in personalized patient care. By streamlining the workflow from medical imaging to implant fabrication, AImp reduces manual effort, accelerates design iterations, and improves overall efficiency, while ensuring that implants are not only patient-specific but also structurally optimized. Beyond implant creation, the incorporation of surgical guides and preoperative planning tools enhances both surgical precision and procedural success. Additionally, the ability to rapidly generate training models supports medical education by providing realistic, patient-specific simulations for skill development.

References

- 1. Biglino et al, 3D Print Med., 9:14, 2023
- 2. Tel et al, Sci Rep, 13(1):12082, 2023
- 3. Oberoi et al, Dent. Mat., 40:1568-1574, 2024

3C: ADVANCES IN HEART PUMP TECHNOLOGY: INNOVATIONS AND FUTURE DIRECTIONS 1

A SOFT ROBOTIC TOTAL ARTIFICIAL HEART CONCEPT

Patricia Castellanos Vaquero 1 , Maziar Arfaee 1,2 , Maria Rocchi 1 , Paul F. Gründeman 1,3 Johannes T. B. Overvelde 2 , and Jolanda Kluin 1

¹Erasmus MC, Netherlands; ²AMOLF, Netherlands; ³University Medical Center Utrecht, Netherlands

Introduction: End-stage heart failure has a high mortality rate (1), and while heart transplantation remains the gold effective treatment (2), the scarcity of donor hearts (3) has led to the development of total artificial hearts (TAHs). A new hybrid TAH concept is proposed, using soft robotics for physiological blood propulsion. It aims to overcome current limitations and improve outcomes for end-stage heart failure patients.

Methods: It comprises two blood-collecting chambers— referred to as "ventricles". Between these ventricles lies a soft pneumatic actuator, so called the "septum" which inflates and deflates using positive or negative air pressure (Figure 1). Inextensible wires arranged in a closed-loop, figure-eight pattern around both the septum and ventricles distribute force evenly. As the septum inflates and its interior expands, more wire length is taken up by the septum; because the total length of each wire remains fixed, the ventricles are squeezed, resulting in blood ejection. Stroke volume is determined by the number and length of wires around each ventricle. During diastole, the septum deflates to allow passive filling of the ventricles. The Hybrid Heart concept uses thin and flexible, yet inextensible materials—nylon coated with thermoplastic polyure-thane (TPU).

Each ventricle has an inlet and an outlet port for blood flow, where any valve type can be installed; in this proof of concept, mechanical heart valve prosthesis was chosen.

The Hybrid Heart's performance was first tested *in vitro* in a mock circulatory loop (MCL). We then evaluated the Hybrid Heart *in vivo* in an acute goat model.

Results: The Hybrid Heart demonstrated a left ventricular output of about 5.71 ± 0.04 L/min at 60 bpm and a slightly lower right ventricular output of 5.02 ± 0.08 L/min *in vitro*. The Hybrid Heart is sensitive to preload changes and increases its stroke volume passively when venous return increases. For each mmHg of preload rise, the Hybrid Heart ejects 198 ml/min extra. Regarding afterload sensitivity, the Hybrid Heart left ventricle ejects 20 ml/min less, for each mmHg afterload rise.

In a proof-of-concept study, we evaluated the Hybrid Heart in an acute goat model. The Hybrid Heart generated a cardiac output of 2.275 \pm 0.035 L/min on both ventricles (35 mL stroke volume). Mean pressures measured were 49 mmHg in the aorta and 17 mmHg in the pulmonary artery, while a sensor in iliac artery recorded systemic pressures ranging from 70/35 mmHg to 105/46 mmHg. After 50 minutes, the experiment ended due to a leak in pneumatic septum caused by delamination at the heat-sealing line between the TPU and nylon.

Discussion: We present first evidence that soft robotic techniques can be successfully utilized to create a TAH capable of delivering adequate cardiac output under physiological hemodynamic conditions *in vitro. In vivo* study showed the feasibility of device implantation and function in a goat model. However, durability and cardiac output need to be improved in future studies.

Figures

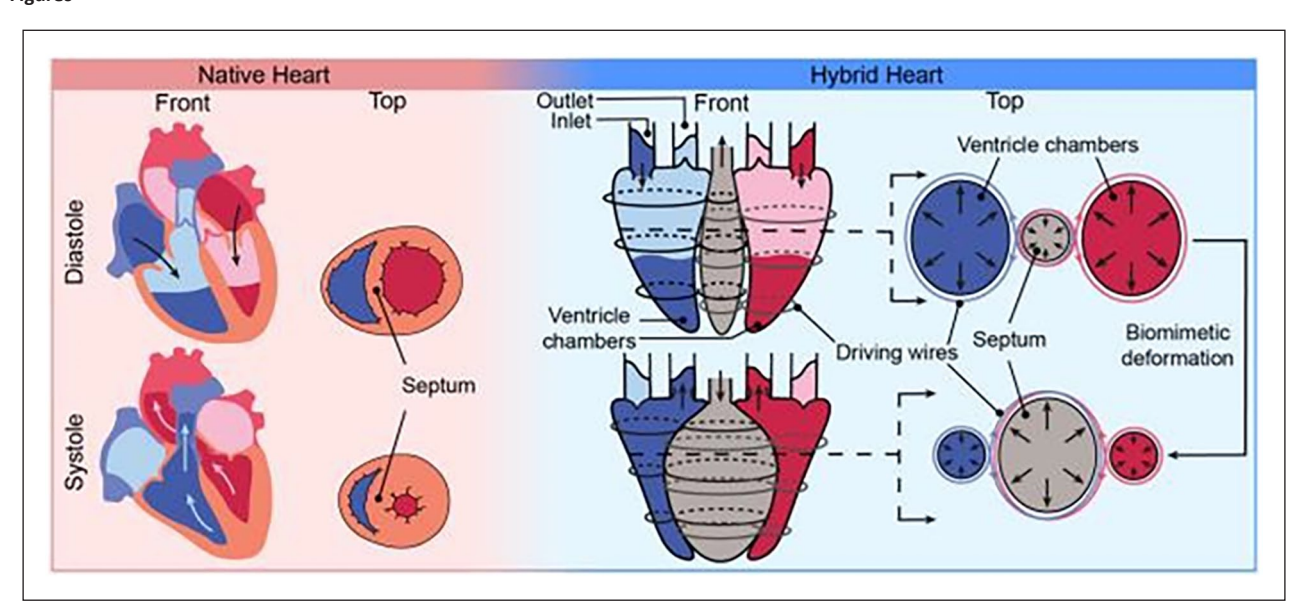


Figure 1. The Hybrid Heart concept.

References

- 1. Bragazzi NL et al. Europ J Prev Card. 2021;28(15).
- 2. Tatum R et al. Heart Fail Rev. 2022;27(5):1819-27.
- 3. Tsao CW et al. American Heart Association. Circulation. 2022;145(8).

Acknowledgements

This work is under review in nature communications journal. The project is initiated within Hybrid Heart consortium funded by European union Horizon 2020 research and innovation programme and being continued within Holland Hybrid Heart consortium, funded by NWA-ORC and Hartstichting.

DRIVE TRAIN DESIGN FOR ADVANCED PERCUTANEOUS VENTRICULAR ASSIST DEVICES: INSIGHTS FROM ENGINEERING

Thomas George Logan ¹, Chiahao Hsu¹, Ifan Yen¹, Tingting Wu ^{1,2}, Mengjie Liu ¹,Jamshid H. Karimov ¹, Po-Lin Hsu ^{1,2}

¹magAssist Co., Ltd., Suzhou, China; ²Artificial Organs Technology Lab, School of Mechanical and Electrical Engineering, Soochow University, Suzhou, China

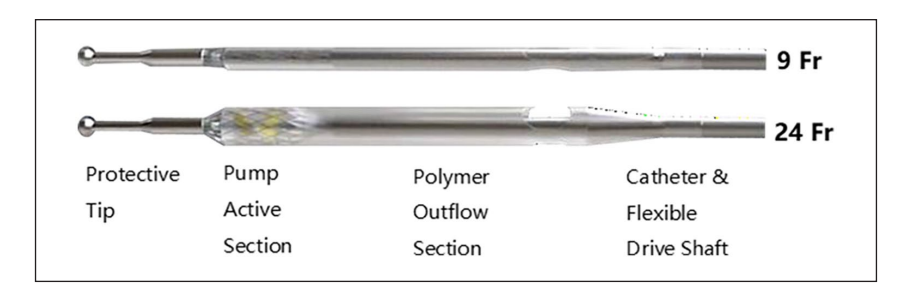


Figure 1. NyokAssist™ pVAD foldable pump structure, 9 Fr folded insertion state (top) and 24 Fr expanded operation state (bottom).

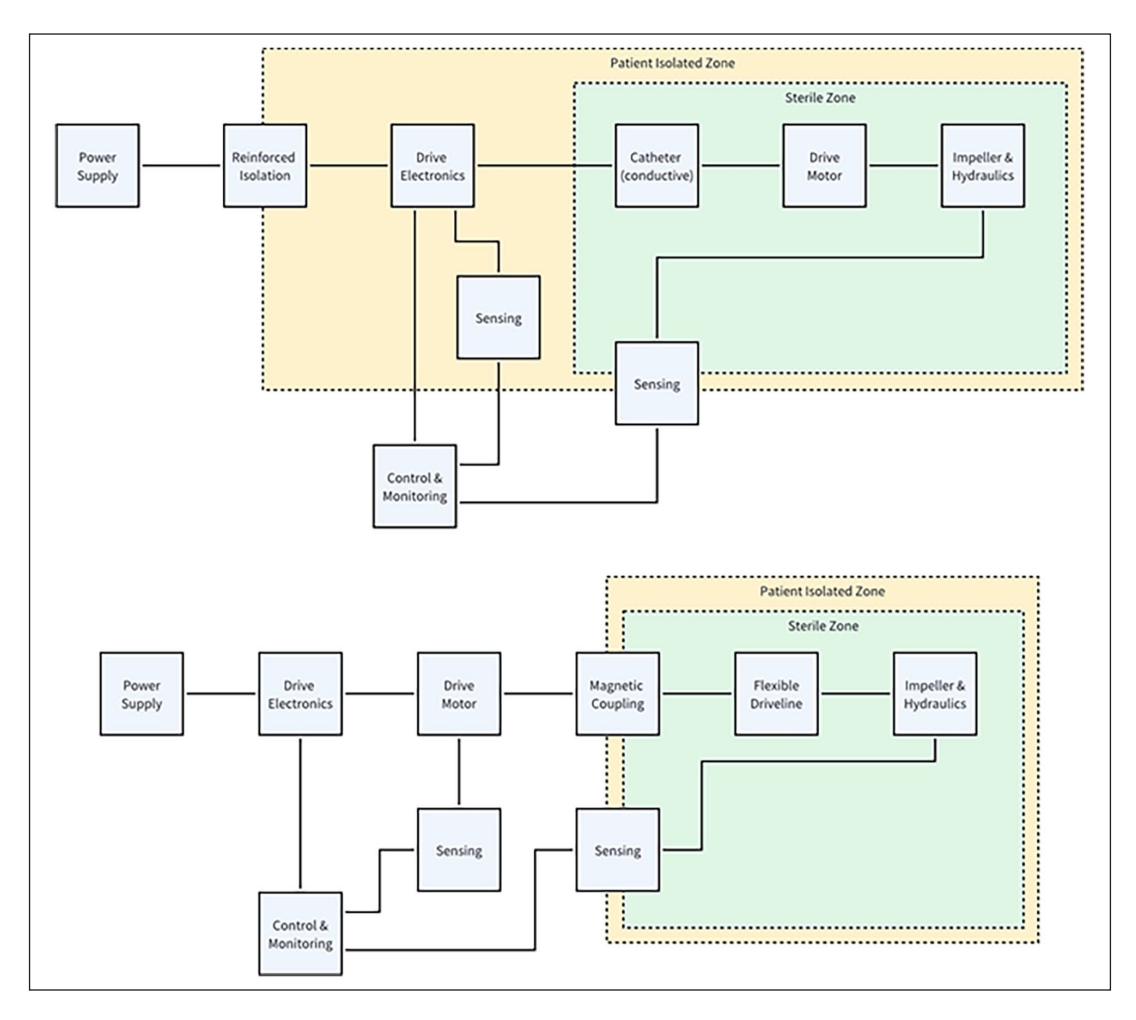


Figure 2. Drive system of a typical internal drive pVAD (top) and external drive pVAD.(bottom).

Introduction: Percutaneous Ventricular Assist Devices (pVADs) are an effective therapeutic option for short-term mechanical circulatory support due to their simple and minimally invasive insertion. Recent trends suggest smaller insertion diameters, in the order of 9-10 Fr, that enable the avoidance of surgical cutdown. The NyokAssist™ (magAssist Co. Ltd., Suzhou, China) is a commercially developed pVAD that initially targets support of patients undergoing high-risk percutaneous coronary interventions (HRPCI). The device is currently undergoing its clinical trial [1].

Methods: Reduction of the insertion diameter impacts on the pump's impeller design, in most cases necessitating a foldable design (figure 1). It also generally prevents the use of the simple drive system based on a motor internal to the patient, as is used in most of the first generation pVADs. Placing the motor outside the patient and transmitting the

rotational power to the internal impeller using a mechanical method such as a rotating flexible shaft overcomes the insertion size problem but at the expense of a much more complicated drive system.

Ultimately the drive system must deliver sufficient torque to the impeller whilst achieving the required speed, insertion size, sealing capability, temperature rise, electrical safety, lifetime, reliability and cost. Solutions driven by internal motors, external single use motors and external reusable motors, and sealed using direct-drive, sliding seals and various types of magnetic couplings can achieve these requirements to different extents. An overview is provided of the drive system strategies that may be deployed (examples in figure 2), performance details of the key components, and their relative advantages and disadvantages, referenced to the example of the NyokAssist™ pVAD.

Results: The reusable external motor drive system used in the NyokAssist™ pVAD permits it to deliver 3.5lpm flows with a 9 Fr insertion size, and do so cost effectively. At time of writing the device has completed 50% of its clinical trial, with demonstrated good performance.

Discussion: A variety of solutions are available as drives for pVADs; their various strengths and weaknesses must be carefully considered to deliver the solution that maximizes benefit to the patient.

References

 R. Wang et al, J American College of Cardiology, 84 (18_Supplement) B213, 2024.

Acknowledgements

This work is sponsored by magAssist Co., Ltd.

CUSTOM DESIGN AND OPTIMIZATION OF VENTRICULAR ASSIST DEVICES FOR LEFT VENTRICLE SUPPORT

Canberk Yıldırım¹, Kağan Uçak², Ali Madayen³, Kerem Pekkan¹

¹Koc University, TR; ²University of Southern California, USA; ³Middle East Technical University, TR

Introduction: Usage of computational tools has become popular in the design and development of ventricle assist devices (VADs) since the 2000s. Recently, computational fluid dynamics (CFD) is the primary tool which provides significant insight on pump hydrodynamic and hemolysis performance. However, this method is mostly based on a trial- error approach requires multiple design cycles to reach an optimal design. Therefore, we introduce a novel approach to improve the pump design process through a patient-specific, target-based lumped parameter model (LPM) tool [1]. By integrating cardiovascular hemodynamics into the optimization process and using an advanced turbomachinery equation, our tool offers a promising, efficient method for optimizing pump performance prior to detailed CFD analysis.

Methods: U.S. Food and Drug Administration (FDA) benchmark pump was chosen as the baseline VAD to be optimized. Acute left ventricle (LV) failure was imposed to the LPM by modifying the LV chamber compliance in the network. FDA pump was improved for LV failure to achieve the same cardiac output (*CO*) and mean aortic pressure (*Pao*), yet with a lower blade tip velocity (*Vtip*), which is the main objective for an improved blood damage performance in this study. Different from the quadratic curves used to model VADs in literature, a parametric approach including all main design dimensions was utilized for the pump modeling:

$$\Delta P_{pump} = \rho (w^2 r 2^2 - w^2 r_1^2) - Q_{pump} \frac{\rho w r_2}{\tan \beta \left(2\pi r_2 b_2 - \frac{tbl, 2}{\sin \beta} \right)} - \Delta P_{loss}$$
 (1)

where 1 and 2 indices represent the inlet and outlet of the pump, respectively. Table 1 shows the design parameters used in Equation (1). Genetic algorithm was used for the optimization and generated pumps at each iteration were compared based on the weight of each target parameter (*Pao*, CO and Vtip) for convergence

Results:

Table 1. Main design parameters to be optimized.

β – Blade angle	<i>r</i> – Impeller radius
b – Blade width	zbl – Blade number
tbl – Blade thickness	Qpump –Flow rate
$\Delta Ppump$ – Actual head	$\Delta Ploss$ – Pump loss

Discussion: Our results showed that the same CO and Pao with the FDA

Table 2. Target parameters of baseline FDA and optimized pumps. Pao: mmHg, CO: I/min, Vtip: m/s.

Target	Healthy	Failure	FDA	Opt
Pao	119/63(92)	88/47(67)	92	92
CO	5.2	3.75	5.2	5.2
Vtip	n/a	n/a	6.8	4.75

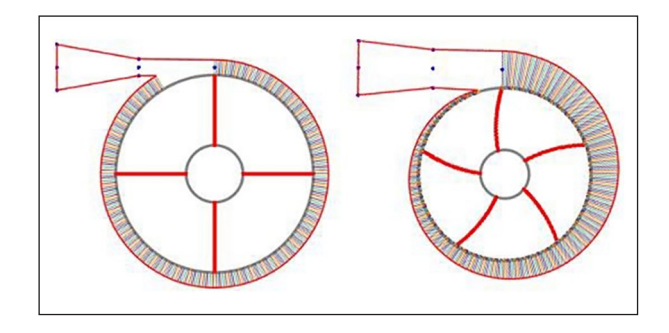


Figure 1. 2D sketches comparison of the baseline FDA (left) and its optimized version (right)

pump can be obtained via the optimized design with the ~30% lower blade tip velocity. The characteristic curve of the optimized pump was also validated through CFD simulations, which showed a lower hemolysis index. Although the blade tip velocity was chosen for this abstract, the developed tool can optimize a wide range of other hemodynamic and design parameters including lower thrombogenicity, target endorgan hemodynamics like coronary/cerebral flow, hepatic/renal conditions and oxygen saturation levels, which will be presented during the conference. Therefore, it is estimated that the proposed model has potential to shorten the traditional pump design approach by providing the main dimensions preliminary before the detailed CFD investigations based on the desired targets.

References

1. Sisli et al, Ann Biomed Eng, 12: 2853-2872, 2023.

4A: ADVANCES IN HEART PUMP TECHNOLOGY: INNOVATIONS AND FUTURE DIRECTIONS 2

THE ONCE AND FUTURE MINIATURE PEDIATRIC, FULLY MAGLEV, AXIAL FLOW VAD

James F Antaki PhD¹, Scott Stelick¹, Joaquin Araos DVM², Michael F Swartz PhD³, Shuichi Yoshitake MD³, Gillian A. Perkins DVM², Salim E. Olia PhD⁴, Mansur Zhussupbekov PhD¹, Rachel Havriliak¹, Jingchun Wu PhD⁵, Josiah Verkaik⁶, Rugveda Thanneeru⁶, Shaun Snyder, Viswajith Siruvallur Vasudevan, PhD¹, Yves D'Udakem, MDⁿ, Harvey S. Borovetz, PhD⁶

¹Meinig School of Biomedical Engineering, Cornell University, Ithaca NY USA; ²Cornell College of Veterinary Medicine, Ithaca, NY, USA; ³University of Rochester Medical Center, Department of Surgery; University of Pennsylvania, Philadelphia, PA, USA; ⁵Advanced Design Optimization, LLC, USA; ⁶Verkaik Innovation, LLC, Boise Idaho, USA; ⁷Children' National Hospital, USA; ⁸University of Pittsburgh, Pittsburgh, PA, USA



Figure 1. PediaFlow PF5 & trumpet cannula.

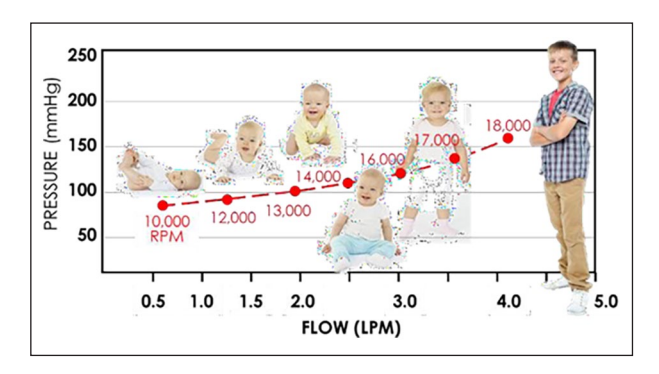


Figure 2. Hemodynamics of PF5.11HF.

Introduction: The PediaFlow™ is a miniature, fully-magnetically- levitated, implantable pediatric VAD intended for extended support in neonates, infants, and adolescents. Its design is derived from the Streamliner™ maglev axial-flow VAD and has evolved through multiple generations to decrease size and improve flow capacity. This report describes progress with the intended clinical, fifth generation, PF5, that operates over a wide range of flow to accommodate the growing child (see Figures 1 & 2).

Methods: Following the latest improvements in the flow path through CFD optimization and in-vitro validation with blood, the PediaFlow (PF5.11HF) was implanted in a sheep, cannulated from left ventricular apex to descending aorta, and operated at 1.2 LPM for 7 days. Anticoagulation was provided by heparin drip to maintain activated clotting time (ACT) near baseline.

Results: Optimization of the flow path by computational fluid dynamics (CFD) was able to increase the maximum output from 1.5 LPM (PF4) to 3.5+ LPM (PF5), with commensurate increase of hydraulic efficiency from 27% to 34%. The inflow and outflow diameters were increased slightly from 5 mm to 6 mm; however, the overall size of the pump was reduced from 17.6 to 14.9 cc displacement. (See Figure 1.) In-vitro Normalized Index of Hemolysis (NIH) remains below 0.01 mg/dL, comparable to PF4.

Postmortem examination of the blood-contacting surfaces was unremarkable and free from adherent thrombus. However, the root of the inflow cannula within the ventricle developed a layer of adherent pannus. PfHb remained under 5 mg/dL throughout the duration, with the exception of an outlier on POD 2 of 7 mg/dL. vWF functional assay fluctuated +/-20% of baseline over the duration of the study. Platelet activation via CD62P expression remained near baseline. End organ function was preserved, and postmortem examinations of the kidneys were unremarkable.

Discussion: A 7-day in-vivo trial of the PediaFlow PF5 demonstrated satisfactory freedom from blood trauma and thrombosis on the blood-contacting surfaces and end organs. Ongoing preparation during the next 12-months in anticipation of first-in- human study involves: manufacturing PediaFlow pumps under GMP requirements and performing chronic (30-day) in-vivo studies. Parallel efforts include development of a miniaturized clinical-use control unit and conducting human factors design for infants and young children, at home.

MODULAR AND VERSATILE THREE-DIMENSIONAL CARDIAC CHAMBER PLATFORM FOR VOLUMETRIC PERFORMANCE MEASUREMENTS

Jana Hecking^{1*}, Mariel Cano Jorge^{1*}, José M. Rivera-Arbeláez^{1,2*}, Danique Snippert¹, Simone Ten Den¹, Anne Braam¹, Loes I. Segerink³, Andries D. van der Meer¹, Robert Passier^{1,3}

¹Applied Stem Cell Technologies, Department of BioEngineering Technologies, TechMed Centre, University of Twente, Enschede, the Netherlands; ²BIOS Lab-on-a-Chip Group, MESA+ Institute for Nanotechnology, Max Planck Institute for Complex Fluid Dynamics, University of Twente, Enschede, the Netherlands; ³Department of Anatomy and Embryology, Leiden University Medical Centre, Leiden, the Netherlands; *Equally contributing authors

Introduction: Engineered three-dimensional (3D) cardiac models have emerged as tools for modeling human (patho-) physiology *in vitro*. Despite their advantages, platforms such as organoids, heart-on-chips, and engineered-heart-tissues cannot replicate the heart's fluid-pumping functionality. To address this challenge, a few cardiac chambers have emerged. While providing a more accurate visual depiction of the heart, these models are capable of fluid- pumping and allow monitoring of hemodynamic metrics. However, their fabrication often relies on complex methods, such as 3D bioprinting and nanotechnology-based scaffolds, which aim to replicate the heart's biological properties [1,2,3]. These approaches, while innovative, lack standardization and scalability, constraining their potential for disease modeling and drug screening.

Objective & Methods: We propose a 3D cardiac chamber platform designed to balance biological complexity with scalability and reproducibility through means of modularity. The platform is compatible with a 12- well plate format. Fabrication of cardiac chambers involves a streamlined three-step process. In the final step, an extracellular matrix mix containing human pluripotent stem cell-derived cardiomyocytes and human cardiac fibroblasts is introduced into the cavity between two molds (figure 1).

Results & Discussion: We have successfully fabricated 3D cardiac chambers in the platform and evaluated performance during spontaneous beating and under electrical stimulation. The 3D cardiac chambers exhibited robust contractions, consistently followed electrical pacing at 2 Hz, and maintained functional activity for over 30 days. Furthermore, cardiac chambers demonstrated fluid-pumping function. Future work will focus on quantification of volume displacement and enhancing biological fidelity. Consequently, this platform will provide new avenues for drug testing and disease modeling applications.

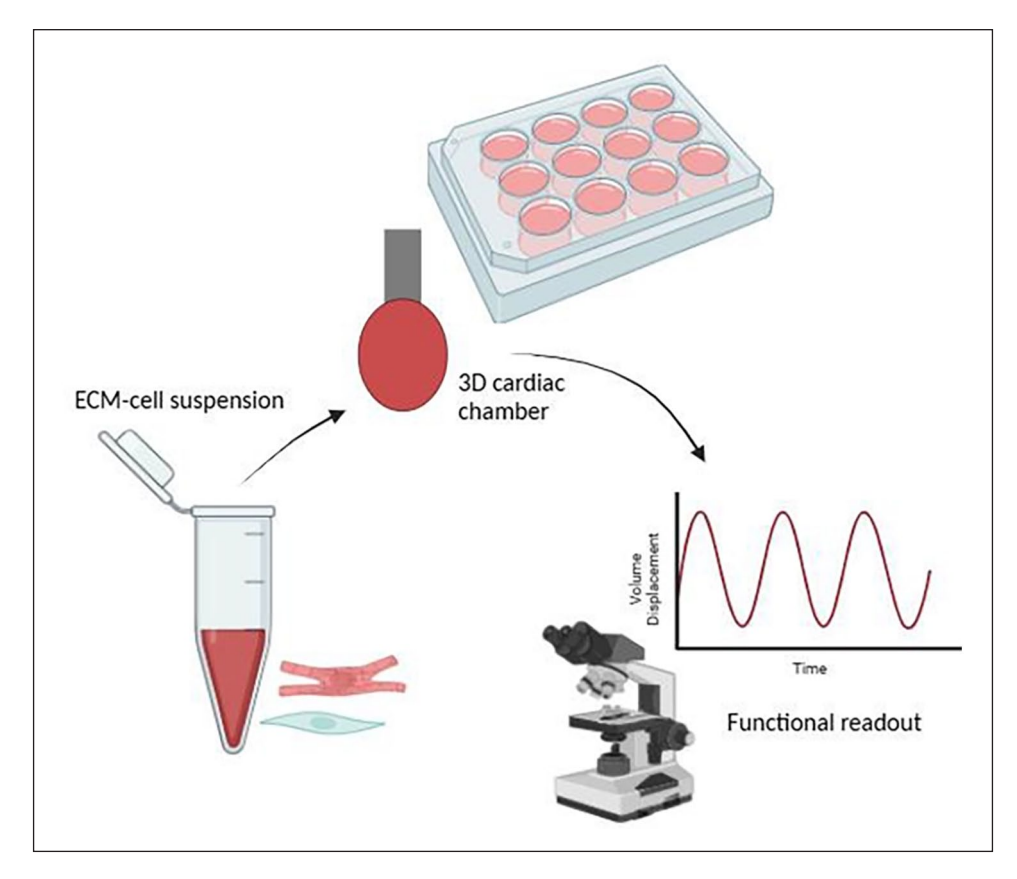


Figure 1. Process flow of 3D cardiac chamber fabrication, culture, and data acquisition.

References

- 1. Kupfer et al, Circ Res, 127(2) 207-224, 2020.
- 2. Chang et al, Science, 377 180-185, 2022.
- 3. Michas et al, Sci Adv, 8(16), 2022.

Acknowledgements

This work is supported by ERC Advanced grant Heart2Beat, Nederlandse Organisatie voor Wetenschappelijk Onderzoek (OCENW.GROOT.2019. 029), and Netherlands Organ-on-Chip Initiative, an NWO Gravitation project (024.003.001). The figure was made using BioRender.

NYOKASSIST™ PERCUTANEOUS TRANSVALVULAR VENTRICULAR ASSIST DEVICE PERFORMANCE IN HIGH-RISK PERCUTANEOUS CORONARY INTERVENTION

Thomas George Logan¹, Tingting Wu^{1,2}, Zheng Lin¹, Huaizheng Ma¹, Chiahao Hsu¹, Ifan Yen¹, Mengjie Liu¹, Jamshid H. Karimov¹, Po-Lin Hsu^{1,2}

¹magAssist Co., Ltd., Suzhou, China; ²Artificial Organs Technology Lab, School of Mechanical and Electrical Engineering, Soochow University, Suzhou, China

Introduction: The NyokAssist™ (magAssist Co. Ltd., Suzhou, China) is a novel transvalvular percutaneous Ventricular Assist Device (pVAD) intended for high-risk percutaneous coronary interventions

(HRPCI) procedures. The pump's unique structure allows it to fold to a 9 Fr diameter during insertion, enabling a rapid, non-surgical procedure through femoral access over a guidewire. Herein, we report the early clinical use of this technology.

Methods: The device self-expands in the descending aorta and is placed across the aortic valve (Figure 1). The device expands to a moderate 24 Fr diameter for operation, maximizing the patient inclusion criteria. Development of the product has been completed, and the device entered the prospective, multi-center randomized control clinical trial (Q4 2024) to assess the safety and efficacy of the NyokAssist™ in supporting patients undergoing HRPCI procedures, with the intra-aortic balloon pump (IABP) as the comparison device. The trial aims to compare patients with the primary endpoint of being free of major adverse cardiovascular and cerebrovascular events 30 days post-PCI.

Results: The pump design is completed; careful optimization enabled the device to deliver 3.5 LPM flow with only a modest 18-25 KRPM operating speed. This low speed greatly assists in minimizing hemolysis. Data for the first (pVAD, n=10; IABP, n=10) patients have been analysed [1]. There were no adverse events in the NyokAssist™ cohort. All devices performed according to design specifications, and no safety concerns were observed.

Discussion: The pVAD clinical trial is ongoing, with almost half the patients now enrolled. This presentation will provide an update on the latest findings of the clinical trial, providing practical insights into the device's performance. It will also share some of the clinicians' key insights regarding device use in high-risk percutaneous coronary interventions.

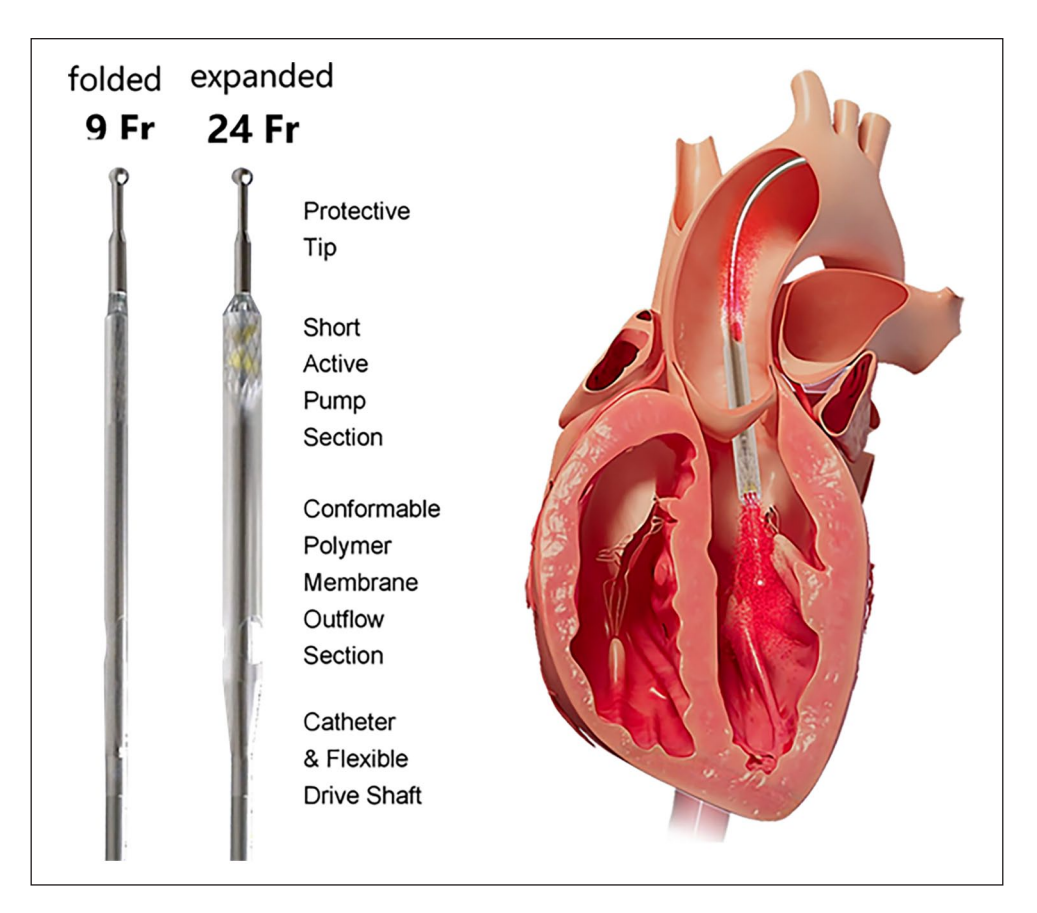


Figure 1. NyokAssist™ pVAD pump structure (left) and operating location when deployed (right).

References

 R. Wang et al, J American College of Cardiology, 84 (18_Supplement) B213, 2024.

Acknowledgements

This work is sponsored by magAssist Co., Ltd.

A PASSIVE BEATING HEART MOCK-LOOP WITH AN UNPUNCTURED NATURAL HEART TO ENABLE CARDIAC DEVICE TESTING

Isabell Schulz^{1,2}, Tim Bierewirtz^{1,2}, Vera Froese^{1,2}, Michael Lommel^{1,2} and Ulrich Kertzscher^{1,2}

¹ Deutsches Herzzentrum der Charité, Institute of Computerassisted Cardiovascular Medicine, Biofluid Mechanics Laboratory, Augustenburger Platz 1, 13353 Berlin, Germany; ² Charité – Universitätsmedizin Berlin, corporate member of Freie Universität Berlin and Humboldt Universität zu Berlin, Charitéplatz 1, 10117 Berlin, Germany.

Introduction: Implantable cardiovascular devices require assessment before proceeding to animal studies and clinical trials to confirm their functionality and effectiveness. Mock circulation loops (MCLs) are versatile tools designed to replicate *in vivo* physiological conditions and serve as essential tools for preliminary testing. A multifunctional passive beating heart mock-loop connected to a porcine heart has been developed to mimic the natural movement of the heart.

Methodes: The operating principle of the *in vitro* MCL is to drive the movement of the ventricular walls throughout the cardiac cycle,

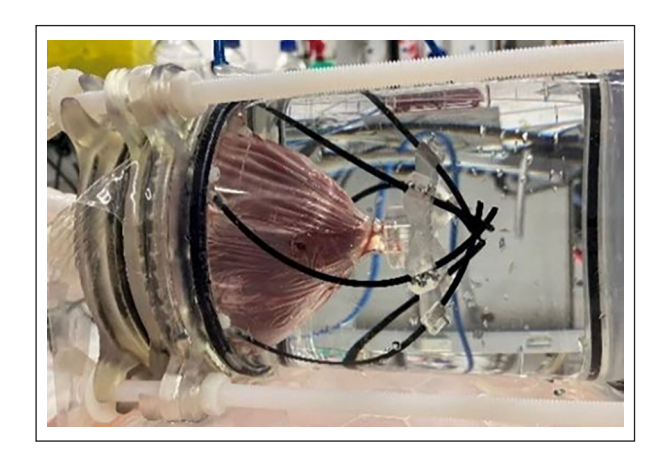


Figure 1. Fluid filled chamber with a porcine heart

mimicking the pulsatile pumping function of the heart. To achieve this, the system pressurizes the ventricles while excluding the atria from external loads. The system consists of a fluid-filled chamber that houses the ventricles and is sealed to isolate the atria from external loads. The heart is held in place by applying a vacuum between two thermally molded polyurethane foils. The thermoformability of the foils allows the mock-loop to handle the high variability of the hearts. In between those foils a vacuum is generated. The chamber with the integrated heart is shown in Figure 1. The chamber is connected to a computer-controlled piston pump that cyclically injects and withdraws fluid in and out of the chamber, hence directly actuating the ventricular walls. The atriae and the large arteries are connected to the two circuits (cardiac and

pulmonary circulation) with silicone tubes and 3D-printed connectors. Each circuit consists of an open and a closed reservoir, a pressure sensor, a flow sensor, and a resistor.

Results: The MCL mimicked the natural movement of the heart with the opening and closing of the heart valves adequately. In the systemic circulation, pressures between 92 mmHg and 72 mmHg were reached at mean flow rates of 1.7 l/min. In the pulmonary circulation, pressures between 7 mmHg and 24 mmHg were achieved at mean flow rates of 2.7 l/min. The flow rates and pressures are shown in Figure 2.

Discussion: The passive beating heart mock-loop mimics the cardiac flow rates and pressures adequately. A key technical challenge—securely fixing the heart—was addressed with two thermally moulded foils between which a vacuum is applied, providing a simple, efficient, and reliable solution for sealing and mounting while enabling physiological ventricular stroke volumes. Combined with the integrated hydraulic

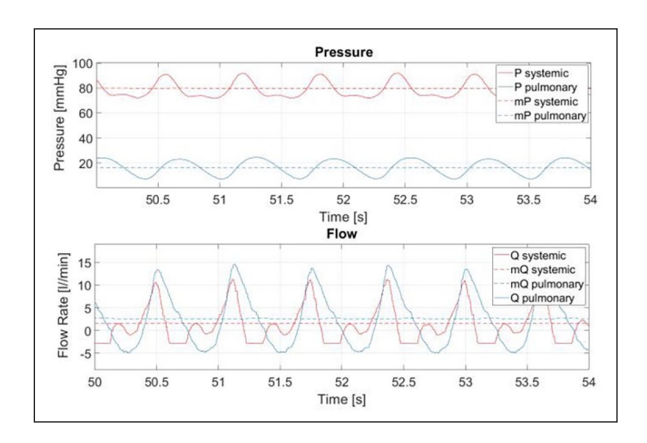


Figure 2. Recorded pressures and flow rates.

modules, this MCL achieves appropriate hemodynamic conditions in the setup, however with regurgitations that might be attributable to valve defects. Further improvements to the mock-loop are required and will be implemented in the coming months.

Acknowledgements

This project is co-financed by the European Regional Development Fund (ERDF).

MODULAR INTEGRATION IN MECHANICAL CIRCULATORY SUPPORT: A UNIFIED PLATFORM FOR MULTI-INDICATION CARE

IFan Yen¹, Kynan Taylor⁴, Xianshan Qi¹, Jialiang Zhang¹, Tingting Wu^{1,2}, Graeme Marshall⁴, Rachel Hook⁴, Justin Yuan⁴, Thomas George Logan¹, Chiahao Hsu¹, Jamshid H. Karimov^{1,3}, Po-Lin Hsu^{1,2}

¹magAssist Co., Ltd., Suzhou, China; ²Artificial Organ Technology Lab, School of Mechanical and Electrical Engineering, Soochow University, Suzhou, China; ³on behalf of Medical Advisory Board; ⁴Cobalt Design Pty Ltd, Melbourne, Australia

Introduction: In clinical settings, the critically ill are surrounded by numerous devices, including mechanical circulatory support (MCS) systems. Accompanied by complex wiring, tubing, and user interfaces, these systems pose significant challenges to operational efficiency and patient safety. We developed an integrated, user-friendly system adaptable to variable, complex clinical scenarios and emergency environments, consolidating multiple devices into a single platform.

Methods: Proprietary modular "Life Support Platform" (magAssist, Suzhou, China) was designed and tested in intensive care units (ICU), emergency departments (ER), and cardiovascular departments. Surveys

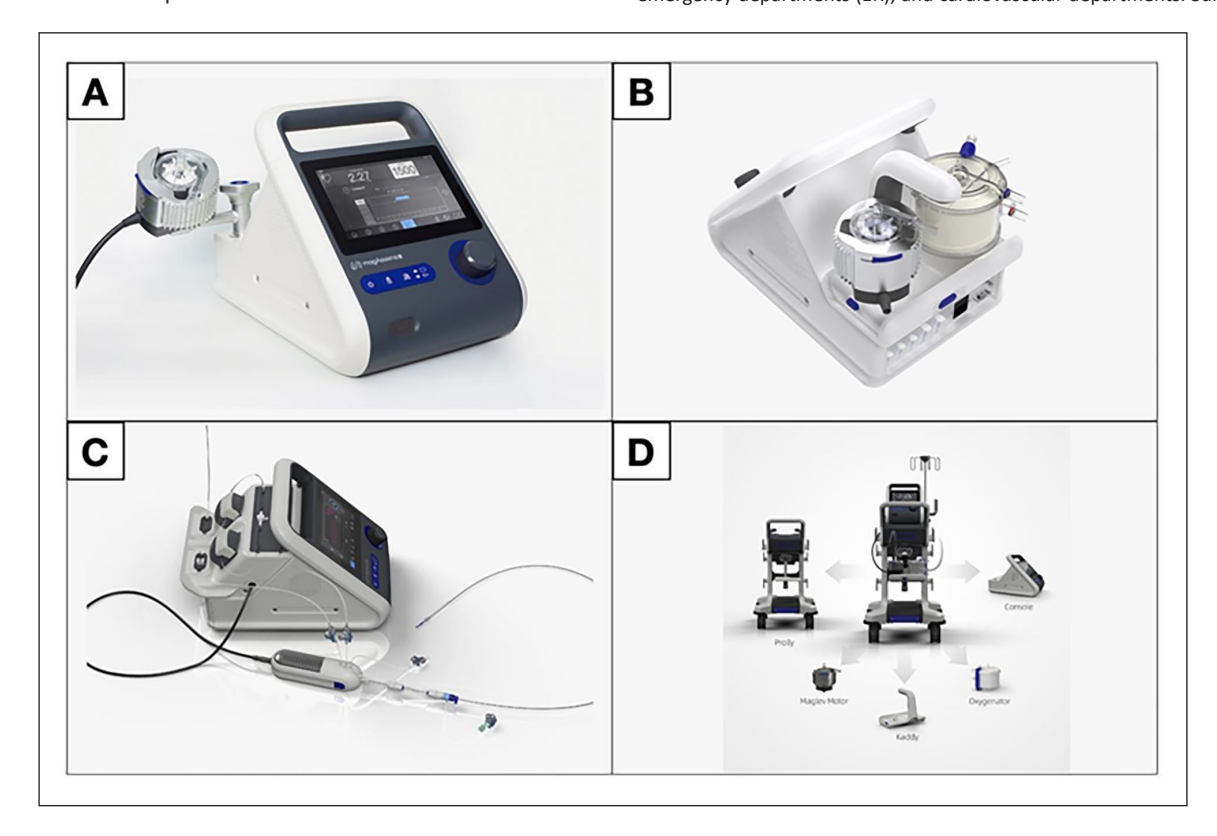


Figure 1. Modular platform architecture.

were conducted at 21 centers (clinical experts and nursing staff, n=39), focusing on functional requirements, environmental adaptability, alert systems, and user interfaces. Data included (Kano model) industrial design analysis and iterations of complex functionalities into a coherent design, validated through usability studies.

Results: The modular platform architecture (Fig. 1) supports three configurations: (Fig. 1A) an extracorporeal ventricular assist system with a magnetic levitation motor and adjustable support arm, (Fig. 1B) an ECMO system incorporating a modular oxygenator and pump, and (Fig. 3C) a catheter-based ventricular assist system featuring a flushing pump system, a drive motor, and a catheter pump head. Weight ranged from 10 to 20 kg based on levels of portability. Usability studies and clinical trials testing confirmed its intended adaptability and effectiveness across ICU, ER, and cardiovascular settings.

Discussion: The proposed "Life Support Platform" modular platform was successfully performed in diverse clinical indications, such as acute cardiogenic shock, pulmonary failure, and high-risk percutaneous coronary intervention. Well-received by clinical and nursing experts, the benefits of modular design have been demonstrated to improve device-based care efficiency, reduce costs, and optimize healthcare practices.

Acknowledgements

This study was funded by magAssist Co., Ltd., Suzhou, China.

4B: BIOMATERIALS AND ORGAN MODELS

DEVELOPMENT OF A PERFUSABLE 3D BIOPRINTED SKIN EQUIVALENT ON A MILLIFLUIDIC CHIP PLATFORM

Monika Belak¹, Lidija Gradišnik¹, Uroš Maver^{1, 2}, Boštjan Vihar¹, Jernej Vajda^{1, 2}, Tanja Zidarič¹, Tina Maver² ¹Institute of Biomedical Sciences, Faculty of Medicine, University of Maribor, Maribor, Slovenia; ²Department of Pharmacology, Faculty of Medicine, University of Maribor, Maribor, Slovenia

Introduction: This study presents the development of a perfusable 3D bioprinted skin equivalent integrated with a cost-effective and customizable millifluidic chip platform. The platform addresses key limitations of static skin cultures, including inadequate nutrient supply, inefficient waste removal, and limited viability [1], which are enabling dynamic microenvironmental control. This innovative system aims to provide a physiologically relevant and robust model for advanced skin research, drug testing, and tissue engineering.

Methods: The millifluidic chip was designed using CAD software and fabricated via photopolymerization- based 3D resin printing (digital light processing). Key design features include compatibility with P6 well plates, precise manufacturing tolerances, direct 3D bioprinting support, and integration with an external perfusion system for continuous nutrient and waste exchange. The dermal layer was bioprinted directly into the chips using an alginate-cellulose hydrogel scaffold embedded with skin fibroblasts (hSF). At the same time, Pluronic F127, as a sacrificial ink, formed placeholders for internal vasculature. Perfusion was initiated to maintain scaffold stability and aseptic conditions. After one week, keratinocytes (HACAT) were seeded onto the dermal construct and cultured under continuous perfusion for three additional weeks to promote cell stratification and maturation.

Results: Out of the tested designs, the cylindrical chip insert compatible with P6 multi-well plates was the most effective. The chip's main frame seamlessly interfaced with the external perfusion circuit and the culture chamber, enabling precise and continuous nutrient and waste exchange. The bioprinted skin equivalent exhibited strong integration with the chip system, maintaining aseptic conditions and stable perfusion over four weeks without seal failures or microbial contamination. Live/Dead staining at predetermined intervals confirmed sustained fibroblast viability

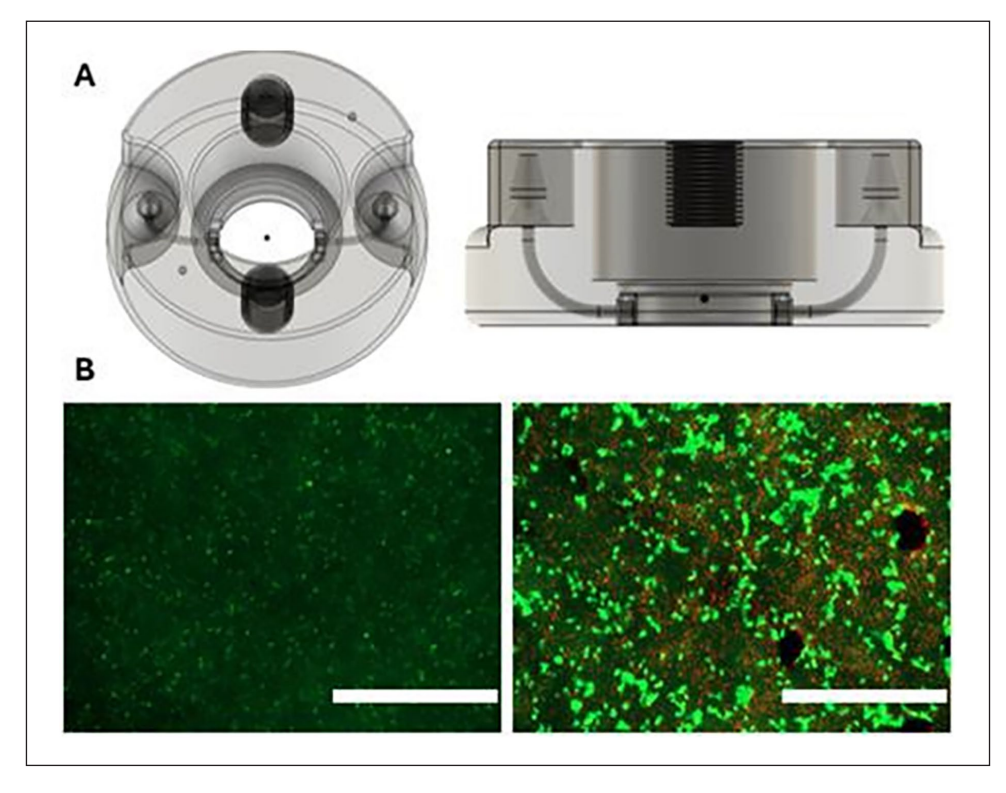


Figure 1. A) Millifluidic chip design (Fusion360). Live/Dead staining images of the dermal (left) and epidermal (right) layers after 2 weeks of cultivation (scale bar = $1000 \mu m$).

within the dermal layer. It demonstrated the successful formation of a viable keratinocyte monolayer on the scaffold surface after two weeks of cultivation.

Discussion: The millifluidic chip platform supports the long-term cultivation of a 3D bioprinted skin equivalent, providing a dynamic and physiologically relevant model for advanced skin research and biomedical applications. Its scalability, cost-effectiveness, and customizability make it an ideal tool for drug testing, toxicity studies, and tissue engineering applications. We are currently working on the optimization of the system for full-thickness skin models with vascularized networks.

References

1. Zidarič et al, Springer Cham. 156 p., 2023.

Acknowledgements

The authors acknowledge the financial support from the Slovenian Research Agency for Research Core Funding No. P3-0036, and for projects Nos. L7-4494, N1-0305, the Young Researcher Program and New Harvest foundation.

SURFACE MICROPATTERNING TO IMPROVE ENDOTHELIALISATION FABRICATED VIA 2-PHOTON POLIMERISATION 3D PRINTER

Marta Bonora^{1, 2}, Christian Grasl^{1, 2}, Barbara Messner³, Francesco Moscato^{1, 2, 4}

¹Center for Medical Physics and Biomedical Engineering, Medical University of Vienna, Austria; ²Ludwig Boltzmann Institute for Cardiovascular Research, Austria; ³Department of Cardiac and Thoracic Aortic Surgery, Medical University of Vienna, Austria; ⁴Austrian Cluster for Tissue Regeneration, Austria;

Introduction: Ventricular assist devices (VADs) are a standard treatment for heart failure. However, at the inflow cannula (IC), hemocompatibility issues arise due to endothelial damage and regions of blood stasis. Endothelialization of artificial surfaces is extensively investigated as a potential solution, but a definitive strategy has yet to be established. Surface micropatterning may stimulate controlled cell proliferation. In this study, we employed, for the first time, a two-photon polymerization (2PP) printing strategy to fabricate high-resolution micropatterns. These micropatterned surfaces will be integrated into a microfluidic system designed to mimic the conditions at the VAD inflow cannula.

Methods: Microfluidic chip was designed with three microchannels micropatterned with riblets of three different sizes (Large, Medium, Small; Figure 1E) on half of its width, while the remaining half is flat as a control (Figure 1A–D). The master for the chip was printed via 2PP, using two photosensitive materials—Upbrix and Up-photo from Upnano GmbH—across three printing modes (conservative, simple, voxel) and three laser power settings (low, medium, high).

The master was replicated in polydimethylsiloxane (PDMS; Sylgard 184). The quality of the printing was verified using microscopy and profilometry techniques.

Results: Uphoto yielded clean, sharply defined prints with minimal post-polymerization debris and was therefore chosen over Upbrix. Figure 2 shows the results for small riblets. The voxel mode (Figure 2G–I) performed better than the other modes, while variations in laser power did

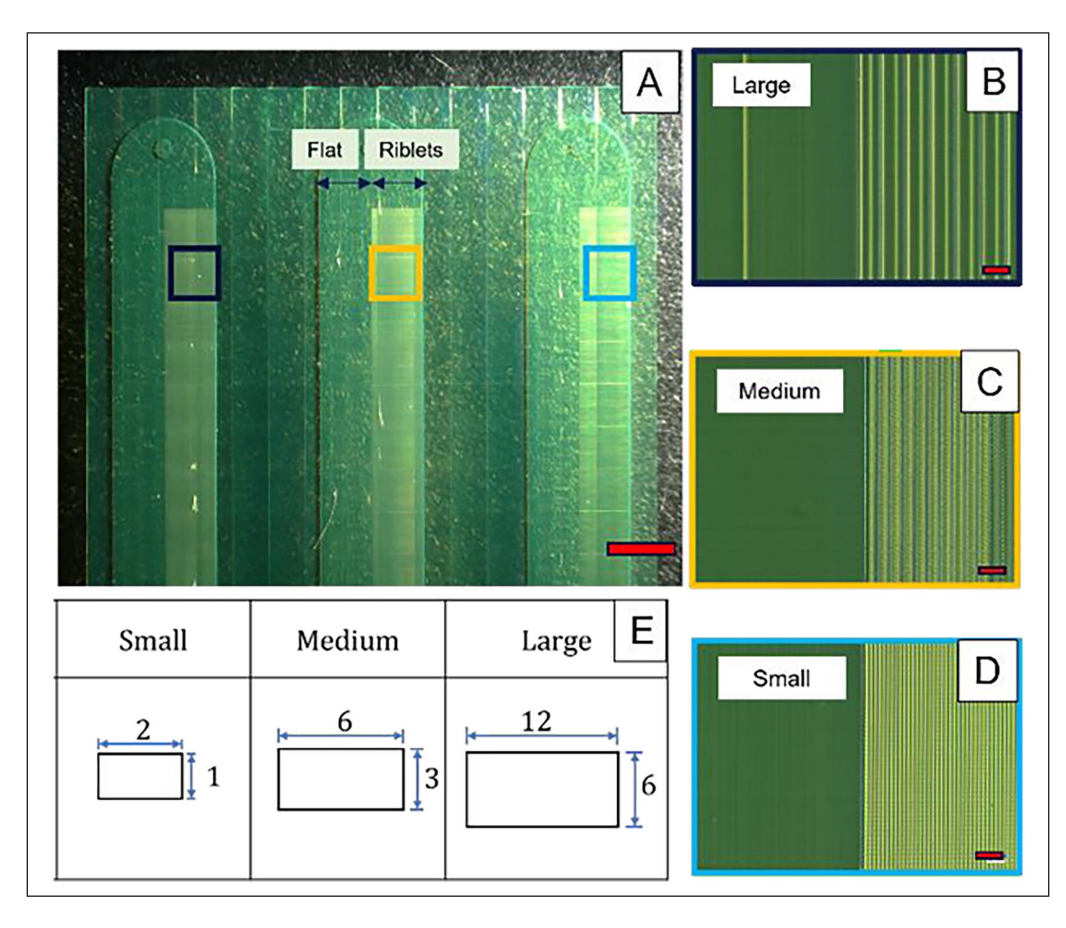


Figure 1A. 2PP master, scale 1 mm - 1B-D respectively flat and large, medium, small riblets magnification, scale 20 μ m - 1E technical drawings of the cross section of the riblets, all the dimensions are in μ m.

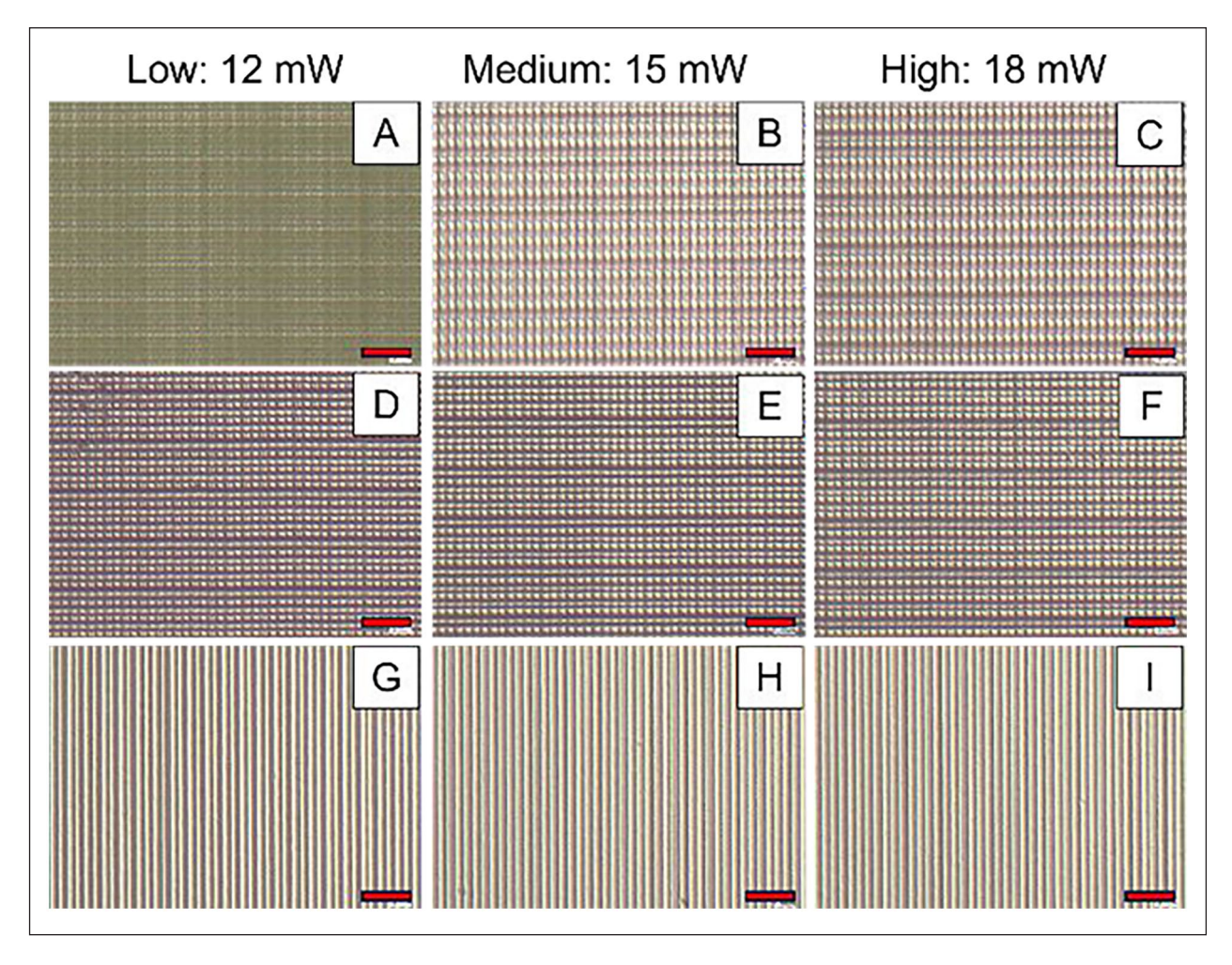


Figure 2A-C. conservative mode - 2D-F simple mode - 2G-I voxel mode; scale 10 μm.

not result in visible differences. Profilometry analysis demonstrated that the riblets achieved the intended height.

Discussion: High precision printing is the first step to get reliable results during cells culture. The next stage of this work will focus on optimizing the PDMS molding process and evaluating endothelialization of the micropatterned surfaces under microfluidic conditions.

Acknowledgements

Funded by FFG: Optiflow 3D (Nr. 891239) and M3dRES (Nr. 858060).

THE CRUCIAL IMPACT OF ANALYZED AREA IN OPTICAL HEMOCOMPATIBILITY EVALUATION

Johanna C. Clauser¹, Judth Maas¹, Jutta Arens¹, Ulrich Steiseifer¹, Benjamin Berkels^{2, 3}

¹Department of Cardiovascular Engineering, Institute of Applied Medical Engineering, Medical Faculty, RWTH Aachen University, Germany; ²AICES Graduate School, RWTH Aachen University, Germany; ³Institute for Geometry and Practical Mathematics, RWTH Aachen University, Germany

Introduction: Hemocompatibility remains a major challenge for blood-contacting artificial organs. Additionally, in- vitro hemocompatibility

assessments lack standardization. A common approach for material evaluation after in-vitro blood contact involves optical analysis of platelet adhesion and activation, but no standardized workflows exist for platelet quantification or microscopy techniques. As a result, manual or semi-manual analysis of a small sample fraction – often less than 1 % of the total material area – has become standard practice.

We hypothesize that such small area fractions do not accurately represent platelet adherence, leading to invalid hemocompatibility assessments. To address this, we evaluated the impact of sample area size on hemocompatibility results and established a threshold for the area that must be analyzed to obtain reliable data.

Methods: A static in-vitro hemocompatibility test series (n=10) was conducted using human platelet-rich plasma. Duplicates of five different polymer materials were incubated for 1 hour, stained with glutaraldehyde, and mounted on microscopy slides. Fluorescence microscopy was performed, imaging as much of the sample area as possible. Following microscopy, a newly developed automated analysis routine classified particles into 'platelet' and 'no platelet' [1]. Additional data on the number and area of adherent components were collected. Small image subsets were randomly selected and analyzed for covered area with 10- fold repetition. Based on this, we determined the necessary threshold of analyzed sample area for statistically valid results.

Results: The optical evaluation revealed significant inhomogeneity in platelet distribution across the material samples. Within just a few

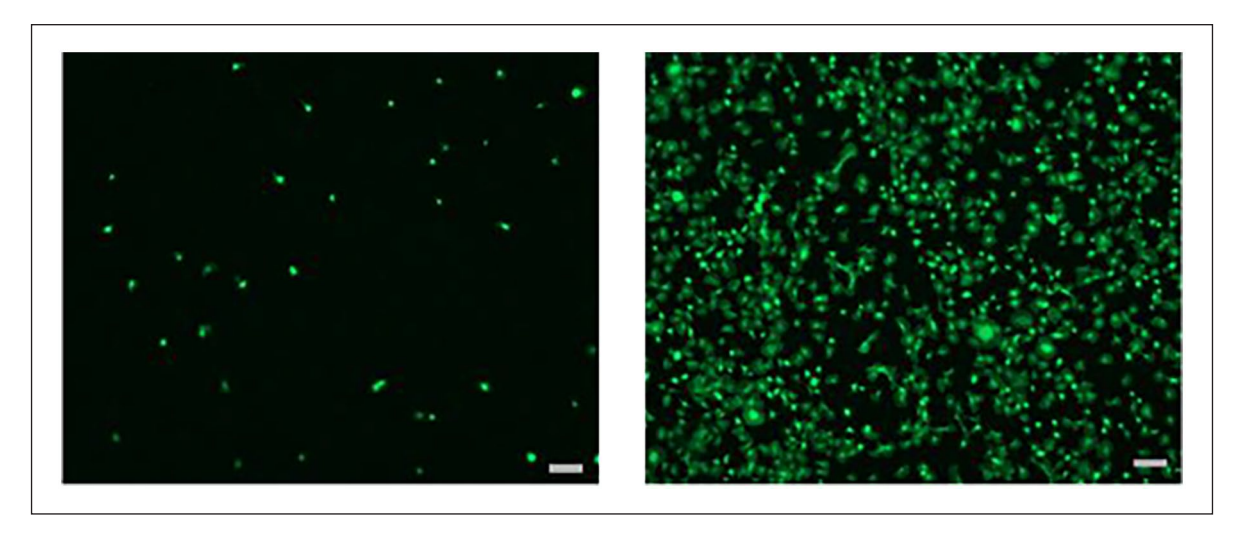


Figure 1. The identical material sample with little (left) and massive (right) platelet adhesion.

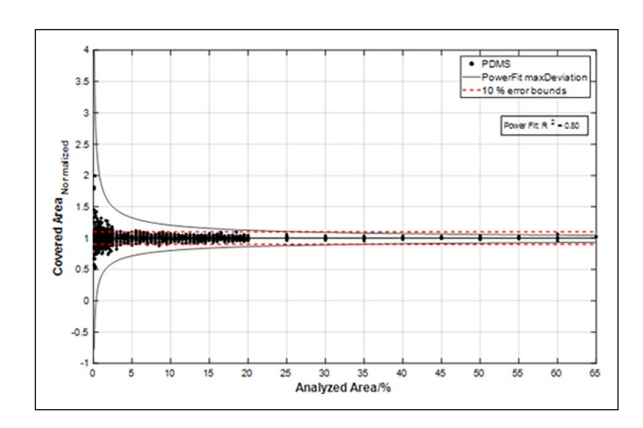


Figure 2. Covered area in dependance of analyzed sample area bis 10 % error bounds (red).

micrometers, platelet adhesion varied drastically, with regions showing either very few or many platelets (Fig. 1). Repeating the random selection of images for a given fraction of the analyzed sample area resulted in large coefficients of variation (CVs) for small sample areas.

However, increasing the analyzed area led to a reduction in CVs for all materials, eventually converging to a plateau (Fig. 2). Comparing results from image subsets to the total analysis, deviations were below 10% once the analyzed sample area reached 40% for all five materials.

Discussion: This study highlights the importance of the analyzed sample area in optical hemocompatibility analysis. For the materials investigated here, 40% of the sample area is the threshold for statistically valid results. These findings should be considered in future hemocompatibility studies and provide a step toward standardizing optical hemocompatibility assessments.

References

Clauser et al. ACS Biomater. Sci. Eng., 2021

Acknowledgements

Simulations were performed with computing resources granted by RWTH Aachen University under project rwth0314.

IN SITU LIVER SPHEROID FORMATION IN A NEW LOW ADSORPTION 3D-PRINTED BIOCHIP

Alexandre Martins^{1,2}, Sylvie Klieber¹, Charlotte Le Graët², Cécile Legallais², Rachid Jellali²

¹Sanofi, DMPK, In Vitro ADME, Vitry-sur-Seine, France; ²Université de Technologie de Compiègne, CNRS, Biomechanics and Bioengineering, Compiègne, France

Introduction: Organ-on-Chips (OoC) have shown an impressive development since the 2010s and offer new ways to improve current static 2D culture models. The main material used for their manufacture is PDMS that exhibits numerous advantages: transparency, biocompatibility, O2 permeability and ease-to-handle. However, it also shows an important unspecific binding (especially for highly lipophilic small molecules), leading to important bias in drug studies [1]. The aim of this work is to design a model of Liver-on-Chip using a fluorinated polymer (FP) with the same advantages than PDMS and a low-binding property. Dynamic cultures were implemented thanks to the IDCCM box developed by the BMBI lab allowing parallelized perfusion of 12-biochips [2].

Methods: The non-specific binding of the FP and PDMS were compared on several standard compounds. A new method was developed to print biochips with different microstructures and integrated standardized adapters using SLA printer. Printing and post-curing parameters were refined to obtain devices suited for long-term cell culture. This new standardized biochip was then compared to PDMS biochips considering several parameters: roughness, transparency, hydrophobicity, and surface energy with various technologies. Cell culture was assessed on this new printed chip for in-situ spheroid formation under perfusion thanks to the IDCCM. Cultures were performed for several days, and their viability and metabolic competency were characterized (LIVE/DEAD, Prestoblue, albumin and urea dosing). Confocal imaging was used to evaluate polarization of created spheroids and their structure. This model was finally used for pharmacokinetics studies of standard compounds.

Results: The tested FP showed a significant reduction of non-specific binding compared to PDMS, especially with high LogP compounds. Similar mechanical and surface properties than PDMS were observed. SLA printing allowed the fabrication of a microstructured

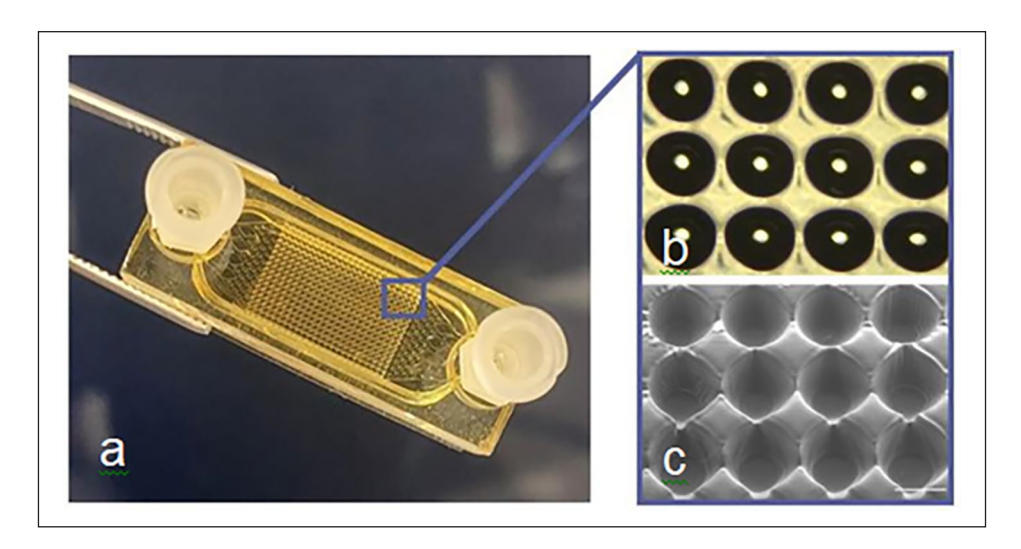


Figure 1. FP printed biochip (a), brightfield (b) and SEM (c) pictures of printed microwells.

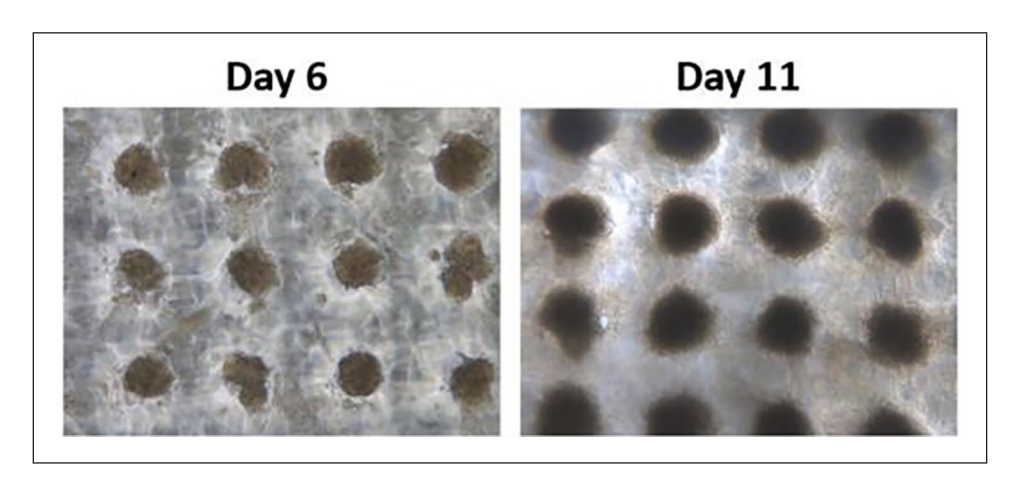


Figure 2. HepG2 spheroids in printed biochip at day 6 and 11.

biochip containing 384 microwells designed for spheroid formation. This technique allows a fast (25 minutes) and standardized fabrication of biochips with a good replication of microstructures (Fig. 1).

Cell culture of HepG2 was maintained for 11 days in PDMS and FP biochips and allowed a quick and repeatable formation of spheroids (Fig. 2). Both materials showed a high maintenance of metabolism, viability and polarization.

Discussion: This study showed that the FP is a suitable alternative of PDMS for the fabrication of biochip. Further experiments need to be completed to complexify this model, by selecting primary sources of cells and other cell types from the liver.

References

- Van Meer B.J. et al., Biochemical and Biophysical Research Communications, Vol. 482, Issue 2, p.323-328, 2017
- Leclerc E. et al., Biochemical Engineering Journal, Vol. 20, p. 143-148, 2004

TOWARDS A LEAK-RESISTANT AND MINIMALLY INVASIVE APPROACH FOR LARGE VASCULAR ANASTOMOSES USING CIRCULAR STAPLERS: OPTIMIZATION AND FUTURE PERSPECTIVES

Siarhei Yelenski¹, Johannes Greven¹, Guangmin Yang¹, Jan Spillner¹

¹Department of Thoracic Surgery, Medical Faculty, RWTH Aachen University, Aachen, Germany

Introduction: Building on previous research demonstrating the feasibility of circular stapling devices for vascular anastomoses, this study focuses on optimizing the technique to enhance stability and minimize leakage. The aim is to develop a minimally invasive and standardized approach for creating large- diameter vascular connections to major central vessels, which is particularly relevant for cardiovascular assist devices and transplantation surgery.

Methods: A proof-of-principle study was conducted in an ex vivo model to refine circular stapler-based anastomoses in large thoracic vessels near the heart. End-to-end and end-to-side anastomoses were performed on the pulmonary artery and descending aorta. Additionally, the effect of a biocompatible adhesive as a reinforcement was examined. The primary objective was to improve anastomotic sealing while ensuring mechanical integrity under physiological and supraphysiological pressure conditions.

Results: Compared to previous findings, the optimized technique led to a significant reduction in leakage while maintaining structural stability. Under high-pressure conditions, leakage remained minimal (<1 ml at MAP 150 mmHg with adhesive; <1 ml at MAP 100 mmHg without adhesive), and no thrombosis was observed (pressure change <2 mmHg, macroscopically unremarkable). The use of a biocompatible adhesive further reinforced the anastomoses but led to a temporary increase in stiffness at the connection site. The refined approach consistently resulted in reproducible anastomoses with improved sealing properties.

Conclusion: This study confirms that further optimization of circular stapler-based anastomoses can enhance their mechanical stability and significantly reduce leakage. A minimally invasive, standardized technique for creating large vascular connections could facilitate broader applications in cardiovascular surgery.

Further refinements, including optimized staple geometry, improved stapler dimensions, and advanced reinforcement methods, may enhance the safety and clinical feasibility of this approach. Future in vivo studies are required to evaluate long-term stability, biocompatibility, and hemodynamic performance.

Acknowledgements

The authors would like to thank Stapleline Medizintechnik GmbH for providing the staplers used in this study as part of the ZIM Project. Their support was instrumental in conducting this research.

4C: RESEARCH ON OXYGENATION AND MEMBRANES FOR ARTIFICIAL ORGANS

MODELING & DESIGN OF AN IMPLANTABLE DIALYSER FOR HEMODIALYSIS WITHOUT NEEDLES

Tadeo Alcerreca¹, Jeroen Vollenbroek^{1,2}, Karin Gerritsen¹, Tugrul Irmak¹

¹Department of Nephrology and Hypertension, University Medical Centre Utrecht, Utrecht, NL; ²BIOS Lab on a Chip Group, MESA + Institute, University of Twente, Hallenweg 15, 7522 NH Enschede, NL

Introduction: Hemodialysis is the most common treatment for end-stage kidney failure, but frequent vascular access via needles limits home care and increases infection risk. An implantable dialyzer module, directly anastomosed with vasculature, would provide continuous blood access. With dimensions of $4\times7\times2$ cm, it allows for subcutaneous implantation. Dialysate is supplied through a dual-lumen catheter from an external reservoir, resembling peritoneal dialysis (PD) in appearance and ease of use. Current hollow-fiber membranes (30–50µm thick) require large surface areas due to their large blood channels (170–200µm), making implantation unfeasible. Ultrathin (~100nm) nanofabricated membranes drastically reduce diffusion resistance. Combined with 3D printing, they enable a ~16-fold increase in diffusive transport, making an implantable device possible. Here, we present the first viable design and manufacturing approach for such a device.

Methods: We used an analytical diffusion model¹, simplifying the system as a rectangular channel with an a diffusive membrane, assuming a perfect sink on the opposite side. The β parameter, representing membrane

characteristics, was included. Urea clearance was determined from the average remaining concentration in the channel. The diffusion coefficient was calculated under physiological blood conditions for small solutes using the Stokes-Einstein equation. The membrane parameters were set at 5 nm pore radius, 160nm thickness, and 15% porosity. We are developing such membranes using silicon nitride (SiN). Total blood flow was fixed at 40ml/min to balance shear forces and manufacturability, with a target clearance of 30 ml/min—sufficient for 7×8-hour nocturnal hemodialysis sessions per week.

Results:



Figure 1. Initial implantable hemodialyzer design.

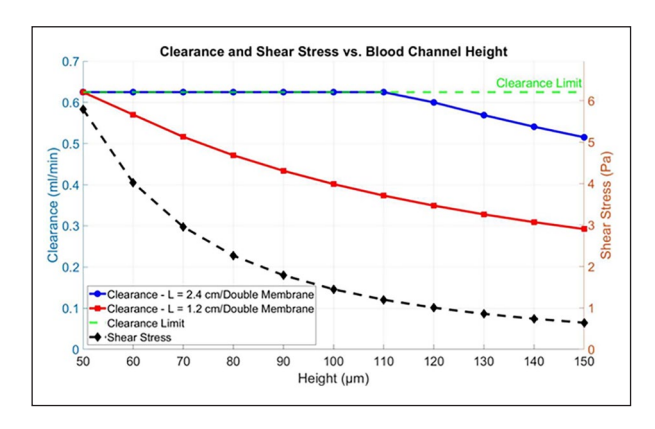


Figure 2. Urea clearance and blood shear vs total blood flow rate for a single unit.

Discussion: The CAD model in Figure 1 consists of 64 membrane units, each containing two 1.2cm-long membranes sandwiching a 100µm blood channel. The current clearance is 25.6ml/min but can be optimized by adjusting channel height or adding more units. The relatively small membrane length and area is to provide space for gradual flow expansion and to therefore minimize turbulent, recirculating zones that trigger platelet activation and thrombus formation. The device maintains a maximum wall shear stress of ~1.5Pa, assuming laminar flow, with physiological flow distribution based on Murray's law. The device measures 5×12×2cm. The above device is contained in a housing through which dialysate is pumped in cross- flow configuration, where each stack is separated by spacers. Conventional manufacturing cannot produce such complex geometries, but vat photopolymerization-based 3D printing enables fabrication as a single monolith, eliminating leakage risks. This demonstrates, for the first time, that an implantable dialysis filter can achieve the necessary clearance within implant size constraints and feature complex, blood-compatible pathing.

References

1. Burgin T et al, Membranes, 6:6, 2015.

Acknowledgements

This project was funded by KIDNEW (HORIZON-EIC-2022 Pathfinder GA 101099092), MICROMERULUS (OCENW.XS24.1.159 from NWO), ACX Grant and Dutch Growth Fund (NXTGEN HighTech, Biomed04 'Artificial Organs').

CARDIOPULMONARY COMPUTATIONAL MODEL TO UNRAVEL MECHANICAL VENTILATION EFFECTS ON CRITICAL HEMODYNAMICS

Federica Colombi¹, Elira Maksuti², Kenny Rumindo², Magnus Hallbäck², Fredrik Jalde², Dirk Donker^{1,3}, Libera Fresiello¹

¹-Cardiovascular and Respiratory Physiology, Technical Medical Centre, University of Twente, Enschede, the Netherlands; ²-Getinge, Acute Care Therapies, Maquet Critical Care AB, Solna, Sweden; ³-Intensive Care Centre, University Medical Centre Utrecht, Utrecht, the Netherlands

Introduction: Hemodynamic management of critically ill mechanically ventilated patients entails complex heart-lung interaction (HLI) between the cardiovascular and respiratory systems. Computational physiological models provide mechanistic and clinical insights into these intricated phenomena, aiding in the development of new monitoring techniques that translate into effective clinical management. We present a computational cardiopulmonary simulator built upon a previously validated closed loop lumped parameter model [1],[2].

Results: The simulations show that at the start of ventilatory inspiration, left ventricular preload and stroke volume increase while the right ventricular hemodynamics decrease (and conversely during expiration), in agreement with literature [3]. As PEEP increases, cardiac output (CO) and mean systemic arterial pressure (MAP) decrease, while pulmonary vascular resistance (PVR) increases (Table 1).

Methods: The original model is a lumped parameter representation of the left heart and right heart, pulmonary and systemic circulation, baroreflex control, metabolic peripheral control, respiratory mechanics and gas exchange [1]. Here, we integrate model elements that capture heart-lung interaction:

- Non-linear mechanical properties for lungs and chest wall
- Implementation of mechanical ventilation in flow and pressure controlled mode. The resulting airway pressure is transmitted into the pleural cavity affecting transmural pressure of the vasculature
- Pericardium modelled as a nonlinear compliance, its total volume being the sum of the heart chambers and the myocardial tissue
- Ventricular septum modelled as a three- compartment elastance
- Pulmonary arterial and venous capillaries and vena cava modelled as nonlinear resistances and compliances allowing to reproduce their collapse for high transmural pressures

The verification of added model elements is performed by comparing the simulator results with literature data of post cardiac surgery patients, undergoing volume controlled mechanical ventilation with different positive end-expiratory pressures (PEEP).

Discussion: This novel, integrated modelling approach of HLI shows a good overall agreement between simulations and literature data. Although further validation of the simulator is required, it represents a promising tool for understanding the critical hemodynamics under mechanical ventilatory support, creating perspectives to aid the development and testing of new diagnostic and therapeutic solutions.

Table 1. Simulation (bold) and literature data [4].

PEEP [cmH2O]	CO [L/min]	MAP [mmHg]	PVR [dynes·cm/sec ⁵]
0	4.1 – 4.2	90.3 – 91.6	160 – 216
5	3.8 – 4.1	86.2 – 91.6	208 – 217
10	3.5 – 3.9	80.7 – 90.2	280 – 256
15	3.2 – 3.6	74.9 – 90.2	382 – 256

References

- 1. Fresiello L et al, Front. Physiol., 2016.
- 2. Fresiello L et al, Front. Physiol., 2022.
- 3. Lansdorp et al, Crit. Care Med., 2014.
- 4. Koganov et al, Crit. Care Med., 1997.

Acknowledgements

This work was conducted in the frame of a research cooperation between the University of Twente and Getinge Acute Care Therapies.

PREDICTIVE NUMERICAL MODELING OF OXYGENATION AND FILTRATION RATES IN A DUAL-FUNCTION OXYGENATOR AND DIALYSIS DEVICE

Imane El Jirari¹, Danny Van Galen², Jutta Arens², Lisa Prahl Wittberg ¹, on behalf of the ArtPlac Research Consortium³

¹FLOW, Dept. of Engineering Mechanics, KTH Royal Institute of Technology, Stockholm, Sweden; ²Dept. of Biomechanical Engineering, Engineering Organ Support Technologies group, University of Twente, Enschede, the Netherlands; ³HORIZON-EIC-2022-PATHFINDEROPEN-01, Grant agreement ID: 101099596

Introduction: Mortality in premature infant population suffering from severe lung or kidney failure is high. Current treatments are less adapted to neonatal physiology, invasive and have side-effects. The Artificial Placenta (ArtPlac) preclinical project aims to provide a miniaturized assist device providing simultaneous pulmonary and renal support. The model configuration of the lung and kidney assists device (LKAD) will be adopted for either microfluid or hollow-fibre approach. To improve and optimize oxygenation and filtration performance. The aim of this study is focused on achieving an efficient species exchange while obtaining a low resistance within the LKAD device as well as minimize the risk of device-induced complications such as blood haemolysis.

Methods: A numerical analysis was carried out to predict the performance of a miniaturised version of the hollow-fibre-based LKAD. A computational fluid dynamics (CFD) analysis was conducted to assess the mass transport through membranes between gas or dialysate and blood and overall, indevice hemodynamic performance. The models were implemented with the commercial COMSOL Multiphysics software. A parametric analysis was conducted to assess the sensitivity of physical quantities of interest (related to both hemodynamic and species transport rates) to the inputs, including the influence of blood structural/rheological model, flow unsteadiness, membrane properties, and species diffusivity. The oxygen transport in the blood is governed by the convection-diffusion equation:

$$\upsilon \cdot \nabla P \theta_2 = D_b \cdot \nabla^2 P \theta_2 \tag{1}$$

where v is blood velocity, PO_2 oxygen partial pressure and Db oxygen diffusivity in blood. To consider the fraction of oxygen bound to

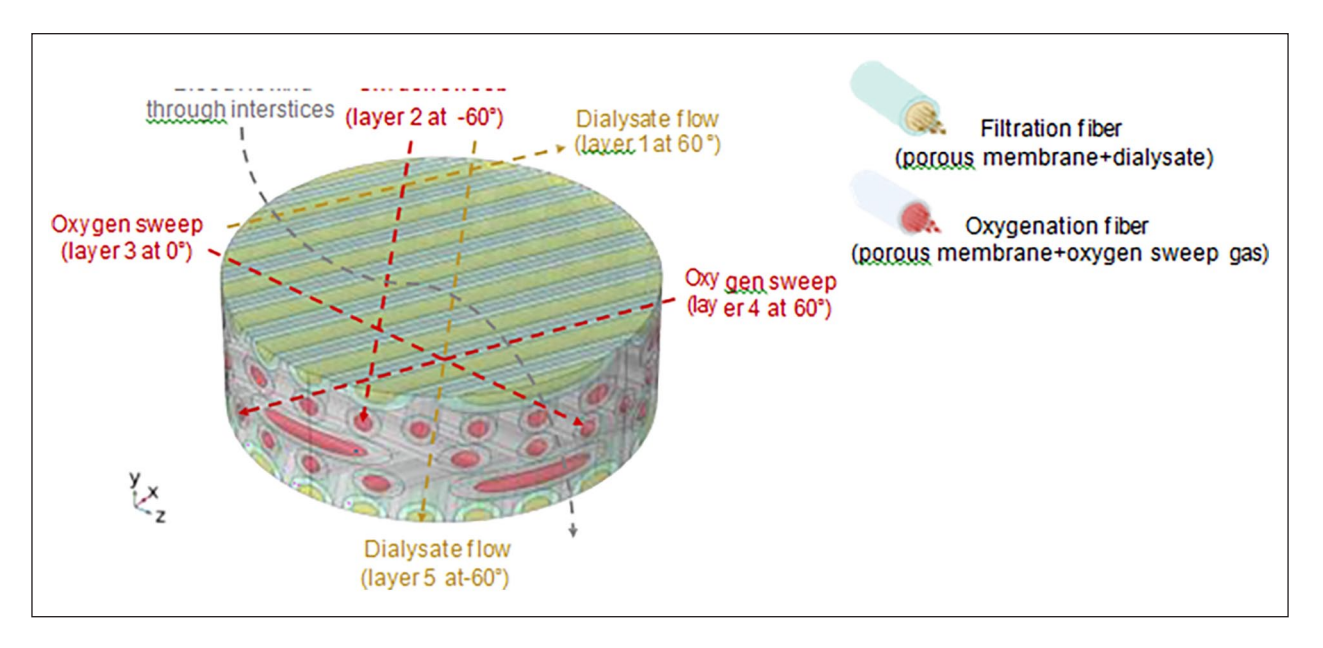


Figure 1. Computational domain corresponding to a portion of the full-scale model, showing the different domains.

hemoglobin, the effective diffusivity approach first introduced in reference [1] was employed:

$$D_{eff} = \frac{D_b}{1 + 1.34 \frac{c[H_b]dSO_2}{\alpha dPO_2}}$$
 (2)

where c[Hb] is haemoglobin concentration, α oxygen solubility in blood and the derivative dSO_2/dBO_2 is the slope of the oxygen- haemoglobin dissociation curve. The increased affinity of foetal haemoglobin for oxygen is included as a conditional statement in the user-defined functions. Toxins (urea and creatinine) and electrolytes (sodium, potassium, and chloride) transport are governed by convection-diffusion. The Debye-Hückel theoretical model [2] is employed to describe the electrolytic activity.

Results and Discussion: The influence of oxygen diffusivity was found to be significant where oxygen concentration varied by a factor of two depending on the assigned oxygen diffusivity (i.e. molecular diffusivity versus effective diffusivity). The influence of the particulate nature of blood was observed to be more pronounced for high blood flow rates. Future directions will assess factors such as interspecies interaction and albumin loss in filtration membranes to enhance species transport within the device.

References

- 1. Vaslef et al, ASAIO Journal, 40:990-996, 1994
- 2. Kontogeorgis et al, Fluid Phase Equilibria,462:130-152

Acknowledgements

ArtPlac is coordinated by Klinikum Nurnberg, Germany and funded by Horizon Europe programme under the European Innovation Council (EIC). Grant agreement ID: 10109. We thank the PDC Center for High Performance Computing, KTH Royal Institute of Technology, Sweden, for providing access to the NAISS large compute project "Large-scale Simulations in Complex Flows" (NAISS 2024/1-13) used in this research.

DESIGN, AND CHARACTERIZATION OF A 3D-PRINTED FLAT SHEET MEMBRANE MODULE FOR EXTRACORPOREAL BLOOD CIRCUITS

Flávia S.C. Rodrigues¹, Rita F. Pires¹, Ricardo Bexiga², Sérgio B. Gonçalves³, Mónica Faria¹

¹Laboratory of Physics of Materials and Emerging Technologies (LaPMET), Center of Physics and Engineering of Advanced Materials (CeFEMA), Instituto Superior Técnico, Universidade de Lisboa, Portugal; ²Faculty of Veterinary Medicine, Universidade de Lisboa, Portugal; ³IDMEC, Instituto Superior Técnico, Universidade de Lisboa, Portugal

Introduction: Hemodialysis (HD) is the most widely used treatment for kidney failure, a condition whose prevalence is progressively increasing worldwide. In HD, blood circulates out of the body and passes through a hemodialyzer for purification, and the clean blood returns to the body [1]. Traditionally, the components of these systems, including membrane modules, are manufactured using conventional methods such as injection molding. However, additive manufacturing (AM) has recently emerged as a promising alternative, offering advantages such as the ability to produce highly complex and customizable designs, which could benefit applications in this field [2].

In a research environment, flat sheet membranes are often used as an initial step in membrane development, requiring specialized modules to support them during testing. This work studies the potential of extrusion-based 3D printing to fabricate flat sheet membrane modules (FSMMs) at a lab- scale that enables flat sheet membrane evaluation. The goal is to demonstrate that AM is a viable alternative for producing customized FSMM for lab- scale studies, and its suitability in HD conditions.

Methods: A FSMM with well-defined microfluidic blood flow channels was developed and coupled to an in vitro circulatory system, operating as an extracorporeal blood circuit (ECBC) to mimic HD at a laboratory scale. The FSMM consists of two modules with microfluidic channels for the flow of either blood or dialysate, and a perforated central module for membrane support.

Two prototypes (FSMM-A and FSMM-B) with well- defined microfluidic flow channels that mimic the hemodynamic conditions of HD at a small scale were designed using the Onshape® CAD software and subsequently fabricated via 3D printing with Acrylonitrile Butadiene Styrene (ABS). Functional validation involved confirming the channel dimensions by imposing flow rates between 30 and 200 mL/min and measuring precise pressures, using aqueous solutions. Hemocompatibility of the prototypes was evaluated in terms of hemolysis using bovine whole blood and imposing shear stresses up to 260 Pa, following international standards [3]. Finally, a proof-of-concept experiment was performed with semi-permeable membranes placed in the prototypes for the filtration of whole blood for a period of 4 hours to demonstrate the feasibility of the FSMM.

Results: Both FSMMs showed no leaks after assembly, and the channel dimensions were very similar to those of the CAD design. The blood/ABS interfaces did not induce hemolysis, and flow conditions correlated with hemolysis degrees through microchannel designs. Prototype FSMM-B demonstrated outstanding performance when compared to FSMM-A and was selected for the proof-of-concept. After 4 hours of whole blood filtration there was hardly any hemolysis, increasing less than 1%.

Discussion: This work highlights the critical role of microfluidic channel design in devices for ECBCs. The results demonstrate the feasibility of using extrusion 3D printing technology to fabricate hemocompatible FSMMs with well-defined microchannels. This approach provides a quick and efficient alternative to traditional manufacturing methods, offering significant advantages for the development of lab-scale HD modules. Additionally, the versatility of 3D printing suggests its potential for designing more complex membrane modules in the future, expanding its

applicability to more advanced experimental setups and possibly clinical applications.

References

- 1. Rodrigues, F.S.C. et al, Toxins, 15:110, 2023.
- 2. Alghamdi, S.S. et al, Polymers, 13:753, 2021.
- ISO 10993-4:2017. International Organization for Standardization, 2017.

Acknowledgements

Fundação para a Ciência e a Tecnologia (FCT): CeFEMA programmatic funding UIDB/04540/2020 and UIDP/04540/2020, CEECIND/CP1651/CT0016 contract grant, UI/BD/150949/2021, and the LAETA Base Funding (DOI: 10.54499/UIDB/50022/2020).

FIRST DESCRIPTION: HEMOGLOBIN BASED DIALYSIS FACILITATES DECARBOXYLATION AND OXYGENATION IN-VITRO

Jan Stange¹, Stine Koball^{1,2}, Jan Klaiber², Adrian Dominik¹

¹University of Rostock Medical Center, Germany ²ProMedTec, Germany

Introduction: Extracorporeal removal of CO² in patients with acute respiratory distress syndrome can be performed using clinically available hemoperfusion devices based on hydrophobic oxygenation membranes like MultiEcco²R (Fresenius) added to dialysis. This is the first description

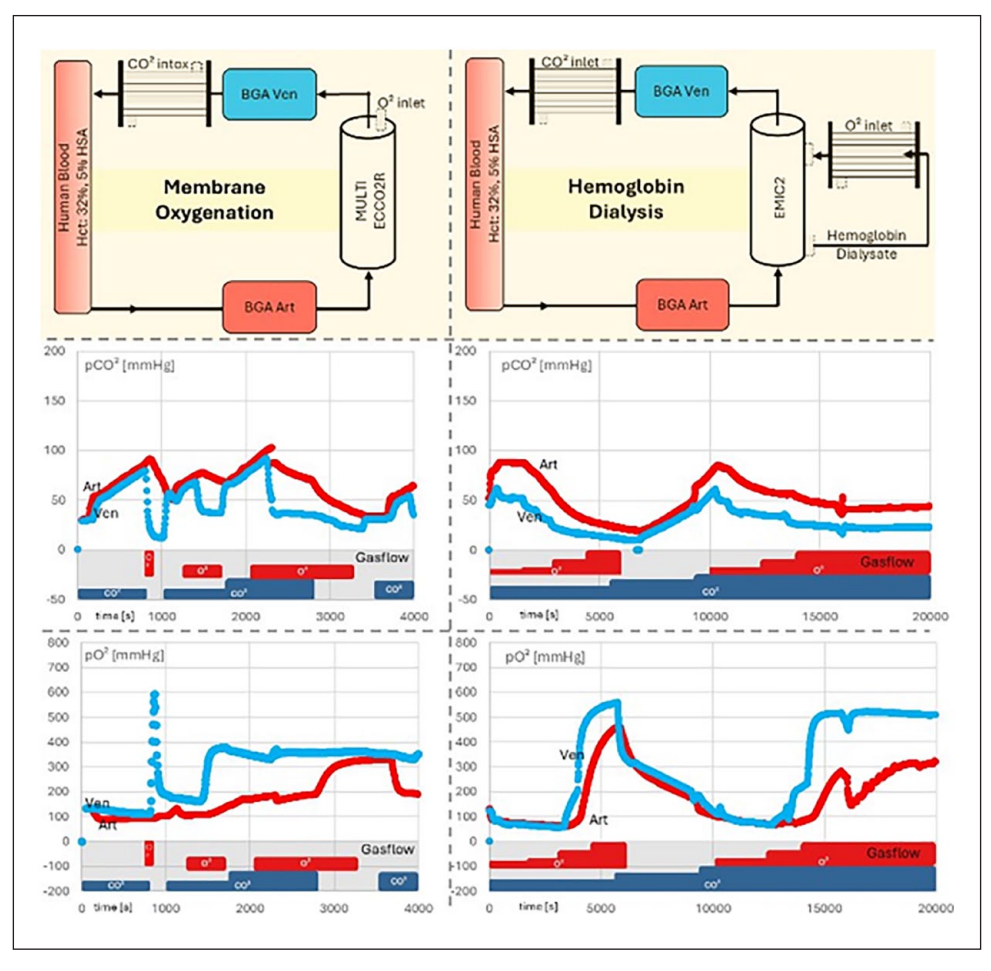


Figure 1. (left) membrane oxygenation (right) hemoglobin dialysis (top row) overview of test setups with denoted blood gas analysis sample points (middle row) Carbondioxide partial pressures with denoted gas flow changes (bottom row) Oxygen partial pressures with denoted gas flow changes.

of a novel Hemoglobin-based dialysis technique1 that uses hydrophilic dialysis membranes to effectively remove CO² and introduce O² simultaneously with dialysis in a pre-clinical model compared to MultiEcco²R.

Methods: A 1,5 Liter Patient was simulated using human erythrocyte concentrate diluted with 5% albumin solution to a Hkt of approx. 31% and adjusted to a pH 7.4. MultiEcco²R served as control experiment. CO² was introduced to the patient side using a silicone membrane gas exchanger (Permselect). Patient was dialysed against Dialysate containing purified human hemoglobin using an Emic²- Hemofilter (Fresenius). Oxygen was introduced to dialysate side using a MultiEcco²R. A blood flow rate of 200 ml/min was used for the patient circuit. Dialysate speed was 200 ml/min. In hemoglobin dialysis blood flow was adjusted to 100 ml/min at t=13000s.

Results: CO² was removed efficiently by both MultiEcco²R membrane oxygenation as well as hemoglobin- based dialysis (Figure 1).

Discussion: CO²-removal and O²-introduction in a dialysis setting using hydrophilic dialysis membranes can be achieved by adding oxygenated hemoglobin to the dialysate. Here, dialysate hemoglobin increases oxygen availability at the membrane pore level and thereby enables oxygen and carbon dioxide transfer over the membrane in the water- soluble phase. Dialysis membranes propose several advantages over oxygenation membranes and are expected to improve hemocompatibility in blood decarboxylation and oxygenation. Membrane wetting is of no concern. The concept could be extended to ECMO.

Finally, dialysis and carbon dioxide removal can be done by only one membrane, thereby reducing clinically significant side effects. Results display encouraging potential for further optimization. On the technological side, gas transfer was limited by blood flow and upper detection was limited by TerumoCDI550. On a biochemical side, gas transfer could be increased by higher concentration of hemoglobin in dialysate as well as effectors of the hemoglobin oxygen dissociation curve like temperature. Technological optimization concerning mass transfer is under current investigation.

References

1. US patent: US20220339333A1 (2022).

Acknowledgements

Study was supported by Federal and State Funds of Germany (BMBF/VDI KMU innovativ).

5A: FUTURE THERAPIES TO REDUCE LEVELS OF UREMIC TOXINS IN CKD

THE DUALITY OF UREMIC TOXICITY

Griet Glorieux 1

¹Nephrology Unit, Department of Internal Medicine and Pediatrics, Ghent University Hospital, Gent , Belgium

Introduction: Uremic toxicity has long been a focus in nephrology, but less attention is given to the potential benefits of metabolites produced alongside uremic toxins.

 $\label{eq:Methods:Tryptophan-derived metabolites} \textbf{Methods:} \ \textbf{Tryptophan-derived metabolites} \ \textbf{were used as an example.}$

Results: We highlight their dual nature: some are toxic (e.g., indoxyl sulfate, kynurenine), some beneficial (e.g., indole, melatonin), and others ambivalent (e.g., serotonin). This dualism extends to their main receptor, the aryl hydrocarbon receptor (AHR), which has both harmful and beneficial effects. We recently also demonstrated that untargeted metabolomics offer a more balanced view of uremic retention than the targeted approaches, with higher chances of revealing the beneficial potential of some of the metabolites.

Discussion: We emphasize the need to consider both positive and negative aspects of uremic metabolites in future therapeutic strategies, aiming for balance rather than indiscriminate elimination.

Acknowledgements

I thank Raymond Vanholder and Stéphane Burtey for their contribution and the European Uremic Toxin Workgroup (EUTox) for supporting this work.

DRUG-TOXIN INTERACTIONS AT ORGANIC ANIONIC TRANSPORTER 1: IMPLICATIONS FOR BIOARTIFICIAL KIDNEY DEVELOPMENT

Silvia M. Mihăilă¹, Jasia King², João F. Faria¹, Nargis Khoso¹, Sabbir Ahmed¹, Leyla Sharafutdinova¹, Leyla, Noroozbabaee¹, Dimitrios Stamatialis³, Karin GF Gerritsen⁴, Aurélie Carlier², Rosalinde Masereeuw¹

¹Division of Pharmacology, Utrecht Institute for Pharmaceutical Sciences, Utrecht University, 3584 CG Utrecht, The Netherlands; ²MERLN Institute for Technology-Inspired Regenerative Medicine, Maastricht University, 6229 ER Maastricht, The Netherlands; ³Advanced Organ Bioengineering and Therapeutics, Faculty of Science and Technology, Technical Medical Centre, University of Twente, 7522 NB Enschede, The Netherlands; ⁴Department of Nephrology and Hypertension, University Medical Center, 3508 GA Utrecht, The Netherlands

Introduction: The bioartificial kidney (BAK) aims to enhance uremic toxin clearance by utilizing proximal tubule epithelial cells (PTECs) with active transporter function. Organic anion transporter 1 (OAT1) plays a key role in protein-bound uremic toxin (PBUT) uptake from the blood, while efflux pumps facilitate their removal into the dialysate. However, chronic kidney disease (CKD) blood contains high levels of PBUTs and pharmaceuticals, such as statins, diuretics, ACE inhibitors (ACEIs), and angiotensin receptor blockers (ARBs), due to polypharmacy. These compounds may compete at OAT1, potentially hampering PBUT excretion and BAK efficiency. This study investigates drug-toxin interactions at OAT1 using computational and experimental approaches to provide insights for BAK development and optimize drug treatment in CKD.

Methods: We used proximal tubule cells with confirmed OAT1 activity to study the competitive uptake of PBUTs and CKD-associated drugs. A fluorescein- based assay assessed OAT1-mediated transport inhibition by selected pharmaceuticals (ACEIs, ARBs, statins, and diuretics). Additionally, we tested functional BAK hollow fiber membranes decorated with PTECs using LC-MS to quantify toxin clearance in single and multi-toxin conditions. A computational model was developed to simulate indoxyl sulfate (IS), a prototypical PBUT, transport dynamics, incorporating transporter density, albumin-binding kinetics, and toxin dissociation rates to predict clearance efficiency under physiological and uremic conditions.

Results: Experiments with the BAK functional unit confirmed effective PBUT removal, but toxin-toxin interactions led to variable clearance rates, underscoring the need to understand their impact on function (1). Anticipating this effect, we examined drug-toxin and toxin-toxin interactions at OAT1. Our findings show that CKD-associated drugs compete with PBUTs for OAT1-mediated uptake, with ARBs and furosemide significantly inhibiting fluorescein uptake at clinically relevant concentrations, a trend exacerbated by PBUTs (2). Computational modeling revealed that transporter density and PBUT dissociation rates are key determinants of clearance efficiency. Experimental data also indicated that albumin enhances PBUT removal (2). However, computational simulations suggested that albumin conformational changes in uremic conditions may reduce PBUT dissociation rates, limiting their availability for clearance (3).

Discussion: This study provides key insights into toxin- transporter interactions, emphasizing drug-toxin competition in BAK system design. By integrating computational modeling with in vitro validation, we offer a

framework to optimize transporter function in BAK. Additionally, we are investigating multi- toxin and drug-toxin interactions by measuring intracellular concentrations and develop a computational framework to predict these interactions, allowing for better-informed strategies in BAK design. Future studies should refine transporter expression strategies and mitigate drug-induced inhibition to enhance BAK efficacy.

References

- 1. Faria J, et al, Int J Mol Sci.24(15):12435, 2023
- 2. Mihaila, SM, et al, Toxins, 12(6), 391, 2020
- 3. King, J, et al,. Toxins, 13(10), 674, 2021

Acknowledgements

This work was supported by DETOX from Dutch Kidney Foundation (22OK1019), EUTox working group of ESAO, the MSCA- doctoral network (RenalToolBox, 813839), and NWO OTP BAKTOTHE FUTURE (Grant nr 20775)

5B: ADVANCES IN BLOOD PUMP DEVELOPMENT

RESTORING VENTRICULO-ARTERIAL COUPLING BY SPEED MODULATING ROTARY BLOOD PUMPS

Theodor Abart¹, Philipp Aigner¹, Kamen Dimitrov¹, David Santer², Michael Röhrich³, Daniel Zimpfer¹, Marcus Granegger¹

¹-Christian Doppler Laboratory for Mechanical Circulatory Support, Department of Cardiac Surgery; ²-Center for Biomedical Research and Translational Surgery; ³-Department of Anesthesia and Intensive Care Medicine all Medical University of Vienna, Austria

Introduction: Recovery rates in patients with implantable left ventricular assist devices (LVADs) remain low. This might be linked to a mismatch between arterial and ventricular elastance (Ea and Ees), as physiological ventriculo-arterial coupling ratio is 0.5 to 1 and it increases in heart failure. [1] We hypothesize that matching ventricular and arterial elastances may promote myocardial recovery. [2] The aim of this study was to investigate whether rotary blood pumps at constant speed and with instantaneous altering of the speed throughout the cardiac cycle can adapt the loading conditions of the heart to restore physiological Ea/Ees ratios.

Methods: A pediatric heart failure lumped parameter model was coupled to a hybrid mock circulatory loop (HMCL). Instantaneous speed control was integrated with two LVADs, the HeartMate 3 (Abbott, North Chicago, USA) and the Berlin Heart NGP (Next Generation Pump, under research, Berlin Heart GmbH, Berlin, Germany). Both pumps were utilized to support the simulated failing heart, with partial and full support (QVAD=2.0 lpm and QVAD=2.8 lpm) at constant speed. This was compared to cardiac cycle-triggered, sine shaped, modulated speed patterns, with different amplitudes (0.5 krpm, 1 krpm and 1.5 krpm) and phase delays (0% to 90% of the cardiac cycle) by pressure-volume loops and elastance calculations. To validate results the NGP was used to support an isolated lamb heart in ex-vivo working mode at different pump speeds (2000 to 5000 rpm) while oxygen consumption was measured in addition to pressures and volumes.

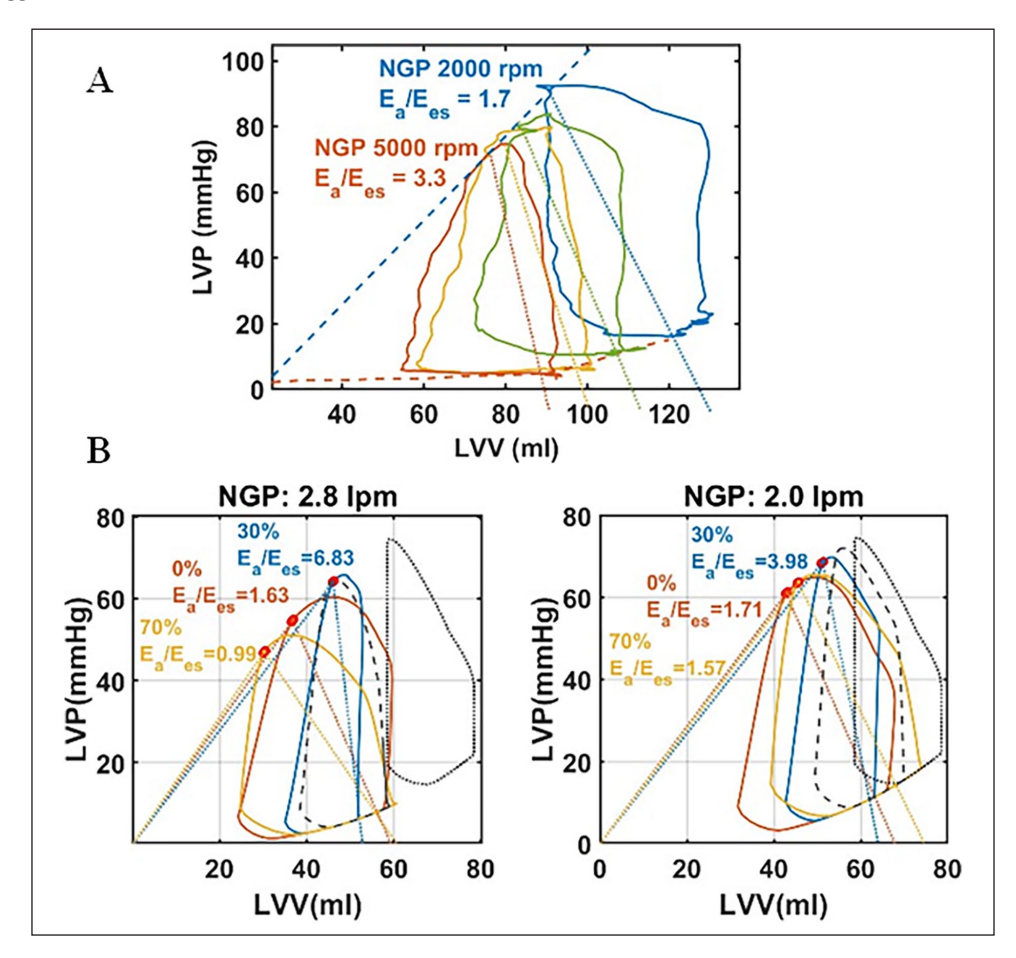


Figure 1A. Isolated heart hemodynamics with NGP support at increasing pump speeds; 1B: NGP in the HMCL supporting the failing heart with phase delayed, modulated speed. Baseline & constant speed (black, dotted & dashed).

Results: In the HMCL, partial and full support baseline were 3 krpm and 4 krpm (HM3) and 2.8 krpm and 3.4 krpm (NGP). The unsupported Ea/Ees ratio was 3.0, while constant speed unloading increased the ratio to 3.2 and 3.6 (at 2 lpm and 2.8 lpm). Similarly, in the isolated heart (Figure 1A), Ea increased with higher pump speeds (range 2.24 - 4.17 mmHg/ml) and also resulted in higher Ea/Ees ratios (1.67 - 3.25) indicating unfavorable support conditions at higher support degrees, as cardiac efficiency correlated negatively with an increasing Ees/Ea ratio ($R^2 = 0.81$). In the HMCL, pulsatile speed control could alter the Ea/Ees ratio with minimal values of 0.99 (NGP) and 1.16 (HM3) reached at the maximal amplitude and a delay of 70% during full support (Figure 1B). While restoring a coupling ratio of close to one, sufficient cardiac unloading was achieved.

Discussion: Constant speed support in LVAD recipients leads to non-physiological ventriculo-arterial coupling ratios. Restoring a physiological coupling ratio is feasible using a rotary blood pump (HM3 or NGP) with a triggered, sine shaped, pulsatile speed control while maintaining sufficient unloading.

References

- 1. García et al, Ann Transl Med., 8(12):795, 2022
- 2. Granegger et al, Scient.Rep., 9:1:20058, 2019

Acknowledgements

The financial support by the Austrian Federal Ministry of Labor and Economy, the National Foundation for Research, Technology and Development and the Christian Doppler Research Association is gratefully acknowledged.

SENSORLESS ESTIMATION OF INSTANTANEOUS FLOW RATE, HEAD PRESSURE AND VISCOSITY IN A ROTARY BLOOD PUMP

Theodor Abart¹, Marko Grujic¹, Stefan Jakubek², Adrian Wisniewski³, Daniel Zimpfer¹, Marcus Granegger¹

¹Christian Doppler Laboratory for Mechanical Circulatory Support, Department of Cardiac Surgery, Medical University of Vienna, Austria; ²Division of Control and Process Automation, Institute of Mechanics and Mechatronics, University of Technology, Vienna, Austria; ³Berlin Heart GmbH, R&D, Berlin, Germany

Introduction: Hemodynamic sensors incorporation is not feasible in durable left ventricular assist devices (LVADs). However, measurements such as flow rate, pressure head and blood viscosity bear important information on the pumps' performance and the patients' condition with potential to predict and prevent adverse events. [1] Therefore, researchers and companies try to estimate these parameters from intrinsic pump signals, however, previous attempts are limited by signal availability, nonlinear characteristics of blood pumps (hydraulic, motor, and bearing), and substantial dynamics effects. [2] The aim of this work was to develop a digital twin of a rotary blood pump in terms of a state observer based on the identified nonlinear differential equations describing the hydraulic pump, the motor and the bearing of a novel blood pump.

Methods: We employed an Unscented Kalman Filter (UKF), which enables the estimation of current states ($Q...pump\ flow;\ H...head\ pressure;\ w...pump\ speed;\ Xdisp...bearing\ displacement;\ \mu...viscosity$) using readily available pump signals (w.lmotor,lbearing,Xdisp) as the sole additional inputs to determine Q.H and Q.H. We identified static and dynamic hydraulic, motor and bearing characteristics of the Berlin Heart NGP (Next Generation Pump, under research, Berlin Heart GmbH, Berlin, Germany) in a hybrid mock loop and acquired realistic hemodynamics of virtual patients coupled to the hybrid loop. The physical states were modeled as differential equations based on static characteristics, and

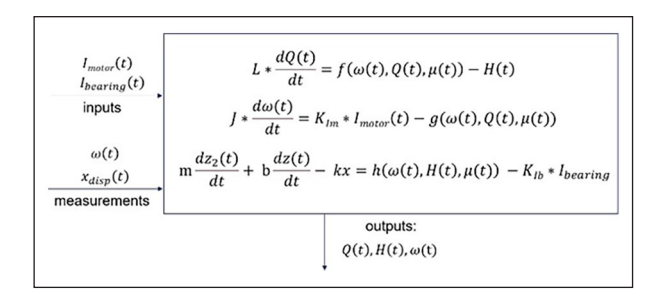


Figure 1. States corresponding to

- (i) hydraulics,
- (ii) motor and
- (iii) bearing used in the UKF.

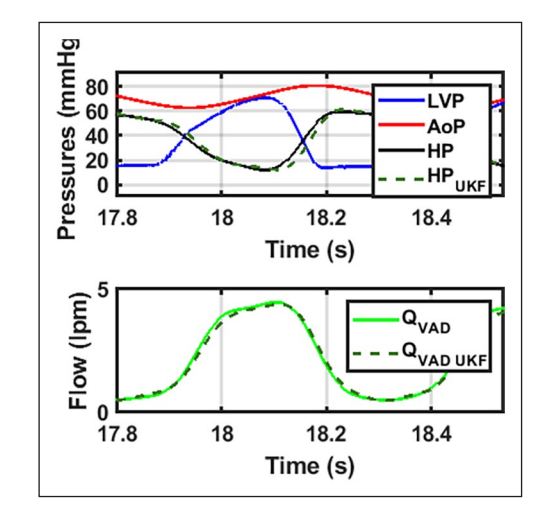


Figure 2. Hemodynamics with flow rate and head pressure estimated by the UKF (dashed).

dynamic parameters optimized before integration in the UKF (Figure 1). μ and ${\it H}$ were modeled as augmented states.

The performance was then evaluated with different hemodynamic signals for 3 rpm to 4.5 krpm.

Results: The UKF estimated Q with an RMSE of 0.22 (\pm 0.02) lpm and a correlation coefficient of r=0.98 (\pm 0.01). H was estimated with an RMSE of 6.0 (\pm 0.2) mmHg and r=0.93 (\pm 0.03). μ was modeled with reduced process noise to prevent adaptation during the cardiac cycle, results showed convergence to a value within \pm 1 mPa*s of the actual viscosity in under one minute.

Discussion: The algorithm has demonstrated the feasibility of applying nonlinear state estimation to the NGP. Its accuracy will further be improved by increasing the complexity and precision of the underlying models. Its application can be extended to fault detection (e.g. sensor drifts, aspiration of particles) or integration with established hemodynamic monitoring algorithms (e.g. suction, contractility).

References

- 1. Ayre et. al., Physiol. Meas., 24, 1, 2003
- 2. Granegger et al., Art.Org., 36(8):691-9, 2012

Acknowledgements

The financial support by the Austrian Federal Ministry of Labor and Economy, the National Foundation for Research, Technology and Development and the Christian Doppler Research Association is gratefully acknowledged.

FRICTION LOSSES IN PIVOT BEARINGS OF ROTODYNAMIC BLOOD PUMPS

Leon Ballabani¹, Simon Klocker¹, Benjamin Torner¹, Michael Hübler², Daniel Zimpfer¹, Marcus Granegger^{1, 2}

¹Department of Cardiac and Thoracic Aortic Surgery, Medical University of Vienna, Vienna, Austria; ²University Heart and Vascular Center Hamburg, University Medical Center Hamburg-Eppendorf, Hamburg, Germany.

Introduction: The use of rotodynamic blood pumps (RBPs) as supportive devices for the cardiovascular system has become a promising therapy for patients with severe heart failure. A key factor for the pump performance and pump reliability is the impeller's bearing concept.

Pivot bearings, a type of mechanical bearing, have been used in left ventricular assist devices like the HeartMate II (HMII, Abbott Laboratories), success- fully supporting thousands of patients worldwide. Building on this concept, our team has developed a cavo-pulmonary assist device (CPAD) with pivot bearings specifically tailored for Fontan patients [1,2]. However, to date, the complex interaction between mechanical pivot bearings, the surround- ding blood flow and its corpuscular components remains unexplored.

In this study, we investigated friction losses and the associated torque in pivot bearings by analyzing the power consumption of two rotodynamic pumps.

Methods & Materials: The HMII and CPAD were evaluated *in-vitro* on a test bench. A wide operational range of both pumps was investigated, covering different flow rates and rotational speeds. Flow rates were determined by an ultrasonic flow meter, while rotational speeds and the associated power consumption were determined by a manufacturer control unit for HMII and a self-developed control unit for the CPAD. Results obtained with heparinized (15000 IU/L) bovine blood (35% hematocrit, 1050 kg/m³, 3.5 mPas) and blood plasma (1025 kg/m³, 1.6 mPas)

were compared to those using single-phase blood analog fluids (water-glycerol, 1110-1127kg/m³, 3.0-4.0 mPas).

Results: Our measurements indicate a significant increase in power consumption during the blood exper- iments compared to those with the blood analog fluids with similar viscosities. This is exemplified in Figure 1 for two rotational speeds of both pumps. This trend was observed across the entire operational range. The increase in power consum- ption is quantified using the root mean square of the relative deviation in power consumption between blood/plasma in comparison to the blood analog, as listed in Table 1.

Notably, tests using low-viscosity blood plasma demonstrated power consumption that was comparable to, or even higher than that observed with the higher-viscosity blood analog fluids.

Discussion: In this study we showed that the friction losses and the associated torque in the pivot bearings are considerably higher in blood compared to water glycerol with similar viscosity.

This discrepancy cannot be explained solely by the presence of erythrocytes in the blood, as even plasma - despite being less viscous - results in a similar or even higher power consumption compared to the more viscous blood analog fluids. Power consumption is strongly influenced by viscosity, with more viscous fluids generating greater frictional losses in the bearings. Our findings suggest that plasma behaves as a significantly more viscous fluid within the bearing.

This observation may be explained by protein denaturation, forming microstructures that increase the apparent viscosity locally, leading to

Table 1. RMS of relative deviation in power consumption.

	HMII	CPAD
RMS of Blood/W-G	1.17	1.31
RMS of Plasma/W-G	1.04	1.24

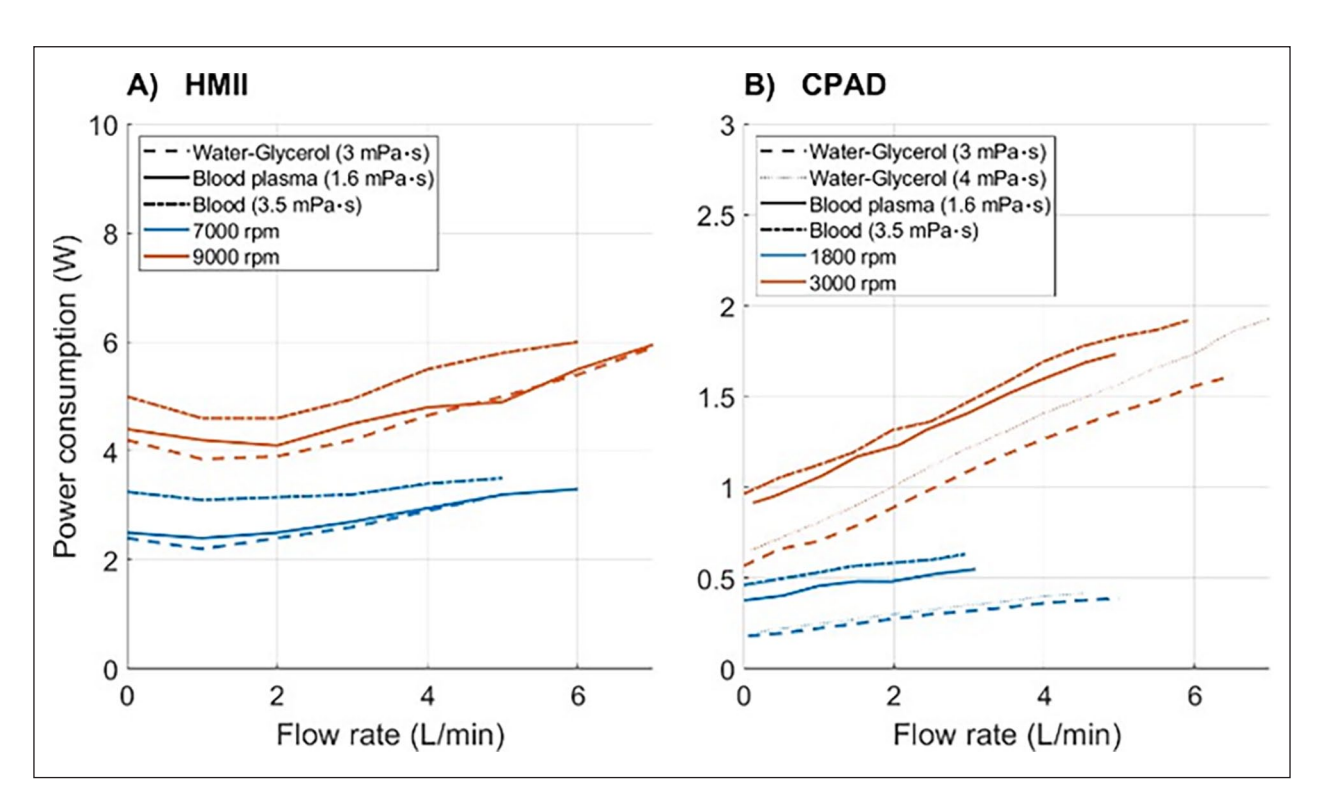


Figure 1. Power consumption at two rotational speeds for the HMII (left) and the CPAD (right).

elevated torque and power consumption. Future work will focus on validating this hypothesis through experimental and computational methods.

References

- Escher et al. (2022): A Cavopulmonary Assist Device for Long-Term Therapy of Fontan Patients. Semin Thorac Cardiovasc Surg. 34(1).
- [2] Escher et al. (2024): Multiobjective Optimization of Rotodynamic Blood Pumps: The Use Case of a Cavo- pulmonary Assist Device. ASAIO J. 70(12).

HEMOCOMPATIBILITY AND HEMODYNAMICS OF THE HEARTMATE 3 IN PEDIATRIC PATIENTS

Manar El-Shaer¹, Rosmarie Schöfbeck¹, Theodor Abart¹, Barbara Messner², Daniel Zimpfer¹, Marcus Granegger¹

¹Christian Doppler Laboratory of Mechanical Circulatory Support, Department of Cardiac Surgery, Medical University of Vienna; ²Cardiac Surgery Research Laboratory, Medical University of Vienna

Introduction: The HeartMate3 (HM3) has become an important treatment option for pediatric patients, despite limitations due to its larger size [1]. However, its hydraulic properties and hemocompatibility in typical pediatric settings, including a potential recovery scenario, was not yet investigated. The aim of this study was to assess the pump's performance (hemodynamics and hemolysis) in typical pediatric conditions, including low- and backflow episodes in recovery scenarios.

Methods: Based on data from a literature review, we parametrized a lumped parameter model to replicate typical hemodynamics of a 6-year-old patient with (i) end-stage heart failure (full support), (ii) less advanced heart failure (partial support) and (iii) a completely recovered cardiovascular system (recovery candidate). Using a hybrid mock circulatory loop we assessed the hemodynamic effect of the HM3 in these three conditions. As the hybrid mock loop was operated with bovine blood from the abattoir, hemolysis was assessed concomitantly according to the ASTM F1841-19e1 standard. The samples were taken every 30 minutes, centrifuged twice and the plasma-free hemoglobin measured with a photometer. The delta free hemoglobin (dfHb) and the Normalized

Index of Hemolysis (NIH) were established to quantify the hemolysis rate. Experiments were repeated ten times and each experiment lasted for 6 hours, with a change of condition every two hours.

Results: For the three conditions the pump speeds were adjusted to 4700 rpm in full support, 4200 rpm in partial support and 4200 \pm 100 rpm in the recovery candidate. The resulting mean pump flows in these conditions were 2.8 L/min, 2.3 L/min and 1.8 L/min, respectively. Flow pulsatilites reached from -2.5L/min to 6L/min, with pronounced backflow during diastole in the partial support patient and recovery candidate (Figure 1A). The calculated NIH was comparable between the three conditions (full, partial, recovery: 9.95 \pm 6.83 mg/100L, 12.22 \pm 5.40 mg/100L, 12.31 \pm 8.09 mg/ 100L, p=0.76), see Figure 1B. Further, no significant difference in dfHb was observed between the three conditions (1.83 \pm 1.11mg/dL, 1.87 \pm 0.92mg/dL, 1.51 \pm 0.85mg/dL; p=0.76).

Discussion: In this study we showed that with the HM3 in pediatric patients and mean pump flows from <3L/min, substantial periodic backflows during diastole (up to -2.5L/min) can be observed especially in patients with recovering cardiovascular function. These frequent backflows did not cause elevated hemolysis compared to the other operating conditions without backflow. The present results underpin our previous finding that periodic low/backflow conditions under dynamic conditions are not associated with higher hemolytic action in contrast to these flows under static conditions. Further studies are required to assess the safety of the HM3 in these patients in terms of thrombogenicity. Of note, considerable backflows during diastole were associated with low diastolic arterial pressures, which may impede coronary perfusion.

References

 Niebler, R.A., et al., Impact of HeartWare ventricular assist device discontinuation on the pediatric population: An Advanced Cardiac Therapies Improving Outcomes Network (ACTION) registry analysis. JHLT Open, 2024. 4.

Acknowledgements

The financial support by the Austrian Federal Ministry of Labor and Economy, the National Foundation for Research, Technology and Development and the Christian Doppler Research Association is gratefully acknowledged.

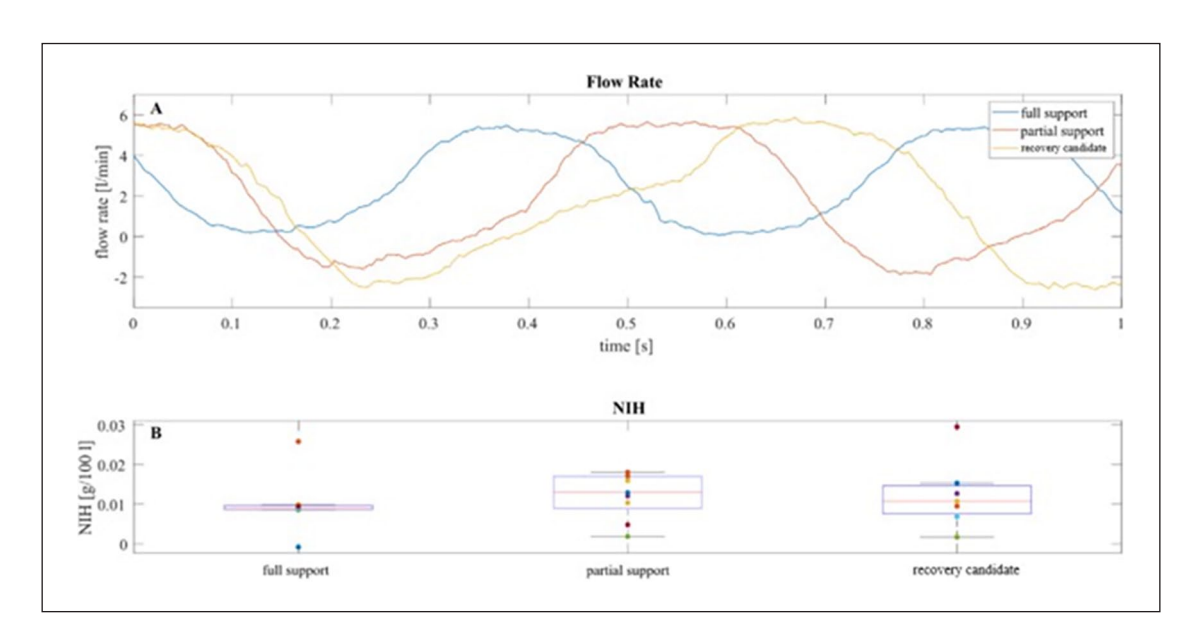


Figure 1. A: Different flow rate conditions for the three scenarios: full- and partial-support & recovery candidate. B: NIH for all three scenarios.

DESIGN OPTIMIZATION OF A RIGHT VENTRICULAR ASSIST DEVICE: BALANCING EFFICIENCY AND HEMOLYSIS RISK

Ilaria Guidetti¹, Elena Cutrì², Maria Laura Costantino¹, Francesco De Gaetano¹

¹Department of Chemistry, Material and Chemical Engineering, Politecnico di Milano, Milan, Italy; ²Université de technologie de Compiègne, CNRS, Biomechanics and Bioengineering, 60203 Compiègne Cedex. France:

Introduction: Right heart failure (RHF) is a complex condition in which the right ventricle (RV) fails to maintain adequate blood flow to the pulmonary circulation, meet tissue metabolic demands, and regulate right atrial pressure [1]. RHF is associated with high morbidity and an in-hospital mortality rate of up to 75%, affecting 40% of patients with a left ventricular assist device (LVAD) [2][3].

In severe RHF cases, a right ventricular assist device (RVAD) is required. However, most current solutions repurpose LVADs, which are not designed for the lower pressure conditions and for the anatomy of the RV. This underscores the need for RVADs specifically engineered for right heart support. This study aims to develop and optimize a novel RVAD prototype, enhancing hydraulic efficiency and reducing hemolysis potential.

Methods: The RVAD prototype was developed as a centrifugal pump with a mixed-flow impeller, designed using classical pump theory.

An optimization strategy was implemented using ANSYS Workbench 2024 to identify the optimal device design that allows to enhance hydraulic efficiency while minimizing potential blood damage. Four key geometric parameters were investigated: impeller blade diameter, gap between blade tips and volute, blade outlet angle, and blade trailing edge inclination. The optimization criterion (OC), minimized in this study, was based on the cost function proposed by incebay, which

accounts for both the modified index of hemolysis (MIH) and the hydraulic efficiency (η) [4].

$$OC = MIH / \eta^2$$
 (1)

A total of 25 different RVAD geometries were analyzed through computational fluid dynamics, and the results were used to construct response surfaces correlating the geometric parameters and the optimization criterion. A genetic algorithm was then employed to determine an optimal pump design.

Results: The characterization of the initial RVAD prototype demonstrated its capability to sustain high flow rates while maintaining pressure drops within the physiological range required for right ventricular support (from 0 to 35 mmHg). Additionally, the device achieved hydraulic efficiencies of approximately 30% across different flow conditions (Figure 1).

The optimization process highlighted the influence of the trailing edge inclination angle and the gap between impeller and volute for enhancing hydraulic efficiency and minimizing the hemolysis risk.

Discussion: The developed RVAD fulfils RV requirements, and its ability to operate efficiently across a wide range of flow rates opens the possibility of implementing an artificial pulsing pump, able to mimic the physiological blood pulsatility.

The optimization strategy allowed to refine the device design to achieve a balance between increasing hydraulic efficiency and reducing the hemolysis risk, further improving overall performance and hemocompatibility.

References

- 1. Dini et al, Heart Fail Rev, 28:757-766, 2023.
- 2. DeFilippis et al, Card Fail Rev, vol. 8, 2022.
- 3. Arrigo et al, Card Fail Rev, vol. 5, 3:140–146, 2019.
- 4. incebay et al, J. Braz. Soc. Mech. Sci. Eng., 2024.

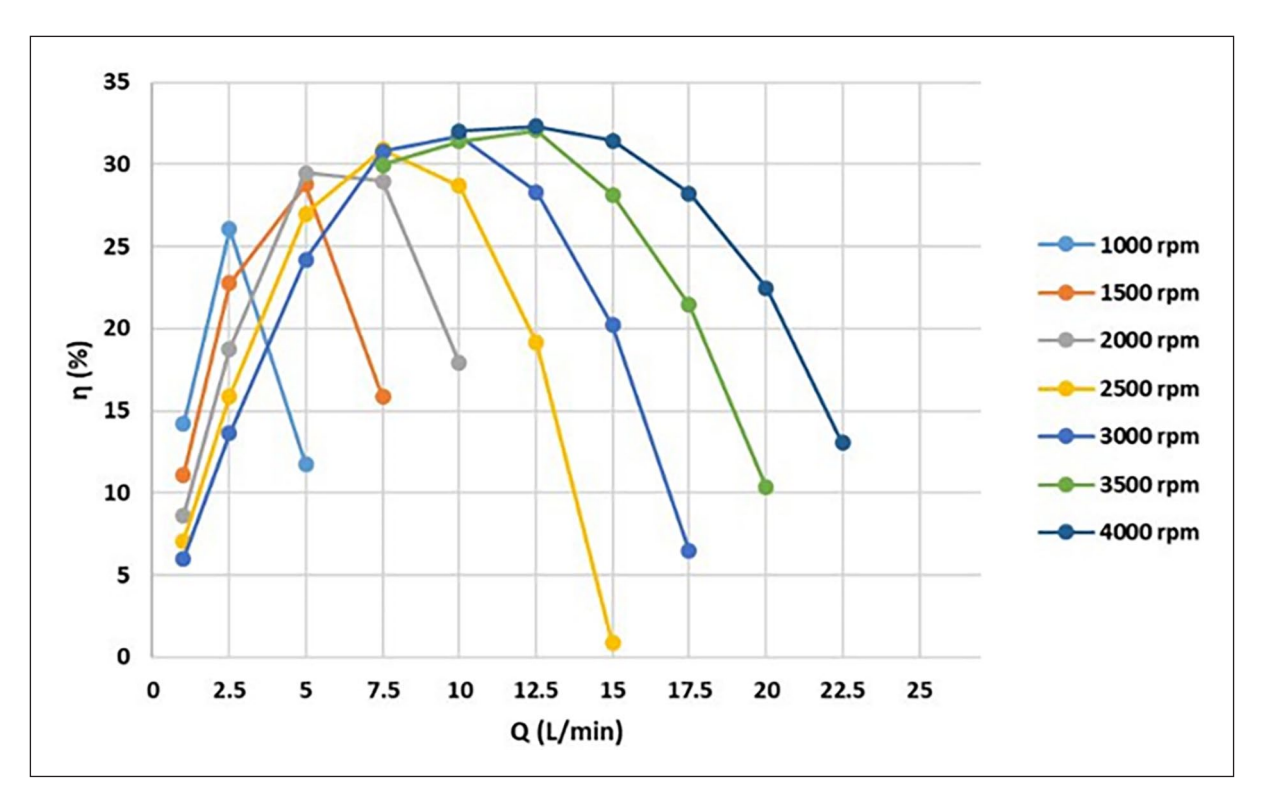


Figure 1. Hydraulic efficiency (η) of the initial RVAD prototype for different rotational speeds and flow rates (Q).

5C: IN-VITRO AND IN-SILICO MICROFLUIDIC AND CELL-CULTURE MODELS

AN IN SILICO MODEL RELATING THE MECHANICS OF CARDIOMYOCYTES TO CARDIOVSACULAR HAEMODYNAMICS FOR THE INVESTIGATION OF HEART FAILURE AND RELATED THERAPIES

Akhilesh Kamtikar¹, Dirk Donker^{1,2} and Libera Fresiello¹

¹Cardiovascular and Respiratory Physiology, Technical Medical Centre, University of Twente, Enschede, The Netherlands; ²Intensive Care Centre, University Medical Centre Utecht, Utrecht, The Netherlands

Introduction: Cardiomyocytes undergo periodic stress and strain cycles due to contraction/relaxation, cardiac chamber condition and surrounding vasculature. Heart failure, tissue remodelling, and circulatory support therapies can alter these mechanical forces. Understanding how these conditions and interventions, including mechanical circulatory support (MCS), affect ventricular mechanics is crucial for developing new therapies for heart failure. This study aims to create a novel simulator integrating the TriSeg model (TSM) of cardiomyocyte mechanics [1] with a cardiovascular simulator (CVS) model [2]. This combined platform allows for in silico representation of different pathophysiological conditions at the systemic level, with the CVS modelling effects on the myocardium and vasculature, while the TSM computes stress and strain on cardiac myofibers.

Methods: The CVS is a closed-loop lumped parameters model that incorporates the four heart chambers and the systemic and pulmonary circulation. The TSM is a representation of ventricular mechanics, split into left and right free walls and interventricular septum, with each component represented by a simplified spherical geometry. The CVS and the TSM were integrated and interfaced in LabVIEW so that the global ventricular pumping activity could be related to the myofiber contracting and relaxing status in each myocardial wall component. Specifically, the CVS provided geometric inputs (ventricular and septal wall volumes) to the TSM, which in turn calculated the corresponding myocardial stress and strain values while satisfying the law of conservation of energy. The CVS was tuned to reproduce the haemodynamic of a healthy subject, and the resulting ventricular stress and strain were retained from the TSM.

Results: The CVS reproduces the general hemodynamic condition of the healthy subject in terms of cardiac output (6.9 L/min), mean systemic arterial pressure (105 mmHg), left and right ventricular volumes (49- 142 ml, 39-136 ml). The TSM provides physiologically relevant values of strain, such as 15% in the left ventricle, 20% in the septum, and 27% in the right ventricle, for accurate normal heart geometric input parameters. The TSM also produces plausible stress-strain waveforms for the cardiomyocytes, that reflect the pressure-volume simulated by the CVS for every simulated heartbeat. Furthermore, insights are provided by the TSM into geometrical parameters of the ventricular walls, with the curvatures obtained being 30 m-1, 20 m-1, and 24 m-1 for the left, right and septal wall, respectively [1].

Discussion: The integrated CVS-TSM simulator offers a comprehensive in silico platform for analysing patient haemodynamic and cardiac myofiber mechanics. While the TSM uses a simplified cardiac geometry for efficient computation and real-time simulation, it provides valuable insights into myofiber stress and strain. The present model will be used to simulate heart failure and investigate the impact of MCS on myocardial stress and strain at different support levels, along with other important parameters such as the geometry of the ventricular walls. By assessing ventricular remodelling and wall motion abnormalities, the model can improve the understanding and optimization of MCS device settings and help reduce the risk for cellular injury. The incorporation of patient-specific data could also be a possibility, with the potential to pave the way

for personalised therapy. This may lead to a better understanding of how different MCS modalities affect the myocardium, ultimately contributing to improve clinical outcome for patients undergoing this therapy MCS.

References

- 1. Lumens et al, Ann Biomed Eng, 37: 2237-2255, 2009
- 2. Fresiello et al, Front. Physiol. 13-2022

Acknowledgements

The work was supported by the UT starter grant.

IN VITRO ASSESSMENT OF CATECHOLAMINE ADSORPTION PROFILES DURING HEMOADSORPTION THERAPY

Andreas Körtge 1,2, Christoph Kamper 1,2, Gerd Klinkmann 1,3,4

¹Department of Extracorporeal Therapy Systems, Fraunhofer Institute for Cell Therapy and Immunology IZI, Germany; ²Division of Nephrology, Center for Internal Medicine, Rostock University Medical Center, Germany; ³Department of Anaesthesiology, Intensive Care Medicine and Pain Therapy, Rostock University Medical Center, Germany ⁴International Renal Research Institute of Vicenza, Italy

Introduction: Hemoadsorption is gaining prominence as an adjunctive therapy in critical care, offering potential benefits in managing systemic inflammation and sepsis. However, its non-selective nature raises concerns about the unintended removal of essential medical substances, which may result in underdosing and adverse clinical outcomes. This in vitro study investigates the adsorption characteristics of two vital catecholamines, epinephrine (E) and norepinephrine (NE), which play a critical role in maintaining hemodynamic stability in critically ill patients.

Methods: The test setup is shown in Figure 1. Miniaturized versions (60 mL sorbent) of the CytoSorb were used in an in vitro circuit with 1 liter of EDTA- anticoagulated human whole blood. The blood was spiked with the respective catecholamine (E: 20 ng/mL; NE: 100 ng/mL) and circulated for 5 h at a flow rate of 40 mL/min. To compensate oxidation and light-induced degradation, catecholamines were continuously infused into the circuit at rates determined by preliminary experiments (E: 15 μ g/h; NE: 17 μ g/h). Samples were taken at the inlet and outlet of the adsorber after 0, 5, 15, 30, 60, 120, and 300 minutes, centrifuged, and stored at -20 °C until analysis. Control samples were taken at the start and kept at 37 °C until the end of the experiments. Experiments were conducted in duplicate, with catecholamines measured using high-performance liquid chromatography and electrochemical detection.

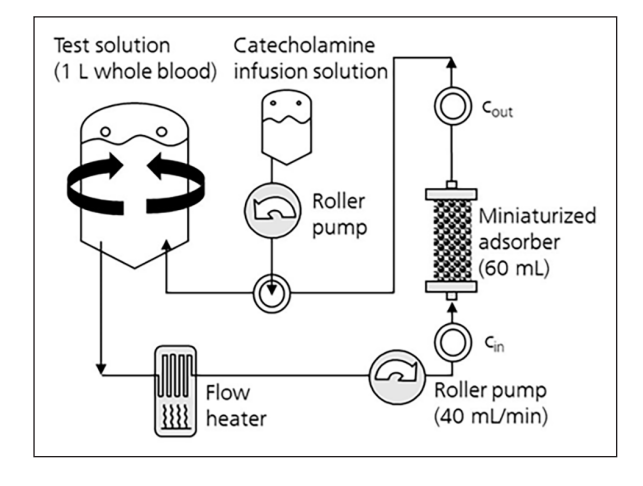


Figure 1. Test setup.

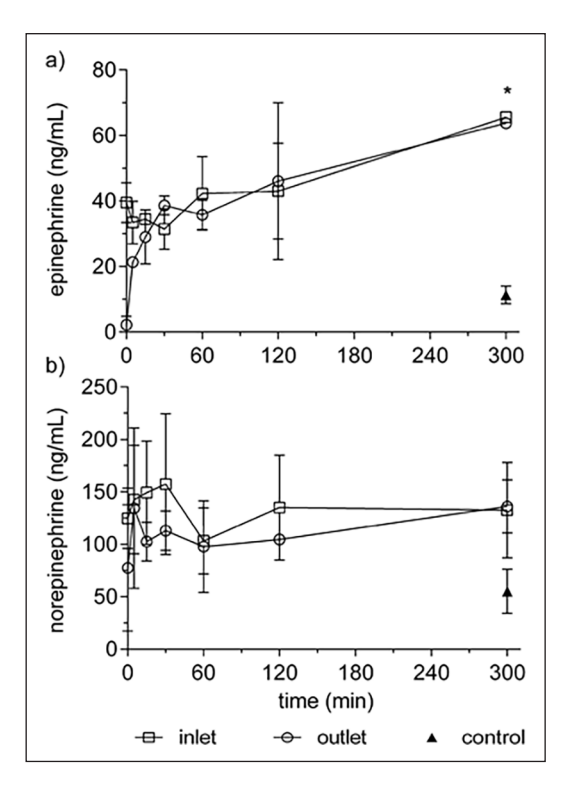


Figure 2. Epinephrine (a) and norepinephrine (b) concentration-time curves (mean+/-SD, n=2). *n=1 for the sampling time 300 min.

Results

The concentration-time curves for both catecholamines are shown in Figure 2. The curves indicate that neither E nor NE are considerably removed by the CytoSorb.

Discussion: This in vitro study demonstrates that CytoSorb has minimal impact on the removal of epinephrine and norepinephrine. Clinically, this supports the feasibility of maintaining standard dosing protocols for hemodynamic stabilization in critically ill patients undergoing CytoSorb therapy. Notably, clinical evidence consistently highlights CytoSorb's role in enhancing hemodynamic stability, often accompanied by a reduced need for catecholamines in unstable patients, further underscoring its therapeutic value in critical care [1,2].

References

- 1. Rugg et al, Biomedicines, 8(539), 2020.
- 2. Boss et al, PLoS One 16(2), 2021.

TOWARDS 3D IN VITRO PERSONALIZED TUMOR MODELS: CHARACTERIZATION OF BIOPRINTED GLIOBLASTOMA TISSUE

Mariachiara Buccarelli¹, Giorgia Castellani¹, Quintino Giorgio D'Alessandris², Giuseppe D'Avenio³, Carla Daniele³, Eleonora Petrucci¹, Enza Cece³, Evaristo Cisbani³, Antonella Rosi³, Giovanna Marziali¹, Lucia Ricci-Vitiani ¹

¹Department of Oncology and Molecular Medicine, Istituto Superiore di Sanità, Rome, Italy; ²Institute of Neurosurgery, Catholic University School of Medicine, Rome, Italy; ³National Center for Innovative Technologies in Public Health, Istituto Superiore di Sanità, Rome, Italy

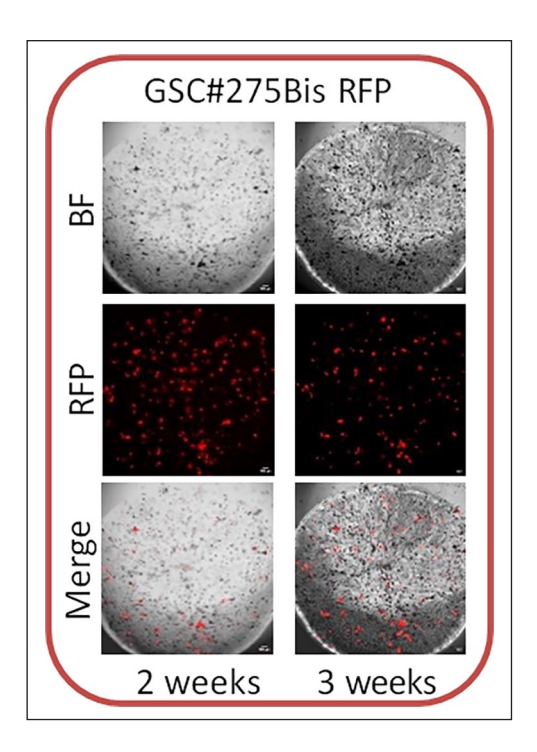


Figure 1. Evolution of GBM stem-like cells (RED), at 2 and 3 weeks after bioprinting with GelMA. Upper, central and bottom panels: brightfield, fluorescence (RFP) and merged images, respectively.

Introduction: *In vitro* modelling of tumors is faced with several challenges. Traditionally, 2D experiments have been carried out, but this approach is currently seen as insufficient to reliably replicate the 3D environment of tumoral cells. Moreover, tumoral tissue is composed by different cell lines, each one of which is possibly marked by genetic heterogeneity, adding up to experimental complexity. As a preliminary step in view of trustworthy *in vitro* modelling of brain tumors, we characterised bioprinted constructs containing patient-derived glioblastoma (GBM) stem-like cells.

Methods: We collected 123 tumor samples from adult glioblastoma (GBM) patients. About 30% of samples included in this collection was characterized by: 1) NMR spectroscopy for metabolic profiling; 2) flow cytometry for immunoprofiling; 3) RNASeq for transcriptomic profiling. GBM stem-like cell (GSC) lines derived from the same samples were analyzed for transcriptomic profiling. This cohort of 35 samples includes 16 females (43.2%) and 21 males (56.8%), with a median age of 61 years and a mean age of 59.9 \pm 11.9 years.

Bioprinting based on Digital Light Processing (DLP) was used to fabricate patient-derived-cell- laden scaffolds, with a cylindrical geometry in which 30- and 50- μm microchannels were alternately arranged in a square lattice, for maximizing solute transport between construct and medium. Gelatin methacryloyl (GelMA) was selected as bioink, given its remarkable compatibility with cells upon bioprinting. Fluorescently labeled patient-derived GBM stem- like cells (GSCs) were cultured in GelMA scaffolds up to three weeks. Representative images were recorded at different time points, under an inverted fluorescence microscope equipped with phase contrast (brightfield, BF) at 5x magnification (Thunder Imager DMi8 Fluorescent Microscope, Leica).

Results: The bioprinting-related stress on the cellular part of the constructs was seen to be negligible: a non-decreasing viable cell density was observed, up to 3 weeks post-printing.

Discussion: The preliminary investigation confirmed the potential of DLP-based bioprinting in crafting tumoral tissues with a controlled 3D

architecture. The extension to constructs with additional cell lines (i.e., endothelial cells) aimed at reproducing the tumor microenvironment is ongoing.

Acknowledgements

This work was supported by the Project PNC 0000001, **D3 4 Health**, "Digital Driven Diagnostics, Prognostics and therapeutics for Sustainable Health Care", funded by the "Piano nazionale per gli investimenti complementari al PNRR", supported by the European Union – NextGenerationEU.

IMMUNE-ENDOTHELIAL CO-CULTURE MODEL WITH MADCAM-1 TO STUDY VEDOLIZUMAB RESPONSE IN CROHN'S DISEASE

Gloria Krajnc^{1,3}, Boris Gole¹, Uroš Potočnik^{1, 2, 3}

¹Centre for human molecular genetics and pharmacogenomics, Faculty of Medicine, University of Maribor, Slovenia; ²Laboratory for Biochemistry, Molecular Biology and Genomics, Faculty of Chemistry and Chemical Engineering, University of Maribor, Slovenia; ³Department for Science and Research, University Medical Centre Maribor, Slovenia

Introduction: Crohn's disease (CD) is a chronic, immune- mediated inflammatory condition of the gastrointestinal tract [1]. Vedolizumab (VDZ), a biologic used to treat CD, blocks interaction between $\alpha 4\beta 7$ integrin on leukocytes and mucosal addressin cell adhesion molecule-1 (MAdCAM-1) on endothelial cells, thereby preventing leukocyte trafficking to the gut and thus excessive inflammation. Despite its efficacy, primary non-response occurs in up to 40% of patients [2]. Our goal is to develop a reliable immune-endothelial co-culture model that mimics the environment of intestinal blood vessels surrounding the inflamed gut of CD patients. The model addresses the lack of predictive biomarkers for VDZ treatment response and MAdCAM-1 expressing endothelial cell lines. By incorporating these cells, it will allow us to predict treatment response in VDZ-naïve patients, explore VDZ response mechanisms, aid biomarker discovery, and advance personalized CD treatment strategies.

Methods: The model is based on a "transwell" system with collagencoated porous inserts (upper chamber) seeded with BOECs transiently transfected to express MAdCAM-1. When BOECs are unavailable, they are substituted with human microvascular endothelial cells-1 (HMEC-1). stably transfected to express MAdCAM-1, and confirmed to form a tight monolayer (ZO-1 staining). The upper chamber therefore simulates a blood vessel environment in which PBMCs are introduced to study leukocyte transmigration. When using the model, venous blood is obtained from CD patients, and PBMCs and BOECs will be isolated. Tumour necrosis factor-alpha (TNF α) is added into the lower chamber as chemoattractant for leukocytes, mimicking the inflamed gut. Moreover, the effect of VDZ on PBMC transmigration is assessed, with responders showing fewer PBMCs in the bottom chamber than non-responders. Transmigration (+/- VDZ) is quantified with Alamar Blue, and transmigrated cell types identified using flow cytometry and immunofluorescence microscopy (IFM). Molecular pathways tied to therapeutic response are analysed using qRT-PCR, RNA-seq, .IFM, and Western blot.

Results: We successfully implemented a BOEC isolation method from a healthy donor in our laboratory and optimized a protocol to obtain a continuous endothelial cell layer with HMEC-1. The formation of tight junctions confirmed its integrity, ensuring the prevention of passive PBMC leakage. We also determined the optimal TNF α concentration and duration of exposure to induce PBMC transmigration while maintaining viability of both incorporated cell types.

Discussion: Models in recent studies assess only PBMC attachment to MAdCAM-1 immobilized on glass and do not evaluate physical

transmigration in the presence of VDZ [3]. Furthermore, no endothelial cell lines or BOECs have been transfected with MAdCAM-1 until now. Therefore, more complex models like ours are needed-enabling active PBMC transmigration after attachment, mimicking the effect of CD, and ultimately allowing prediction of patient response to VDZ treatment.

References

- 1. M. Luzentales-Simpson et al, Front. Cell Dev. Biol., 9:612830, 2021.
- 2. B. Verstockt et al, Clin. Gastroenterol. Hepatol., 18:5, 2020.
- 3. C. Allner et al, BMC Gastroenterol., 20:103, 2020.

STUDY OF EMBOLIC AGENT INJECTION VIA A MICROFLUIDIC-BASED MODEL OF A VASCULAR NETWORK

Julien Massoni^{1,2}, Rachid Jellali¹, Gwenaëlle Bazin², Anne-Virginie Salsac ¹

¹-Université de Technologie de Compiègne, CNRS, Biomechanics and Bioingineering (UMR 7338), France; ²-Research and Innovation Department. Guerbet. France

Introduction: A new indication of vessel embolization concerns the treatment of joint pain commonly associated with musculoskeletal disorders. It involves the intra-arterial injection of an embolic agent meant to be temporary, but capable to occlude neovessels for enough time to destroy the associated sensory nerves. An emulsion prepared by mixing two contrast agents, one oily (Lipiodol) and one aqueous, is used as an embolic agent. Clinical trials demonstrated its safety and its efficacy in reducing pain. To better understand the mechanisms involved, a microfluidic model of a simple vascular network was developed and used to measure the resident time of the embolizing solution and study the influence of the geometry, fluid and flow conditions.

Methods: A polydimethylsiloxane (PDMS)-based microfluidic chip was prepared using photolithography and replica molding.1 The geometry was selected to mimic vessels. To obtain a hydrophilicity comparable to that of vascular endothelium (which has a contact angle of about 30°), a copolymer PDMS-(polyethylene glycol) (PDMS-PEG) was added to PDMS and the chip was treated with plasma.2,3 Blood was mimicked with a mixture of water and glycerol of viscosity 4.7 mPa.s. The model blood was at a flow rate fixed of 10.5 μ L/min. The embolizing fluid is injected selectively into one branch of the chip and its evacuation is monitored

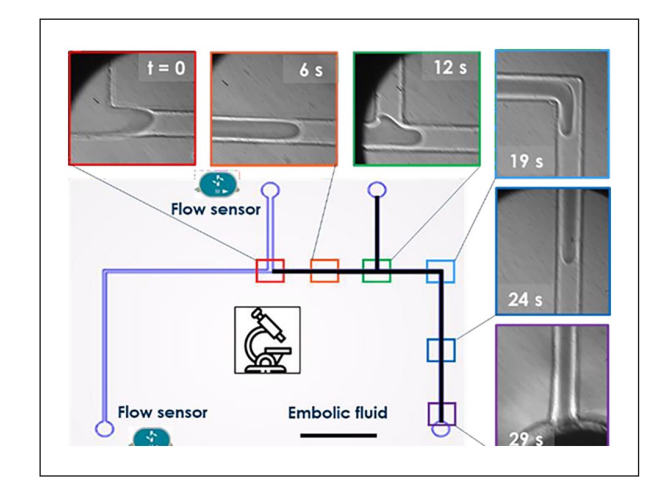


Figure 1. Evacuation of an aqueous fluid (600 mPa.s) observed under microscope.

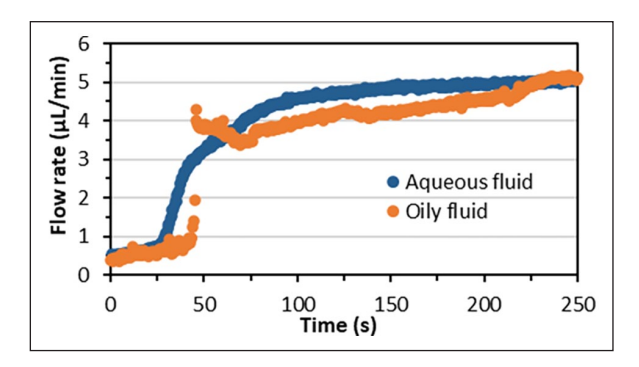


Figure 2. Kinetics of evacuation in the embolized branch upon injection of a 600 mPa.s embolic agent.

with a microscope. Flow sensors are placed in the embolic free branch and at the model blood entry (Figure 1).

Results: After plasma treatment, the PDMS contact angle decreases from $105 \pm 4^{\circ}$ to $78 \pm 16^{\circ}$. The higher the PEG concentration in the formulation, the greater the angle reduction. To maintain the angle as low as possible, the microfluidic chips are stored in pure water. Compared to ethanol and air, it is indeed the most efficient storage medium, as the PDMS/PDMS-PEG (0.3%w) chips keep a contact angle below $19 \pm 4^{\circ}$ for 2 weeks. Various oily and aqueous fluids were injected into the microfluidic chip. As shown in Figure 2, the flow rate is progressively restored as the plug is evacuated. The higher the fluid viscosity, the slower the return to the initial flow rate. At similar viscosities, oily embolic fluids reduce the flow rate more efficiently than aqueous embolic fluids.

Discussion: After the injection of the embolic fluid, the flows depart from the evenly distributed case between the two branches of the microfluidic chip. Since the embolic agent is more viscous than blood, its presence leads to a reduction in flow rate in the branch with the embolic. The time required to remove the embolic is a function of the viscosity and phase of the injected fluid.

References

- 1. Puryear III, & al, Micromachines 2020, 11 (8), 730.
- 2. Sherman, I. A, Microvasc Res 1981, 22 (3), 296–307.
- 3. Gökaltun, A, & al. Sci Rep 2019, 9 (1), 7377.

Acknowledgements

This work has been supported by the ANRT (Association nationale de la recherche et de la technologie) through CIFRE funding.

6A: EUROELSO

AN IN SILICO – IN VITRO CARDIOVASCULAR SIMULATOR WITH AN ULTRASOUND COMPATIBLE 3D AORTA PHANTOM FOR THE INVESTIGATION OF VA-ECMO

Alessia Ferranti^{1,2}, Hadi Mirgolbabaee³, Erik Groot Jebbink³, Vincenzo Piemonte², Dirk W. Donker^{1,4} and Libera Fresiello¹

¹Cardiovascular and Respiratory Physiology, University of Twente, Enschede, the Netherlands; ²Unit of Chemical-physics Fundamentals in Chemical Engineering, Department of Engineering, University Campus Bio-Medico of Rome, Italy; ³Multi-Modality Medical Imaging Group, TechMed Centre, University of Twente, Enschede, The Netherlands; ⁴Intensive Care Centre, University Medical Centre Utrecht, Utrecht, the Netherlands

Table 1. Mean pressure (MAP), pulse pressure (PP), right atrial pressure (RAP), LV/VA-ECMO flow ratio (QLV/QE), end-diastolic LVvolume (EDV).

	MAP [mmHg]	PP [mmHg]	RAP [mmHg]	QLV/QE [-]	EDV [mL]
CS	58.5±0.3	29.4±0.3	7.1±0.0	NA	127±0
Test1	59.5 ± 0.2	26.3 ± 0.3	5.3 ± 0.0	3.0	127 ± 0
Test2	67.0±0.0	19.5 ± 0.5	3.1 ± 0.0	0.6	131±0
Test3	53.8 ± 0.1	6.2 ± 0.2	$0.7\!\pm\!0.0$	0.0	137±0

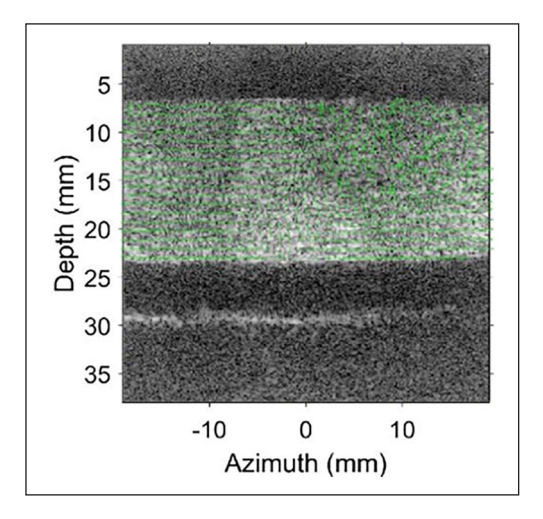


Figure 1. Watershed in the 3D aorta for Test1.

Introduction: Veno - arterial extracorporeal membrane oxygenation (VA-ECMO) is an effective therapy for cardiogenic shock (CS) patients. The management of this therapy is challenging, due to the complex interaction between the left ventricle (LV) and the device pumping blood into the aorta, in adjacent anatomical regions and in opposite direction to one another. Aim of this work is to investigate these complex hemodynamics and flow patterns using an in silico — in vitro cardiovascular simulator.

Methods: The simulator is a further development of an already validated system [1]. The in silico part is a closed loop lumped parameter model of the 4 heart chambers, pulmonary and systemic circulation. It is tuned to reproduce the hemodynamic condition of a CS patient, whose target values are obtained by averaging the data of 10 literature papers. The in silico model is interfaced with an in vitro system bidirectionally and in real time. This has 3 hydraulic chambers: one mimics the right atrium, the other two create a physiological flow into a 3D aorta phantom. This phantom is implemented in silicone through a mold casting technique, with the geometry of a generic subject and a compliance of 1.2 mL/mmHg. The VA-ECMO is connected to the hydraulic right atrium and to the descending 3D aorta, to simulate a peripheral arterial cannulation. Tests are executed for different LV contractilities and VA-ECMO speeds, to progressively reduce LV output until the aortic valve (almost) does not open. For each test, hemodynamic measurements are collected and high framerate ultrasound particle imaging velocimetry system (Vantage 256 research) is conducted on the 3D aorta.

Results: Tests refer to: CS, CS+VA-ECMO 1.0 L/min (Test1), CS+VA-ECMO 3.5 L/min (Test2), CS+VA-ECMO 5.0 L/min + worse LV contractility (Test3).

Discussion: The hemodynamic data evidences a reduction of MAP, PP and RAP for decreasing QLV/QE. EDV increases with VA-ECMO support, as the LV pumps against a higher afterload with an impaired contractile function. This effect is exacerbated in Test3, where the LV has a strongly impaired contractility. These hemodynamic findings are corroborated by the ultrasound measurements: a watershed is observed in the aorta phantom, as a result of the LV and VA-ECMO pumping in opposite directions. The watershed moves closer to the aortic valve in Test 2 and disappears in Test 3. Overall the simulator offers a high-fidelity anatomical and physiological test bench, suitable for the hemodynamic and ultrasound investigation of VA-ECMO and other medical devices.

References

1 Fresiello et al. Front. Physiol. 13 – 202, 2022.

6B: DIALYSIS IMPROVEMENTS & CLINICAL STUDIES

IN-VITRO PERFORMANCE OF THE NEOKIDNEY™ PORTABLE HD DEVICE UNDER VARIOUS SIMULATED PATIENT CONDITIONS

Christian G. Blüchel¹, Paiboon Khaopaibul², Han Jie Tan², Yu En Toh², Jacobus A.W. Jong³

¹Nextkidney S.A., Switzerland; ²Nextkidney SG, Singapore; ³Nextkidney B.V.. The Netherlands

Background and Aim: The Neokidney is a miniaturised dialysis device intended for Short Daily Hemodialysis (SDHD). Neokidney requires only 4.5L of dialysate to generate a total of 36L for each therapy. This is achieved by continuous regeneration of spent dialysate in a sorbent cartridge (SC), re-using the fluid multiple times rather than discarding it after only one single use. The device has been successfully tested in 2 clinical studies involving a total of 7 patients [1, 2].

The objective of this in vitro study was to test the latest Neokidney development prototype in a matrix of simulated standard and extreme SDHD conditions, covering most of the expected patient conditions.

Methods: The test setup replicated the Neokidney therapy setup, but replaced the "Patient" with a carboy containing 40L of a dialysate solution. This represented the combined fluid of blood and body water, and the total amount of dissolved uremic toxins in a 70Kg patient. During the experiment, this simulated patient fluid was continuously dialysed through a standard high-flux hemo- dialyser (Fresenius FX80), at a flow rate of 300mL/min. The dialysate side of the dialyser was connected to the Neokidney dialysate circuit, where spent dialysate was continuously regenerated in the sorbent cartridge.

The simulated patient conditions were chosen to map out the expected patient conditions for typical SDHD therapies. Four serum biochemical parameters were identified as crucial (Na $^+$, HCO3 $^-$, Urea and K $^+$), and were each varied to reflect minimum, normal, and maximum expected concentrations. The test results were evaluated for biochemical stability, with particular attention on acid-base balance.

Results: All SDHD experiments proceeded with efficient toxin clearance (reduction ratios of approx. 50% for urea, creatinine and phosphate). The post-dialysis Na-, HCO3 and Cl- concentration in the simulated patient remained mostly within +/- 1mmol of the pre-dialysis concentration. Most experiments proceeded with a net release of 0 – 40mmol HCO3 to the "patient". Exceptions were the high-urea experiment, which provided a net release of 86mmol of bicarbonate to the patient, and the low- urea experiment, which proceeded with a slight net removal of 30mmol from the patient. The dialysate Na concentration followed the intended isonatraemic behaviour, i.e. it adjusted within 15min to the simulated patient's pre-dialysis Na concentration and then remained approx. stable at that concentration. Three experiments had detectable

Table 1. Variable parameters (in mmol/L) for simulated patient plasma concentrations.

	Na	HCO3	Urea	К
Low (L) Normal (N)	125 138	14 22	15 20	3.5 4.5
High (H)	145	30	25	5.5

amounts of ammonia in dialysate towards the end of the experiments (all below the specified limit of 20ppm).

Discussion: The present study was based on a single point variation matrix, representing the minimum set of conditions for probing the proposed range of patient conditions. Within this set, the Neokidney system met its design specifications in all simulated patient conditions.

The experimental setup had some shortcomings, such as a missing representation of the 2- compartment-model and missing respiratory contributions to acid/base equilibria which would be found in a real patient. Nevertheless, it allowed a clear view on the corresponding equilibria on the dialysate side, on toxin removal efficacy, and on the behavior of the sorbent cartridge under the tested conditions.

Future studies will be conducted on the final configuration of the device, and will include a broader set of simulated patient conditions with multiple variations of plasma parameters

References

- Lau TW et al., Journal of the American S ociety of Nephrology. 2024:35.
- Ficheux M. 9ÈME ,CONGRÈS ANNUEL DE LA SFNDT. Bordeaux; 2024.

particularly for startups as well as small and medium enterprises (SMEs), which typically have limited resources to bridge the "valley of death" between product development and start of product sales. Unfortunately, disruptive technologies are by definition not yet included into existing regulations and standards [1].

Methods: Fortunately, most existing *national* regulations typically point to *international* standards that describe requirements to establish compliance. When working on disruptive medical technologies like Artificial Organs, it is thus wise to early involve international standards issuing bodies (see fig. 1). The Dutch national standardization institute (NEN) cooperates within the NXTGEN Hightech Biomed04 project that focuses on creating production technology of modular components for Artificial Organs, with automated cell-cultivating and artificial kidney as well as bioresorbable stents and grafts as spearpoints.

Results: Via NEN, cooperations are established with:

- IEC TC62D/MT20 Dialysis devices
- ISO/TC276/WG4 Bioprocessing for cells and related entities
- ISO TC150/SC2/WG5 Renal replacement, detoxification and apheresis
- ISO/TC150/SC2/WG7 Cardiovascular absorbable implants

See also Fig. 2.

Discussion: Participation in these standardization workgroups opens the possibility to explain new disruptive technologies and to create objective judgement criteria for notified bodies and governmental agencies that must assess new medical devices. This, in turn, shortens time to market. Furthermore, when patient organizations support the value of the developed technology, this greatly increases the chance of reimbursement by payor parties (e.g. health care insurers).

when writing a research proposal, another reason to pay attention to standardization is that the European Union recently has published a report which pronounces the weight of this aspect when assessing research proposals: "It is recommended to analyse the existing standards landscape and assess the contribution which standardization can

INTERNATIONAL STANDARDIZATION FOR ARTIFICIAL ORGANS

Fokko Wieringa^{1, 2}, Suzie Noten³, Saliha Lalout³

¹IMEC, Netherlands; ²UMC Utrecht, Netherlands; ³Dutch Standardization Institute (NEN), Netherlands

Introduction: International differences in regulations create additional complexity and costs for medical device developers. This holds

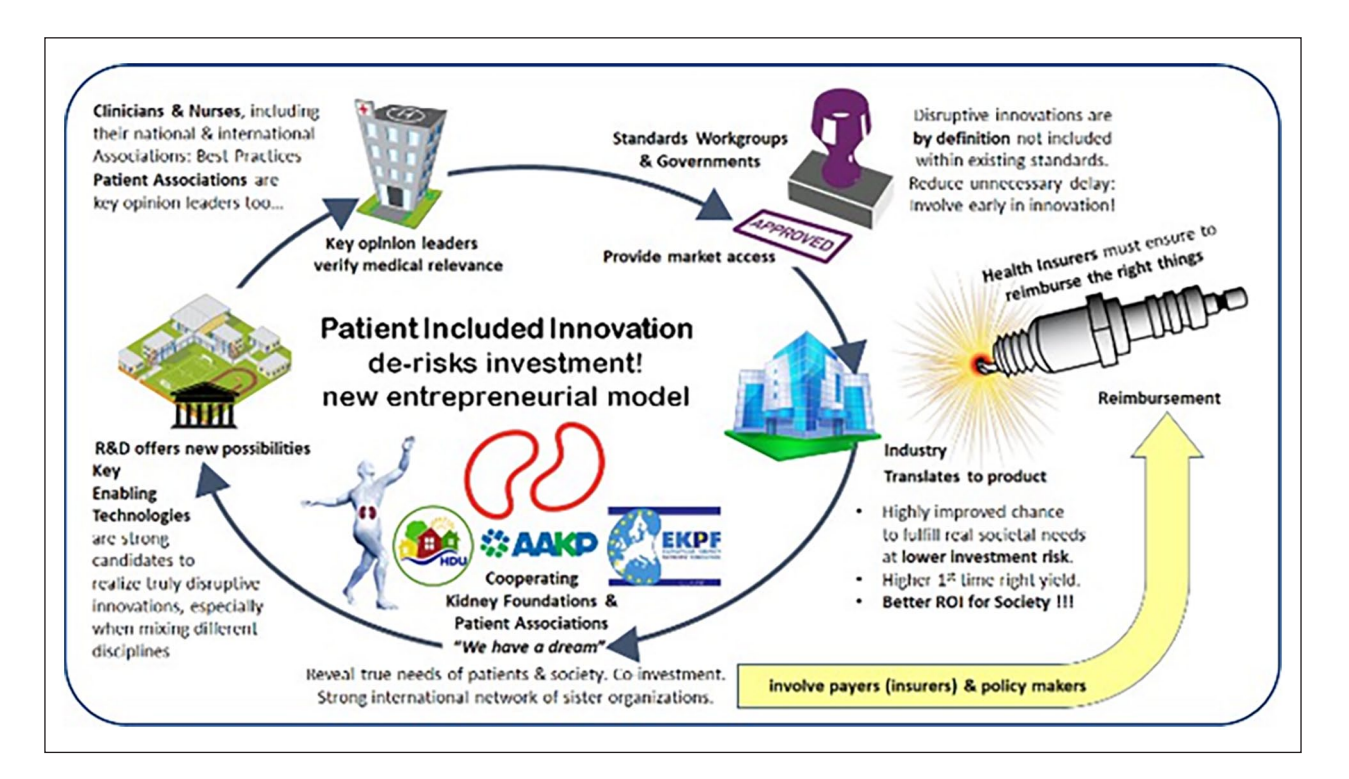


Figure 1. Proper attention for standardization helps to de-risk investments for industrial parties, while involving patients in the process increases the chance to create a "first-time-right" solution [2].

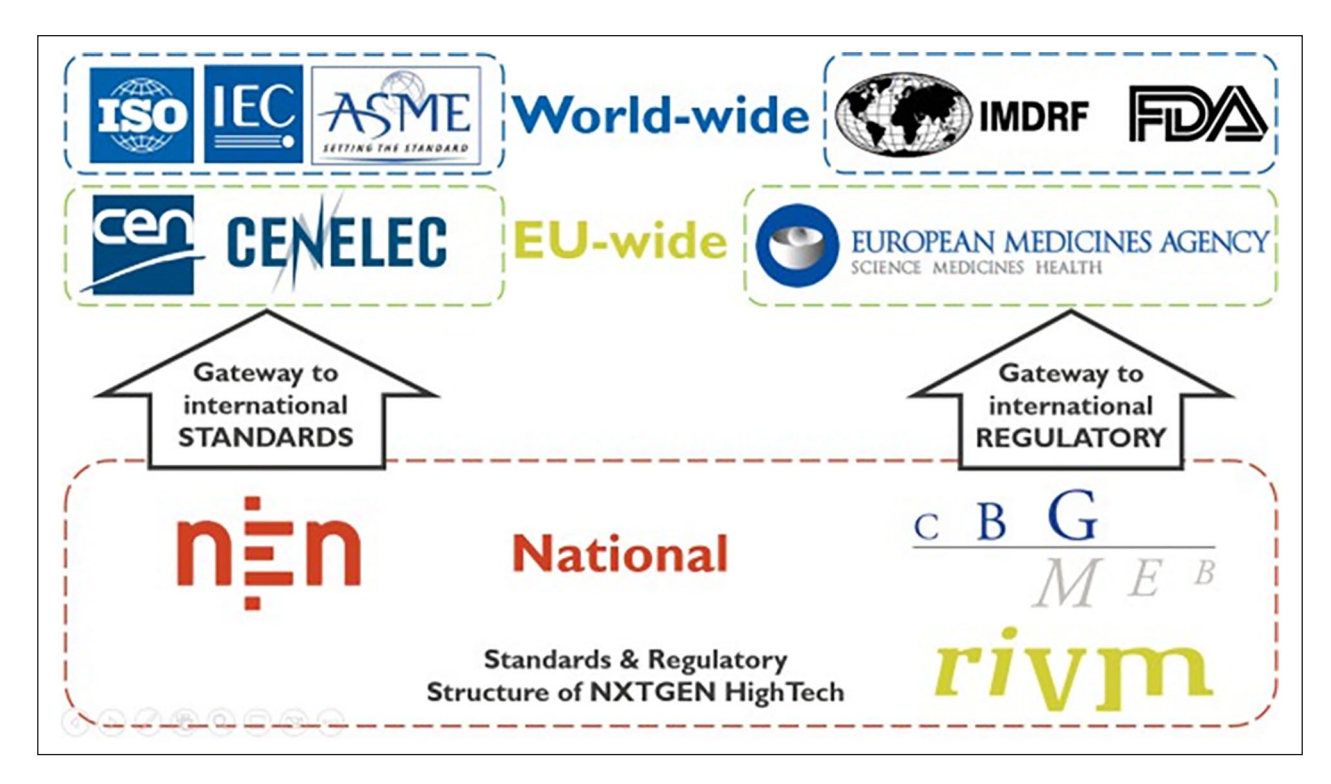


Figure 2. NXTGEN Hightech is an R&D project that leverages standardization to speed-up time-to- market by early involvement of standardization workgroups in disruptive medical technology.

offer to the research and innovation project" as well as "in case of a collaborative project, it is recommended to create in the consortium a common understanding as well as a common strategic position on standardization and standardization issues" [3].

References

- Wieringa et al, Clinical Kidney Journal, 2023, vol.16, no.6, 885–890, 2023.
- 2. Wieringa et al, Artificial Organs, 44:111–122, 2020
- EU Commission, Off. Journal of the European Union, Commission Recommendation (EU) 2023/498, 2023.

Acknowledgements

We acknowledge financial support from the Dutch National Growth Fund (project NXTGEN Hightech).

ALBUMIN LEAKAGE DURING HEMODIALYSIS: A NOVEL OPTICAL DETECTION APPROACH

Jana Holmar¹, Annika Adoberg^{1, 2}, Liisi Leis^{1,2}, Merike Luman^{1,2}, Joosep Paats¹, Kristjan Pilt¹, Risto Tanner ¹, Ivo Fridolin ¹

¹Tallinn University of Technology, Department of Health Technologies, Tallinn, Estonia; ²Centre of Nephrology, North Estonia Medical Centre, Tallinn, Estonia

Introduction: Roughly 13% of the population suffers from chronic kidney disease (CKD) globally [1]. To replace kidney function, hemodialysis is the primary treatment option for CKD stage 5 (end-stage renal disease - ESRD) patients. The global number of individuals receiving dialysis treatment reached 2.7 million in 2016 and is estimated to reach 5.4 million by

2030 [2]. During dialysis therapy, uremic toxins are filtered out from the blood regularly. However, during the procedure, all the substances fitting the cut-off size of the dialysis membranes are transported to spent dialysate, among them many beneficial substances, including albumin. Washout of proteins, e.g., albumin (MW 66 kDa), is considered a disadvantage of the more effective dialysis [3]. The cut-off value for super high-flux dialysis, it can reach 65 000 Da [4]. The study aimed to demonstrate the efficacy of dialysis in different modalities in particular interest of albumin loss and its detection from the spent dialysate using optical method.

Methods: The clinical study was performed in Tallinn, Estonia, and six chronic hemodialysis patients, 5 males and 1 female were included. For each patient two treatments in two different dialysis modalities were performed (hemodialysis-HD and hemodiafiltration-HDF - HDF). Two types of dialyzers (FX1000 and Theranova500) were used. Spent dialysate samples from the drain tube of the dialysis machine were taken at 5, 120, and at the end of each dialysis session (240 min). Concentrations of albumin were measured in the Clinical Chemistry Laboratory, and UV-absorbance of dialysates samples were measured with a spectrophotometer UV-3600 (Shimadzu corp., Japan) over the wavelength range 220-360 nm.

Logistic regression and Reciever Operating Characteristics (ROC) analysis was used to evaluate possibility to predict albumin content in the spent dialysate (albumin leakage).

Results: Concentration of albumin throughout dialysis procedure with different settings is given in the figure 1.

Logistic regression revealed the statistically significant parameters in the model of albumin content detection were the UV-absorbances at 225 and 240 nm. Receiver Operating Characteristic (ROC) curve was generated for albumin detection based on UV-absorbance with area under the curve (AUC) 0.893.

Discussion: The study indicates that the optical method combined with the statistical tools could be used for albumin leakage detection during hemodialysis. Although longitudinal studies are needed to evaluate the long-term impact of chronic albumin loss, in patient-tailored prescriptions with or without albumin replacement the use of MCO can be justified.

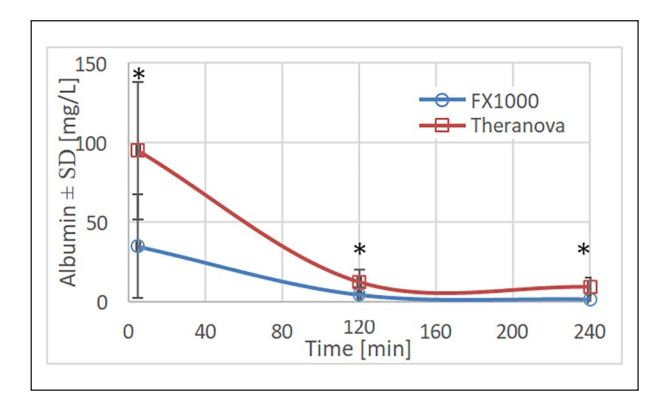


Figure 1. Mean albumin concentrations over the course of dialysis. *-results were statistically different, p < 0.05.

References

- 1. Hill, N.R. et al, PLOS ONE, 11, e0158765, 2016.
- 2. Himmelfarb, J. et al, Nat Rev Nephrol 16, 573-585, 2020.
- 3. Gayrard, N. et al, PLOS ONE, 12, e0171179, 2017.
- I. Olczyk, P. et al, Polim Med, 48, 57-63, 2018.

Acknowledgements

The research was funded by the Estonian Research Council grant PSG819.

DEVELOPMENT AND EVALUATION OF AN IN-VITRO MODEL FOR COMPARATIVE STUDIES OF MINI-DIALYZERS FOR HEMODIALYSIS

M. Torrents Yeste¹, D. Ramada¹, O.E.M ter Beek¹, J. de Vries², B.H. Lentferink², K.G.F. Gerritsen² & D. Stamatialis¹

¹Advanced Organ bioengineering and Therapeutics, University of Twente, The Netherlands; ²Department of Nephrology and Hypertension, University Medical Centre Utrecht, Utrecht, The Netherlands.

Introduction: Hemodialysis (HD) is nowadays the most used therapy option for End-Stage Renal Disease (ESRD) patients, due to the

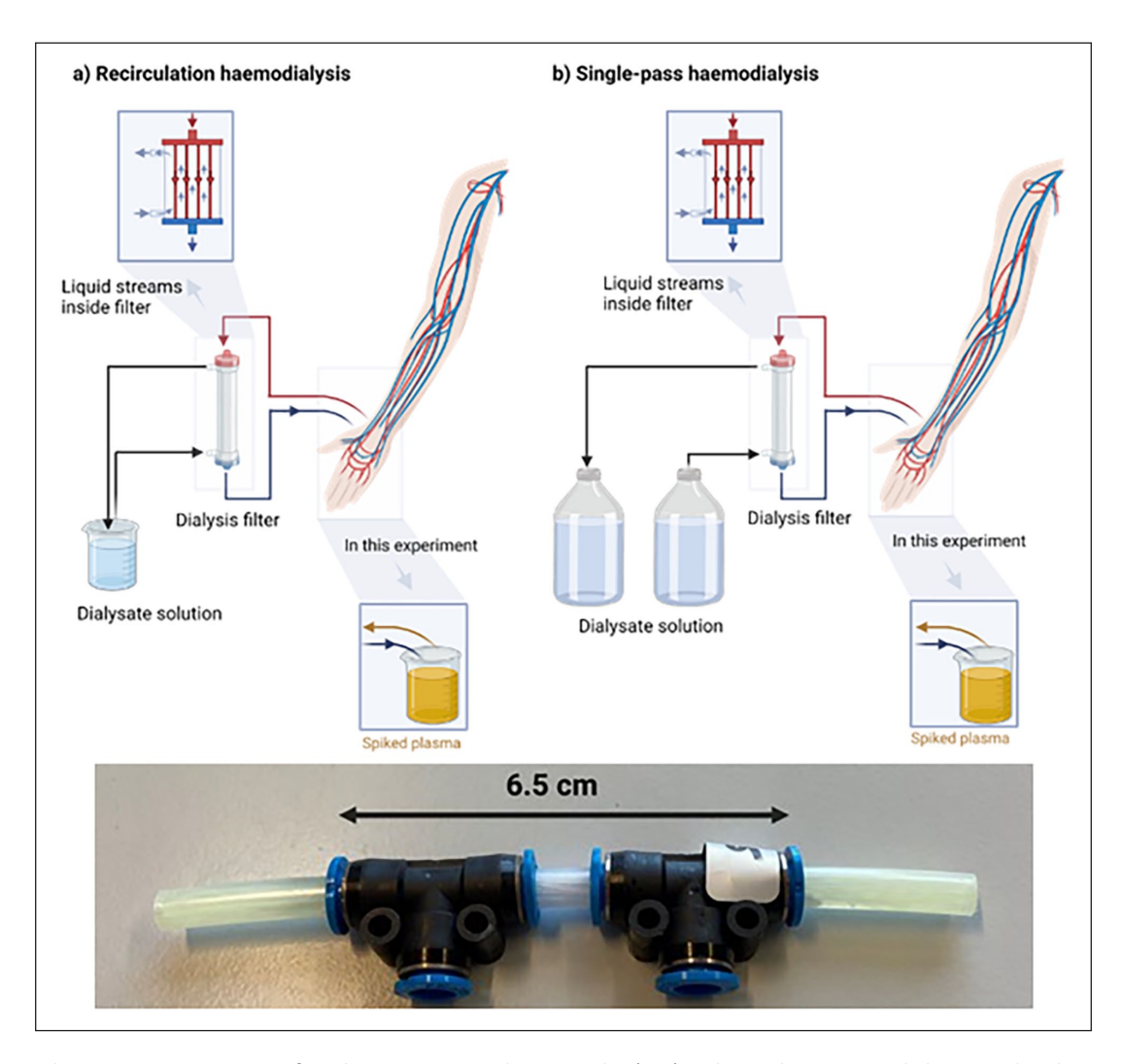


Figure 1. Schematic representation of single-pass vs recirculation modes (top) and an in-house mini- dialyzer used in this study (bottom).

low availability of donor organs [1]. However, current HD presents major drawbacks such as the non-continuous nature of the therapy (3 times a week for 4 hours each session) [1,2], and the ineffective removal of toxins, such as protein-bound uremic toxins (PBUTs) [3]. Therefore, new hemodialysis membranes and/or techniques are being developed to tackle these issues. However, there is a lack of a standardized protocol for evaluating different dialysis membranes in a comparable and reliable way.

This study aims to establish a comprehensive, in- vitro model based on mini dialyzers for comparative studies of dialysis conditions. This could be used for investigating newly developed membranes, and for comparative studies with commercially available membranes. The following HD parameters are investigated: (1) single-pass versus recirculation of the dialysate fluid, (2) flow rates of plasma and dialysate fluid, (3) direction of plasma flow; Inside-Out Filtration (IOF) versus Outside-In Filtration (OIF) application and (4) human plasma versus full human blood. Here, we investigate the above parameters using mini dialyzers prepared using hollow fiber (HF) membranes obtained from commercially available dialyzers as well as in house developed matrix membranes (MMMs), which combine adsorption and filtration for PBUTs removal.

Methods: Mini dialyzers were prepared using HF from FX1000 dialyzers (Fresenius) and MMMs (separately) with effective surface area of 1.24 cm² (6.5 cm of eff. length and 31 HF membranes). The HF membranes were characterized using Scanning Electron Microscopy (SEM). For the mini dialyzers we performed Clean Water Flux to determine the HF ultrafiltration coefficient (Kuf), and uremic toxin removal studies by tailoring the above mentioned parameters using a commercial device (Convergence).

Reverse-phase HPLC and UV-VIS (Nanodrop) measurements were used to study uremic toxin removal. For the studies with full human blood (provided by donor service of University of Twente from healthy donors) a detailed protocol for testing toxin removal was developed.

Results and Discussion: Our results show no significant difference for PBUTs removal between single-pass vs recirculation of dialysate fluid when similar intraluminal plasma flow (1 mL/min) is applied.

There is no significant difference in toxin removal when a dialyzer is operated in IOF or OIF mode (0.25 mL/min intraluminal flow and 25 mL/min extraluminal flow).

 $\ensuremath{\mathsf{MMMs}}$ improve significantly PBUTs removal compared to standard HD membranes.

References

- Stamatialis, Dimitrios, ed. Biomedical membranes and (bio) artificial organs. Vol. 2. World Scientific (2017).
- Ter Beek, Odyl, et al. Separation and Purification Technology 225 (2019): 60-73.
- Pavlenko, D. et al. New low-flux mixed matrix membranes that offer superior removal of protein- bound toxins from human plasma. Sci Rep 6, 34429 (2016).

Acknowledgements

This project is made possible in part by a contribution from the National Growth Fund program NXTGEN Hightech.

6C: (BIO)ARTIFICIAL LIVER

"AGGRAVATED SEPSIS, ACUTE KIDNEY INJURY AND MICROBIOLOGICAL RESISTANCE IN FOUR YEARS PRE-POST COVID OUTCOME STUDY"

Aleksandra Canevska-Taneska, Lada Trajceska, Zvezdana Petronijevik, Irena Rambabova-Bushljetik, Nikola Gjorgjievski, Gjulsen Selim University Clinic of Nephrology; Medical Faculty, Ss Cyril and Methodius University, North Macedonia, Republic of

Introduction: COVID 19 pandemic consequences, like the long- term alterations in the immune system and the rising trend of antimicrobial resistance after the overuse of antibiotics, it may have influenced on the incidence, manifestation, and mortality of diseases globally. The aim of our study is to compare the prevalence, etiology and outcomes of sepsis and associated AKI in pre- and post-COVID 19 era.{1}

Method: We conducted a retrospective observational analysis in 144 patients with sepsis and AKI, in two periods of time, two years before and after COVID 19 pandemic, with two years washout period. Out of 3801 hospitalisations in the pre- COVID 19 era in 50 (1,3%) and 94 (2,5%) from 3760 hospitalisations in post-COVID 19 era were diagnosed as sepsis, with urinary tract being dominant door of entrance. The patients were divided as hospitalized in pre- and post- COVID era (50(34% vs. 94 (64%)), respectively. Comparative analysis, Kaplan-Meier and Cox-Regression analysis and MAR index calculation with Kolmogorov-Smirnov one sample test were performed.

Results: Out of 144 hospitalised septic patients, 50.7% (74) were man with a mean age of 67 \pm 11.47 years. 41.1% (60) of the examined population had diabetes and 42.5% (62) had established obstructive uropathy. Blood culture test was performed in 123 (84.2%) patients in the first days of hospitalisation, and in 100 (68.5%) patients disease-causing germ was confirmed. Regarding causative agents' (positive isolates) the comparative analysis showed similar distribution in both periods, but what was worthy of attention was that the multiple antibiotic resistance index (MAR) was significantly higher in the post COVID 19 period for Staphylococcus coagulase negative (0.48 vs. 0.62, p=0.001). Striking evidence of appearance of fungi and Enterobacter cloacae as sepsis causative agents only in the post COVID 19 period was noted, indicating more immunocompromised patients in this period. In the comparative analysis the two periods did not differ in respect of age, gender, diabetes, hypertension, and malignancy, but we noted higher values of inflammatory markers – C reactive protein (192±91.70vs.268.26±12.38,p=0.001) Also our study demonstrated more severe forms of sepsis (multiorgan affection and septic shock dominating in post pandemic period (5(10%) vs. 23(25%), p=0,037).{2} According AKI staging respectively we found AKI stage 3 more frequently present after pandemic and more patients needed dialysis and died in the post COVID 19 era ((35(70%)vs.79 (84%), p= 0.04); (31(62%)vs.78 (54%), p=0.02); (16(32%) vs. 51%(54%), p=0.018)), respectively. Patients in post-COVID 19 era survived less longer (22,66 \pm 11,32 vs. 17,132 \pm 12.66, p=0,021) with almost doubled risk for mortality HR:1.977; CI [1,127 \pm 3.469], p=0.018.

Conclusion: Sepsis and associated AKI occurrence, morbidity and mortality are significantly higher in the post- COVID 19 era. The overuse of antibiotics in the pandemic and the subsequent increase the drug resistance for sure provides explanation for to the rising incidence and mortality of sepsis.

Further studies on larger groups of patients are needed to evaluate additional contributing factors, including potentially long-term impaired coagulation and immunological disorders. {3}

References

- Boccabella L et al Post-Coronavirus Disease 2019 Pandemic Antimicrobial Resistance. Antibiotics (Basel). 2024 Feb 29:13(3):233.
- Sprung et al The new sepsis consensus definitions: the good, the bad and the ugly. *Intensive Care Med* 42, 2024–2026 (2016).
- Teodoro AGF et al, Inflammatory Response and Activation of Coagulation after COVID-19 Infection. Viruses. 2023 Apr 10;15(4):938.

THE NUMBER OF APHERESIS PROCEDURES TO TREAT IMMUNE-MEDIATED NEUROLOGICAL DISEASES IS ON THE RISE

Kaatje Le Poole¹, Hans Vrielink¹, Anders Svenningsson², Bernd Stegmayr³ on behalf of the WAA registry group.

¹Sanquin Blood Supply Foundation, Unit of medical Affairs, Amsterdam, the Netherlands; ²Department of Clinical Science, Karolinska Institute, Danderyd, Sweden; ³Department of Public Health and Clinical Medicine, Unit Medicine, Umea University, Umea, Sweden

Introduction: Apheresis is applied in the treatment for many different diagnoses, especially when the conventional therapy is insufficient while in some diseases it is the first choice of treatment. The aim of this study was to investigate the extent and change over time of neurological diseases in which apheresis played a role in the treatment within the frame of the World Apheresis Association registry.

Methods: During the period 2003-2023, a total of 23,699 apheresis procedures in 2,963 patients with a neurological disease were performed. Data were collected during different periods by 44 centers, while some interrupted registration, approximately 22 centers had been registering continuously during the latest 10 years.

Results: An increase in the proportion of neurological diseases developed over the period (p<0.001) while the overall burden by apheresis procedures remained stable (p=NS). Most procedures were due to either Multiple Sclerosis (MS; n=2,665 in 17.7% of patients), Neuromyelitis Optica (NMO; n=650 in 2%), Guillain Barré (GB; n=3,247 in 30%), Chronic Inflammatory Demyelinating Polyradiculoneuropathy (CIDP; n=2,367 in 3.4%), and Myasthenia Gravis (MG; n=11,049 in 31%). A change in the proportion of these diseases was noted over time. Side effects differed significantly between the diseases (Table 1). A symptom panorama of side effect for various the diseases will be presented.

Discussion: The panorama of different neurological diseases may well cause different side effects based on the variation in neurological response to the apheresis procedure and replacement. It is favorable to expand knowledge in both fields for those who are prescribing and performing the apheresis.

Table 1. Frequency of side effects during apheresis in various diseases treated.

	Mild AE %	Moderate AE%	Severe AE%
Multiple sclerosis	3.3	1.5	0.1
Neuromyelitis optica	2.3	1.7	0.5
Guillain Barré	2.5	2.3	0.7
CIDP	2.4	1.6	0.3
Myasthenia gravis	1.9	1.1	0.2
Other diagnoses	1.8	1.3	0.4
Total	2.2	1.4	0.3

FINDING THE OPTIMAL STERILIZATION METHOD FOR HUMAN DECELLULARIZED LIVERS: ASSESSING MICROBIOME, MATRIX PROTEINS, AND BIOCOMPATIBILITY

E.V.A. van Hengel, J. Willemse, L.J.W. van der Laan, J. de Jonge & M.M.A. Verstegen

Department of Surgery, Erasmus MC Transplant Institute, University Medical Center Rotterdam Introduction: Liver tissue engineering holds great promise for addressing the growing demand for transplantable organs. Decellularization technology has been widely used to create liver matrices that may serve as native scaffolds for tissue engineering. [1] However, to meet the quality criteria toward clinical applications, it is essential to assess the presence of microorganisms and potential pathogens. Only then, safety and compliance with medical device regulations is ensured. [2] Sterilization procedures can, however, negatively impact the ECM quality. Therefore, this study aimed to evaluate the effectiveness of five sterilization techniques.

Methods: Human livers (N=3), deemed unsuitable for transplantation, were decellularized by perfusion with 4% Triton-X-100 and 1% ammonia solution. The resulting ECM was sterilized using Gamma radiation (1000 Gy), UV radiation (254 nm), exposure to Supercritical Carbon Dioxide (sCCO2), Peracetic acid (0.5%), or Antibiotic-Antimycotic (10%) treatment. The microbial burden was determined using standardized microbiological methods. The effect on the extracellular matrix composition and biomechanical properties, including collagen content, fiber orientation, and stiffness was assessed. Particularly, crosslinking or denaturation of proteins was studied using two- photon microscopy, Picrosirius Red (PSR), H&E, and Collagen IV staining. Furthermore, the biocompatibility of the sterilized matrices was assessed by analyzing cell viability after recellularization with intrahepatic cholangiocyte organoids (N=3) and HepG2 cells.

Results: Peracetic acid and UV radiation were not effective to remove micro-organisms, demonstrating a poor sterilization. Assessing how these techniques affected the ECM by nanoindentation and microscopy, demonstrated that the overall structure of collagen fibers was altered, and modifications in Effective Young's modulus and fiber-to-fiber orientation of collagens were found after exposure to UV and Gamma radiation. Cells remained viable and proliferated in all scaffolds, confirming that none of the sterilization methods affected the biocompatibility of the scaffolds.

Conclusion: Exposure to UV radiation and Peracetic acid were not effective for sterilization. However, while Gamma radiation did remove microorganisms well, this technique showed alterations in protein composition and fiber orientation. No technique hampered the biocompatibility. We therefore suggest sCCO2 or Antibiotic-Antimycotic treatment to sterilize scaffolds after decellularization as it results in an overall effective removal of pathogens, while causing only little damage to the matrix proteins. This study demonstrates the importance of sterilization of decellularized liver matrices for tissue engineering and potential clinical applications.

References

- 1. Willemse et al, Mater Sci Eng C Mater Biol Appl, 108:110200, 2019.
- 2. van Hengel et al, Bioengineering, 12(2):136, 2025.

PURIFIED GRANULOCYTES IN EXTRACORPOREAL CELL THERAPY: UNIQUE DOSING REGIMENS CHALLENGING CONVENTIONAL BLOOD PURIFICATION TECHNIQUES

Gerd Klinkmann^{1,2,3}, Sophie Brabandt¹, Marlene Möller¹, Jens-Christian Schewe¹, Jens Altrichter⁴, Steffen Mitzner^{2,5}

¹Department of Anaesthesiology, Intensive Care Medicine and Pain Therapy, University of Rostock, Germany; ²Department of Extracorporeal Therapy Systems, Fraunhofer Institute for Cell Therapy and Immunology, Germany; ³International Renal Research Institute of Vicenza (IRRIV), Italy; ⁴Department of Research and Development, Artcline GmbH, Germany ⁵Department of Medicine, Division of Nephrology, University Medical Center, Germany

Introduction: Immune cell dysfunction plays a central role in sepsis-induced immunoparalysis (1). Targeted treatment using healthy donor immune cell transfusions, in particular granulocyte concentrates (GC) potentially induces tissue damage. Initial trials using GC in an extracorporeal immune cell perfusion system provided evidence for beneficial effects with fewer side effects, by separating patient and donor immune cell compartments (2). The extracorporeal immune cell therapy is a plasma treatment technology. To date, treatment duration has been empirically set at 6 hours, although no evidence exists for specific dosing concepts (3). Thus, this *ex vivo* study examines technical feasibility and cellular effects of an extended treatment interval of up to 24 hours.

Methods: Plasma is continuously filtered from the patient's extracorporeal blood circuit and transferred into a closed-loop 'cell circuit', where the patient's plasma is brought into direct contact with therapeutically effective, human-donor immune cells. Standard GC were purified to increase the potential storage time and subsequently used in the extracorporeal immune cell perfusion system. The extracorporeal circuit, comprising three plasma filters (PF), operated as follows: PF BC separated patient's plasma from blood, PF CC1 housed donor immune cells for perfusion, and PF CC2 served as a redundant safety measure in the plasma backflow (Figure 1). A "10-hour setting" (33 ml/min plasma filtration) and a "24-hour setting" (13.5 ml/min) was defined, differing both in therapy duration and varying plasma filtration rates. After treatment, donor immune cells were discarded. Parameters assessed included phagocytosis activity, oxidative burst, cell viability, cytokine release, and metabolic parameters of purified GC.

Results: After a storage of 72 hours granulocytes were viable throughout the study period and exhibited preserved functionality and efficient metabolic activity. Lactate dehydrogenase activity as an indication for potential cell damage revealed no signs of impairment of the cells. The findings highlight a time-dependent nature of cytokine release by neutrophils in the extracorporeal circuit, as cytokine secretion patterns

showed IL-8 peaking within 6 hours, while MCP-1, IL-6, IL-1 β , and TNF- α significantly increased (p < 0,001) after 24 hours of circulation.

Discussion: Purified GC remain functional after 72 hours of storage and an additional 24 hours in the circulating treatment model. Cytokine secretion patterns showed a time-dependent response characterized by a significant increase, especially between 10 and 24 hours of treatment. Extending treatment time holds promise for enhancing immune response against sepsis-induced immunoparalysis. These findings provide valuable insights for optimizing therapeutic interventions targeting immune dysfunction.

References

- Yeghen T et al. Granulocyte transfusion: a review. Vox Sang 2001;81:87–92.
- Mitzner SR et al. Use of Human Preconditioned Phagocytes for Extracorporeal Immune Support: Introduction of a Concept. Therapeutic Apheresis and Dialysis. 2001;5:423–32.
- Sauer M et al. Bioartificial Therapy of Sepsis: Changes of Norepinephrine-Dosage in Patients and Influence on Dynamic and Cell Based Liver Tests during Extracorporeal Treatments. BioMed Res Int. 2016

NORMOTHERMIC MACHINE PERFUSION OF EXPLANTED HUMAN METABOLIC LIVERS: A PROOF OF CONCEPT FOR STUDYING INBORN ERRORS OF METABOLISM

Riccardo Cirelli^{1,2}, Gionata Spagnoletti^{1,2}, Diego Martinelli³, Giulia Bravetti⁴, Paola Francalanci⁵, Annamaria D'Alessandro⁶, Giovina Di Felice⁶, Marta Maistri^{1,2}, Elena Baldissone ¹, Alberto M Fratti^{1,2}, Raffaele Simeoli³, Elisa Sacchetti³,

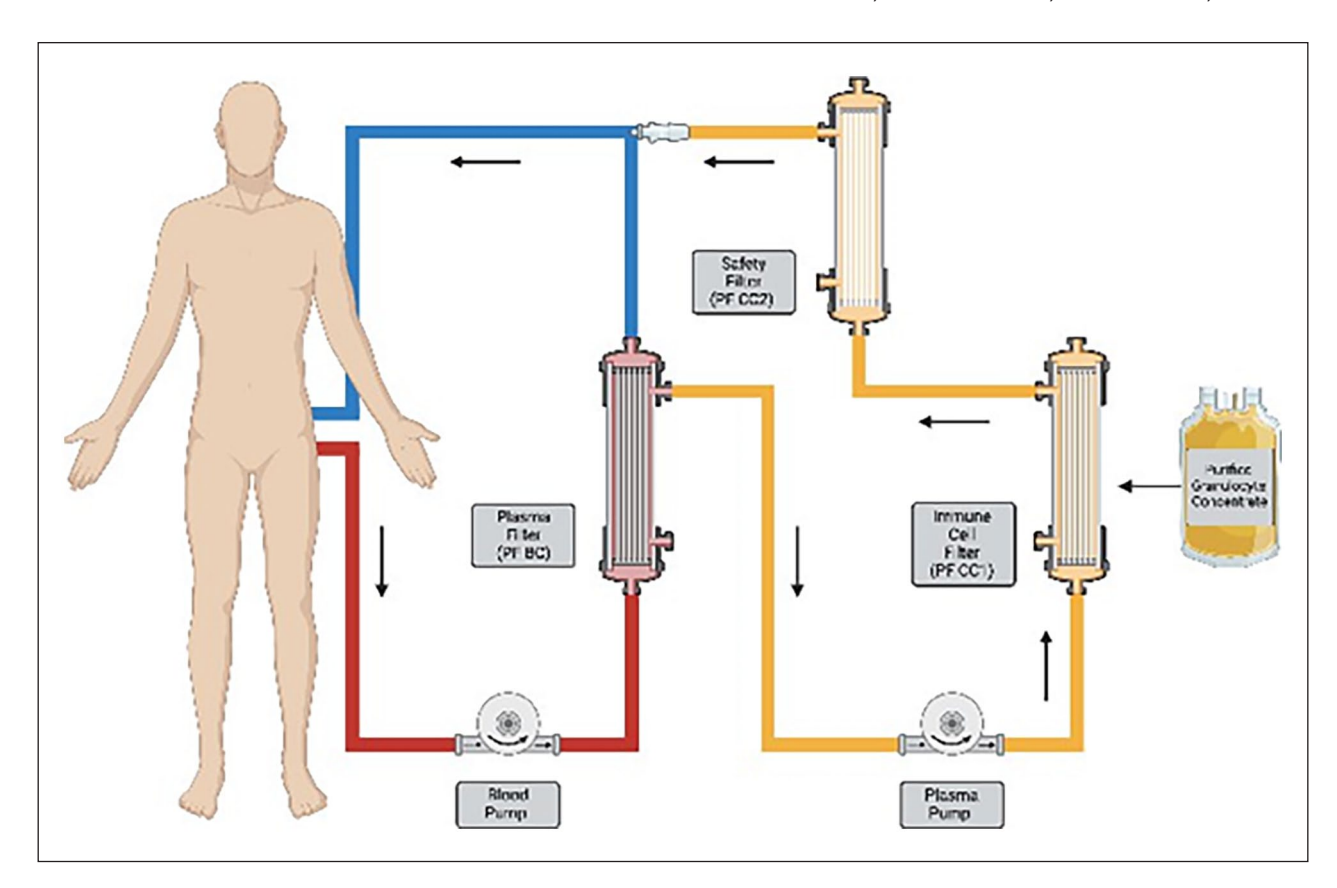


Figure 1. Schematic illustrations of the Immune- Competence-Enhancement System.

Sara Cairoli³, Cristiano Rizzo³, Simone Reali⁷, Michele Vacca⁸; Andrea Cappoli⁹, Christian Albano¹⁰, Andrea Pietrobattista^{1,11}, Samira Safarikia^{1,2}, Marco Spada^{1,2}, Carlo Dionisi Vici³

¹Clinical Hepatogastroenterology and Transplantation Research Unit, Bambino Gesù Pediatric Hospital IRCCS (OPBG), Italy; ²HPB Surgery, Liver and Kidney Transplantation division, OPBG, Italy; ³Metabolic Diseases and Hepatology division, OPBG, Italy; ⁴Cardiac Surgery Unit, OPBG, Italy; ⁵Division of Pathology, OPBG, Italy; ⁶Clinical Analysis Laboratory, OPBG, Italy; ⁷Anesthesiology and Intensive Care division, OPBG, Italy; ⁸Transfusion Medicine division, OPBG, Italy; ⁹Nephrology division, OPBG, Italy; ¹⁰B Cell Research Unit, Immunology Research Area, OPBG, Italy; ¹¹Hepatology and Transplant Clinic Unit, OPBG, Italy;

Introduction: Inborn errors of metabolism (IEM) are a broad category of liver-imbalancing monogenic disorders [1]. Liver transplantation (LTx) improved patient metabolic control, providing enzyme replacement. The introduction of ex-vivo liver normothermic machine perfusion (NMP) enhanced LTx outcomes, besides providing ex-vivo platform for diseases study [2].

Methods: Twelve explanted livers from patients with IEM (propionic aciduria, urea cycle defects) undergoing LTx not eligible to "domino" procedures were flushed with heparinized cold storage solutions and then underwent NMP to investigate disease- related liver metabolism and function. The majority (n=11) was perfused after static cold storage (SCS), one (n=1) after hypothermic machine perfusion (HMP). NMP pressures were set to achieve perfusion flow target of 100 ml/min/100 g liver parenchyma, 25% through hepatic artery (HA), 75% through portal vein (PV) with haematocrit between 25-27%. During perfusion, biochemical, hematologic, and metabolic profile were evaluated by serial sampling. Histological evaluation of the liver parenchyma and biliary tract was carried out before, during, and after NMP. The duration of NMP was established case-by-case looking at liver viability. The grafts were perfused after a mean SCS time of 565±372 min. Seven were perfused for 8 hours, 3 for 18 hours, 1 for 48 hours and 1 for 72 hours of NMP, the last after 12 hours of HMP.

Results: The perfusion parameters allowed adequate oxygenation and CO2 extraction (p<0.0001). Livers were perfused $80\pm7\%$ through PV and $20\pm7\%$ through HA. PV flow remained stable, whereas HA flow significantly increased during perfusion (T0 120 ± 85 vs. T8 178 ± 94 ml/min, p<0.01). Perfused livers demonstrated decreasing values of lactate (T0 6.7 ± 1.9 vs T8 3.7 ± 1.1 mmol/L). Histological examination of the livers during NMP revealed preserved architecture with intact hepatocytes, patent sinusoids and normal bile ducts. Biochemically, the characteristic disease-related biomarkers profiles (i.e. ammonia, aminoacids, organic acids) evaluated ex-vivo throughout NMP were consistent with those seen in vivo pre-LTx. A perfused propionic acidemia liver treated by glycine supplementation produced its ester propionyl-glycine, indicating the "druggability" of the ex-vivo system [3].

Discussion: The perfused livers demonstrated both viability and disease-specific targeted metabolomics, proving that this novel ex vivo model expresses the biochemical disease characteristics and responds to therapeutic intervention. This unique "physiological" milieu represents a pioneering and human-mirroring setting to study disease pathophysiology and novel treatments.

References

- 1. Ferreira CR et al, J Inherit Metab Dis. 2021;44(1):164-177.
- 2. Goldaracena N et al, Am J Transplant. 2017;17(4):970-978.
- 3. Roe CR et al, Lancet. 1982;1(8286):1411-1412.

Acknowledgements

The Division of Metabolic Diseases and Hepatology is an affiliated member of the MetabERN and partner of the UIMD and of the E-IMD. The

Division of HPB Surgery, Liver and Kidney Transplantation is an affiliated member of the ERN TransplantChild and of the ERN Rare Liver. The Unit of Hepatology and Transplant Clinic is an affiliated member of the ERN Rare Liver.

7B: OTHER ORGANS - CROSSTALK

THE REBOUND IN SERUM BILIRUBIN LEVELS AFTER PLASMA EXCHANGE (PE) FOR BILIRUBIN REMOVAL IS PRONOUNCED IN THE NON-SURVAIVER-GROUP

Junko Goto, Takeshi Moriguchi, Norikazu Harii, Daiki Harada, Junichi Takamino, Masateru Ueno, Hirobumi Ise, Akino Watanabe, Hiroki Sakata, Natsuhiko Myose, Fuki Natori, Ryo Iino

Yamanashi University School of Medicine, Department Twenty patients were performed PE during the study period. Data 1 shows the patients characteristics. of Emergency and Critical Care Medicine, Japan

Aim: It is believed that the hyperbilirubinemia is not the cause but the result of the liver failure. However, plasma exchange (PE) is performed for the bilirubin removal in patients with hyperbilirubinemia in Japan occasionally, and we sometimes find it clinically effective in the patient who underwent PE against hyperbilirubinemia. The aim of this study is to evaluate the relationship between the changes in blood bilirubin level before and after PE and the outcome of the PE-treated patients.

Methods: We retrospectively assessed the changes in blood bilirubin level before and after treatment of PE and 28 days mortality. Among patients with hyperbilirubinemia with a bilirubin level of 10 or higher treated in the ICU from December 2006 to September 2024, we calculated the rate of bilirubin elevation before PE, the rate of bilirubin removal in PE and the rebound rate after PE.

Results:

Table 1.

	Survival) group(10)	Non-survival group(10)
Age Male (%)	69.4 ± 14.0 6 (60%)	65.5 ± 12.4 8 (80%)
SOFA score	12.0 ± 2.3	12.8 ± 4.5
APACHE II	26.7 ± 5.7	29.6 ± 9.4

Table 1 shows the patients characteristics. The blood bilirubin level just before plasma exchange was 25.5 \pm 8.5 mg/dL in survival group, and 24.7 \pm 8.9 mg/dL in non-survival group.

Figure 1 shows Bilirubin Increase, Removal and Rebound Rate. (1) removal rate: the rate of the change in bilirubin level from just after finish PE to just before starting PE. (2) rebound rate: the rate of the change in bilirubin level from 12 hours after finish PE to just after PE.

Discussion: In this study, despite the lack of statistically significant differences in pre-PE bilirubin levels or bilirubin removal rates during PE, the rebound in bilirubin levels at 12 hours post-PE was significantly higher in the mortality group. Generally, the molecular weight of bilirubin is relatively large, which causes its movement between different compartments within the body (intracellular, extracellular, interstitial fluid, and intravascular) to be time-consuming. Therefore, even if the intravascular concentration decreases due to bilirubin removal during PE, bilirubin stored intracellularly gradually migrates into the intravascular compartment over time after PE. This phenomenon is considered the mechanism behind the rebound effect. The pronounced rebound observed in the

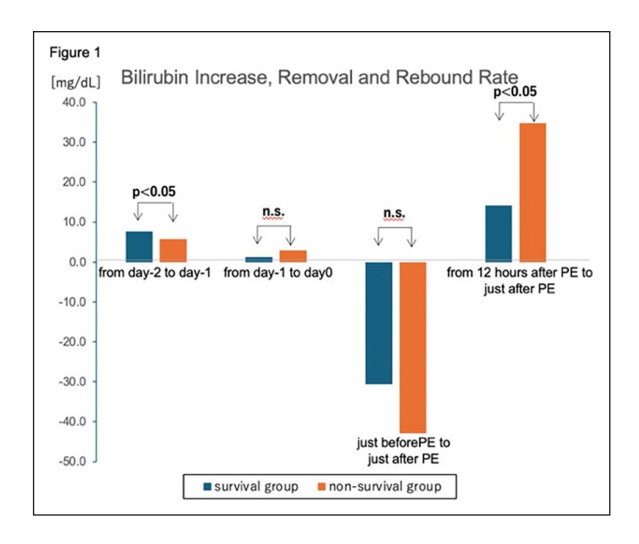


Figure 1.

mortality group may reflect the failure of PE to achieve sufficient improvement in liver function. It remains unclear whether PE was the cause or the consequence of the observed outcomes in this study. However, this finding is important as it suggests the potential clinical benefit of this treatment.

Conclusion: We can conclude that the lower rebound rate of blood bilirubin level after PE is predictive of favorable patient outcome.

References

- 1. Hong Seok Han, et al, PLoS One, 5;16(8): e0255230, 2021.
- 2. Aritz Perez de Garibay, et al, Crit Care, 26(1) 289: 1-16, 2022.

HAEMODYNAMIC AND HAEMOLYTIC CHARACTERIZATION OF AN EX- VIVO HUMAN UMBILICAL CORD MODEL

J. Heyer¹, L. Jeremiah¹, S. Koc², L. Eichmann², U. Steinseifer¹, M. Schoberer², S.V. Jansen¹,

¹Department of Cardiovascular Engineering, Institute for Applied Medical Engineering, Medical Faculty, RWTH Aachen University, Aachen, Germany; ²Department of Paediatric and Adolescent Medicine, Section of Neonatology and Paediatric Intensive Care Medicine, University Clinic RWTH Aachen, Aachen, Germany

Introduction: Artificial Placenta (AP) technologies aim to support the developing organs of Extremely Preterm Infants (EPI), for example, the lungs, by connecting an Extracorporeal Membrane Oxygenation via the umbilical cord vessels [1–4]. Cannulation has only been tested in large animal models so far, with huge limitations due to the different anatomy and size of the umbilical cord vessels [4, 5]. We recently developed an ex-vivo human umbilical cord setup to overcome these limitations. In this study, we verify the physiological haemodynamic behaviour of the ex-vivo setup together with a haemolytic characterization.

Methods: 15 umbilical cords and placentas were harvested, of which 9 umbilical cord cut-offs (>15 cm) and fetal blood collection (> 40 mL) could be included in this study. The umbilical cord was cannulated at

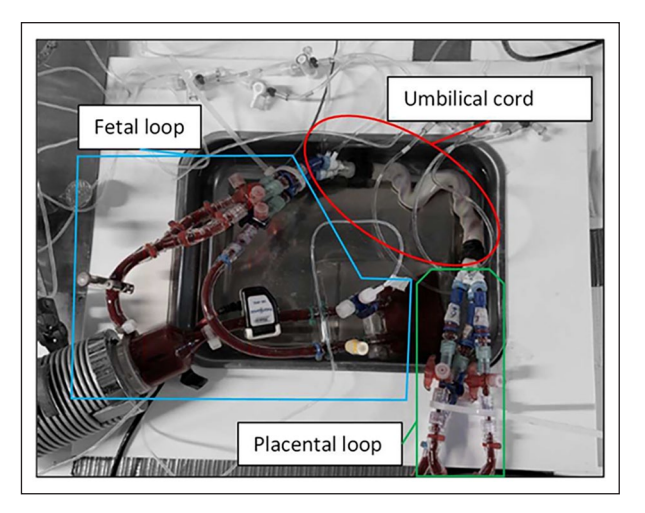


Figure 1. Operating ex-vivo human umbilical cord setup.

both ends and connected to a testing circuit representing the fetoplacental system in a fetal and placental loop (cf. Figure 1). The circuit was primed with fetal blood adjusted to a hematocrit of 30 %. Flow was increased incrementally to a target flow of 70 mL/min, representing a physiological flow in EPI. Pressure drop over the umbilical vessels was measured along with flow. When the target flow was reached, blood samples over a period of 3 h were taken to measure haemolysis induced by the setup.

Results: Target flow of 70 mL/min could be achieved in all (n = 9) experiments. Hydrodynamic parameters were found to be within the physiological magnitude of EPI and following the Hagen- Poiseuille equation despite the viscoelastic behaviour of the umbilical cord vessels. Hemolysis production of the ex-vivo setup alone was measured to NIH of 0.199 \pm 0.092 g/100L (mean \pm SD).

Discussion: The ex vivo model of a perfused human umbilical cord is a physiological model for testing ECMO cannulation devices and procedures within physiological flow and pressure conditions of EPI, the target patient group of AP technologies. This marks an important step towards translating AP.

References

- Arens, J, et al. NeonatOx: a pumpless extracorporeal lung support for premature neonates. Artificial organs 2011;35(11): 997–1001.
- Charest-Pekeski, A, et al. Impact of the Addition of a Centrifugal Pump in a Preterm Miniature Pig Model of the Artificial Placenta. Front Physiol 2022;13:925772.
- Miura, Y, et al. A Parallelized Pumpless Artificial Placenta System Significantly Prolonged Survival Time in a Preterm Lamb Model. Artif Organs 2016;40(5):E61-8.
- Hornick, M, et al. Toward Physiologic Extracorporeal Support of the Premature Infant: Technical Feasibility of Umbilical Cord Cannulation in Mid-Gestation Fetal Lambs. *Journal of the American College of Surgeons* 2016;223(4):S91-S92.
- Hornick, M, et al. Umbilical cannulation optimizes circuit flows in premature lambs supported by the EXTra-uterine Environment for Neonatal Development (EXTEND). The Journal of physiology 2018;596(9):1575–85.

COMBINED ARTIFICIAL LUNG AND KIDNEY DEVICE (RENOX): EXTRA LUNG SUPPORT DELIVERED BY DIALYSIS FIBERS

Ana Martins Costa^{1*}, Laura Guarino^{1*}, Frank R. Halfwerk^{1,2}, Bettina Wiegmann^{3,4,5}, Jutta Arens¹

¹University of Twente, Netherlands; ²Medisch Spectrum Twente, Netherlands; ³Hannover Medical School, Germany; ⁴Lower Saxony Center for Biomedical Engineering, Germany; ⁵German Center for Lung Research (DZL), Germany. * Both authors contributed equally to this work

Introduction: Extracorporeal membrane oxygenation (ECMO) patients frequently suffer from acute kidney injury (AKI). For these patients, a novel and safer treatment is being developed, consisting of a combined artificial lung and kidney assist device (RenOx). The RenOx integrates 75% of gas exchange fibers and 25% of dialysis fibers for oxygen and carbon dioxide transfer, blood dialysis, and filtration [1]. Nevertheless, for patients who temporarily do not require kidney support, dialysis fibers could be repurposed to provide extra gas transfer, Fig.1. Reutilizing dialysis fibers to boost gas exchange could be beneficial to 1) explore treatment flexibility with the RenOx, and 2) counterbalance eventual losses of CO2 removal caused by the replacement of gas exchange fibers by dialysis fibers [1]. This study evaluates the feasibility of transferring O2 and CO2 by recirculating fully oxygenated and decarboxylated dialysis fluid through dialysis fibers under standardized blood test conditions.

Methods: Blood with standardized venous inlet conditions was pumped through a dialyzer with similar dialysis fiber area as the RenOx (0.6 m²).

Simultaneously, fully oxygenated and decarboxylated dialysis fluid flowed through the dialysate chamber. CO2 and O2 exchange was measured at a blood flow rate of 200 mL/min and 300 mL/min, at different blood to dialysate flow ratios equal to 1, 3, or 6.

Results: The use of fully oxygenated dialysis fluid resulted in CO2 removal rates between 10 mL/Lblood flow to 37 mL/Lblood flow. On average, the level of CO2 removal could be adjusted by the blood to dialysate flow ratio. The highest amounts of CO2 could be eliminated with the lowest blood to dialysate flow ratio of 1 (i.e. equal blood and dialysate flow). In addition, blood oxygenation up to 17 mL/Lblood flow was provided with this method.

Discussion: Recirculation of fully oxygenated dialysis fluid could provide minimal supplementary CO2 clearance (10 mL/Lblood flow) up to the full metabolic requirement of CO2 removal for an adult patient (~40 mL/Lblood flow). Dialysis fibers could compen- sate for the loss of CO2 transfer caused by the replacement of gas exchange fibers in the RenOx [1].

Conclusions: When kidney support is not necessary with the RenOx, dialysis fibers can deliver supplementary lung support. The level of support can be regulated by the blood to dialysate flow ratio.

References

[1] Martins Costa et al, J. Membr. Sci, 680, 2023.

Acknowledgements

This work was granted by the German Research Foun- dation (DFG, project no. 447746988) as part of the priority program `Towards an Implantable Lung' (SPP 2014).

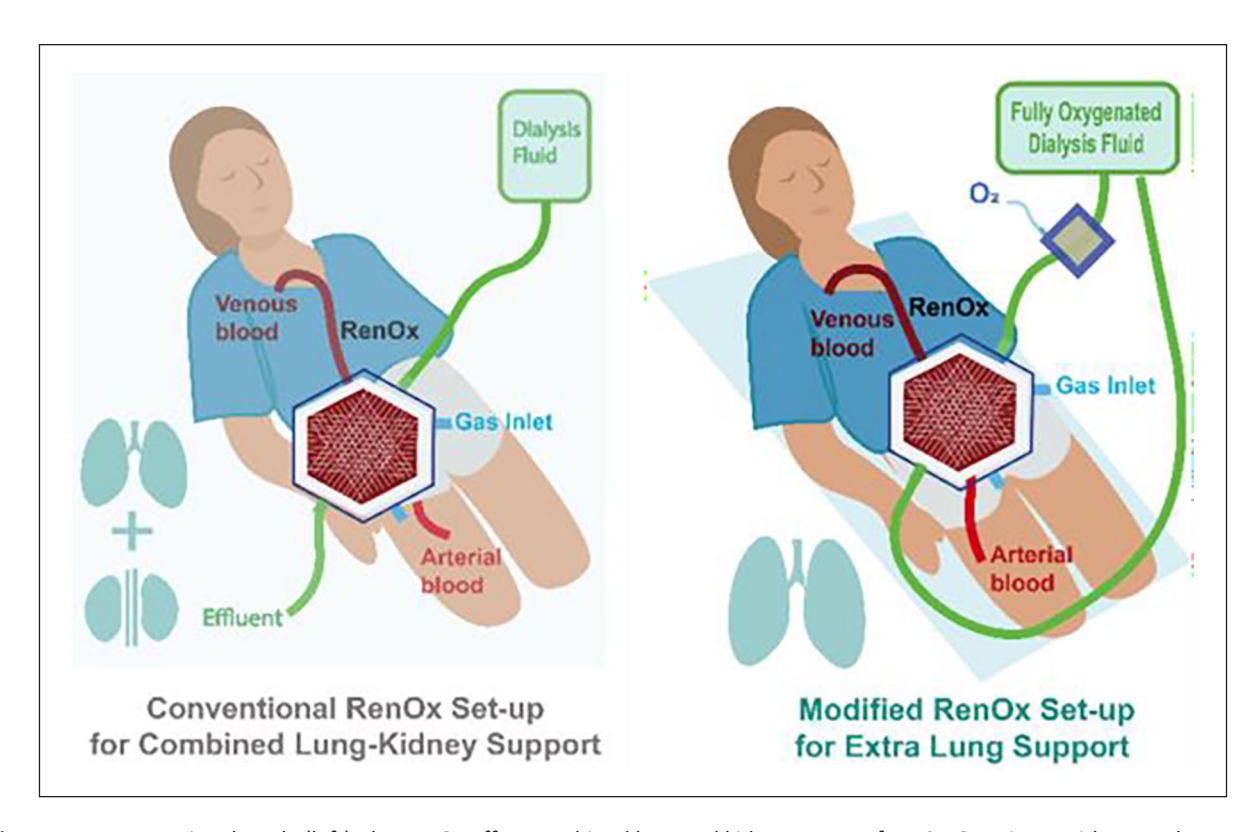


Figure 1. In conventional mode (left), the RenOx offers combined lung and kidney support for ECMO patients with AKI. When kidney support is not required (right), the RenOx circuit can be modified to provide extra gas transfer by recirculating fully oxygenated and decarboxylated dialysate through the dialysis fibers.

COMBINED LUNG AND KIDNEY SUPPORT IN A SINGLE EXTRACORPOREAL DEVICE: DEVELOPMENT OF THE FIRST RENOX PROTOTYPE

Ana Martins Costa¹, Jan-Niklas Thiel², Frank R. Halfwerk^{1,3}, Danny J.M. van Galen¹, Bettina Wiegmann^{4,5,6}, Michael Neidlin², Jutta Arens¹

¹University of Twente, Netherlands; ²RWTH Aachen University, Germany; ³Medisch Spectrum Twente, Netherlands; ⁴Hannover Medical School, Germany; ⁵Lower Saxony Center for Biomedical Engineering, Germany; ⁶German Center for Lung Research (DZL), Germany

Introduction: Extracorporeal membrane oxygenation (ECMO) is a life-saving therapy for > 20,000 patients/year who suffer from severe respiratory and/or cardiac diseases. Combined impairment of lungs and kidneys is one of the most common complications, affecting up to 70% of ECMO patients. These patients are conventionally treated with ECMO and continuous renal replacement therapy in two separate circuits. However, the need for additional pumps, cannulas, tubing, and devices, increases risks, and hospital costs. Therefore, a novel artificial lung device with integrated kidney support (RenOx) is developed to reduce current treatment limitations.

Methods: For the development of RenOx, first, we gathered clinical needs including patient target group, and level of lung and kidney support. Second, the design and configuration of the RenOx membrane bundle was defined based on previous findings [1, 2] on the combination of gas exchange and dialysis fibers. Third, all device parts including the blood flow path, housing, and lids were designed considering clinical requirements, ease of use, and manufacturing processes. The device's blood flow path was optimized by means of computational fluid

dynamics (CFD) to reduce blood stagnation areas and blood cell damage. Forth, the RenOx feasibility will be tested in vitro using full blood.

Results: The first RenOx prototype was designed for small adult patients (30–40 kg) comprising a total 1.2 m² of membrane area arranged with every 4^{th} gas ex- change fiber layer (0.9 m²) replaced by a dialysis fiber layer (0.3 m²). This configuration proved to maintain sufficient gas exchange capacity [1] while providing additional kidney support. The fiber bundle is arranged in a hexagonal configuration creating separate compartments for blood, gas, and dialysate flow, see Fig.1. CFD analysis showed that designed lids with a 10° inlet and outlet angle reduced blood stagnation volume to 0.0004% of total blood volume, and pressure drop in inlet/outlet < 8mmHg. Full in-vitro results will be presented at ESAO.

Discussion: The RenOx integrating a membrane bundle with 75% of gas exchange fibers and 25% of dialysis fibers is indicated to provide sufficient lung [1] and kidney support [2]. The highly integrated bundle allows the RenOx to be a compact device with similar surface area as a single oxygenator, while providing support for two organs. The design, manufacture, and testing of the first RenOx prototype is a step towards safer and more economic treatment for ECMO patients with underlying acute kidney injury (AKI).

References

- [1] Martins Costa et al, J. Membr. Sci, 680, 2023.
- [2] Martins Costa et al, J. Membr. Sci, 698, 2024.

Acknowledgements

This work was granted by the German Research Foun- dation (DFG, project no. 447746988) as part of the program `Towards an Implantable Lung' (SPP 2014).

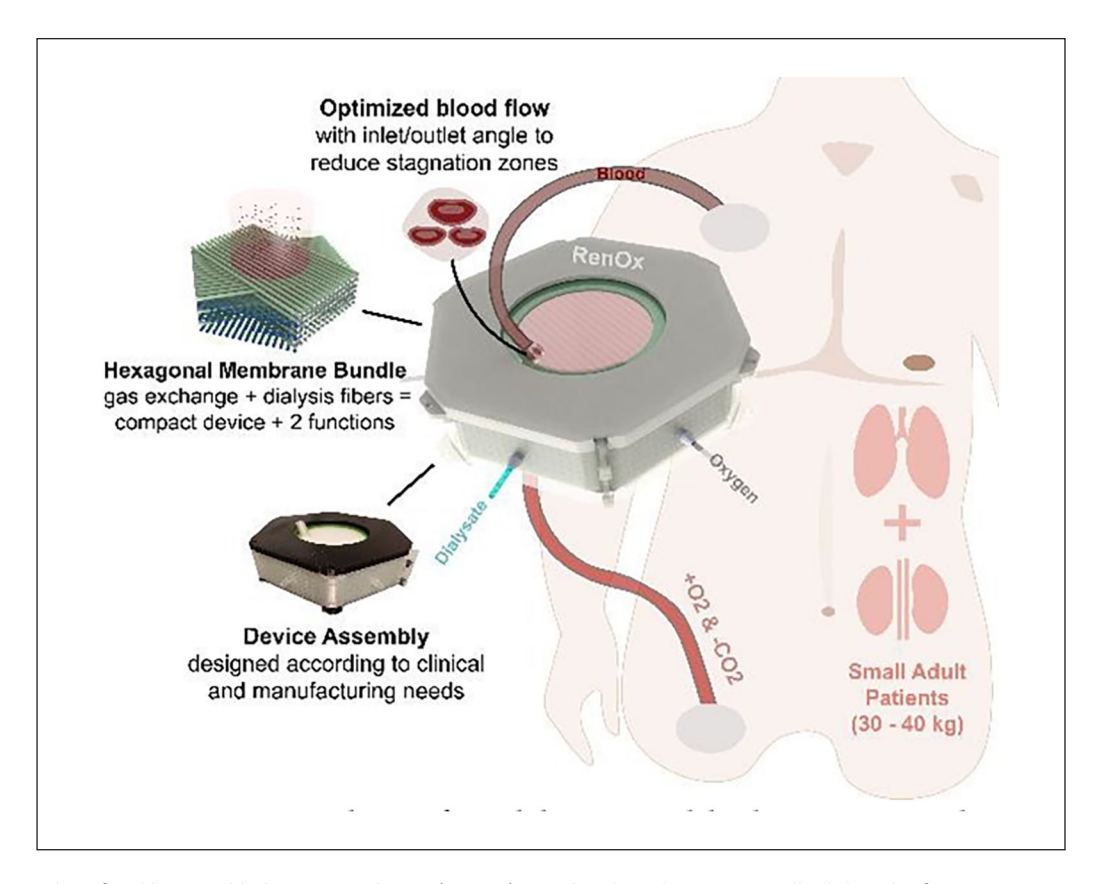


Figure 1. Novel artificial lung and kidney assist device (RenOx) was developed to treat small adults. The first prototype is optimized to compactly combine gas ex- change and dialysis fibers in one device and to reduce blood stagnation. The RenOx was manufactured for the first in-vitro tests with full blood.

7C: SUPPORTING LUNG FUNCTIONS - THE GOALS, CHALLENGES AND ADVANCES

BIO-INSPIRED ARTIFICIAL LUNG BASED ON A THREE-DIMENSIONAL CAPILLARY NETWORK – PROOF OF PRINCIPLE

Kai P. Barbian, Ulrich Steinseifer, Sebastian V. Jansen

Department of Cardiovascular Engineering, Institute of Applied Medical Engineering, Medical Faculty, RWTH Aachen University, Forckenbeckstr. 55, 52074 Aachen, Germany

Introduction: Hollow fiber membranes (HFM) are the standard technology in clinically used artificial lungs for extracorporeal life support (ECLS). Despite their efficacy, significant limitations exist in this membrane type limiting ECLS availability for patients and worsening outcome. Suboptimal blood flow conditions lead to reduced gas transfer efficiency and increased risk of thrombosis reducing device durability. Moreover, large foreign surface areas are needed for sufficient blood-gas transfer requiring mediation with anticoagulation. This puts the patient at risk of internal bleeding. [1-3] To overcome these limitations, we propose a bio-inspired design for artificial lungs based on a three-dimensional capillary network creating physiological blood flow conditions. In this study, we demonstrate the feasibility of this concept in combination with a hybrid additive-subtractive manufacturing approach.

Methods: First, a miniaturized prototype of the bio-inspired artificial lung was designed using in-silico methods. Subsequently, the geometry of the blood flow path was 3D printed in masked stereolithography with a dissolvable polymer (xMold, Addifab, Denmark). Afterwards, a thin membrane out of medical grade siloxane (Elastosil RT620, Wacker, Germany) was formed on the surface of the 3D print using a dip-spin coating process. Finally, the 3D printed polymer was etched away using sodium hydroxide (cf. Figure 1). The manufacturing results were analyzed using digital microscopy. After integrating the membrane structure into a housing (cf. Figure 2, left), performance testing was carried out in-vitro according to ISO 7199 measuring oxygen and carbon dioxide transfer rates and pressure drops.

Results: The bio-inspired membrane structure was manufactured successfully yielding minimal membrane thicknesses of 100 μ m and smooth blood flow channels with diameters of 300 μ m. Significant gas transfer rates were measured (cf. Figure 2, right) as well as pressure drops below 1.5 mmHg. During the in-vitro testing period, no blood clotting was observed.

Discussion: For the first time, we have successfully manufactured a bioinspired artificial lung based on a micro-scale capillary network membrane structure. Significant gas transfer rates as well as low pressure drops were measured during the testing. This proves the feasibility of

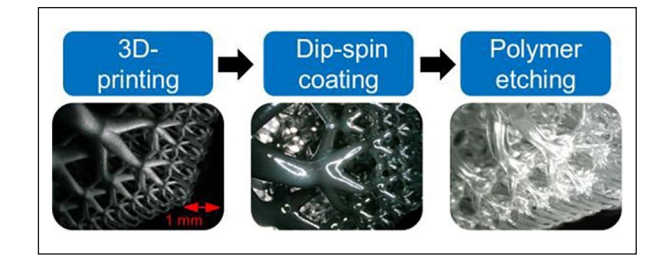


Figure 1. Process steps for manufacturing the bio-inspired membrane structure.

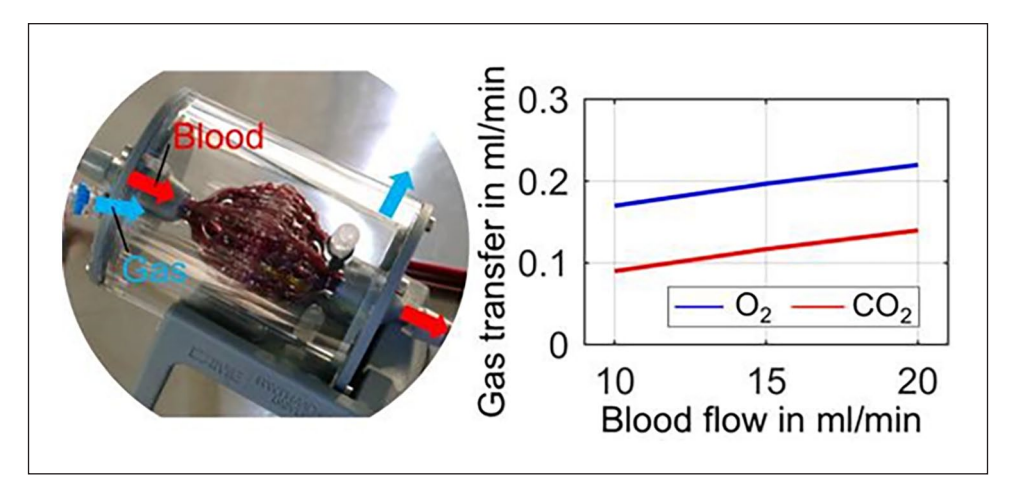


Figure 2. Prototype of the bio-inspired artificial lung (left), results of gas transfer measurements (right).

our approach to create an artificial lung that is based on this completely novel concept. Nevertheless, our bio- inspired artificial lung does not yet match the small geometric scales that are required to be competitive to HFM in terms of area-specific gas transfer rates. Still, these early results clearly show the capability of our artificial capillary network technology. By further miniaturizing the capillary network channels to achieve higher efficiency, a novel artificial lung concept might be at hand that is superior to HFM.

References

- 1. T. Tonetti et al, ICMx, 11(1):77,2023
- 2. D.B. Tulman et al, BMC Anesthesiol. 14(1):65, 2014
- ELSO, ELSO Live Registry Dashboard of ECMO Patient Data, https:// www.elso.org/registry

IN VITRO STUDY OF SAFETY AND EFFICENCY OF A NOVEL OXYGENATOR USING MICROSPHERES: OXYGENATION, HEMOLYSIS AND THROMBOGENICITY

Leonid Goubergrits¹, Katharina Vellguth¹, Benedikt Franke¹

¹Institute of Computer-assisted Cardiovascular Medicine, Deutsches Herzzentrum der Charité, Germany

Introduction: Long-term use of oxygenators is despite advances in material science, anticoagulation administration by coating, and optimization of the flow design limited. Use of oxygenators is associated with complications (e.g. acute kidney injury), failure (e.g. thrombus) and pure outcome due to lack of hemocompatibility and up to three times higher priming blood volume if compared with human lungs. We propose a novel oxygenator design with a reduced size and priming volume by filling blood compartment with microspheres. The aim of the presented studies was to evaluate in vitro the ability of the novel oxygenator design (OptOx) principle to achieve the same oxygen saturation performance as by a standard device (Control) without increasing hemolysis and thrombogenicity.

Methods: To perform in vitro tests with human blood samples, scaled-down (cross-section size) prototypes of a Control and OptOx were fabricated for parallel tests (**Control**: Length – 80 mm, Diameter - 3 mm, number of capillary membranes - 8; **OptOx**: Length – 30 mm, Diameter - 4 mm, number of capillary membranes - 16). Capillary membranes PMP 90/200 (OXYPLUS, 3M Membrana) were used. The blood

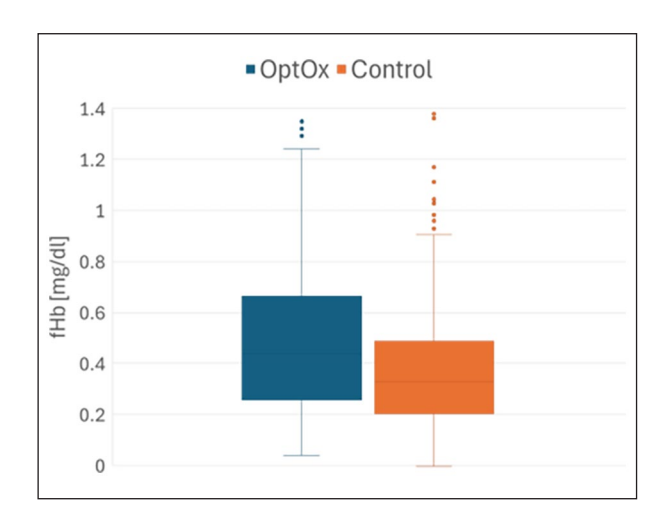


Figure 1. Results of hemolysis tests.

compartment of the novel oxygenator was filled with polyethylene microspheres of ~230µm diameter, which were fixed using metal filter with a mesh size of 200µm. Filled microspheres reduce priming volume by approximately 50-60%. Oxygenation tests were performed in a setup allowing first deoxygenation of the blood to 60%. Tests were done under temperature of 37°C. Oxygenation level was measured using Terumo gas analyse device. To assess the thrombogenicity three direct parameters (Fibrinogen or TPZ, INR, and aPTT) as well as four specific biomarkers (VWF:Ag, VWF:CBA, Factor VIII, and VWF:RCo) were measured. Prior to thrombogenicity tests prototypes were covered by NOF Lipidure solution (polymer of 2-methacryloyloxyethyl phosphoryl- choline): prototypes were filled with a Lipidure- solution for 1 hour. Thrombogenicity tests were done for two conditions simulating normal blood flow of 5 L/min as well as low flow conditions with 1 L/min: 10 parallel tests per flow rate of 2 hours duration. Blood tests were performed by Labor Berlin. Hemolysis was measured by free released hemoglobin fHb [g/100l], which was measured by the Harboe method recording absorbance at three wave lengths (380 nm, 414 nm, and 450 nm) with a spectrometer, 10 parallel experiments simulating 5 L/min blood flow were done. During each test fHb was measured five times every 30 min.

Results: During oxygenation tests the OptOx prototype achieved the same oxygen saturation levels >97% as the Control prototype. Thrombogenicity tests found no significant (all p values > 0.2) differences for all seven investigated biomarkers for both flow conditions (paired student T-test). All measured parameters were inside a range of healthy values. Furthermore, we found no significant differences in hemolysis tests for both prototypes (fHb: 0.49 \pm 0.23 vs. 0.41 \pm 0.25 g/100l paired student T-test, p = 0.484, see figure 1).

Conclusion: It was shown that microsphere proposed to reduce size and priming volume of the novel oxygenator allows to increase oxygenation rate without increasing a risk of blood damage and thrombogenicity. Next, full-size prototype will be designed and in vitro tests using animal blood will be repeated.

Acknowledgements

This work was supported by SPARK program of the Charité-BIH.

IN-SILICO ANALYSIS OF THE RENOX DEVICE: COMPARISON OF HEMO- DYNAMICS AND GAS EXCHANGE DURING INTEGRATED LUNG AND KIDNEY SUPPORT IN AN ECMO COHORT

Jan-Niklas Thiel¹, Ana M. Costa², Bettina Wiegmann³, Jutta Arens², Ulrich Steinseifer¹, Michael Neidlin¹

¹RWTH Aachen University, Aachen, Germany; ²University of Twente, Enschede, Netherlands; ³Hannover Medical School, Hannover, Germany

Introduction: Extracorporeal membrane oxygenation (ECMO) is commonly used in intensive care for cardiac and respira- tory support, yet up to 70 % of these patients also suffer from acute kidney injury. To treat this, continuous renal replacement therapy (CRRT) is connected to the ECMO circuit, but there is no gold standard for the configura- tion of this connection. However, differences in hemo- dynamics e.g. 200 %

variation in pulmonary artery pres- sure were found in a previous study [1]. Hence, the RenOx project is developing a new device that combines lung and kidney support in a single device [2]. This study quantifies the hemodynamic and gas exchange performance of the RenOx device and benchmarks it against conventional CRRT support in a cohort of veno-arterial ECMO (V-A ECMO) patients (Figure 1).

Methods: A computational cardiovascular model was extended by the respiratory system incl. lung mechanics, lung and tissue gas exchange and mechanical ventilation. Model parameters identified in a sensitivity analysis were cali- brated on each of the 30 data points of the eight patients listed in Table 1. The influence of different CRRT con- nection modalities was then investigated for all patients and compared with a manufactured RenOx prototype.

Results: Figure 2 shows results for cardiovascular pressures and the right ventricular pressure-volume (RV PV) loop of a single patient. Arterial blood pressure is lowest when the CRRT is connected downstream of the ECMO pump and upstream of the oxygenator, while the highest pressures occur with the RenOx device.

Placement of the CRRT before the pump and after the drainage cannula results in the highest end-systolic and end-diastolic volumes and stroke volume of the right ventricle.

Discussion: Initial results indicate a similar hemodynamic performance of the RenOx device compared to existing commercial CRRT solutions yielding high systemic pressures and high right ventricular stroke work. Investigation of the gas exchange potential and performance of the device over a wider range of patients and ECMO flows is ongoing.

References

- Thiel et al., J CIBM, 186, 2025.
- 2. Martins Costa et al., J Membrane Science, 698, 2024.

Acknowledgements

This project is funded by the DFG SPP2014 "Towards the Ar-tificial Lung" - PN: 447746988.

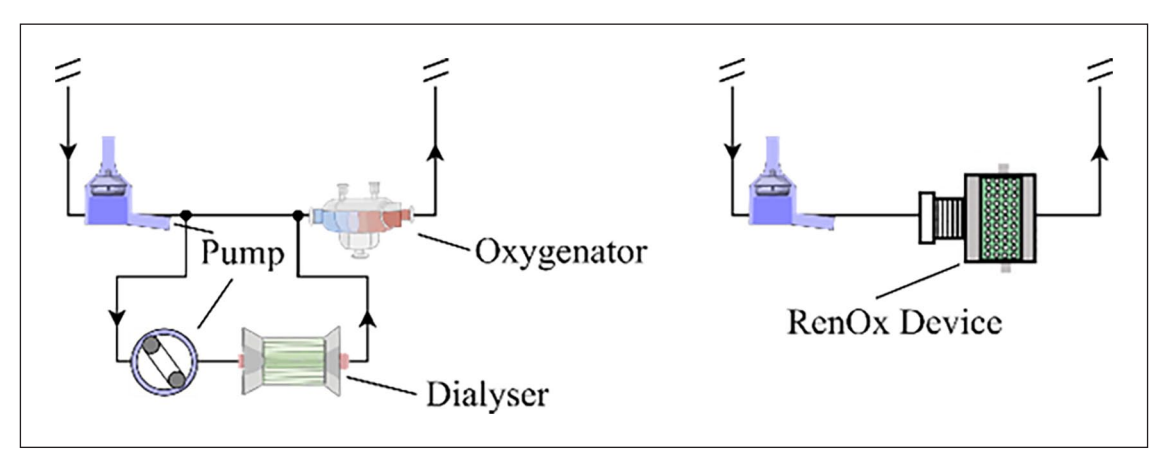


Figure 1. Example for combination of CRRT and ECMO (left) and RenOx device (right).

Table 1. Data from patients under V-A ECMO.

Parameter	Median	(Min, Max)
Mean arterial pressure	79.0	(55.0, 113.0) mmHg
Mean pulmonary arterypressure	19.5	(6.0, 30.0) mmHg
Pulmonary capillary wedge pressure	11.0	(7.0, 15.0) mmHg
Cardiac output	3.4	(1.5, 7.5) L/min
Pump flow	2.5	(1.2, 3.8) mmHg

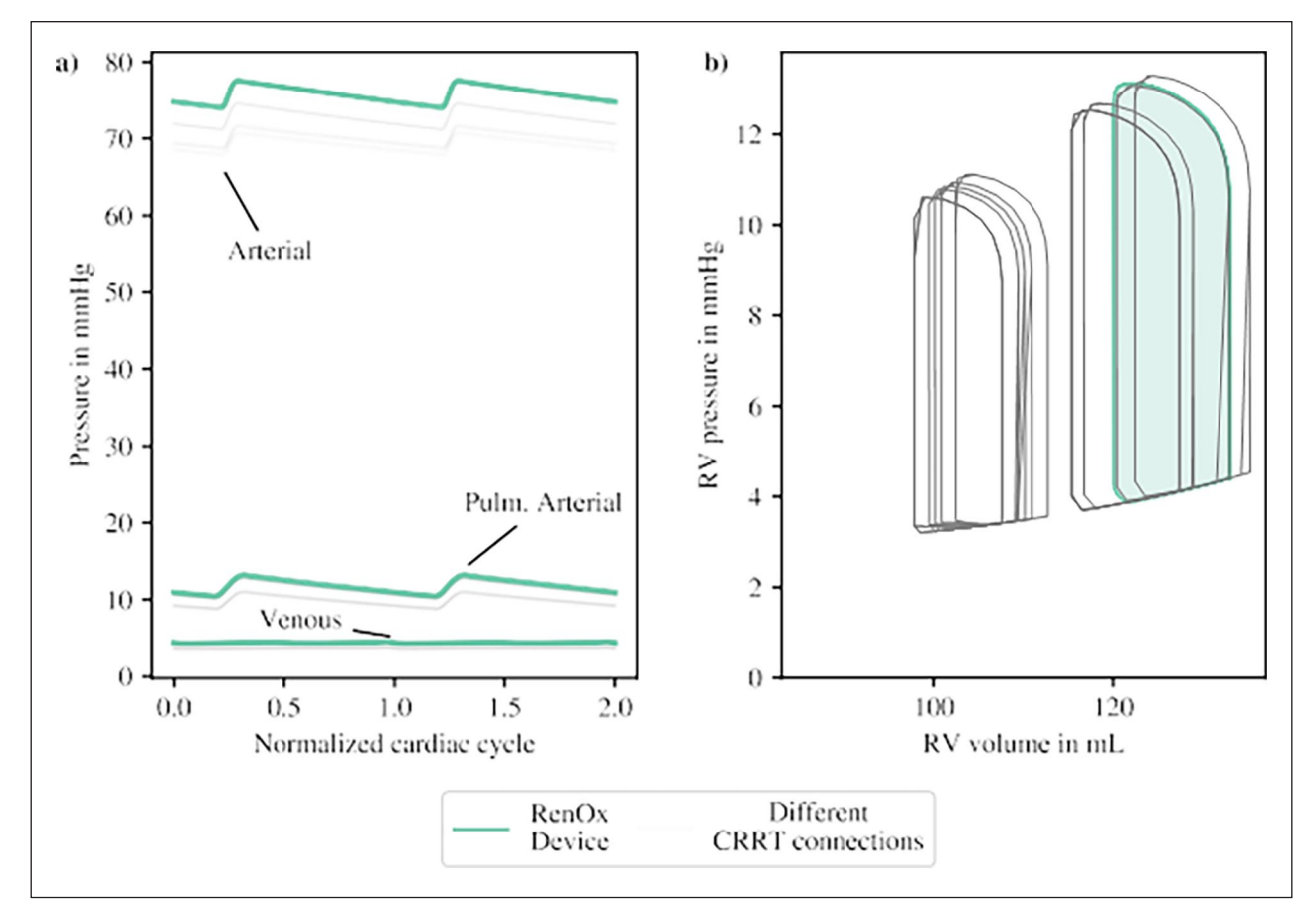


Figure 2. Influence of CRRT connections schemes and RenOx device on the a) cardiovascular system and b) RV PV loop.

ARTPLAC: ADVANCING NEONATAL CARE WITH AN INNOVATIVE ARTIFICIAL PLACENTA FOR LUNG AND KIDNEY SUPPORT

D.J.M. van Galen¹, A. Martins Costa¹, N. Rochow^{2,3}, F.R. Halfwerk^{1,4}, J. Arens¹, on behalf of the ArtPlac Research Consortium⁵

¹Engineering Organ Support Technologies, Department of Biomechanical Engineering, Faculty of Engineering Technologies, Technical Medical (TechMed) Centre, University of Twente, Enschede, the Netherlands; ²Department of Pediatrics, Paracelsus Medical University, Nuremberg, Germany; ³Department of Pediatrics, University Medicine Rostock, Rostock, Germany; ⁴Department of Cardio-Thoracic Surgery, Thorax Centrum Twente, Medisch Spectrum Twente, Enschede, the Netherlands; ⁵HORIZON-EIC-2022-PATHFINDEROPEN-01, Grant agreement ID: 101099596

Introduction: Despite a decline in neonatal mortality in recent years, preterm birth remains the leading cause of death among newborns [1]. Many cases are caused by immaturity of the lungs, often exacerbated by renal failure [2,3]. Current therapies include mechanical ventilation, extra- corporeal membrane oxygenation, and continuous renal replacement therapy. However, these interventions are highly invasive, associated with lifelong disability, and limit family care integration [4,5]. Therefore, we de- velop a combined lung-kidney assist device that

addres- ses the needs of extremely preterm infants (>24 weeks gestational age) through a less invasive and family- centered approach.

Methods: User requirements were defined by stakeholder analysis (clinicians, parents, etc.) and converted into design requirements. Design concepts for the device were developed and manufactured. Hexagonal polymethyl- pentene-hollow-fiber-membrane bundles were produced by a round-potting process utilizing silicone. Device performance was tested in vitro according to ISO standards.

Results: The ArtPlac device is intended for neonates aged 24 to 40 weeks of gestational age, with body weights ranging from 400 to 5000 grams. The device will be connected like in a fetus through the umbilical vessels. The system will operate pumpless to reduce the risk of hemolysis and platelet activation. The hexagonal shaped mem- brane bundle contains a 60° angle between respective layers of oxygenation and dialysis hollow fiber mats. This allows the device to provide both lung and kidney support in customizable proportions in one device (Figure 1). A first prototype will be designed for neo- nates aged 28 to 37 weeks gestational age, weighing between 1000 and 2500 grams. This prototype shall include a gas exchange area of 0.12 m² and an estimated priming volume of 12 mL. Various device sizes will be developed to ensure compatibility with all targeted neonates.

Discussion: This novel hexagonal design combines oxygenation and dialysis in a single device. Future design goals include balancing pressure drop and hemodilution to our patients' needs. ArtPlac represents a

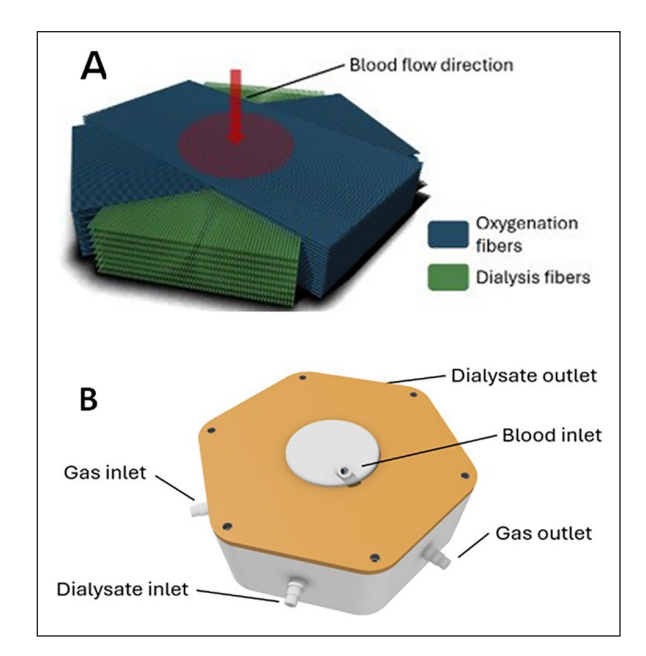


Figure 1. Design of ArtPlac providing lung and kidney support in one device. A) Hexagonal configuration of the hollow fiber membrane bundle allowing blood, gas, and dialysate flow. B) Device exterior with inlet and outlet ports.

groundbreaking treatment approach for enhancing survival rates and quality-of-life in neonatal intensive care.

References

- 1. Cao et al, JAMA Pediatr, 176 (8):787-796, 2022.
- David Sharrow et al, Levels & Trends in Child Mortality Report 2023 - Estimates developed by the United Nations Inter-agency Group for Child Mortality Estimation: 6,2024.
- 3. Nada et al, Semin Fetal Neonatal Med 22 (2): 90-97, 2017.
- 4. Stoll et al, JAMA 314 (10): 1039-51, 2015
- 5. Amodeo et al, Eur J of Pediatr, 180 (6): 1675-1692, 2021.

THE HYBRID (PNEUMATIC-NUMERICAL) RESPIRATORY SYSTEM SIMULATOR DESIGNED FOR NEW STRATEGIES OF INDEPENDENT LUNG VENTILATION

Krzysztof Zielinski¹, Zofia Knapinska¹, Anna Stecka¹, Maciej Kozarski¹, Marek Darowski¹

¹Nalecz Institute of Biocybernetics and Biomedical Engineering PAS,

Introduction: Independent lung ventilation (ILV) is a non-routine clinical procedure of mechanical ventilation used in patients suffering from respiratory failure and asymmetrical lung diseases. ILV can be performed by two ventilators, synchronized or working independently, where each ventilator supports one lung separately. An alternative way for ILV is to use a special pneumatic divider together with only one ventilator.

Physical simulators also called artificial patients play an important role in the process of evaluation of newly developed medical devices. In our Institute we have developed a specialized divider for ILV called Ventil [1] and implemented new control algorithms in it to, among others, prevent barotrauma. To access the performance of this divider we have developed a hybrid, pneumatic- numerical respiratory simulator (HRS), designed specially for ILV. The goal of this study was to evaluate the properties of the HRS by simulating ILV procedure with the Ventil connected between the HRS and a clinical ventilator.



Figure 1. The hardware of the hybrid respiratory simulator, two piston-based pressure sources, and the computer simulating the pathophysiology of the respiratory system in real time.

Methods: The HRS consists of two piston-based pneumatic pressure sources reproducing the pressure in the left and right bronchi. These pressure sources are the part of the pneumatic-numerical interface and are coupled with the real time digital model of the respiratory system mechanics [2] executed in the industrial PXI computer. This interface provides real time mutual communication between the real and digital worlds. The Ventil, a pneumatic divider for ILV, was connected to the HRS and the ventilator Draeger Evita V600. The ventilator was set in pressure control ventilatory mode. In the HRS, several asymmetrical lung diseases were simulated - resistive and elastic properties of the respiratory system were adjusted to obtain the desired pathology. The simulations were also performed for various control pressures, respiratory rates, inspiratory to expiratory values and positive end-expiratory pressures, as well as for different Ventil's parameters. All hardware signals and digital respiratory system model variables were recorded and analyzed.

Results: The HRS properly simulated unilateral lung diseases – the Acute Respiratory Distress Syndrome (reduction in parenchyma's compliance) and the Chronic Obstructive Pulmonary Disease (increased affected lung's bronchial tree resistance and emphysema, i.e., elevated parenchyma's compliance) for a wide range of changes from 25% to 1600% of the predicted values (simulated healthy patient). The HRS remained stable for all parameters adjusted in the ventilator and the Ventil.

Discussion: Simulation results proved that HRS is able to simulate both obstructive and restrictive asymmetrical lung diseases and then is a valuable tool to evaluate the systems for independent lung ventilation as well as to optimize ventilation therapy to improve ventilated patients' outcomes.

References

- 1. Zielinski et al, Sci Rep, 12(1):22591, 2022.
- 2. Zielinski et al, Membranes, 12(6):548, 2022.

Acknowledgements

This work was supported by the National Science Centre, Poland (Grant No 2021/43/D/ST7/01912).

8A: INNOVATIVE APPROACHES IN ALBUMIN-BASED THERAPIES: FROM RESEARCH TO CLINICAL APPLICATIONS IN ARTIFICIAL ORGANS

EXTRACORPOREAL MULTIORGAN SUPPORT
EFECTIVELY CORRECTS ACIDOSIS AND IMPROVES THE
STANDARDIZED MORTALITY RATIO: ANALYSIS OF
PATIENTS WITH ACIDOSIS FROM THE EMOS-REGISTRY

Tobias Bingold¹, Valentin Fuhrmann², Aritz Perez¹

¹ADVITOS GmbH, Munich, Germany; ²Universitätsklinikum Hamburg-Eppendorf, Klinik für Intensivmedizin, Hamburg, Germany

Introduction: The Advanced Organ Support (ADVOS) multi hemodialysis system (ADVITOS GmbH, Munich, Germany) effectively combines kidney, liver, and lung support together with acid-base balance correction for patients with multiple organ failure within a single device.

The present work aims to summarize the effect of ADVOS on acidosis correction and standardized mortality ratio (SMR) in a subgroup of patients with acidosis within the EMOS-Registry (DRKS00017068).

Methods: The Registry for Extracorporeal Multiorgan Support (EMOS Registry), designed as a non-interventional, multi-center, and non-randomized initiative for post-marketing surveillance, aimed to capture realworld clinical data from the patients that required multiple organ dialysis support with the ADVOS hemodialysis system.

The clinical data collected spans the period from 18/01/2017 to 31/08/2020. A total of 282 critically ill patient with an indication for

hemodialysis with ADVOS were enrolled in the study, with participation from 5 clinical sites in Germany. The subgroup of patients with acidosis included participants with pH < 7.35 at baseline (n = 146). The SOFA Score-Standardized Mortality Ratio (SMR) served to evaluate patient outcomes in the absence of a control group. To calculate the SMR, the observed number of deaths in the treated patients was compared to the expected number of deaths that would have occurred considering their SOFA score at baseline (i.e., immediately before the first ADVOS session).

Results: In the subgroup of patients with acidosis at baseline, a significant correction of acid-base balance was achieved for pH (7.26 vs. 7.39, p<0.001), serum bicarbonate (16.7 vs. 24.0 mmol/l, p<0.001) and base excess (-10.3 vs. -0.5 mmol/l, p<0.001) (Table 1). Moreover, only 27% of the patients with acidosis at baseline had a pH < 7.35 after the first ADVOS session (40 out of 146).

SOFA Score was available from 105 patients with acidosis (Figure 1). Those subjects showed a Standardized Mortality Ratio of 0.90 (CI95%: 0.70- 1.10), an absolute risk reduction (AAR) of 9% and a Number Needed to Treat (NNT) of 11.7.

Conclusion: ADVOS effectively corrects acidosis in critically ill patients, significantly improving pH, bicarbonate, and base excess. The SMR of 0.90 suggests a potential survival benefit. These findings support its use in multiorgan failure, warranting further research.

References

[1] Ferreira FL, et al. JAMA. 2001; 286(14): 1754-8

Table 1. Rapid change of bloom	ood gas parameters a	after the first ADVOS	session in patients with acidosis.

Parameter	Time	Median (IQR)	T test			
			Mean	Lower	Upper	Significance
Blood pH	Baseline	7.26 (7.17, 7–30)	0,14	0,11	0,16	0,000
	Post 1st Treatment	7.39 (7.31, 7450				
Serum Bicarbonate	Baseline	16.7 (14.2, 19.2)	6,7	5,6	7,8	0,000
	Post 1st Treatment	24.0 (20.0, 27.8)				
Base Excess	Baseline	-10.3 (-13.8, -6.7)	8,7	7,3	10,1	0,000
	Post 1st Treatment	-0.5 (-5.1, 4.0)				

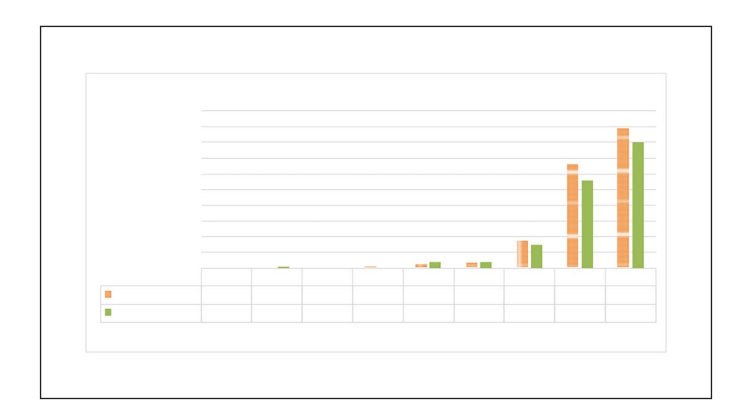


Figure 1. Expected (orange) vs. observed (green) deaths in each of the SOFA groups [1].

1-YEAR-FOLLOW-UP: ALTERATIONS OF ALBUMIN FUNCTION AFTER KIDNEY TRANSPLANTATION

Lea Marie Berntsen¹, Margret Paar², Katja Waterstradt ³, Kerstin Schnurr³, Max Lennart Westerbarkei¹, Gerd Klinkmann ⁴, Steffen Mitzner⁵, Karl Oettl², Andreas Kribben¹, Kristina Boss ¹

¹Department of Nephrology, University Hospital Essen, University Duisburg-Essen, Germany; ²Division of Medicinal Chemistry, Otto Loewi Research Center, Medical University of Graz, Austria; ³MedInnovation GmbH Berlin, Germany; ⁴Department of Anaesthesiology, Intensive Care Medicine and Pain Therapy, University of Rostock, Germany; ⁵Department of Medicine, Division of Nephrology, University of Rostock, Germany

Background: Patients with chronic kidney disease (CKD) have increased morbidity and mortality. This is mainly driven by chronic inflammation and increased level of oxidative stress. Albumin function is a suitable marker for investigating this in interaction with kidney function [1,4]. It is known that albumin function is altered in several ways in the first weeks after kidney transplantation (KT) but there is currently no data on the level to which albumin function improves when there is stable and sometimes even very good graft function

Methods: Albumin redox state (ARS) was determined by fractionating it into reduced human mercaptalbumin (HMA), reversibly oxidized human non-mercaptalbumin 1 (HNA-1), and irreversibly oxidized human non-mercaptalbumin 2 (HNA-2) by high-performance liquid chromatography. In healthy individuals, albumin circulates roughly in the following proportions: HMA 70–80%, HNA-1 20–30% and HNA-2 2–5% [2].

The binding and detoxification efficiency of albumin (BE and DTE) were assessed by electron paramagnetic resonance spectroscopy using a spin-labelled fatty acid. BE reflects strength and amount of bound fatty acids under certain ethanol concentration. DTE reflects the molecular flexibility of the patient's albumin molecule, thus the ability to change the conformation depending on ethanol concentration. Percentage of BE and DTE are depicted in relation to healthy individuals (100%) [3]. ARS, BE and DTE were determined at 9 time points up to one year after KT, as were renal function according to CKD-EPI eGFR and albuminuria as recommended by KDIGO guideline.

Results: 42 patients (29 male, median age 43.5 years) were analyzed. In the period of 180-365 days after KT, graft function further improved: eGFR increased by approximately 7 ml/min/1.73m². All patients showed stable, 23 patients even very good KT function with CKD stage G1 or G2. Albuminuria decreased in most patients to less than 30 mg/g creatinine.

Although kidney function increased, there was no further improvement of ARS in the total cohort (HMA 63.9% IQR 61.8-69.9%, HNA-1 29.6% IQR 24.6-32.7%, HNA-2 5.8% IQR 5.4-6.4%). BE also maintained its level one year after KT at 83% (IQR 74-101%), whereas DTE fell slightly to 85% (IQR 72-117%). In patients with good and very good graft function (CKD stage 1 and 2) albumin function is better than in the total cohort, but did not reach the level of healthy persons (BE 85.5% IQR 75.5- 94.5%, DTE 85% IQR 72.5-104.8%, HMA 67.4% IQR 63.4-70.3%, HNA-1 27% IQR 24.4-30.7%, HNA-2 5.7% IQR 5.4-6.1%).

Conclusion: This first multimodal one year follow-up after KT shows improvement of albumin function. However, even if graft function is at the level of healthy persons, albumin function remains limited.

References

 Jager KJ et al. A single number for advocacy and communicationworldwide more than 850 million individuals have kidney diseases. Kidney Int 2019;96:1048–50

- Oettl K et al. Redox state of human serum albumin in terms of cysteine-34 in health and disease. Methods Enzymol. 2010;474:181–95.
- Kazmierczak SC et al. Electron spin resonance spectroscopy of serum albumin: a novel new test for cancer diagnosis and monitoring. Clin Chem 2006;52:2129–34. 10.1373/clinchem.2006.073148
- Klammt S et al. Albumin-binding capacity (ABiC) is reduced in patients with chronic kidney disease along with an accumulation of protein-bound uraemic toxins. Nephrol Dial Transplant. 2012 Jun;27(6):2377-83.

Acknowledgements

The excellent technical assistance of Doris Payerl is highly appreciated. We thank the Albunet e.V. group for their constructive ideas for this project. This research received external funding from Stiftung Universitätsmedizin Essen (2023 4699 108).

ONLINE MONITORING OF THE EFFECTIVENESS AND CAPACITY OF ALBUMIN DIALYSIS PROCEDURES FOR EXTRACORPOREAL LIVER REPLACEMENT THERAPY

Sebastian Koball, Stine Koball, Jan Stange

Organization(s): ¹University of Rostock, Internal Medicine, Nephrology and Dialysis, Germany; ²Albutec GmbH, Rostock; Germany ³ProMedTec Germany GmbH, Rostock; Germany

Introduction: Various albumin dialysis procedures (MARS, OPAL, SPAD, Albunique) are used to treat patients with acute or acute to chronic liver failure. The principle of these procedures is similar. Dialysis therapy is carried out against a dialysate containing albumin. This absorbs protein-bound substances, especially those bound to albumin (for example bilirubin, bile acids, indoxyl sulfate, para-cresyl sulfate and others). The albumin-containing dialysate is then discarded or cleaned by adsorbers and reused in the circuit. The use of larger amounts of albumin increases the costs of the procedure.

Bilirubin, as a surrogate parameter for albumin- bound toxins, passes from the blood into the dialysate and is also removed from the dialysate again with the help of adsorbers in albumin- recirculating procedures. Bilirubin causes a clearly concentration-dependent discoloration of the dialysate, which can be measured using optical methods.

Methods: By quantitatively assessing the discoloration of the dialysate, it is possible to monitor the effectiveness of the liver replacement procedure. By measuring at different points in the dialysate circuit (behind the filter - before the adsorber and after the adsorber - before the filter), it is possible to optimize the control of the flow rates (particularly important for SPAD). In recirculating procedures, it is also possible to assess the adsorber capacity. The adsorber capacity is exhausted when there is no longer a difference in concentration before and after the adsorber. The adsorber should then be replaced.

Results: We would like to present initial results (in vivo and in vitro) of an optical measuring device for optimized control of the dialysate flows and monitoring of the adsorber capacity. The measurement is carried out spectroscopically and nephelometrically in a serial measurement construction. The combination of spectrophotometry and nephelometry makes the measurement robust against interferences.

Spectroscopic colour differences were measured on an individual patient basis, the significance of which is the subject of further investigations. A correlation between the optical measurement values and the bilirubin values measured in the laboratory was demonstrated. A computer-assisted evaluation of the data also allows online adjustment of the control to individual patient conditions (different bilirubin variants, hemolysis, etc. are recognized). It is shown that the capacity of some adsorbers is sufficient for treatment sessions longer than 48 hours. When used in SPAD treatments, the flow rate of the dialysate could be adapted to the transport capacity of the dialyser.

Discussion: The procedure is intended to enable more effective treatment of patients and reduce the costs of treatment (through lower albumin consumption and better utilization of the adsorber capacity).

THE ROLE OF ALBUMIN IN ARTIFICIAL ORGAN TECHNOLOGIES: INSIGHTS AND FUTURE PERSPECTIVES

Steffen Mitzner^{1,2}, Gerd Klinkmann^{2,3,4}

¹Department of Medicine, Division of Nephrology, University Medical Center, Germany; ²Department of Extracorporeal Therapy Systems, Fraunhofer Institute for Cell Therapy and Immunology, Germany; ³International Renal Research Institute of Vicenza (IRRIV), Italy; ⁴. Department of Anaesthesiology, Intensive Care Medicine and Pain Therapy, University of Rostock, Germany

The Role of Albumin in Artificial Organ Technologies: Insights and Future Perspectives: Albumin, an abundant and multifunctional plasma protein, is a pivotal component in maintaining physiological homeostasis and has become an indispensable element in artificial organ systems and extracorporeal therapies. Its unique biochemical and biophysical properties, including its high binding affinity for various endogenous and exogenous molecules, make it a critical agent in addressing complex pathophysiological conditions such as liver failure, sepsis, and multiorgan dysfunction. This lecture will provide a detailed exploration of the fundamental role of albumin in artificial organ technologies, its current applications, and the emerging innovations driving future advancements in the field.

The presentation will begin with an overview of albumin's structural and functional characteristics that underpin its clinical utility. Albumin serves as a molecular carrier for a wide range of substances, including bilirubin, fatty acids, and toxins, while also acting as a detoxification agent by binding protein-bound toxins and facilitating their removal. These properties are particularly significant in extracorporeal systems, where albumin enhances the efficacy of treatments designed to mimic or support organ function.

A primary focus will be on the application of albumin in liver support systems, such as albumin dialysis, where its ability to bind and clear protein-bound toxins has shown remarkable benefits in patients with acute and chronic liver failure. Similarly, in renal replacement therapies, albumin's role in modulating fluid balance, detoxification, and immune responses highlights its importance in optimizing treatment outcomes. These clinical applications are supported by robust evidence from case studies and clinical trials, which demonstrate improved survival rates, reduced inflammation, and enhanced quality of life for patients undergoing albumin-based therapies.

The lecture will also address recent innovations in the field, including the integration of albumin into hybrid devices and bioengineered materials to enhance biocompatibility and reduce the inflammatory complications

often associated with extracorporeal circuits. Advances in nanotechnology and material science are enabling the development of albumin-functionalized biomaterials, which have the potential to revolutionize artificial organ design by improving device efficiency and patient safety. Despite these advancements, several challenges remain, including the need to optimize albumin dosing strategies, address economic constraints related to albumin production, and ensure sustainable supply chains for clinical use. Additionally, ongoing research into the immunomodulatory properties of albumin is opening new pathways for its application in treating systemic inflammatory conditions and reducing complications in critically ill patients.

Future perspectives will focus on emerging technologies and personalized medicine approaches that aim to tailor albumin-based therapies to individual patient needs. These innovations include the potential use of recombinant albumin and synthetic albumin mimetics, which could offer greater stability, reduced immunogenicity, and enhanced functionality in artificial organ systems.

In summary, this lecture will synthesize current knowledge on albumin's role in artificial organ technologies, providing an evidence-based assessment of its therapeutic potential and identifying key challenges that must be addressed to fully realize its clinical impact. Attendees will gain a comprehensive understanding of how albumin- based innovations are shaping the future of extracorporeal therapies and advancing the management of life-threatening conditions in critical care settings.

NXECAD REDUCES CLIF EXPECTED 6 MONTHS MORTALITY IN ACLF SUPERIOR TO MARS IN LINE WITH SIGNIFICANT IMPROVEMENT OF ALBUMIN BINDING FUNCTION

Jan Stange ¹, Sebastian Koball ¹, Michael Hinz ¹, Hartmut Schmidt ², Andreas Kortgen ³, Matthias Dollinger ⁴, Steffen Mitzner ¹

¹University of Rostock Medical Center, Germany; ²University of Essen Medical Center, Germany; ³University of Jena Medical Center, Germany, ⁴University of Ulm Medical Center, Germany

Introduction: Albumin bound toxins, accumulating in liver failure, have a broad effect and role in manifestation and progression of multiorgan failure. Among others, toxic serum levels of Bile Acids are emerging as direct inducers of haemodynamic failure¹, renal failure², pulmonary damage³, mitochondrial toxicity and sarcopenia³, mental deterioration in acute liver failure⁴, cholestatic pruritus⁵, severe immune deficiency generally seen in jaundiced patients⁶, coagulation disorders⁷, disseminated intravascular coagulation⁸ and apoptosis in hepatocytes, therefore, inhibiting hepatic regeneration and recovery⁹. High Albumin binding rate makes extracorporeal removal in a selective (safe), effective and usable challenging. Only Extracorporeal Albumin Detoxification/dialysis (ECAD) using MARS has shown reduction of Acute on Chronic

Table 1. Effect on ACLF expected mortality.

CLIF-Calc.	preMars	postMars	p-Value		preNxECAD	postNxECAD	p-value	
exp. Mortality	Mean+SD	Mean	paired	unpaired	Mean	Mean	paired	unpaired
1 Month 3 Months 6 Months	37 + 33 49 + 33 52 + 33	31+32 42+33 46+32	0.007 0.008 0.006	0.454 0.420 0.426	37+32 49+34 53+33	27+30 38+33 41+33	0.006 0.004 0.002	0.226 0.206 0.197
Time Regression	Median 25%-75%	Median 25%-75%	Wilcoxon	MWU	Median 25%-75%	Median 25% 75%	Wilcoxon	MWU
cumulative	41(18-79)	31(10-69)	<0,001	0,23	43(17-75)	26(6-64)	<0.001	0.037

Liver Failure, a surrogate biomarker for survival, in multiple prospective randomized trials $(RCT)^{10-13}$. The aim of this research is to present "next generation MARS" data for ECAD (NxECAD) sessions using highly purified albumin (HepalbinTM) as dialysate on improvement of ACLF compared to MARS in a RCT.

Methods: 24 subjects with ACLF grade 1-3 were randomized to receive either MARS™ first and Hepalbin™ second or vice versa. ACLF grade was determined pre and post treatment using https://efclif.com/researchinfrastructure/score-calculators/clif-c-of-aclf-ad/, change of outcome prognosis was compared for ECAD sessions between groups.

Results: MARS and OPAL resulted into a significant improvement of calculated expected mortality at 30, 90 and 180 days after one treatment session, supporting earlier MARS trials reporting a survival benefit¹⁰⁻¹³. However, NxECAD significantly improved Albumin Binding Function in patients detected by Dansylsarcosine Binding to Sudlow II and ESR Spectroscopy of fatty acid binding, while MARS did not. MARS and NxECAD both removed Bile Acids significantly, while NxECAD Bile Acid reduction was significantly more effective. In line with this observation, reduction of calculated mortality over time (1-6 months) cumulatively was more prominent for NxECAD, which was significant not only in paired analysis (Wilcoxon signed rank) but even in unpaired analysis (MWU), as seen in Table 1.

Discussion: Analysis of the Opalesce trial support significant effect of ECAD on survival, which was more prominent for NxECAD, supported by qualitative improvement of patients albumin binding function.

References

- Fiorucci, S. et al. Am. J. Physiol.-Heart Circ. Physiol. 312, H21–H32 (2017).
- 2. Tinti, F. et al. Life 11, 1200 (2021).
- 3. Abrigo, J. et al. Biol. Res. 56, 30 (2023).
- 4. McMillin, M. et al. Am. J. Pathol. 186, 312-323 (2016).
- 5. Krawczyk, M. et al. Liver Int. 37, 743-747 (2017).
- Leonhardt, J. et al. Cell. Mol. Gastroenterol. Hepatol. 12, 25–40 (2021).
- 7. Reusswig, F. et al. Platelets 35, 2322733 (2024).
- Baker, K. S. et al. Arterioscler. Thromb. Vasc. Biol. 39, 2038–2048 (2019).
- 9. Faubion, W. A. et al. J. Clin. Invest. 103, 137–145 (1999).
- 10. Heemann et al. Hepatology 36(4Pt 1):949-58. (2002)
- 11. Hassanein et al. Hepatology 46(6):1853-1862 (2007)
- 12. Gerth Crit Care Med Oct;45(10):1616-1624 (2017)
- 13. Banares. Therap Adv Gastroenterol 2019 Sep 27;12:1756

Acknowledgements

Study was supported by EU and Federal and State Funds of Germany and Mecklenburg-Western Pommerania.

8B: IN-SILICO INVESTIGATIONS FOR FUTURE CLINICAL TRANSLATION

VIRTUAL CLINICAL TRIAL FRAMEWORK FOR EVALUATING MECHANICAL CIRCULATORY SUPPORT DEVICES

Prashant Chand¹, Andrew Stephens^{1,2}, Shaun Gregory¹

¹Advanced Cardiorespiratory Engineering Laboratory, Centre for Biomedical Technologies and School of Mechanical, Medical, and Process Engineering, Queensland University of Technology, Australia; ²School of Electrical Engineering and Robotics, Queensland University of Technology, Australia.

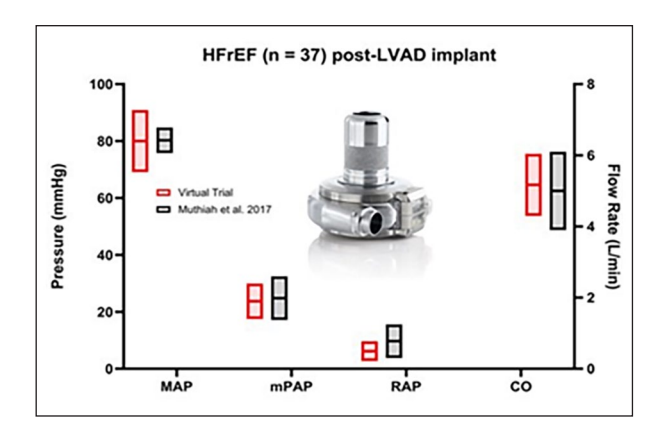


Figure 1. LVAD post implant Clinical vs Virtual Trial results [1].

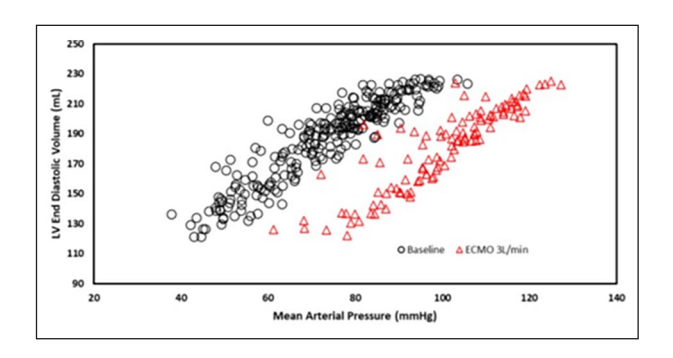


Figure 2. MAP vs EDV for baseline and VA ECMO.

Introduction: Mechanical circulatory and respiratory support devices are vital for patients with severe cardiac or pulmonary failure, yet their effectiveness varies across patient populations. This study aimed to establish a virtual clinical trial framework for evaluating these devices in a simulated environment. By generating "virtual patients" from clinical data, the model enables preclinical assessment of different device intervention and hemodynamic impact, allowing for detailed comparisons across various scenarios. Unlike traditional single-patient numerical simulations, this platform accounts for real-world patient variability, enhancing device evaluation, performance prediction, and design optimization.

Methods: In this study, a virtual clinical trial framework was developed and validated using published clinical data. The validation dataset included HFrEF patients (N=37) assessed before and after LVAD implantation. Heart rate and vascular resistance parameters were used to generate a synthetic population, incorporating systolic and/or diastolic dysfunction. Randomly combining these variables created "virtual patients," which were simulated in an advanced cardio-respiratory numerical model. Once validated, the platform was used to simulate Veno-Arterial (VA) ECMO patients (N=250), with cardiogenic shock pathophysiology, to analyze ECMO-induced hemodynamic changes. These patients were simulated under VA ECMO via central cannulation at a flow rate of 3 L/min.

Results: Figure 1 compares post-LVAD clinical data with virtual trial results, showing no significant differences, as indicated by p>0.05 for MAP, mPAP, and cardiac output. Figure 2 shows the virtual framework outcomes with and without VA ECMO support, revealing a scattered linear relationship between mean arterial pressure and end-diastolic volume (EDV). Among the 250 virtual patients simulated under VA ECMO, 100% experienced an increase in end-systolic volume. However, only 4%

showed an increase in EDV, 3.6% exhibited no change, and 92.4% had a reduced EDV compared to baseline hemodynamic state- further highlighting the diverse loading conditions in patients under VA ECMO that would otherwise be missed in single-patient simulations.

Discussion: The strong statistical alignment of LVAD virtual trial data with actual clinical results validates the application of the developed virtual framework in evaluating other MCS devices.

When applied to evaluate VA ECMO in a virtual cohort of 250 patients; with cardiogenic shock, significant variability in hemodynamics was observed, particularly concerning LV distention. This aligns with the different ECMO clinical data reported in the literature, where the precise mechanisms causing LV distention during VA ECMO remain an open question. These large- scale simulations capture patient variability often overlooked in single-patient models, enabling more detailed hemodynamic analysis and device evaluation. Consequently, this approach facilitates more patient-specific interventions, in particular LV decompression strategies when placed on VA ECMO.

References

1 Muthiah. K et al, J Heart Lung Transplant, 36(7):722-731, 2017.

IMPACT OF MITRAL VALVE REGURGITATION ON FLOW DYNAMICS IN VENTRICULAR ASSIST DEVICES

Mario Hahne¹, Thorben Kreutzfeldt¹, Frank-Hendrik Wurm¹

¹Institute of Turbomachinery, University of Rostock, Germany

Introduction: Cardiovascular diseases, including heart failure (HF), are increasing worldwide. For patients with advanced HF, ventricular assist devices (VADs) serve as a long-term alternative or as a bridge to heart transplantation. However, the high rate of rehospitalization and device replacement due to adverse events remains a major challenge. Continuous advancements in VAD technology are therefore crucial to improving patient outcomes.

Computational fluid dynamics (CFD) has proven to be a valuable tool for optimizing VAD performance. Traditionally, CFD analyses focus on steady-state conditions with constant VAD flow [1,2]. However, due to residual cardiac activity, VAD patients exhibit pulsatile flow patterns, leading to dynamic variations in operating conditions. While initial studies have investigated pulsatile flow in VADs [3,4], these are often limited to single HF cases. In reality, cardiovascular parameters vary significantly among HF patients. Previous studies have demonstrated that incorporating cardiovascular dynamics into CFD simulations significantly impacts VAD flow characteristics.

A common condition in VAD patients, particularly those classified according to AHA/ACC guidelines, is mitral valve regurgitation (MR). MR is characterized by retrograde blood flow from the left ventricle into the left atrium, potentially influencing VAD performance. To assess this impact, we implemented varying degrees of backflow in a bidirectionally coupled VAD-CFD simulation integrated with a cardiovascular system model.

Methods: The bidirectional coupling consists of a VAD-CFD model of the HeartMate 3 (Abbott Inc.). The VAD flow is simulated using a $k\text{-}\omega$ SST URANS approach. The cardiovascular system is represented by an electric-analogy 0D/1D Lumped Parameter Model (LPM). The LPM calculates the pressure in the left ventricle and aorta, which serve as inlet and outlet boundary conditions for the VAD- CFD. The VAD-CFD, in turn, determines the outlet flow rate, which is incorporated as the bypass flow between the left ventricle and aorta within the LPM. This bidirectional coupling ensures that both the VAD-CFD and the LPM are solved at each timestep, with continuous exchange of pressure and flow rate data. To model backflow caused by mitral valve regurgitation, an additional diode

and resistance are introduced in the LPM between the left ventricle and left atrium, opposing the main flow direction.

The methodology is validated against the H-Q characteristics of the HeartMate 3 as reported by Boes [5].

Results: Four backflow conditions up to 75 mL per heartbeat were analyzed, with a range of 40 to 90 mL corresponding to the mitral valve regurgitation backflow reported in a previous study [6].

As backflow increases, the pressure-volume (p-V) loop shifts toward lower end-systolic and end- diastolic volumes in the left ventricle. Additionally, maximum left ventricular pressure decreases with increasing backflow, ranging from 80 mmHg to 45 mmHg. Consequently, the minimum pressure head of the VAD increases from 18 mmHg to 48 mmHg, as the pressure difference between the aorta (VAD outlet) and the left ventricle (VAD inlet) rises. Furthermore, VAD flow decreases with increasing backflow, from 7 L/min to 6 L/min.

Discussion: Mitral valve regurgitation has been shown to affect the operating parameters of a VAD. By shifting the H-Q characteristic, the operating range is reduced, preventing the VAD from functioning under high overload conditions with excessive flow rates. As previously demonstrated, patient-specific boundary conditions significantly influence the operating point and blood damage behavior. The inclusion of mitral valve regurgitation further enhances the patient-specific VAD simulation.

References

- 1. Bourque K et al, ASAIO J, 62:375-383, 2016.
- 2. Thamsen B et al, Artif Organs, 39:651-659, 2015.
- 3. Horvath DJ et al, J Artif Organs, 23:123-132, 2020.
- 4. Fresiello L et al, Front Physiol, 13: 967449, 2022.
- 5. Boes et al, IEEE Trans Biomed Eng, 66:1618-1627, 2019.
- 6. Bennati L et al, Cardio Eng Tech, 14:457-475, 2023.

Acknowledgements

We thank Bente Thamsen for sharing the VAD geometry.

NUMERICAL SIMULATIONS OF THE IMPACT OF RUGOUS ARTIFICIAL SURFACES ON THE DEPLOYMENT OF VON WILLEBRAND FACTOR

Pierre-Louis Martin¹, Simon Mendez¹, Stéphane Pagano², Franck Nicoud^{1,3}

¹IMAG, University of Montpellier, CNRS, Montpellier, France; ²LMGC, University of Montpellier, CNRS, France; ³Institut Universitaire de France

Introduction: Von Willebrand factor (VWF) is a large multimeric mechano-sensing protein found in blood, playing a key role in shear-induced platelet aggregation (SIPA). At high shear rates (> 1500 s $^{-1}$ [1]), VWF transitions from a resting "globular" conformation to a filament-like unfolded conformation due to hydrodynamic forces. When unfolded and exposed to sufficient tension [2], VWF becomes activated and binds to platelets, slowing them down and initiating their adhesion. While many studies have explored platelet adhesion on microstructured artificial surfaces in the absence of flow [3], the impact of such surfaces on SIPA remains poorly understood. The present work uses numerical simulations to investigate the key step of SIPA by modelling VWF deployment under shear flow.

Methods: The flow configuration and the protein are illustrated in figure 1. The fluid is Newtonian, with a viscosity $v=3.10^{l^{m}}\,m^{\#}.\,s^{l5}$, and a density $\rho=1050\,kg.\,m^{1\%}.$ VWF is modeled as a coiled filament, and its mechanical behavior is described in equations (1-3).

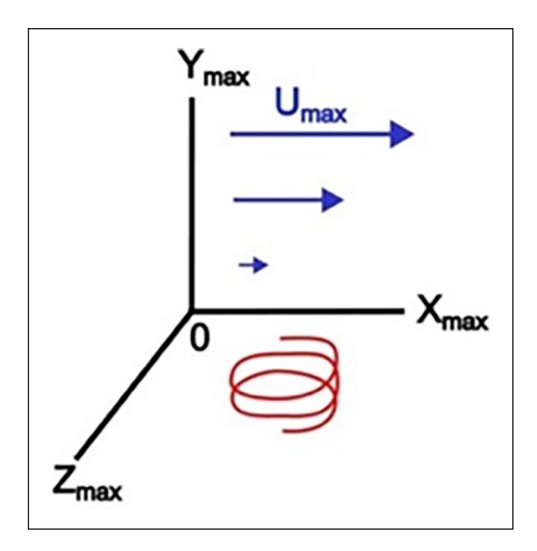


Figure 1. Flow configuration, and the protein (red) position at the initial time step. Xmax, Ymax and Zmax values are 2.5L, 1.3L and L respectively, where L is the contour length of VWF. A no-slip condition is applied in the (XZ) plane, and wall-slip conditions are applied at Z=0; Zmax. Periodic boundary conditions are used at X=0; Xmax. The wall at Y=Ymax moves at velocity Umax.

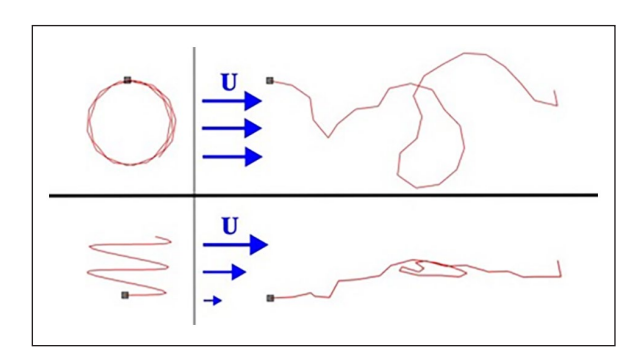


Figure 2. VWF in the absence of flow (left part), and VWF unfolding under shear flow (right part). The top part of the figure is a view from the top, and the bottom part is a view from the side. Black squares represent the anchoring point of VWF.

Fluid-structure interactions are handled using an immersed boundary method [4]. The protein having no inertia, the hydrodynamic forces balance the inner forces of VWF, which derive from three potentials: stretching (1), bending (2) and torsion (3). The variable X represents the coordinates of the protein, $E_{\rm g}$ its stretching stiffness, $E_{\rm g}$ its bending stiffness, κ its curvature, $E_{\rm g}$ its torsion stiffness, τ its torsion, and s the arclength. Terms with zero subscript are properties of VWF in the absence of flow. Please note that torsion here refers to out of plane bending, and not to twisting. Simulations are run with the YALES2BIO solver [5].

$$U_{\&} = {}_{\#}^{\$} E_{\&} \int (X - X_{1})^{\#} ds$$
 (1)

$$U_{\cdot} = {}^{\$}_{\#} E_{\cdot} \int (k - k_{1})^{\#} ds$$
 (2)

Table 1. Parameters used for the simulation presented in figure 2.

γ·L/U _{+,-}	$Re = \gamma L^{\#} / \nu$	E. / E _{&} Ľ	E. / E _c
0.75	3.10-8	1.5.10 ⁻³	1

$$U_{i} = {}^{\varsigma}E_{i} \int (\tau - \tau_{i})^{\sharp} ds$$
 (3)

Results: A representative result is presented in figure 2, illustrating the unfolding of adsorbed VWF under shear flow along a flat surface. This serves as a proof of concept for the implementation of equations (1-3). The parameters used for this simulation are provided in table 1.

Discussion: The presented results show the unfolding of a coiled filament under shear flow along a flat wall. The effect of rugosity on this mechanism will be discussed at the conference, should the abstract be accepted.

References

- 1. Lehmann M. et al, J Thromb Haemo 2018;16:104-15.
- 2. Bergal HT et al, Blood. 2022;140(23):2490-2499.
- 3. Ding Y et al, J Biom Mater Res 2013:101A:622-632.
- 4. Sigüenza J et al, J. Comput. Phys. 2016;322:723-746.
- 5. Mendez S et al, Biological Flow in Large Vessels. 2022;183-206.

VIRTUAL POPULATION STUDY OF BLOOD PRESSURE VARIATIONS BY AGE AND GENDER USING A 0D-1D CARDIOVASCULAR MODEL

Girindra Wardhana¹, Libera Fresiello¹, Dirk W. Donker^{1,2}

¹Cardiovascular and Respiratory Physiology, University of Twente, Enschede, the Netherlands; ²Intensive Care Centre, University Medical Centre Utrecht, Utrecht, the Netherlands

Introduction: In recent years, blood pressure monitoring has gained attention for its role in supporting therapy decisions and enhancing the understanding of complex (patho)physiological phenomena. This interest has led to the development of 0D and 1D computational cardiovascular (CV) models. In these models, heart and vessel parameters are tuned according to the patient status and possible CV pathologies to capture the related blood pressure alterations. The flexibility of these simulators can be capitalized on creating virtual populations (VPs) that summarize the main differences in blood pressure expected across a patient cohort. The development of a realistic and valuable VP strongly relies on the CV model and the tuning of its parameters.

So far, the effects of aging on 0D-1D CV parameters have been widely implemented, while the impact of gender remains underexplored. This work addresses this gap, by proposing an approach on how to simulate blood pressure profiles over healthy VPs, incorporating both age- and gender-related variations.

Methods: This study uses an open-loop CV simulator [1], with a 0D left ventricular (LV) model and a 0D-1D arterial network. CV parameters are tuned to represent subjects of different ages and gender (Figure 1). For aging, the simulator is tuned to reproduce decreased cardiac output and reduced vascular compliance, according to Charlton et al. [2]. For gender- specific variations, smaller cardiac dimensions and shorter and narrower arterial structures are considered in females compared to males, according to Zeid et al. [3]. The simulated VPs account for a total of 12 subjects, with 6 subjects for each gender. For validation, the

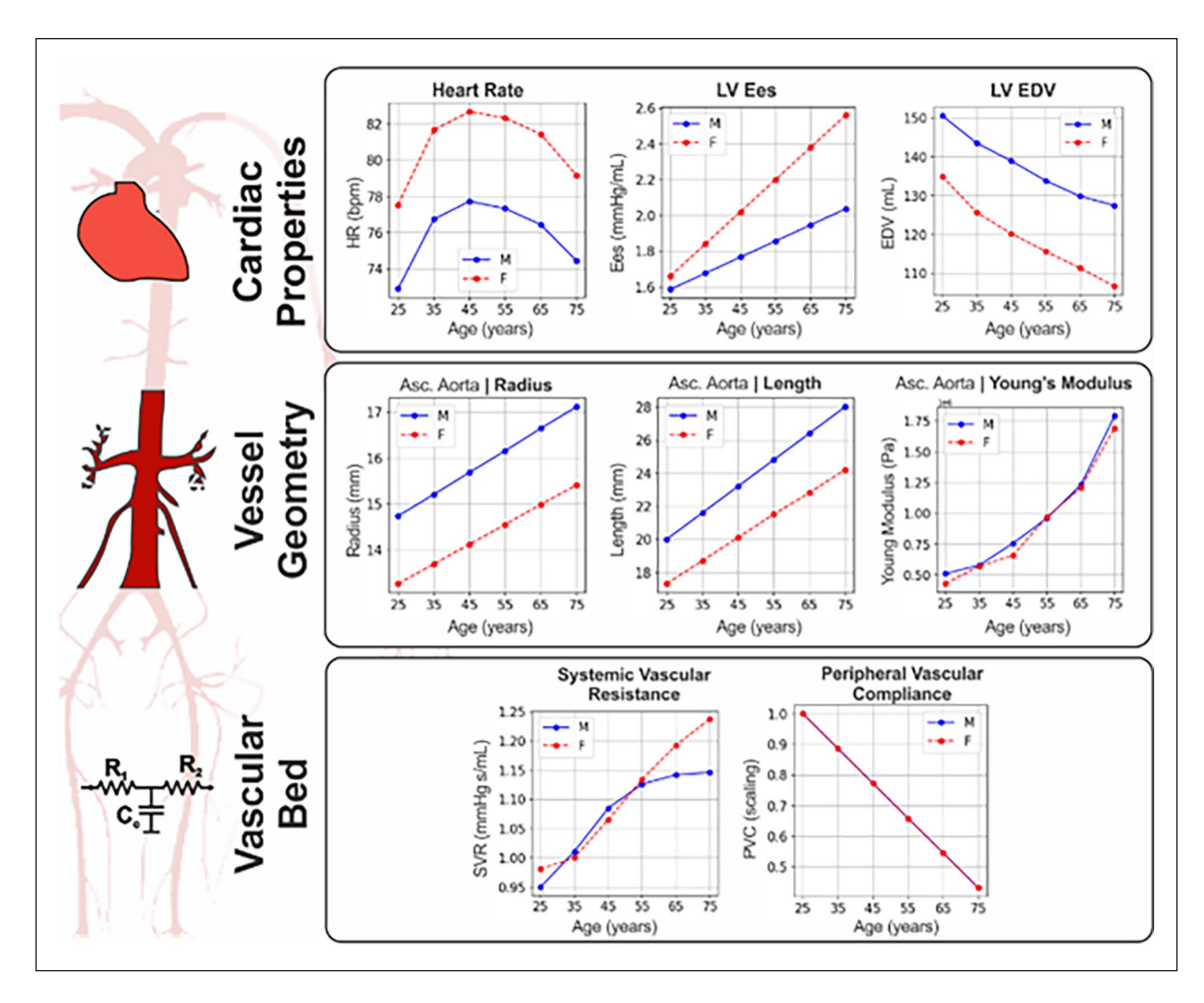


Figure 1. Adjusted parameters for modelling age and gender in virtual populations.

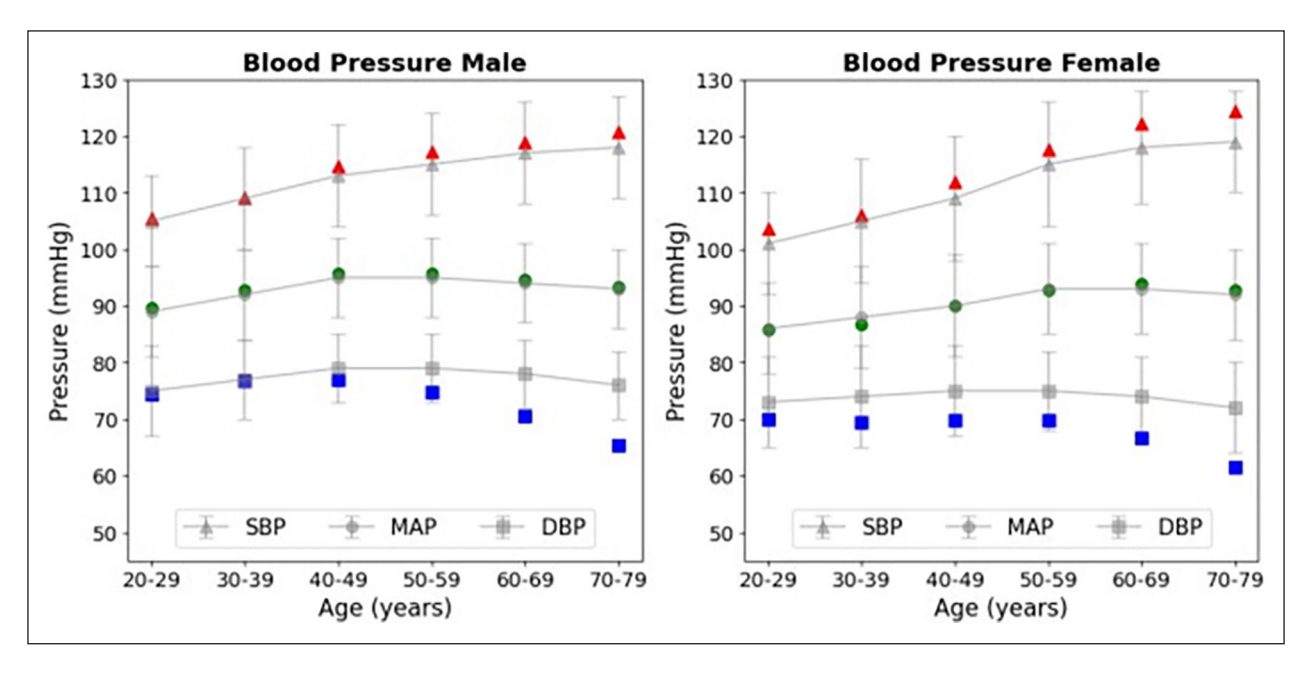


Figure 2. Blood pressure comparison between virtual populations (colored shapes) and literature data (gray shapes)[4].

simulated mean, systolic, and diastolic blood pressure (MAP, SBP, DBP) are compared with literature data from 4001 healthy subjects [4].

Results: RMSE of simulated vs. literature MAP, SBP, and DBP is 0.67, 1.79, and 5.65 mmHg for males and 0.68, 3.48, and 6.48 mmHg for females, respectively.

Discussion: Overall, the pressures of the VPs align with the literature data. A widening of pulse pressure with age is observed in both males and females, due to increased arterial stiffness [4]. The model provides a more accurate simulation of SBP and DBP for the younger male groups (<50 years) compared to older male groups (>50 years). Concerning the female VP groups, further parameter refinements are needed, as the model tends to underestimate diastolic blood pressure.

As future work, additional key factors that influence blood pressure will be included, such as body mass index and CV diseases, to provide more comprehensive VPs and even data for rare conditions. These VPs would be suitable to investigate specific pathophysiologies and to test related therapies while reducing reliance on costly clinical trials and avoiding ethical concerns.

References

- 1. Benemerito et al., Physiol. Meas., 45: 12, 2024
- Charlton et al., Am. J. Physiol.-Heart Circ. Physiol., v317, 5:H1062–H1085, 2019.
- 3. Zaid et al., Front. Cardiovasc. Med., v10, p1215958, 2023
- 4. McEniery et al., J.Am. Coll. Cardiol., 9:1753-1760, 2005

Acknowledgment

The work was supported by a research collaboration between the University of Twente and Sonion Nederland B.V.

CONTINUOUS VS PULSATILE ARTERIAL CANNULA FLOW FOR VENOARTERIAL EXTRACORPOREAL MEMBRANE OXYGENATION: A MULTISCALE COMPUTATIONAL FLUID DYNAMICS ANALYSIS

Avishka Wickramarachchi¹, Michael Neidlin², Mehrdad Khamooshi¹, Jessica Benitez^{3,4}, Eric L. Wu^{3,4}, John F. Fraser^{3,4,5}, Shaun D. Gregory ¹

¹Queensland University of Technology, Brisbane, Australia; ²RWTH Aachen University, Aachen, Germany; ³Critical Care Research Group, Brisbane, Australia; ⁴The University of Queensland, Brisbane, Australia; ⁵St. Andrews War Memorial Hospital, Spring Hill, Australia.

Introduction: Venoarterial extracorporeal membrane oxygenation (VA ECMO) is a treatment strategy that provides temporary circulatory and respiratory support for refractory cardiogenic shock patients. VA ECMO uses an extracorporeally placed pump to generate a continuous flow (CF) of blood which is delivered to the patient via an arterial cannula. Pulsatile flow (PF) VA ECMO has been proposed as an alternative method for delivering flow to diminish the risk of complications associated with CF, such as differential hypoxemia and left ventricular (LV) distension, which limit myocardial recovery and contribute towards the low survival rates of VA ECMO [1]. The aim of this study was to utilise a multiscale computational fluid dynamics (CFD) model to evaluate and compare the flow dynamics and hemodynamics generated by CF and PF VA ECMO.

Methods: A patient-specific aortic geometry was segmented from a computed tomography scan of a VA ECMO patient. A 19 Fr arterial cannula was then 3D modelled within the right external iliac artery. The inlet and outlet boundary conditions were controlled by a closed-loop lumped parameter network (LPN) adapted from Neidlin et al. [2]. Acute left heart failure was modelled in the LPN by reducing LV elastance. Then, 3, 3.5, 4, and 5 L/min VA ECMO flow rates were implemented at the arterial cannula's distal end surface. PF was modelled by switching off the LPN's VA ECMO compartment during LV systole and ramping up the pump speed during LV diastole. Differential hypoxemia was modelled by setting oxygen partial pressures of 37 and 200 mmHg to blood ejected by the LV and cannula, respectively, and then computing oxygen saturation (SO2) via the oxygen-hemoglobin dissociation curve.

Results: The hemodynamic results demonstrated increased ejection fractions and coronary flow during PF VA ECMO, and decreased afterload and pressure- volume areas, when compared to CF VA ECMO (Figure 1A). When simulating differential hypoxemia, the delivery of > 90% SO2 blood from VA ECMO to the arch vessels varied between PF and CF VA ECMO only at support levels of 3.5 and 4 L/min (Figure 1B). Even still, only slight improvements were observed during PF, such as increased SO2 in the right subclavian artery (94.0% vs 90.2% for PF and CF, respectively) during 4 L/min support. Lastly, wall shear stress (WSS) markedly increased during PF VA ECMO. For instance, during 5 L/min support, WSS was > 100 Pa higher during PF VA ECMO than CF VA ECMO.

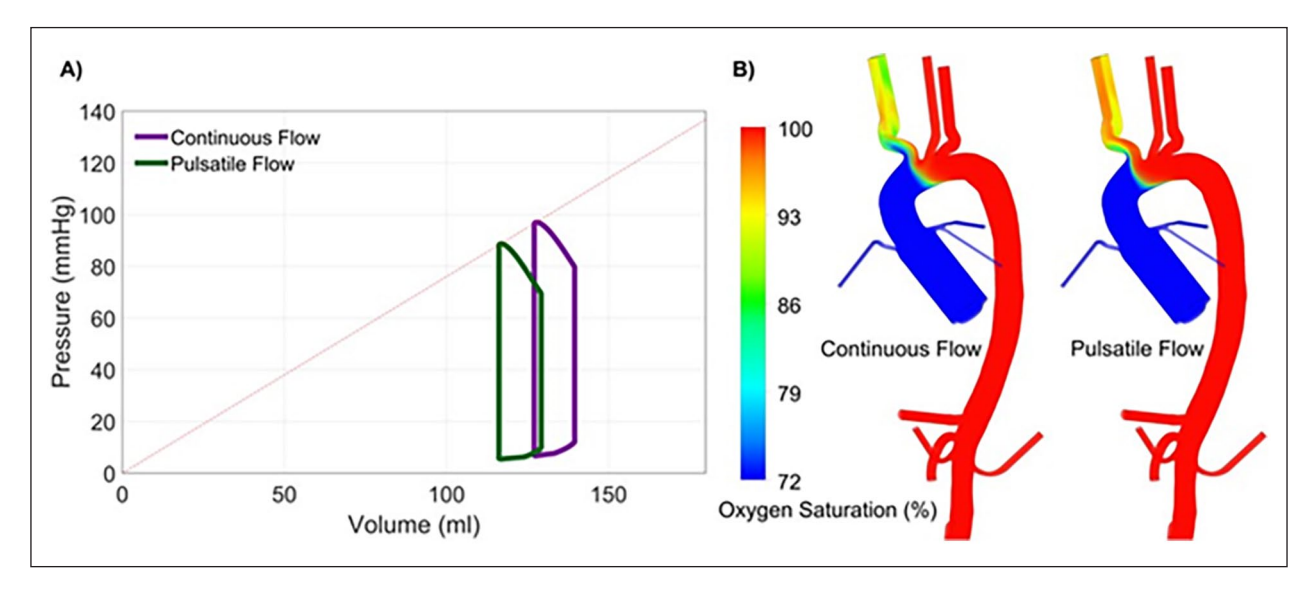


Figure 1. A) Left ventricular pressure-volume loops and B) watershed regions taken at end-diastole, both during 4 L/min continuous and pulsatile flow.

Discussion: Our findings indicate that PF may be able to mitigate the harmful hemodynamic effects of CF VA ECMO by increasing myocardial oxygen delivery and reducing oxygen demand. Marginal improvements in watershed region location suggest that PF VA ECMO may not be able to significantly improve cerebral oxygenation or significantly reduce the risk of differential hypoxemia. Lastly, increased WSS during PF VA ECMO may increase the risk of endothelial damage and blood trauma.

References

- M. Guglin, M. J. Zucker, V. M. Bazan, et al., "Venoarterial ECMO for adults: JACC scientific expert panel," *Journal of the American College of Cardiology*, vol. 73, pp. 698-716, 2019.
- M. Neidlin, C. Corsini, S. J. Sonntag, et al., "Hemodynamic analysis of outflow grafting positions of a ventricular assist device using closed-loop multiscale CFD simulations: Preliminary results," Journal of biomechanics, vol. 49, pp. 2718-2725, 2016.

9A: IFAO

DIFFERENTIATED FUNCTION OF PRIMARY RENAL TUBULE CELLS IN EXTENDED ARTIFICIAL CULTURE: RESULTS AT ONE YEAR

Rachel C. Evans¹ Alissa Ice¹ Shuvo Roy² William H. Fissell¹

¹Vanderbilt University Medical Center USA; ²University of California, San Francisco, USA

Introduction: End-stage Kidney Disease (ESKD) affects over 600,000 Americans and nearly 3 million worldwide. Treatment options are few and highly morbid. Our team has developed platform technologies for a new treatment option for ESKD that combines the universal availability of mass manufacturing with the cardiac and nutritional benefits of continuous therapy[1]. We combine a novel silicon nanopore membrane filter [2] to remove toxins with a bioreactor of cultured renal tubule cells to concentrate filtered toxins into urine [2-4]. This approach relies on durable function of cultured cells, which has not been a focus of previous cell culture protocols. Here, we demonstrate prolonged stable function of primary human renal tubule cells in culture out to one year.

Methods: Primary human renal tubule cells were purchased from Lonza and seeded at first passage at 0.5×10^5 cells/cm² onto permeable supports pre-coated with extracellular matrix proteins. After 48 hours of culture at 37C and 95/5 air/CO2 culture trays were placed on an orbital shaker to produce 2 dyne/cm² fluid shear stress averaged across the area of the culture well. Media (50:50 F12/low-glucose DMEM with T3, hydrocortisone, ITS, supplemental ascorbic acid and SB431542, a TGF}R2 inhibitor, and metformin, and inhibitor of Complex I) was changed thrice weekly.

Monolayer integrity was assessed by measuring leak of fluorescent dextrans from apical compartment to basolateral compartment. Active transport was assessed by measuring fluid volume transport in the absence and presence of tenapanor, furosemide, or hydrochlorothiazide. Mitochondrial fucntion was assessed by high-resolution respirometry using the Agilent Seahorse system.

Results: At 46 weeks in culture, renal tubule cells retained transport activity (not shown). SB431542 and metformin additivelty increased oxygen consumption compared to cells that received neither treatment (Fig 1).

Discussion: Primary renal tubule cells require TGF} inhibition for differentiation sufficient to support active transport *in vitro*. These cells are usually seen as prone to irreversible dedifferentiation in artificial culture. Prolonged culture is unusual in the context of discovery science but essential to bioengineering an artificial kidney. We have overcome the fundamental barriers to a mass- produced bioartificial kidney.

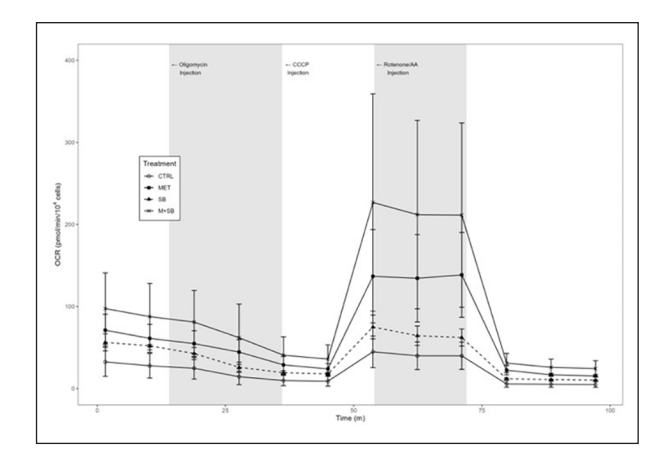


Figure 1. SB431542 (triangles) and metformin (squares) additively (circles) increased Renal Proximal Tubule Cells oxygen consumption at 46 weeks.

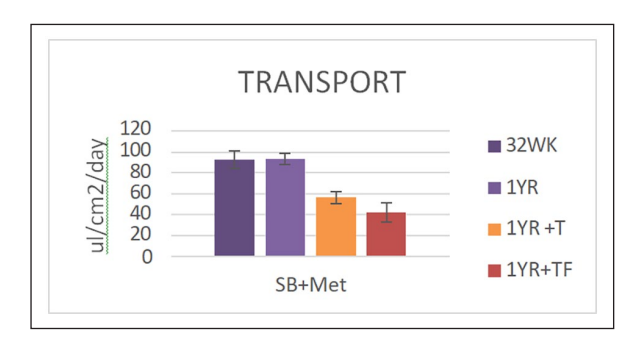


Figure 2. At 52 weeks, renal tubule cells in artificial culture retain diuretic-inhibitable active transport. T denotes tenapanor; TF denotes tenapanor and furosemide in combination.

References

- [1] Groth T et al Artif Organs. 2023;47(4):649-666.
- [2] Kensinger C et al ASAIO J. 2016;62(4):491-5
- [3] Kim EJ et al Nat Commun. 2023;14(1):4890.
- [4] Hunter K et al Tissue Eng Part A. 2023;29(3-4):102-111

A NOVEL OXYGENATOR OPTIMIZATION METHODOLOTY MITIGATING DUAL-LOW REGION

Tingting Wu^{1,2}, Xuhui Hua², Han Wu², Xianshan Qi², Thomas George Logan², Jamshid H. Karimov², Po-Lin Hsu^{1,2}

¹Artificial Organ Technology Lab, School of Mechanical and Electrical Engineering, Soochow University, Suzhou, China; ²magAssist Co., Ltd., Suzhou. China

Introduction: One of the many reasons that the Oxygenator is not suitable for long-term use is device coagulation. This study propose a novel design methodology to improve oxygenator blood compatibility, specifically mitigating coagulation. Efforts have been made for identifying low velocity area for lower the risk of thrombotic deposition [1]. Some study relates the low shear rate to thrombotic risks [2]. The concept connects the region prone to affecting the device coagulation performance to the identified low flow velocity and low shear rate areas ("dual-low regions").

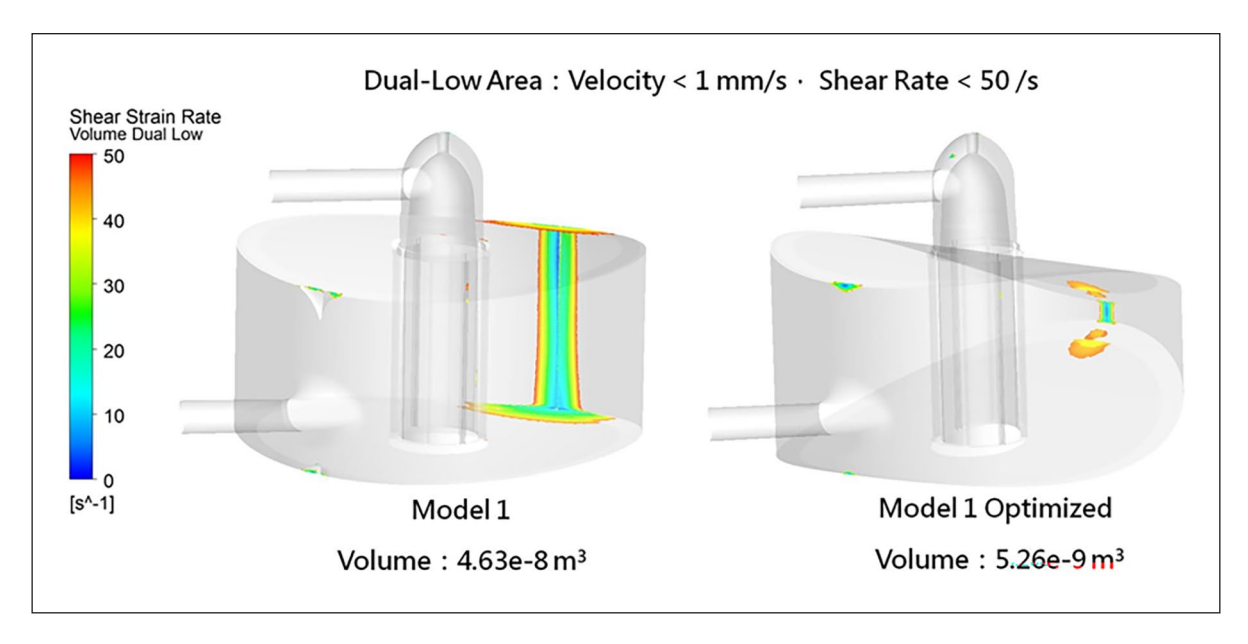


Fig.1. Dual-Low region decrease observed after structural modification.

Methods: Dual-low regions were defined as low flow velocity (<1 mm/s) and low shear rate (<50/s). A Computational Fluid Dynamics (CFD) simulation model of BreathMo® oxygenator iteration was employed to identify the dual-low regions. A morphological assessment of the flow field was performed to observe structural flow obstructions and alteration to flow direction.

The dual-low regions identified in the oxygenator by CFD fitted well with the thrombus formation observed in vivo. Flow field analysis elucidated the underlying factors contributing to their formation. Structural modifications were conducted and effectively reduced the volume of dual-low regions by 88.6% (Fig. 1). These changes may lead to a more optimized flow field conducive to enhanced blood compatibility.

Results: The dual-low regions identified in the oxygenator by CFD fitted well with the thrombus formation observed in vivo. Flow field analysis elucidated the underlying factors contributing to their formation. Structural modifications were conducted and effectively reduced the volume of dual-low regions by 88.6% (Fig. 1). These changes may lead to a more optimized flow field conducive to enhanced blood compatibility.

Discussion: The proposed study design methodology incorporating dual-low region identification using CFD analysis, flow field examination, and structural flow optimization has demonstrated its feasibility and successfully provided essential insights. The approach can mitigate risk- associated adverse effects of dual-low regions, improve the oxygenator hemocompatibility performance. Future work will focus on validating the model with coagulation tests and quantify the relationship between the dual-low region and the coagulation performance.

References

- 1. Gartner et al, Artificial Organs, 24(1), 29-36, 2000.
- 2. Lauren et al, Journal of Vascular Surgery, 61(4),1068-1080, 2015.

Acknowledgements

This work is sponsored by magAssist Co., Ltd..

9B: TOXIN REMOVAL IN DIALYSIS

WARMING UP TO IMPROVE HEMODIALYSIS: UREMIC TOXIN CLEARANCE NON-LINEARLY RISES WITH TEMPERATURE

João Brás¹, Fokko Wieringa¹,2,3, Jeroen Vollenbroek¹,2,4, Karin Gerritsen¹

¹Department of Nephrology and Hypertension, University Medical Centre Utrecht, Utrecht, The Netherlands; ²IMEC, Holst Centre, Eindhoven, The Netherlands; ³EKHA WG3, Brussels, Belgium; ⁴BIOS Lab on a Chip Group, MESA + Institute, University of Twente, Enschede, The Netherlands

Introduction: Current hemodialysis (HD) techniques are weak at removing protein-bound uremic toxins (PBUTs), which strongly associate with plasma proteins like albumin. PBUT accumulation contributes to complications as cardiovascular disease, accelerated aging and uremic syndrome. Various strategies to enhance PBUT removal are under investigation, including the use of adsorbents, chemical displacers, increased ionic strength, and pH-shifts [1], but further research is needed before clinical implementation. In this study, building on our findings presented at ESAO 2024, we explored whether further increasing albumin temperature (up to 45°C) safely enhances uremic toxin removal, as protein binding is temperature-dependent, with higher temperatures reducing bound fractions [2]. In addition, temperature-augmented PBUT removal is reversible and compatible with current HD machines, while maintaining circuit sterility.

Methods: PBUT free fractions were determined by static in- vitro "Rapid Equilibrium Dialysis" (RED, Thermo Scientific™) protein binding assays. 40g/L albumin solutions were spiked with 3 toxins at uremic concentrations: Indoxyl Sulfate (IS), p-Cresyl Sulfate (pCS), and Hippuric Acid (HA) (150 μM, 200 μM & 400 μM respectively). These solutions were

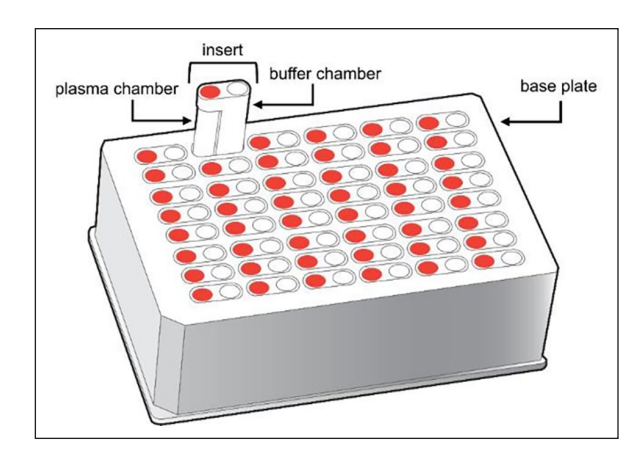


Figure 1. The rapid equilibrium dialysis device can warm up to 48 RED dialysis cells simultaneously.

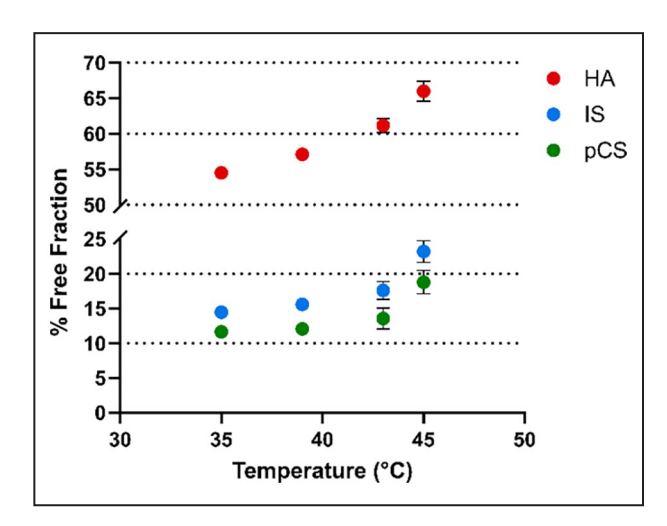


Figure 2. Free fractions of IS, pCS, and HA at incubation temperatures between 35-45°C.

incubated in triplicate for 4h at 35, 39, 43, and 45°C. PBUT concentrations were measured with HPLC. The free fraction was calculated by Eq. 1:

Results: For all 3 PBUTs, free fractions increased when elevating temperature from 35°C to 43°C (IS 1.2- fold, pCS and HA 1.1-fold). At 45°C, the increase was more pronounced: pCS 1.6-fold, IS 1.5-fold, and HA 1.2-fold (with a stronger effect per °C).

Discussion: The temperature effect was more notable for the highly bound toxins (IS, pCS) than for the least bound (HA), which aligns with previous reports [2,3]. The temp. range is still within reversible conformation changes in albumin [4]. We present work-in-progress; more research is required on understanding the observed non-linear behavior, max. safe whole blood temp., blood integrity after prolonged temp. cycling, and possible adverse effects. Yet, the approach seems promising.

References

- 1. Sánchez-Ospina D. et al, J. Clin. Med, 13:1428, 2024.
- Deltombe O. et al, Anal. Methods, 9:1935-1940, 2017.

- 3. Berezhkovskiy L. Drug Discov Ther, 2(2):74-6, 2008.
- 4. Rezaei-Tavirani M. et al, BMB Rep, 39:530-36, 2006.

Acknowledgements

This project was funded by a KidneyX Prize (MI-TRAM) and the Dutch national growth fund (NXTGEN HighTech Biomed04). We thank the Albunet e.V. and Eutox group for their input on this project.

ENGINEERING THE FUTURE OF HEMODIALYSIS: INNOVATIVE MEMBRANES FOR OPTIMAL BLOOD PURIFICATION

Beatriz Nunes¹, Flávia S.C. Rodrigues¹, Ricardo Bexiga², Rita F. Pires¹, Mónica Faria¹

¹Laboratory of Physics of Materials and Emerging Technologies (LaPMET), Center of Physics and Engineering of Advanced Materials (CeFEMA), Instituto Superior Técnico, Universidade de Lisboa, Portugal; ²Faculty of Veterinary Medicine, Universidade de Lisboa, Portugal.

Introduction: Chronic kidney disease affects 10% of the global population and is a significant health concern with high mortality rates. When patients reach End- Stage Renal Disease, they rely on hemodialysis (HD) to survive [1]. However, despite HD's ability to remove approximately 45% of all known toxins, it is ineffective at eliminating Protein-Bound Uremic Toxins (PBUTs) due to their strong binding to essential proteins such as Human Serum Albumin (HSA).

Various strategies have been explored to tackle this issue. Among them, mixed matrix membranes (MMMs) composed of a polymer matrix incorporating porous additives with adsorption capacity (e.g. activated carbon) have shown promising results in trapping toxins and enhancing PBUT removal [2]. Metal-Organic Frameworks (MOFs), crystalline materials made from organic ligands and metal ions, have demonstrated excellent adsorption capacity and stability, making them promising candidates for HD applications.

Zirconium-based MOFs (Zr-MOFs), such as NU-1000-comprising zirconium metal ions and pyrene-based linkers-exhibit high PBUTs adsorption efficiency in aqueous solutions [3], making them an interesting option for enhancing PBUT removal during HD. In this study, for the first time, NU-1000 was incorporated into cellulose acetate-based (CA)-based casting solutions to create novel integral asymmetric CA/ NU-1000 MMMs. The adsorption capacity of these membranes towards indoxyl sulfate (IS), a well- known PBUT, was investigated, along with their hemocompatibility.

Methods: The adsorption capacity of the NU-1000 towards IS was evaluated through direct contact studies in phosphate-buffered saline (PBS) and in human blood plasma solutions. Computational docking studies were also performed to understand the nature of interactions between the NU-1000 and IS.NU-1000 (2% wt.) was incorporated into CA- based casting solutions to fabricate novel integral asymmetric CA/NU-1000 MMMs using the phase inversion method. The resulting CA/NU-1000 MMMs were characterized by FTIR, SEM, AFM, and 3D computed tomography (CT) scanning. Their permeation performance was assessed in terms of hydraulic permeability and molecular weight cut-off. The removal of IS from spiked human blood plasma by the CA/NU-1000 MMMs was studied in an extracorporeal HD setup over a 4-hour period, with results compared to pure CA membranes. The hemocompatibility of CA/NU- 1000 MMMs was evaluated through platelet adhesion, thrombosis and whole blood filtration studies.

Results: Docking studies showed strong interactions between the NU-1000 and IS, leading to an adsorption capacity of 60% for a 20 ppm IS solution (in PBS) after 3 hours when NU-1000 was placed in direct contact with PBS. Additionally, NU-1000 disrupted the interaction between IS and HSA, increasing the concentration of unbound IS when introduced into IS-spiked blood plasma. 3D CT scans and SEM

micrographs of the CA/NU-1000 confirmed the membrane's asymmetry, revealing a total thickness of 89 \pm 1 μm , a porosity of 60 % and a uniform distribution of NU-1000 throughout the membrane. Although the CA/NU-1000 MMMs contained only 2wt.% NU-1000, IS clearance studies demonstrated that after 4 hours, these membranes removed 1.3 and 1.05 times more IS via permeation compared to pure CA membrane from PBS and blood plasma solutions, respectively. Despite the thrombosis experiment showing high thrombus formation after 1 hour of direct contact ~92% for pure CA membranes and 95-99% for CA/NU-1000 MMMs), low platelet adhesion and negligible hemolysis were observed after 4 hours of whole blood filtration.

Discussion: NU-1000 exhibited a high adsorption capacity for IS. Its successful incorporation into the CA matrix, resulting in the development of CA/NU-1000 MMMs, offers a promising hemocompatible alternative for PBUT removal via adsorption. This approach has the potential to be applied in future hemodialyzers, enhancing toxin clearance during hemodialysis.

References

- 1. Rodrigues, F.S.C. et al, Toxins, 15:110, 2023.
- 2. Kim, D.L. et al, J Membr Sci, 609:118187, 2020.
- 3. Wang, T.C. et al., Nat Protoc, 11:149-162, 2016.

Acknowledgements

Fundação para a Ciência e a Tecnologia (FCT, Portugal) supported this work through programmatic funding UIDB/04540/2020, UIDP/04540/2020, grants UI/BD/150949/2021 and CEECIND/CP1651/CT0016.

OPTIMIZED BLENDING OF DANAPAROID INTO DIALYSIS MEMBRANES FOR LONG TERM HEMOCOMPATIBILITY

Roberto Nese¹, Odyl ter Beek¹, Edwin Kellenbach², Dimitrios Stamatialis¹

¹AOT, Faculty of Science and Technology, TechMed Centre, University of Twente, The Netherlands; ²BioChemOss B.V., FX2123, Kloosterstraat 6, 5349AB, Oss, the Netherlands

Introduction: Recent studies affirm that Chronic Kidney Disease may become the fifth cause of death among the population of the world by 2040 [1]. To face this challenging situation, innovations and new technologies for dialysis therapies are urgently needed. For example, more continuous dialysis therapies, like home or portable hemodialysis, could better mimic the function of a healthy kidney and thus achieve higher removal of uremic toxins from the blood of patients [2]. However, this requires innovative dialyzers and membranes with excellent hemocompatibility. Recent innovations are focusing on the use of new materials for membrane fabrication, like cellulose triacetate or heparin-like polymers, but limitations in their use for longer dialysis sessions are still present. To significantly improve the hemocompatibility of dialysis membranes, we aim to incorporate Glycosaminoglycans (GAGs) in the polymeric structure of the membranes; GAGs are long linear polysaccharides that can be found in human's kidney glomerulus, providing natural anticoagulating and antifouling properties. In our group we previously assessed that Danaparoid (DP), which is a mixture of different GAGs, shows an improved hemocompatibility in comparison to other types of GAGs [3]. In this study, we present an optimized process to blend DP and other GAGs in hollow fiber membranes and report the first results of hemocompatibility studies.

Methods: A water solution containing GAGs was blended with a polymeric solution made of polyethersulfone (PES), polyvinylpyrrolidone (PVP) and N-methyl-2- pyrrolidone (NMP). The polymer solution containing GAGs was extruded with a lab scale spinning setup to produce hollow fiber membranes with a small inner diameter. After the spinning process, the fibers were rinsed in a water solution containing glycerol to

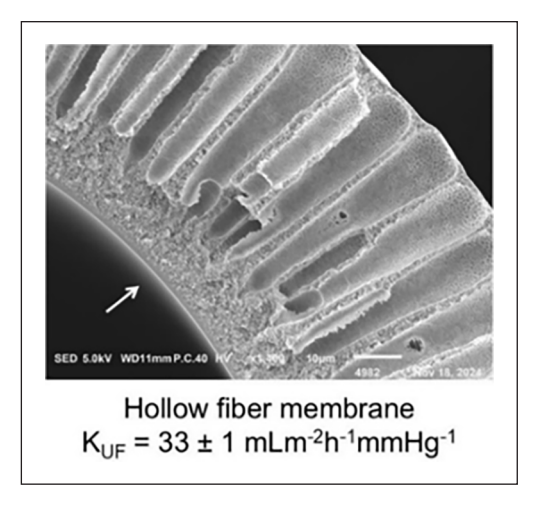


Figure 1. SEM image of a hollow fiber membrane with DP.

preserve the pores of the selective layer during the drying process. The presence of GAGs in the fibers was verified by immunostaining, color-staining and other material analysis like SEM-EDX and Inductively Coupled Plasma Optical Emission Spectroscopy (ICP- OES). To assess the hemocompatibility of the obtained fibers, we performed various biological assays, like anti-factor Xa and IIa activity and thrombin generation analysis.

Results and Discussion: Figure 1 shows a SEM image of a hollow fiber membrane containing DP. The fiber was spun with the optimal spinning conditions to obtain an inner diameter of 250 μ m and a wall thickness of 50 μ m with relatively small macro-voids. The permeability of the fiber is mainly affected by the pores that are present in the selective layer (indicated by the white arrow in Figure 1). During the drying process, the addition of glycerol is essential to preserve these pores and provide fibers with an ultrafiltration coefficient (KUF) that varies between 20 and 30 mLm-2h-1mmHg-1. Material and color-staining analysis indicate that DP is mainly present in the lumen of the fiber.

Conclusion: We found that blending is a simple and effective way to incorporate and concentrate GAGs in the lumen of the fibers. Moreover, the KUF of the obtained fibers is suitable for dialysis. We are currently performing experiments with full human blood to verify the toxin removal efficiency and the hemocompatibility of these membranes compared to commercial dialysis membranes and hollow fiber membranes without GAGs.

References

- 1. Foreman K.J. et al. (2018). 392(10159):2052-90
- 2. Stamatialis, Dimitrios, World Scientific (2017). ISBN: 9813221755
- 3. Kim, DooLi, et al. (2024). 122669.

Acknowledgements

This project is made possible in part by a contribution from the National Growth Fund program NXTGEN Hightech. We thank Erik ter Voert for his assistance and technical support in SEM-EDX analysis.

A MEMBRANE-DRUG-DENDRIMER SYNERGIC SYSTEM TO ENHANCE PROTEIN BOUND UREMIC TOXIN CLEARANCE

Rita F. Pires¹, Johanna Grimm¹, Vasco D.B. Bonifácio², Mónica Faria¹

¹Laboratory of Physics of Materials and Emerging Technologies (LaPMET), Center of Physics and Engineering of Advanced Materials

(CeFEMA), Instituto Superior Técnico, Universidade de Lisboa, Portugal; ²Institute of Bioengineering and Biosciences (iBB) and Institute for Health and Bioeconomy (i4HB), Bioengineering Department, Instituto Superior Técnico, Universidade de Lisboa, Portugal.

Introduction: Patients with end-stage renal disease (ESRD), rely on hemodialysis (HD) to survive. While traditional HD removes many uremic toxins, it struggles to clear Protein-Bound Uremic Toxins (PBUTs) due to their strong binding to human serum albumin (HSA), increasing patient mortality and morbidity [1].

Among the different approaches to address this issue, using drugs with competitive binding properties has emerged as a potential solution. A 2019 clinical trial showed that infusing 800 mg of ibuprofen (IBU) into the HD circuit during the first 19 minutes of a 4-hour session increased indoxyl sulfate (IS) clearance by 2.4 times. However, this effect diminished quickly, returning to baseline between 60 and 240 minutes. Additionally, residual IBU was found in patients, raising safety concerns and questioning this approach's sustainability [2]. To overcome these challenges, we developed a two-component extracorporeal lab-scale HD setup composed of: (1) polyurea-based dendrimer (PUREG4) nanocarriers [3] for controlled drug release to enhance PBUT dissociation from HSA, and (2) integral asymmetric cellulose acetate (CA) membranes for removing the free PBUT fraction from the blood [4].

Methods: Two pharmaceutical drugs, IBU and Furosemide (FUR), were encapsulated into 4th generation polyurea dendrimers (PUREG4) rendering IBU@PUREG4 and FUR@PUREG4 nanoformulations and the release profiles were evaluated in PBS and human blood plasma. Integral asymmetric monophasic CA membranes were fabricated by the phase inversion method and characterized in terms of hydraulic permeability, molecular weight cut-off and hemocompatibility. A lab-scale extracorporeal blood circulation circuit was constructed where IBU (<8 mg) was gradually released into the blood plasma line over a 4-hour period. *In vitro* competitive displacement assays were performed through the gradual release of 8 mg of IBU and or FUR into the IS-spiked blood plasma line and by monitoring the concentration of free IS. The concentrations of IS in the blood plasma circuit and in the permeate were measured by fluorescence spectroscopy throughout the entire 4 hours at different time points.

Results: Furosemide and IBU were successfully encapsulated into the PUREG4.The release studies showed that, after 4 hours, 73 and 63% of the encapsulated IBU was released into PBS and blood plasma, respectively. *In vitro* competitive displacement assays showed that the continuous release of IBU, up to a total of 5 mg, resulted in a 3.7-fold increase of the concentration of unbound IS in blood plasma and a 3.8-fold increase in the clearance of IS.

Discussion: This innovative approach combines drugs displacement action with the selective membrane filtration, throughout the entire treatment in contrast to the direct infusion of high doses of IBU at the beginning of the HD session.

This synergistic effect of the slow release of IBU, combined with IS permeation through the semipermeable CA membrane, not only improves the efficiency of PBUT removal, but also reduces the risk of accumulation of nonsteroidal anti- inflammatory drugs, such as IBU, in patients undergoing regular HD, making it a safer long-term solution for ESRD management.

References

- 1. Rodrigues, F.S.C. et al, Toxins 15:110, 2023.
- 2. Madero, M. et al., Clin J Am Soc Nephrol 14:394-402, 2019.
- 3. Restani, R.B. et al., Part Part Syst Charact, 33:851-858. 2016.
- 4. Almeida P. et al, Sep Purif Technol, 359:130519, 2025.

Acknowledgements

This work was supported by Fundação para a Ciência e a Tecnologia (FCT, Portugal) through the CeFEMA programmatic funding UIDB/04540/2020, UIDP/04540/2020, contract grant CEECIND/CP1651/CT0016.

DEVELOPMENT OF DUAL-LAYER MIXED MATRIX HEMODIALYSIS MEMBRANES FOR OUTSIDE-IN FILTRATION

Ramada, D.¹, de Jong, E.¹, ter Beek, O.E.M¹, Labib, M.² Stamatialis, D.¹

¹-Advanced Organ Bioengineering and Therapeutics, Faculty of Science and Technology, University of Twente, Zuidhorst 28, Drienerlolaan 5, 7522 NB Enschede, The Netherlands; ² NovaFlux, 1 Wall Street, Princeton, NJ 08540, USA

Introduction: Hemodialysis is the standard therapy for End- Stage Renal Disease (ESRD) but has limited efficacy in removing Protein-Bound Uremic Toxins (PBUTs), contributing to complications and high mortality rates [1,2]. Mixed Matrix Membranes (MMMs) offer an innovative solution by combining diffusion and adsorption for improved PBUT removal [3]. When paired with prolonged hemodialysis, further improvements are possible. However, extended blood exposure to dialyzer materials increases the risk of clotting, reducing the effective surface area for toxin removal. The outside-in filtration mode (OIF), where blood flows outside rather than inside the fibers can mitigate clotting and supports longer treatments. This study focusses on development of MMM for OIF for achieving improved PBUT removal with minimal clotting. In an earlier study [4], we have developed MMM fabrication for OIF. Here, we focus on further improving the membrane morphology to minimize albumin leakage combined with high PBUT removal.

Methods: OIF-MMMs were fabricated by dry-wet spinning using two new polymer dope solutions – particle free and particle rich – based on polyethersulfone /polyvinylpyrrolidone polymer (PES/PVP) blends. The fibers' physical and transport properties (ultrafiltration coefficient, protein-bound uremic toxin, hippuric acid (HA) and indoxyl sulphate (IS), removal from human plasma) were studied.

Results - Discussion: Figure 1 presents typical SEM images of OIF-MMMs, showing particle-free and particle-rich layers. Table 1 presents the main characteristics of the membranes. The developed fibers have lower KUF and PBUT removal (shown here with plasma dialysance, DLp), while having higher albumin sieving coefficient than those reported earlier [4].

To improve fiber permeability, minimize protein leakage and improve toxin removal, we aim to: 1) optimize PES/PVP ratios to achieve a more balanced outer layer structure (large enough pores to enhance permeability for toxins, but small enough to limit protein leakage), 2) optimize bore solution composition to influence inner layer morphology (fewer macrovoids, more sponge-like structure) and 3) refine spinning conditions to reduce fiber size.

References

- 1. Pavlenko, D. et al., Scientific Reports (2016)
- Stamatialis, D., Biomedical membranes and (bio) artificial organs. Vol. 2. World Scientific (2017)
- 3. Kim, D., et al., Journal of Membrane Science, 609 (2020): 118187
- 4. Ter Beek, O.E.M, et al., Acta Biomaterialia, 123 (2021): 244-253

Table 1. Properties of new OIF-MMMs and previously developed [4] fibers.

OIF MMM	This study	Ref. [4]
ID/OD/Wall (μm)	486/851/184	329/518/92
KUF (mL m ⁻² h ⁻¹ mmHg ⁻¹)	31 ± 6	100 ± 19
HA DLp (mL min ⁻¹ m ⁻²)	27	370
IS DLp (mL min-2 m-2)	15	145
Sieving Coefficient (BSA)	0.69 ± 0.09	0.00 ± 0.01

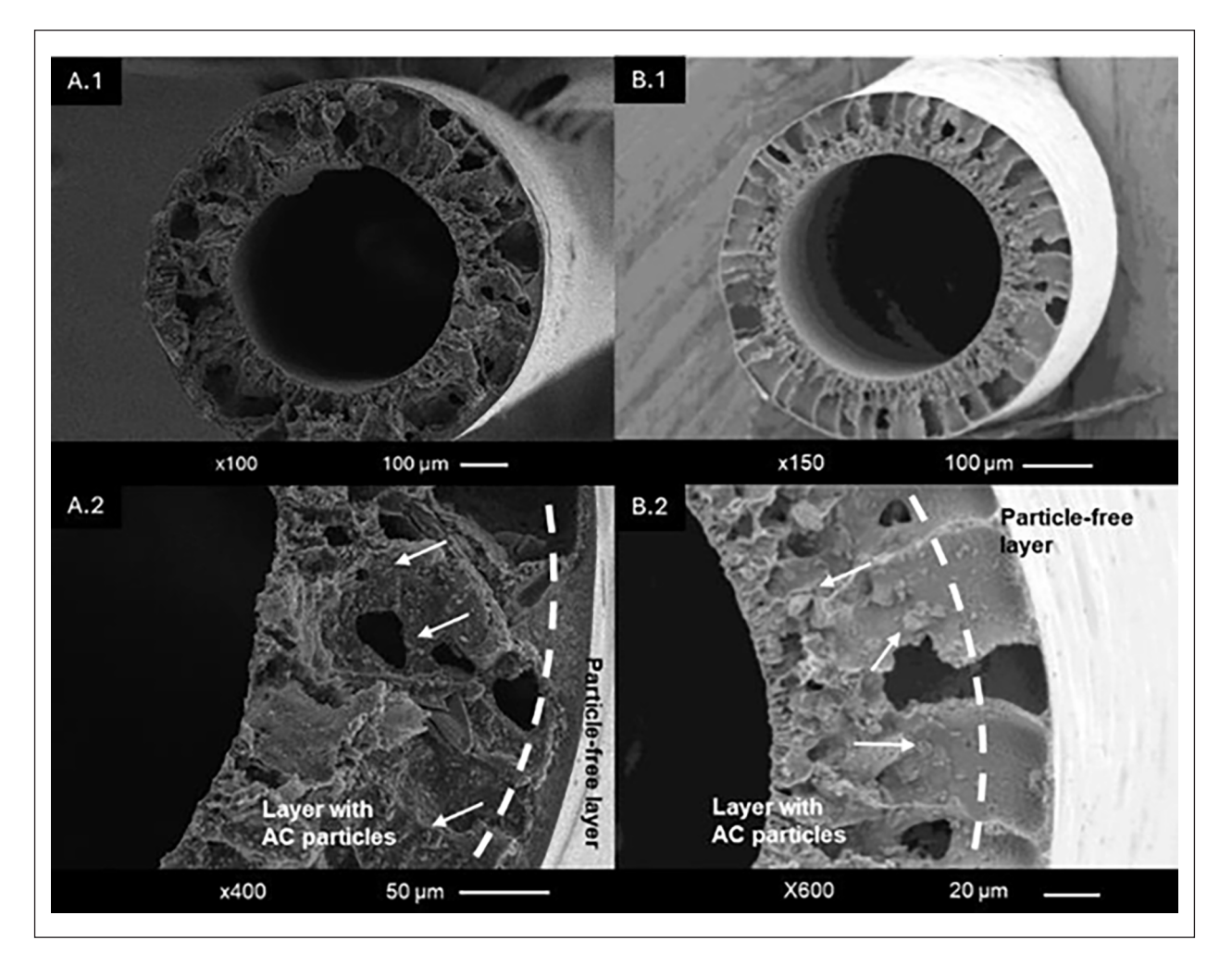


Figure 1. SEM images of OIF-MMM: A, this study and B, previous study ([4]), showing a cross-section and a close-up of the fiber wall, with both layers clearly visible.

Acknowledgements

D. Ramada acknowledges the financial support of the Top Sector Life Sciences & Health (Health $^{\sim}$ Holland), NODIAL project 210P+035).

9C: COMPUTATIONAL MODELS TO ASSESS PATIENT-SPECIFIC HEART SUPPORT

ASSESSMENT OF A FONTAN ASSIST DEVICE DURING EXERCISE WITH 0D-3D MODELLING

Phong Tran¹, Yaxin Wang², Christopher Broda³, Katharine Fraser⁴, Joseph Cavallaro¹

¹Rice University, USA; ²Texas Heart Institute, USA; ³Baylor College of Medicine, USA; ⁴University of Bath, UK

Introduction: Patients with Fontan circulation suffer from a multitude of internal organ complications primarily related to chronic venous hypertension and relatively low cardiac output. Due to the absence of an active pulmonary circuit pump, Fontan patients also experience low exercise capacity. In a previous study, we examined the effect of a Fontan Assist Device (FAD) under various medications and observed how these combined treatments can improve patients' conditions. This study

Table 1. Cycle averaged pressures (in mmHg) from simulations and literature (shaded grey). MCP: mean circulatory filling pressure; PAP: pulmonary artery pressure; MAP: mean arterial pressure; LAP: left atrial pressure; CO: cardiac output.

state	MCP/ Fontan	PAP	MAP	LAP	СО
rest	12.0	_	83.0	8.0	4.5
rest +FAD +diuretic walk	11.8 10.6 7.4 16.0	11.7 14.4 13.8	81.2 90.8 84.7 102.0	7.8 9.9 9.4 11.0	4.5 5.2 5.0 5.8
walk +FAD +diuretic run	16.0 14.9 10.5 19.0	16.0 18.5 17.9	103.5 116.9 109.6 106.0	10.8 12.5 12.0 13.0	5.9 6.8 6.6 7.0
run +FAD +diuretic	19.5 18.3 13.0	19.4 22.2 21.5	112.8 125.6 118.0	13.1 15.0 14.5	7.5 8.6 8.45

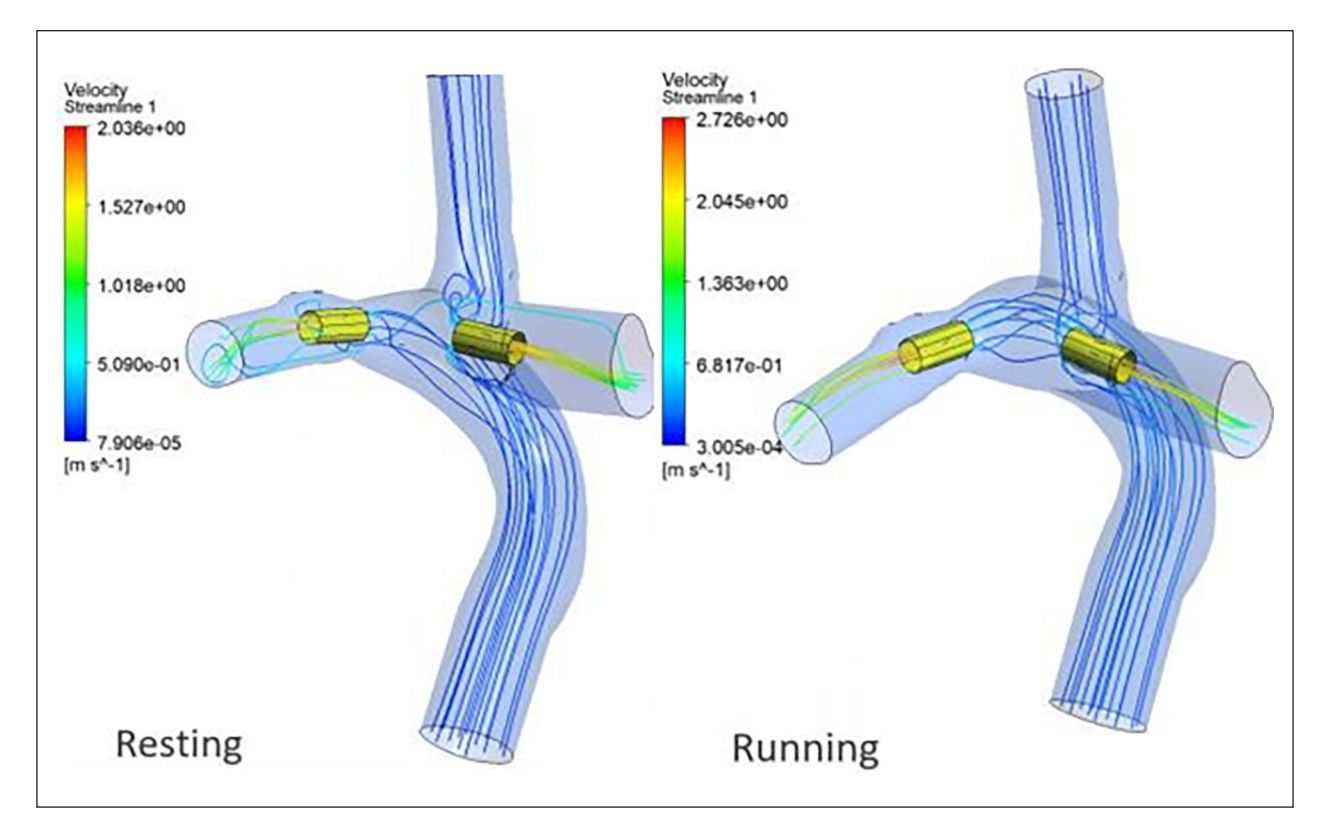


Figure 1. Example streamline plots for rest+FAD and running+FAD.

investigates how the FAD treatment can support Fontan patients during demanding exercise by examining their effect on hemodynamic change.

Methods: A customized 0D-3D lumped parameter-CFD model of the Fontan circulation, using Matlab Simulink and Ansys CFX, was utilized to simulate patient-specific hemodynamics. Three distinct clinical data stages: resting, walking, and running (each with specific heart rates, pressures, and flow rates) were established to replicate the hemodynamic conditions of a single patient. The model was tuned to match the same hemodynamic condition and used as the baseline before treatments. For the FAD treatment simulation, two axial pumps inside the pulmonary arteries were added and run at 15000 RPM, 19500 RPM, and 24500 RPM at resting, walking, and running, respectively. Additionally, FAD treatment with diuretic simulation was achieved by reducing the total circulation volume to 80%.

Results: In general, the simulation was able to closely replicate the clinical data, although there was one notable difference in the exercise trial where the cardiac output was 0.5L/min higher in the simulation. When FAD was activated in all three condition stages, the Fontan pressure decreased by 1.2 to 1.2 mmHg. In contrast, the cardiac flow increased by 0.7 L/min during rest, 1.0 L/min during walking, and 1.1 L/min during running, which could significantly improve exercise capacity. By combining FAD treatment with diuretics, Fontan pressure can be substantially enhanced while slightly reducing the increase in cardiac output. In the FAD and medication pairing treatment, Fontan pressure was decreased to 7.4 mmHg, 10.5 mmHg, and 13.0 mmHg during resting, walking, and running, respectively. Such treatment can help alleviate the hemodynamic pressure on internal organs and improve overall cardiac flow, leading to a better quality of life for patients with Fontan circulation. The 3D modelling allowed changes in flow patterns between the different conditions to be studied. Wall shear stresses were low, up to 12 Pa,

but flow leakages around the FAD were observed suggesting changes in the geometry are required.

Discussion: In conclusion, FAD treatment can be valuable in supporting Fontan patients during exercise. When combined with diuretic medications, Venous pressure lowers further and relieves pressure in internal organs. The improvement of this study highlights the potential benefits of FAD treatment for patients with Fontan circulation.

Acknowledgements

Research supported by: the National Heart, Lung, and Blood Institute of the National Institute of Health under Award Number 1R01HL153538; and Adult Congenital Heart Association.

MECHANICAL CIRCULATORY SUPPORT FOR VENTRICULAR SEPTAL DEFECTS: SIMULATION USING A LUMPED-PARAMETER MODEL

Mengjie Liu¹, Tingting Wu^{1,2}, Ifan Yen¹, Yuxin Zhu¹, Chiahao Hsu¹, Po-Lin Hsu^{1,2}, Thomas George Logan¹, Jamshid H. Karimov¹

¹magAssist Co., Ltd., Suzhou, China; ²Artificial Organ Technology Lab, School of Mechanical and Electrical Engineering, Soochow University, Suzhou, China.

Introduction: Ventricular septal defect (VSD) is a serious complication of post-acute myocardial infarction (AMI), occurring in ~2% of cases. The VSD results from ventricular septum necrosis, leading to abnormal hemodynamics. Mechanical circulatory support (MCS) can be used for patient stabilization [1]. However, its effects on VSD remain unexplored.

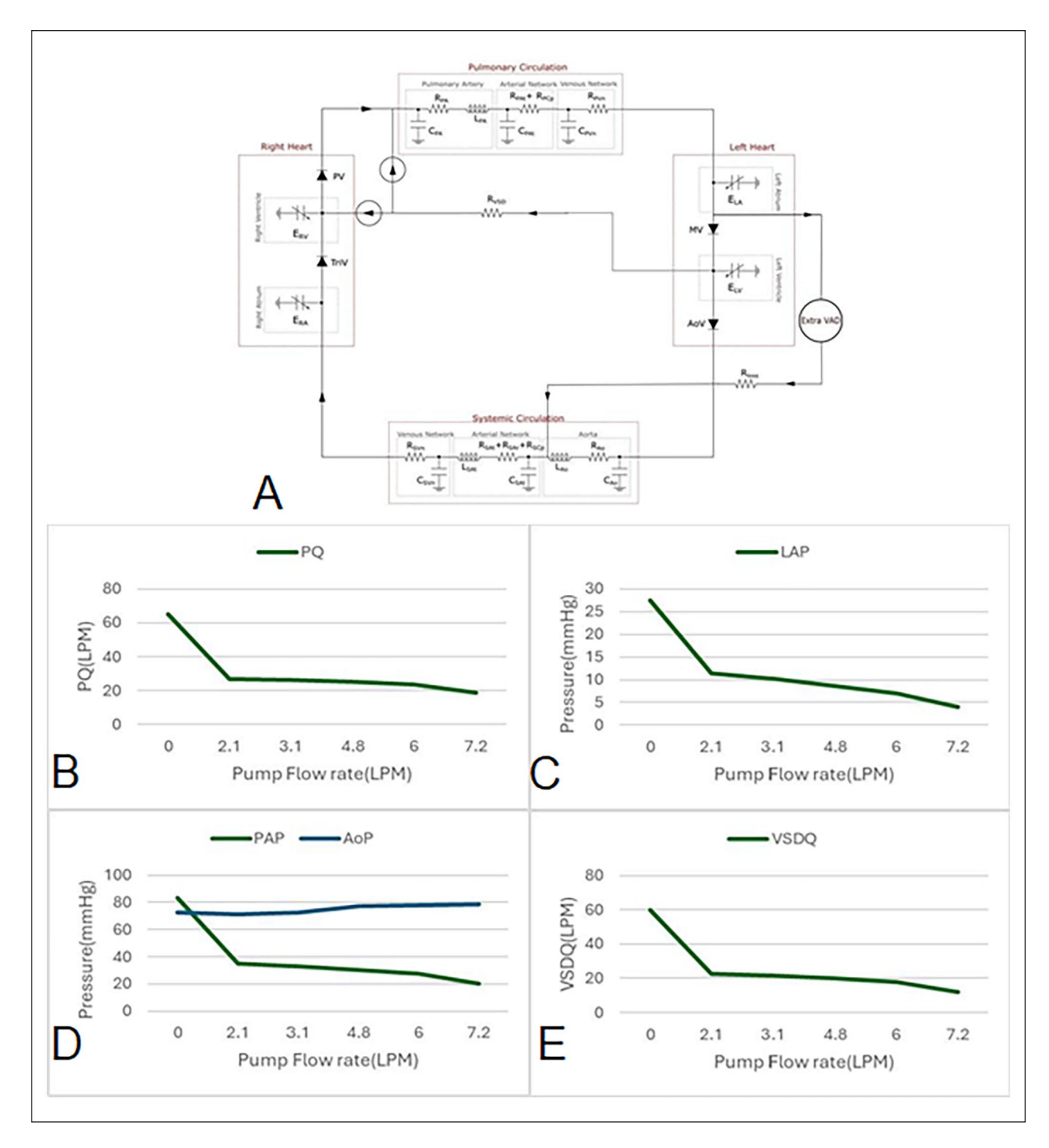


Figure 1.

We simulated the cardiovascular response in VSD patients supported by temporary MCS using a lumped- parameter model (LPM).

Methods: The cardiovascular system (Simulink; MATLAB R2016a, MathWorks, Natick, MA) consisted of an extra corporeal ventricular assist device (Extra VAD) (MoyoAssist™, magAssist, Suzhou, China), cardiac, systemic, pulmonary, and coronary circulations, as well as resistance (R), compliance (C), initial volume (V0), blood inertance, heart rate, and time-varying elastance. Flow drainage from the left atrium and perfusion to the axillary artery was modified in the model to simulate the

actual cannulation in the patient (Fig. 1A). Model validation and hemodynamic response to different support flow rates were performed.

Results: Patient hemodynamic data under no support condition and 3.1 L/min flow support were well- fitted, most parameters within 10% difference between simulated and clinical data (Table 1). The Extra VAD, flow support from 0 to 3.1 L/min, reduced pulmonary flow (PQ) by left ventricular unloading (Fig. 1B). The left atrial pressure (LAP) decreased due to the pump drainage directly from the left atrium (Fig. 1C), and pulmonary artery pressure (PAP) reduced from 78.9 to 32.8 mmHg. The mean

Pump	Category	/ VSDC	Q PQ	SQ	PAP	RAP
Flow	(LPM)	(LPM) (LPM)	(mmHg)	(mmHg)	(LPM)
Table 1	l.					
Clinical	l	59.2	64.4	5.2	73	22
Simula	tion	61.3	66.4	5.09	78.9	10.4
1 Clir	nical	21.7	27.6	5.9	21	15
Simula	tion	21.3	26.1	4.9	32.8	7.83

aortic pressure (AoP) remained stable (75 mmHg) because of the baroreflex mechanisms (**Fig. 1D**). The flow difference (pulmonary and systemic circulation difference) stabilized with 3.1 L/min flow support and remained unreversed (**Fig. 1E**).

Discussion: The LPM demonstrated good performance, providing a useful framework for insights into the hemodynamic effects of the Extra VAD support in post-AMI VSD. Extra VAD effectively reduced pulmonary pressures and improve left ventricular diastolic function. Further assessment would be useful to develop customized models for patients and provide reference information for doctors to select the optimal support flow rate.

References

1. Pahuja, M., Schrage, B., Westermann, D., Basir, M. B., Garan, A. R., & Burkhoff, D. (2019). Hemodynamic Effects of Mechanical Circulatory Support Devices in Ventricular Septal Defect. Circulation. Heart failure, 12(7), e005981.

OPTIMIZING INTRA-AORTIC PUMP PERFORMANCE FOR CARDIAC SUPPORT USING CFD AND AI

Maxime Renault¹, Philippe Meliga¹, Elie Hachem¹

¹CFL CEMEF Mines Paris - PSL. France

Introduction: Intra-aortic pumps provide a promising alternative to traditional ventricular assist devices (VADs) by offering minimally invasive

circulatory support. Unlike extracorporeal or intraventricular pumps, intra-aortic designs must function within complex hemodynamic conditions while ensuring effective unloading and perfusion. This study focuses on optimizing an intra-aortic pump through computational simulations, assessing its performance in a physiological environment and in controlled conditions.

Methods: The simulations were performed using an in-house finite element code, leveraging the Variational Multiscale (VMS) method [1] to accurately capture fine fluid structures.

To model the cardiovascular environment, we implemented lumped parameter models: Classical Windkessel Model – Used for the main arteries. Special Coronary Model – Incorporating intra- myocardial pressure variations to account for the unique perfusion dynamics of coronary circulation. Left Ventricle Active Model – Simulating the contractile dynamics of the ventricle to provide physiologically accurate inflow conditions.

The intra-aortic pump was embedded in this full cardiovascular framework using an immersed volume method to analyze its interaction with native circulation (see Figure 2). Additionally, a simplified pump-in-pipe model was developed to isolate pump performance, enabling direct efficiency and pressure head comparisons between rotor designs. Physiologically relevant boundary conditions were applied in both models to ensure realistic flow behavior.

Results: The full cardiovascular model provided insight into pumpinduced flow patterns, coronary perfusion effects, and hemolytic risks. In particular, it highlighted the potential risk of drawing blood from the coronary arteries, which increases with more powerful pumps or weaker cardiac function.

The pump-in-pipe simulations enabled direct comparison of rotor designs, exposing trade-offs between pressure generation and efficiency. When integrated into a parametric framework, these simulations—coupled with a single-step DRL algorithm [2]—guided the optimization of rotor geometry for improved performance.

Discussion: These results emphasize the importance of coupling detailed anatomical simulations with simplified performance assessments to refine intra-aortic pump designs. Key optimization parameters include rotor geometry, placement within the aorta, and active interaction with native cardiac function. Future work will focus on experimental validation of the optimized designs to assess real-world feasibility and hemodynamic impact.

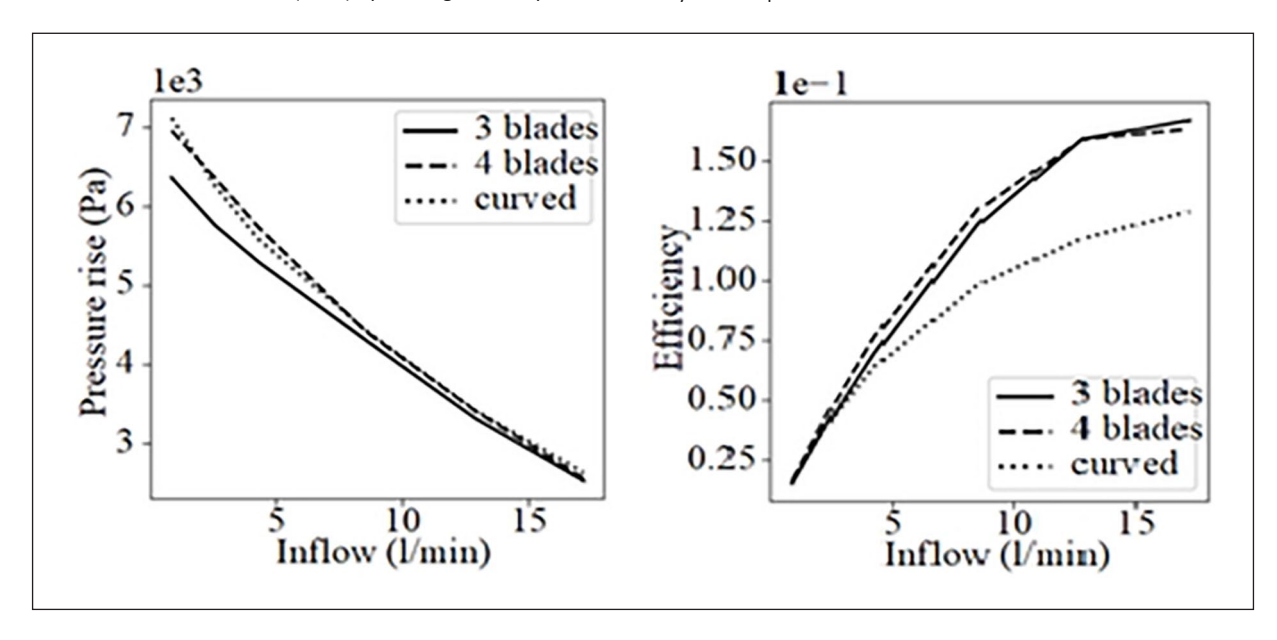


Figure 1. Example of comparison between three designs based on pressure rise and efficiency.

References

- 1. E. Hachem et al, JCP, Volume 229, Issue 23, 2010.
- 2. J. Viguerat et al, Neural Comput. Appl., 2023.

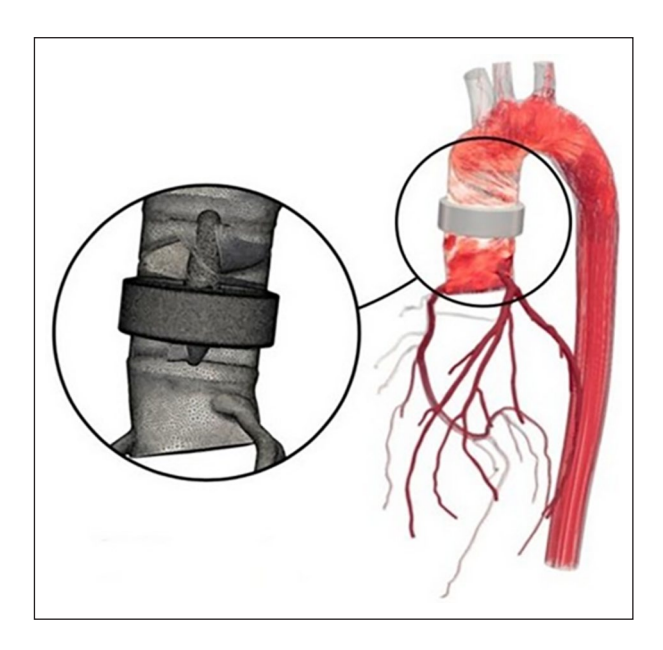


Figure 2. Flow velocity in the aorta model with a detailed view of the pump mesh integration.

UNCERTAINTY QUANTIFICATION OF 4D FLOW MRI SEQUENCE VARIABILITY ON COMPUTATIONAL AORTIC HEMODYNAMICS MODELS

Tianai Wang¹, Levi Juhl¹, Teresa Lemainque², Theresa Degreif², Shuo Zhang^{3,4}, Ulrich Steinseifer¹, Michael Neidlin¹

¹Department of Cardiovascular Engineering, Institute of Applied Medical Engineering, Medical Faculty, RWTH Aachen University, Germany, ²Department of Diagnostic and Interventional Radiology, Medical Faculty, RWTH Aachen University, Germany, ³Philips GmbH Market DACH, Hamburg, Germany, ⁴Philips Healthcare, Best, The Netherlands

Introduction: The onset and progression of cardiovascular diseases are closely linked to altered blood flow. The use of non-invasive imaging tools, e.g. 4D Flow MRI, as input data for Computational Fluid Dynamics (CFD) models enables the assessment of these flow features with high spatio-temporal resolution and holds the potential of virtual diagnostic and treatment planning tools. However, these 4D Flow MRI-based CFD models can be hampered by variability in the imaging data. One determining characteristic of 4D Flow MRI scans are acceleration factors (AF). These are chosen by the practicing clinician and offer faster acquisition with a reduced quality, which is still highly attractive for clinical practice. However, the sensitivity of derived hemodynamic parameters to these variabilities is unknown. The goal of the study was to quantify the sensitivity of hemodynamic parameters to these inter-sequence variabilities in the underlying 4D Flow MRI scans.

Methods: 4D Flow MRI scans of the aortic flow of N=15 volunteers were acquired and reconstructed using five different AF and therefore with up to five-fold reduction in scan time. Velocity profiles were

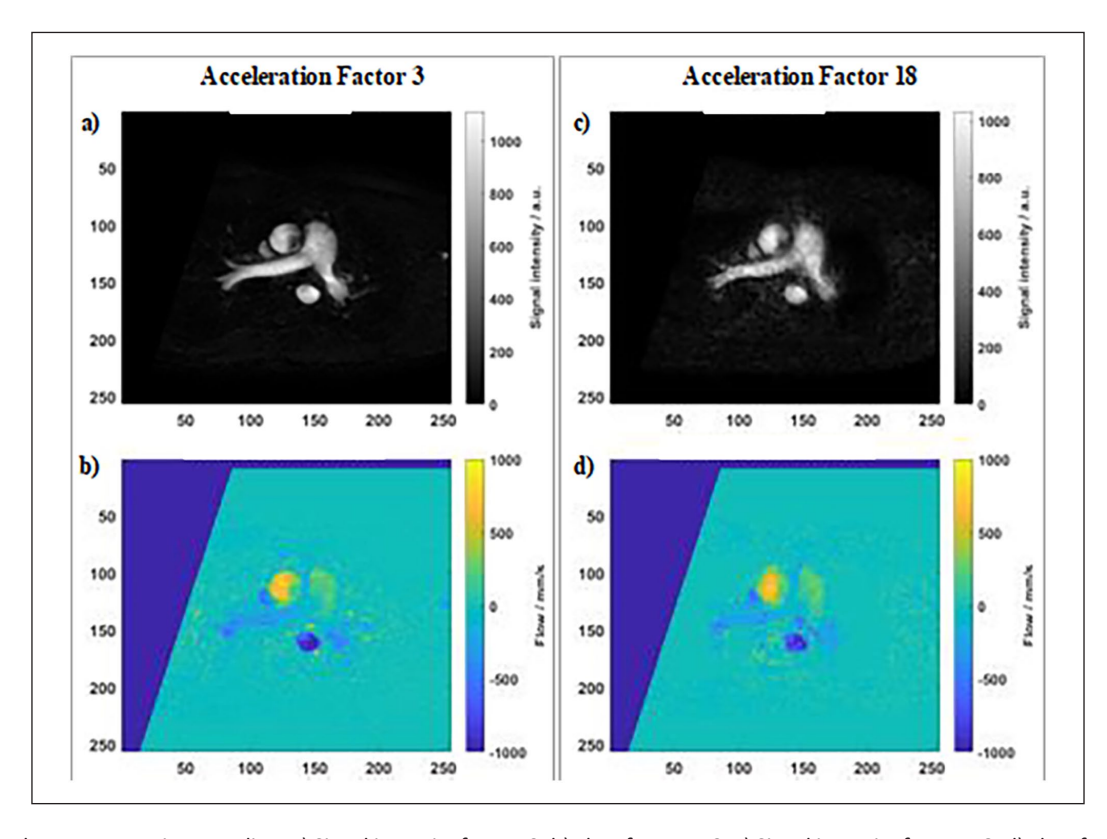


Fig. 1. 4D Flow MRI scans in ascending: a) Signal intensity for AF=3, b) Flow for AF = 3, c) Signal intensity for AF=18, d) Flow for AF = 18.

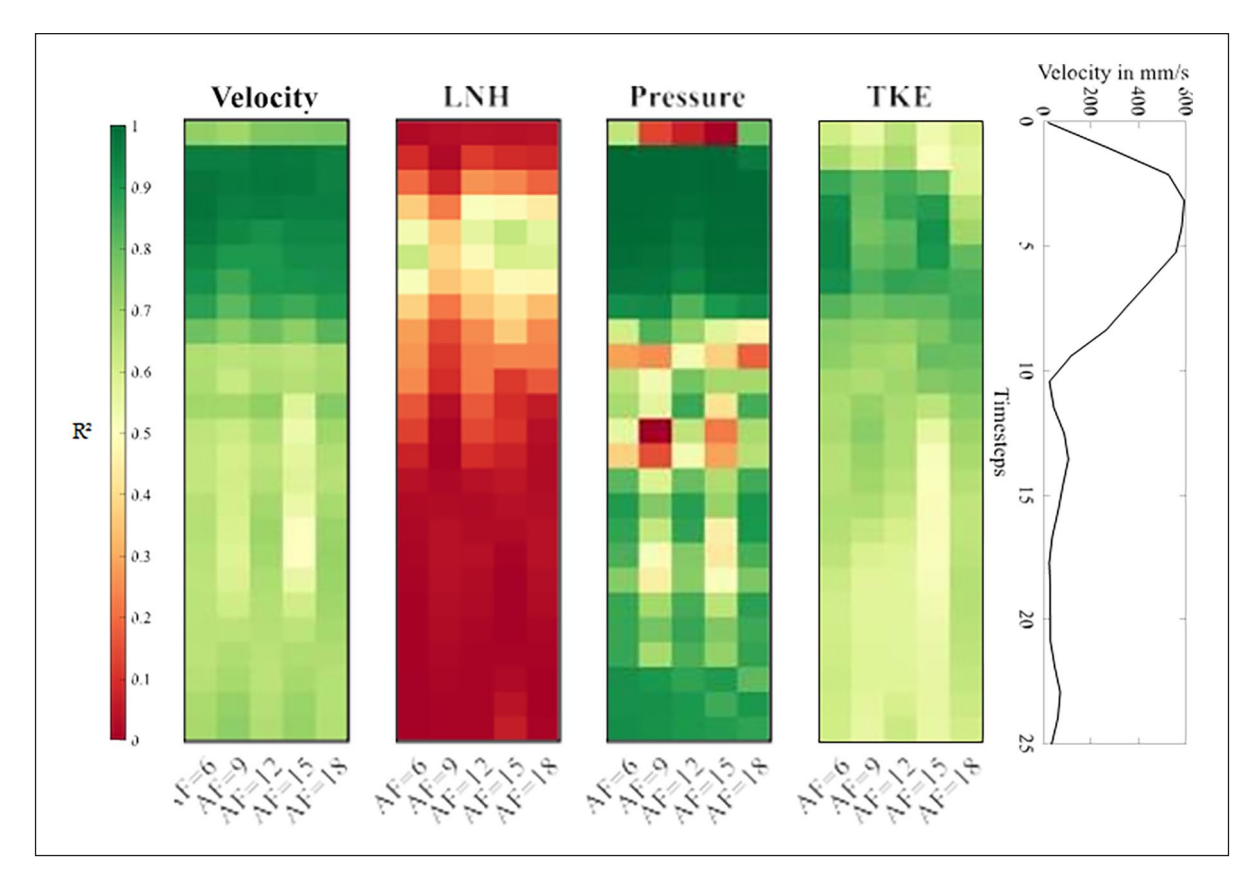


Fig. 2. Correlation heatmaps between AF=3 and higher AF- 4D Flow MRI-based CFD models for velocity, pressure, LNH and TKE.

extracted to serve as inlet conditions for 4D patient- specific CFD models. Finally, the sensitivity of important flow markers such as pressure, local normalized helicity (LNH), and turbulent kinetic energy (TKE) was statistically evaluated.

Results: Fig. 1 shows the signal intensity and corresponding velocity derived from exemplary 4D Flow MRI scans acquired in the ascending aorta for the lowest (left) and highest AF (right). The decrease in image quality with increasing acceleration factor is observable with an increase in overall blurriness.

Next, we analyzed pointwise correlation between flow markers derived from the CFD model based on lowest AF scans to the ones with higher accelerations. Varying degrees of sequence- sensitivity characterize higher-order hemodynamic parameters (Fig. 2). While TKE remains largely unaffected by input data variability, LNH fields deviate strongly from the AF=3 reference model.

Discussion: In summary, the AF cannot be chosen arbitrarily as it leads to non-negligible changes in the image quality and measured velocity field. After prescribing these in CFD models, our results show that pressure and TKE are insensitive to sequence settings, while helicity is highly dependent on the scan settings. It is important to keep these sensitivities in mind when identifying robust markers in hemodynamic analyses. In particular, LNH should be treated with caution when used as a biomarker for diagnostic or planning purposes.

Acknowledgements

This study was funded by the START-Program of the Faculty of Medicine RWTH Aachen University, the Studienstiftung des Deutschen Volkes, and the Joachim Herz Foundation.

INTEGRATIVE MODELING FRAMEWORK FOR MECHANICAL CIRCULATORY SUPPORT: ENABLING REAL-TIME HEMODYNAMIC INSIGHTS AND OPTIMIZATION

Ifan Yen^{1,4}, Michael Neidlin⁴, Yuxin Zhu¹, Lars Fischer⁴, Jamshid H. Karimov^{1,3}, Po-Lin Hsu^{1,2}

¹.magAssist Co., Ltd., Suzhou, China; ². Artificial Organ Technology Lab, School of Mechanical and Electrical Engineering, Soochow University, Suzhou, China; ³.on behalf of Medical Advisory Board; ⁴.Department of Cardiovascular Engineering, Institute of Applied Medical Engineering, RWTH Aachen University, Aachen, Germany

Introduction: Current mechanical circulatory support (MCS) systems lack standardized guidelines for setting critical parameters (rotation speed and flow rate), which limits care optimization. Indirect assessments such as blood-gas analysis provide delayed feedback, emphasizing the need for rapid, non-invasive prediction methods. We report our model, which enables MCS parameter adjustments and predicts hemodynamic optimization.

Methods: An integrated digital model of the human circulatory system and MCS device was developed using lumped parameter modeling (LPM) and reduced-order modeling (ROM) derived from the device's high-resolution computational fluid dynamic simulations. Sensitivity analysis and Bayesian algorithms were employed to fit the model to specific patient conditions, enabling the simulation of hemodynamics and physiological states to predict outcomes at different support levels.

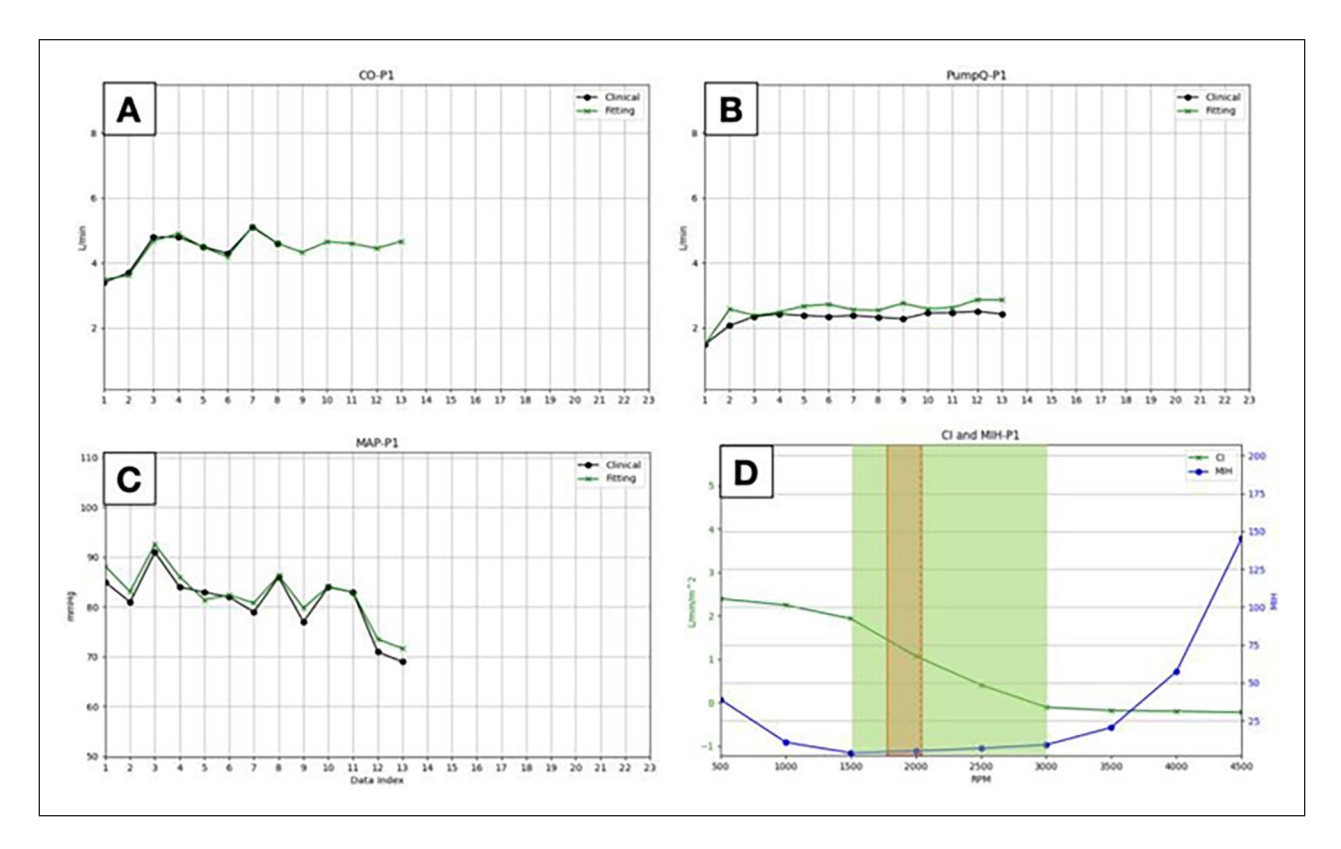


Figure 1. Output of the model; A): Cardiac output, B): Pump flow, C): mean arterial pressure plotted over the treatment duration of one patient. Green: Model data, black: clinical data, D): explores the relationship between cardiac index, rotational speed and device hemolysis. Red shaded area are the clinically set values and green area shown the safe range as identified by the model.

Results: The model demonstrated high computational efficiency, requiring only five parameters to accurately fit clinical records (n=11) at the initial time point and just two of these parameters for subsequent points, significantly reducing complexity(Fig.1A,B,C). It outputs key physiological metrics, including left ventricular elastance, pressure-volume (PV) loops, and hemolysis risk (MIH) from the ROMs. Additionally, it revealed the relationship between rotational speed and cardiac index(CI), providing insights for achieving target hemodynamic and suggesting optimal speed adjustment ranges(Fig.1D).

Discussion: This model demonstrates feasibility for application in MCS systems, enabling rapid calculation of PV loops and ventricular elastance right after device deployment. The relationship between rotational speed and CI provides a reliable basis for defining target CI values and recommending rotational speed adjustments, supporting the optimization of MCS clinical use.

Acknowledgements

This study was funded by magAssist Co., Ltd., Suzhou, China.

A NOVEL APPROACH TO IMMUNE MODULATION: POOLED PURIFIED BUFFY COATS IN AN EXTRACORPOREAL CIRCULATION MODEL

Sophie Brabandt¹, Steffen Mitzner^{2,3}, Jens Altrichter⁴, Daniel Reuter¹, Gerd Klinkmann^{1,3,5}

¹Department of Anesthesiology University Medical Center Rostock, Germany; ²Department of Nephrology, University Medical Center Rostock, Germany; ³Fraunhofer Institute for Celltherapy and Immunology, Germany ⁴Department of Research and Development Artcline GmbH, Germany; ⁵International Renal Research Institute of Vicenza IRRIV, Italy.

Introduction: Sepsis remains a life-threatening condition with persistently high mortality rates, largely attributable to immune cell dysfunction (1). While granulocyte transfusion has been explored as a therapeutic intervention, its clinical application is limited due to the potential for tissue damage (2), highlighting the necessity for alternative strategies. In this regard, extracorporeal immune cell therapy emerges as a promising approach (3).

Although granulocyte concentrates are considered the standard of care, their clinical utility remains inadequate. Currently, two primary production methods exist, with apheresis being the established technique in Germany. However, this method is associated with significant limitations, including donor-related strain and prolonged processing times. As an alternative, granulocyte isolation from Buffy Coats has demonstrated proof of concept and offers considerable potential for optimizing therapeutic efficacy (4).

To improve clinical feasibility, this study investigates the use of purified pooled Buffy Coats within the extracorporeal Immune-Competence-Enhancement System ARTICE.

Methods: Preparation of ppBC: 20 ABO-identical Buffy Coats were pooled and sedimented with gelafundin. The leucocyte supernatant was specially purified in three washing steps with saline solution and by centrifugation to remove platelet and erythrocyte contamination. The finished ppBCs were transferred to gas-permeable storage bags, resuspended in plasma.

Circulation experiments: The extracorporeal circulation system consists of a blood circuit and a plasma circuit, separated by a filter with a pore

size of 0,5 µm (PF CC1). Prior to the start, the ppBCs were introduced into the plasma circuit, so only patient plasma is treated with healthy donor cells. A second filter serves as a safety filter (PF CC2). The total circuit volume was 900 ml. The blood flow rate was 150 ml/min. Plasma from healthy donors was used to simulate the patient. The circulation ran for a period of six hours. Samples were taken from the plasma every hour and after three and six hours before and behind PF CC1 and cell samples by backflushing the filter.

Results: The circulation process was performed without technical problems for 6 hours. Once equilibrium was reached, a decrease in glucose and pH values and an increase in lactate were observed. LDH values remained within the physiological range throughout the entire period. Functional measurements showed good phagocytosis activity above 70.51% over the entire period. Viability remained at 83.48 \pm 7.78% even after 6 hours. Cytokine analysis of plasma showed significant production of IL-1, IL-2, IL-4, IL-6, IL-8, TNF- α and G-CSF 6 hours compared to baseline.

Discussion: Purified Buffy Coats subjected to an extracorporeal circuit for a duration of six hours exhibited robust cell viability, preserved metabolic activity, and sustained functional integrity. A significant increase in cytokine production was observed, underscoring a pronounced immunomodulatory effect. Moreover, the progressive elevation of cytokine levels over the six-hour period suggests a time-dependent dosing response. These findings highlight the potential of this approach to enhance immune competence, offering a promising avenue for therapeutic advancement.

References

- Van Der Poll T, Shankar-Hari M, Wiersinga WJ. The immunology of sepsis. Immunity. November 2021;54(11):2450–64.
- Marfin AA, Price TH. Granulocyte Transfusion Therapy. J Intensive Care Med. Februar 2015;30(2):79–88.
- Klinkmann et. al. Purified granulocytes in extracorporeal cell therapy: A multifaceted approach to combat sepsis-induced immunoparalysis. Int J Artif Organs. 23. Juli 2024;03913988241262901.
- Klinkmann G et. al. Purified Granulocyte Concentrates from Buffy Coats with Extended Storage Time. Transfus Med Hemotherapy. 12. April 2024;1–10.

OPTIMIZATION OF ROTOR DESIGN FOR A CATHETER-IMPLANTABLE VENTRICULAR ASSIST DEVICE

Gustavo Andrade^{1,2,3}, Rafael Nunes^{1,2,3}, Aron Andrade^{1,2}, Oswaldo Horikawa², Edir Leal¹, Jeison Fonseca^{1,2,3}

¹Institute Dante Pazzanese of Cardiology, Brazil; ²University of Sao Paulo, Brazil; ³University Sao Judas Tadeu, Brazil

Introduction: Ventricular assist devices (VADs) have become crucial in treating heart failure [1], a global health problem with increasing prevalence [2]. This study focuses on continuous axial flow blood pumps VAD [3]. The catheter implantation method is a minimally invasive procedure, which poses a lower risk of complications and results in a shorter hospital stay. Computational Fluid Dynamics (CFD) simulations have emerged as essential tools for evaluating VAD performance and understanding flow patterns [4]. The objective of this study is to analyze different geometries of a Catheter-Implantable VAD toward pressure and shear stress and determine the best combination of variables.

Methods: CFD simulations were conducted using water as the fluid, considering 15,000 rpm and 3 L/min aiming to maximize pressure with low shear stress minimizing hemolysis. The rotor design parameters, in Figure 1, were analyzed. All the data were stored and plotted into various graphics showing the analyzed variable and the influence on the pressure and shear stress.

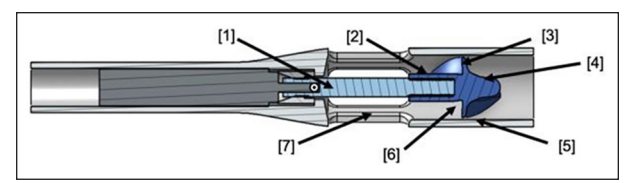


Figure 1. [1] axle length (8.5-11 mm); [2] rotor length (5-12 mm); [3] number of blades (1-6); [4] rotor internal hub diameter (2.2-3 mm); [5] blade tip gap (0.1-0.55 mm); [6] blade pitch (0.5-3 revolutions); [7] outlet width (4-4.8 mm).

Results: Regarding the rotor length, the Shear Stress remained the same from 6 to 10 mm, increased with 5 and 12 mm and has the lowest with 11 mm, but the pressure had a significant gain with 8 mm and lower at the other lengths. The blade pitch, the Shear Stress had a minimum at 1.5 revolutions and was inversely proportional to the pressure, which was maximum at 1.5 revolutions. The axle length, the Shear Stress remained stable from 8.5 to 10 mm and rose sharply from 10 to 11 mm, the pressure decreased linearly from 8.5 to 11 mm. The number of blades, the Shear Stress was practically the same from 1 to 5 blades, and with 6 it decreased a little, the pressure increased from 1 to 4 blades, remained the same from 4 to 5 and decreased with 6 blades. The gap, a distance of less than 0.3 mm considerably increases the SS, and the pressure increases as the Gap decreases, almost linearly. The hub diameter, pressure was highest at 2.2 mm and 2.4 mm, while it remained lower and stable between 2.6 mm and 3 mm. Shear Stress peaked at 2.4 mm but remained stable at other widths, rising slightly again at 3 mm. The outlet width, pressure remained low and stable between 4.0 mm and 4.4 mm, peaked at 4.6 mm, then dropped to zero at 4.8 mm, indicating complete pump failure. Shear Stress showed a different trend, reaching a minimum at 4.2 mm and peaking at 4.8 mm.

Discussion: Thus, the best combination of geometries variables should be a rotor with a length of 8 mm, 1.5 revolutions of pitch, 5 blades, 0.3 mm gap, an axle of 8.5 mm, a hub diameter of 2.2 mm and an outlet width of 4.2 mm. Future CFD and In Vitro tests will be performed combining these variables to evaluate the impact of one variable to another. The results demonstrate the feasibility for the development of a Catheter-Implantable-VAD with dimensions small enough for catheter implantation and with satisfactory hydrodynamic performance.

References

- 1. Bock, E.; et al: in Artificial Organs, 32(4):329-333, 2008.
- Avezum A, Maia LN, Nakazone M. in Manual of Cardiology. 1(1):1-1, 2012
- 3. Andrade, A., et al. in Artificial Organs, 23(9): 876-880, 1999
- 4. Andrade G, et al. in Artificial Organs, 44(8): 803-810, 2020.

Acknowledgements

This study was conducted under financial support from "Fundação de Amparo à Pesquisa do Estado de São Paulo" (FAPESP, Sao Paulo, BRAZIL) and "Fundação Coordenação de Aperfeiçoamento de Pessoal de nível Superior (CAPES, São Paulo, BRAZIL) por meio do Programa de Apoio à Pós-Graduação (PROAP).

EVALUATION OF SLIPS COATINGS FOR COCHLEAR IMPLANTS: WETTING PROPERTIES OF LUBRICANT-SUBSTRATE COMBINATIONS

Tom Bode¹, Jan Drexler¹, Gerrit Paasche² Marc Müller¹, Birgit Glasmacher¹

¹Institute for Multiphase Processes, Leibniz University Hannover; Germany ²Institute of Otorhinolaryngology, Hannover Medical School, Germany

Introduction: As a foreign body reaction to the implantation of a cochlear implant (CI), connective tissue forms, electrically insulating the electrodes [1]. The integration of SLIPS (Slippery Liquid-Infused Porous Surfaces) can lead to reduced connective tissue growth and trauma due to reduced friction, and thus improved overall electrode performance. [2, 3]. Following our previous results [4], this study evaluates different materials for their suitability to create SLIPS by assessing their wetting properties.

Methods: SLIPS coatings were prepared by impregnating electrospun poly(vinylidenefluoride trifluoroethy- lene) (P(VDF-TrFe)), polycaprolactone (PCL), and polyurethane (PU) substrates with the following lubricants: silicone oil (20cSt, S), perfluorodecalin (PFD), almond oil (M), coconut oil (C) and lanolin (L). Untreated polymer samples were used as controls. The contact angle (θ) to deionized water was measured using the sessile drop method (Krüss, FM 40 EasyDrop). Roll-off angles were determined using a custom-built setup. Fiber diameters were determined by SEM.

Results: The average fiber diameter of the PU samples was 1.33 μm , that of PCL 1.76 μm and that of PVDF0.74 μm . The results of the contact angle measurements (see Table 1) showed the highest value for the untreated reference and PFD followed by S, L and C, depending on the substrate material. PFD achieved θ in the range of the untreated substrates. PVDF based SLIPS showed the highest θ .

The PFD samples showed no drop roll-off (see Table 2). Only PVDF showed drop slip for the reference materials. The samples with almond oil and silicone oil showed the lowest roll-off angles. The other combinations showed intermediate slip angles in the experiments.

Discussion: SLIPS reduced the contact and roll-off angles of all combinations compared to the reference except PFD. Here, no roll-off was

Table 1. Contact angles for untreated polymer and SLIPS systems.

Lubricant	PCL	⊕ in °	
		PU	PVDF
-	132,2	133,7	143,8
S	99,8	107,5	108,1
PFD	155,8	137,4	147,3
M	90,0	88,2	94,4
С	103,3	98,7	113,7
L	94,0	109,4	109,0

Table 2. Roll-off angles for untreated polymer and SLIPS systems. 90° roll-off angle shows no slip.

Lubricant	Roll-off angle in °			
	PCL	PU	PVDF	
-	90,0	90,0	66,4	
S	9,8	13,2	7,6	
PFD	90,0	90,0	90,0	
M	8,2	10,0	8,9	
С	12,1	24,0	14,5	
L	24,5	25,0	19,2	

observed, which can be explained by the rapid evaporation of PFD resulting in an uncovered substrate. PVDF was the only reference that showed slip, which may be due to its smoother surface due to smaller fibers. All other combinations were able to reduce the roll-off angle, indicating improved anti-adhesion, with PVDF- based SLIPS showing the best performance on average. M and C were able to achieve comparable values to S. Therefore, these two oils represent a good alternative for the production of natural lubricant-based SLIPS. Future research should further investigate the role of lubricant viscosity, fiber diameter and the cell response.

References

- 1. Seyyedi et al, Otol Neurotol, 35:1545–1551, 2014.
- 2. Gheorghe et al, Biomedicines, 9, 2021.
- 3. Howel et al. Adv Matter. 30. 2018.
- Bode et al, Current Directions in Biomedical Engineering, 10(4):99-102, 2024.

Acknowledgements

This project has been funded by the Deutsche Forschungsgemeinschaft (DFG, German Research Foundation) – 60443918. We also thank the French Embassy in Germany for their support through the Procope Mobility Grant.

TOWARDS FUNCTIONAL *IN VITRO* ISLETS OF LANGERHANS: DUAL MICROFLUIDIC APPROACHES FOR MICROSPHERE-BASED PSEUDOISLET FABRICATION

Amadeja Brečko^{1, 2}, Marko Milojević^{1, 2}, Uroš Maver^{1,2}, Boštjan Vihar¹

¹Institute of Biomedical Sciences, Faculty of Medicine, University of Maribor, Maribor, Slovenia, ²Department of Pharmacology, Faculty of Medicine, University of Maribor, Maribor, Slovenia

Introduction: There is a growing need for innovative models of the pancreas, that give us insight into pancreatic islet (PI) biology, β -cell dysfunction, and potential new treatment options for diabetes mellitus. Currently animal models are widely used in diabetes research, however, concerns such as species-specific differences limit their translational potential [1]. On the other hand, conventional two-dimensional (2D) cell cultures cannot fully replicate the microarchitecture of the native pancreas, which is crucial for maintaining islet function [2]. In vitro three-dimensional (3D) models could bridge the gap by providing a 3D environment that closely mimics the structural and functional properties of native PIs. In this study we present the preliminary results towards the development of such a model.

Methods: To develop a robust *in vitro* model of PIs, we investigated the biocompatibility of different biomaterials with pancreatic beta cells using Live/Dead staining and the Alamar Blue assay. Given the different properties of the various bioink formulations, we used two complementary biofabrication techniques:

- Centrifuge-based microfluidic extrusion for viscous bioinks where we used a coaxial nozzle and a SrCl₂ cross-linking bath to produce stable, cell-encapsulating microspheres.
- Droplet microfluidics for low-viscosity bioinks, generating coreshell droplets in an oil phase. While optimized for bioink stability, this method has yet to be tested with pancreatic cells.

Results: Biocompatibility testing using Live/Dead staining and the Alamar Blue assay confirmed that gelatin- based bioinks provide optimal support for pancreatic beta cells. Using the centrifuge-based microfluidic extrusion

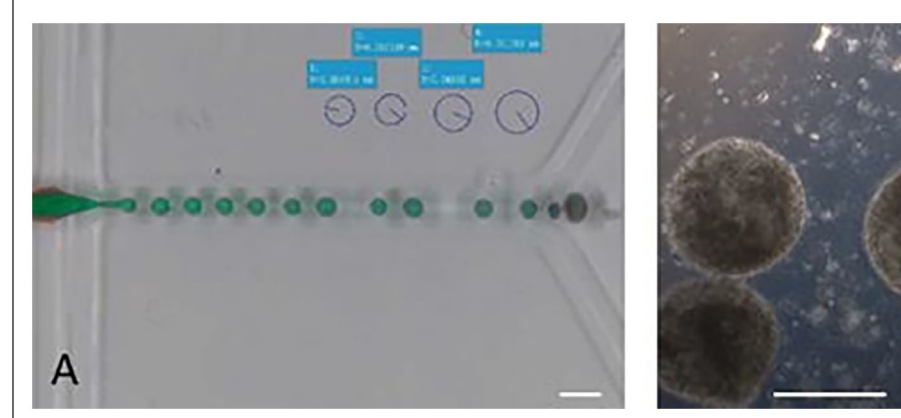




Figure 1. In vitro microspheres produced by using droplet microfluidics (A) or centrifuge-based microfluidic extrusion (B) (scale bar = 400 μm).

technique, we successfully produced microsphere-based pseudoislets with encapsulated pancreatic cells. The size of the microspheres ranged from 400 to 700 μm in diameter, depending on the biofabrication parameters such as rotational speed and bioink composition. Using the microfluidic droplet method, we were able to successfully produce stable microspheres based on GelMA, approximately 200 to 500 μm in diameter.

Discussion: This study demonstrates the feasibility of two microfluidic biofabrication techniques for the production of microsphere-based pseudoislets which can be integrated into more complex *in vitro* models of Pls. The centrifuge method has successfully encapsulated pancreatic cells, while the microfluidic droplet method has proven effective in producing stable microspheres, although its application to pancreatic cells remains to be explored. Both approaches offer scalability and reproducibility, with the size of pseudoislets comparable to native islets. Future work will focus on long-term functionality, refining the formulations of the bioink and integrating these constructs into microphysiological systems to create more physiologically relevant *in vitro* islet models for diabetes research

References

- Dolenšek et al, Islets, 7(1):e1024405, 2015.
- 2. Diane et al, Cell Commun Signal, 21(1):151, 2023.

Acknowledgements

The authors acknowledge the financial support from the Slovenian Research Agency for Research Core Funding No. P3-0036, for projects Nos. Z3-4529, N1-0305, and research funding from the European Comission, grant agreement 872662.

PATIENT-SPECIFIC SIZE AND AGE SCALING IN A 0D CARDIOVASCULAR MODEL

August Lundquist¹, Elira Maksuti \$, Dirk W Donker^{‡;‡}, Michael Broomé[§],¹

¶Anaesthesia and Intensive Care, Dept. of Physiology and Pharmacology, Karolinska Institute, Sweden; §Getinge, Acute Care Therapies, Maquet Critical Care AB, Solna, Sweden; †Dept. of Intensive Care Medicine, University Medical Center Utrecht, Utrecht University, The Netherlands; ‡Cardiovascular and Respiratory Physiology, University of Twente, Enschede, The Netherlands; §ECMO Department, Karolinska University Hospital, Stockholm, Sweden

Table 1. Example of cardiac scaling factors.

Cardiac parameter	Scale factor
Heart rate	BSA-0.33
Contractility and stiffness – right atrium and ventricle	BSA-1.5
Contractility and stiffness – left atrium and ventricle	BSA ⁻¹
V0	BSA
Lambda	BSA ⁻¹
Starling max volume	BSA
Maxflow	BSA
Coronary resistance	BSA-0.8
Myocardial volume	BSA1.2

Introduction: Computational cardiovascular models hold great promise for clinically realistic simulations in education and bedside decision support. To enhance patient-specific modeling, individual anthropometrics are imperative as human physiology varies with body size by fundamental energetic relations expressed in allometric scaling laws.

We hypothesize that computational cardiovascular models can be advanced towards individualization by implementing scaling laws based on patient age, weight, height, and sex.

Methods: A scaling methodology was developed and evaluated in the lumped-parameter cardiovascular model Aplysia Cardiovascular Lab (1). Male and female subject sizes and ages were based on Swedish growth charts from birth to adult size and simulated to test model realism.

Results: Realistic physiology was generated for underweight, overweight, and average male and female patients from birth to 80 years. Model output included comprehensive measures of hemodynamics, cardiac function, respiratory function, gas exchange and mechanical ventilation as well the body's energy expenditure.

Discussion/Conclusion: Allometric scaling laws can be used to generate parameter sets of males and females of disparate sizes and ages enabling simulation of a diverse patient population in computational cardiovascular models. This sets the stage for novel approaches towards individualized modelling for clinical applications.

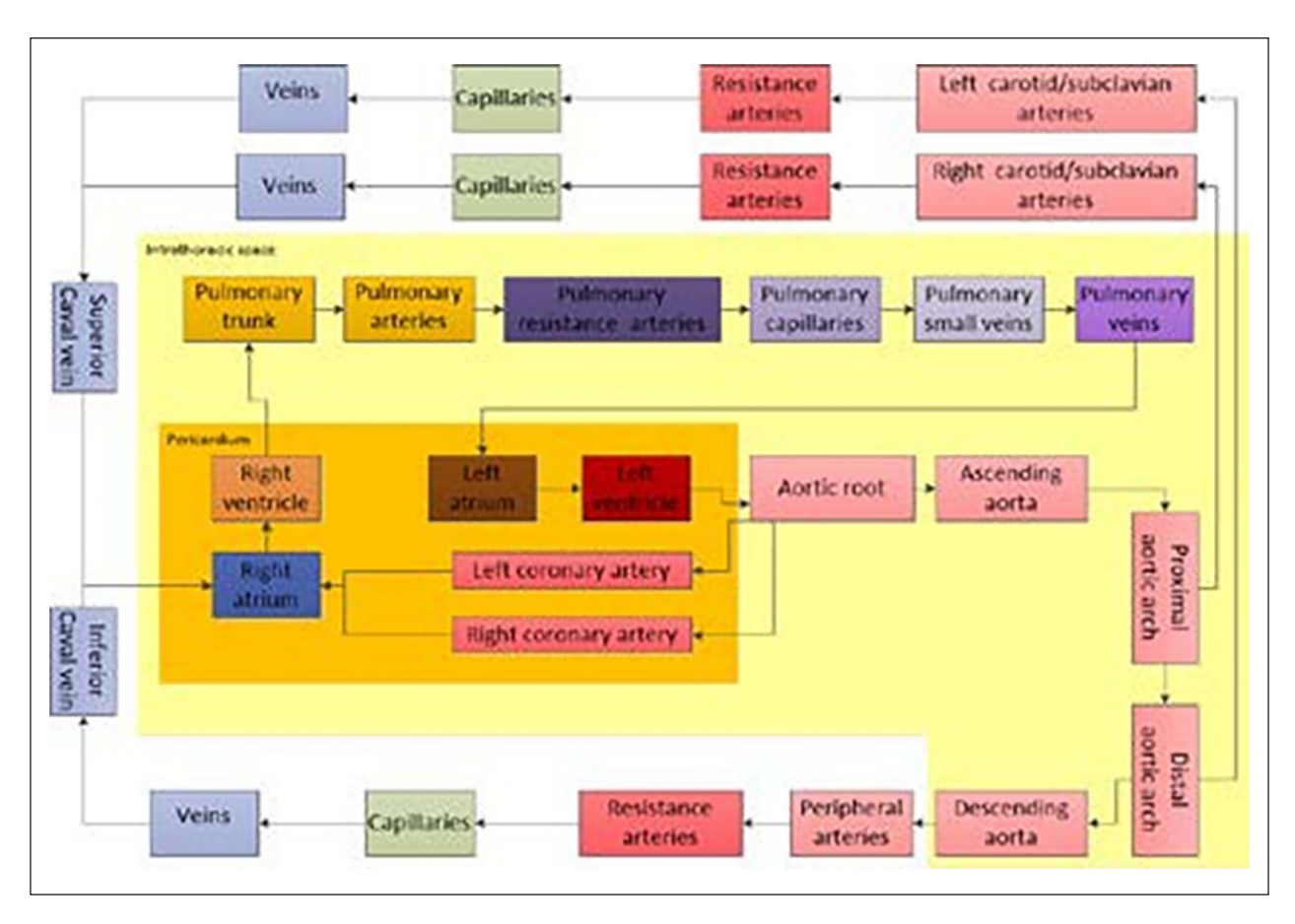


Figure 1. Overview of Aplysia cardiovascular model compartments.

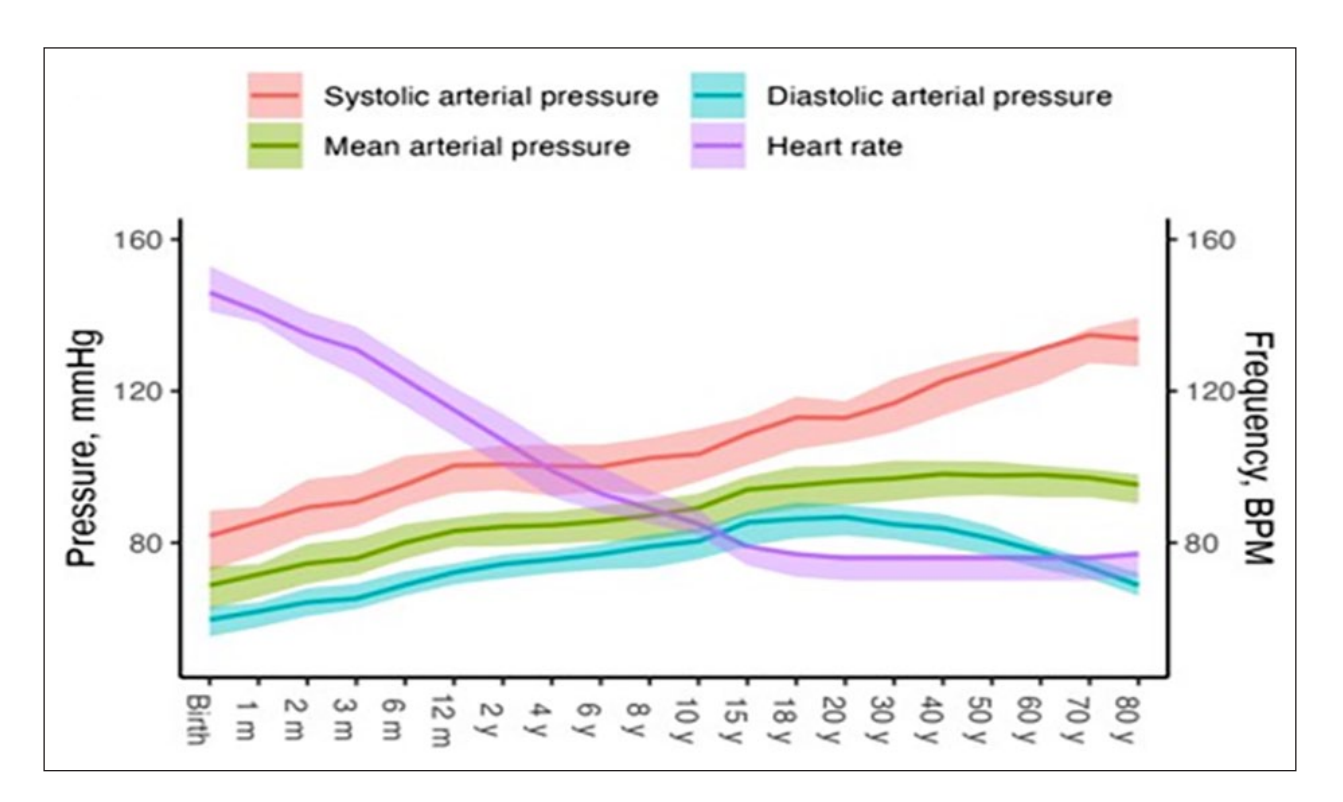


Figure 2. Scaling output of heart rate, systolic, mean and diastolic arterial pressures in ages from birth to 80 years. Solid line represents an average female subject. Upper limit is a 2SD overweight man and lower limit is a 2SD underweight woman.

References

 Broome M, Maksuti E, Bjallmark A, Frenckner B, Janerot-Sjoberg B. Closed-loop real-time simulation model of hemodynamics and oxygen transport in the cardiovascular system. Biomed Eng Online. 2013;12:69.

Acknowledgements

This work was supported by grant No 20180265 from the Swedish Heart-Lung Foundation.

DEVELOPING A MULTI-PURPOSE PHYSIOLOGY MODEL- EMERGING BEHAVIOR AND INTERNAL VALIDATION

August Lundquist[¶], Elira Maksuti^{\$}, Dirk W Donker^{‡ + ‡‡}, Michael Broomé [§], [¶]

[¶]Anaesthesia and Intensive Care, Dept. of Physiology and Pharmacology, Karolinska Institute, Sweden; \$Getinge, Acute Care Therapies, Maquet Critical Care AB, Solna, Sweden; [‡]Dept. of Intensive Care Medicine, University Medical Center Utrecht, Utrecht University, The Netherlands; ^{‡‡}Cardiovascular and Respiratory Physiology, University of Twente, Enschede, The Netherlands; [§]ECMO Department, Karolinska University Hospital, Stockholm, Sweden

Introduction: Multi-purpose 0-D computational cardiovascular and respiratory physiology models are used in education of health care professionals and hold promise in research and future clinical decision support systems. Model validation is often insufficient, and model output may

therefore be difficult to trust. Conventional validation with real world patient data is the standard, but not enough since realistic models often have more parameters than can be determined by clinical measurements. Moreover, the most valuable use of a model is often in complex cases outside the range of the validation data set.

Testing internal consistency and correspondence with known physics, physiology, dimensions and tissue properties are strong tools in model validation and should systematically be used to improve model reliability.

Methods: A previously published 0D closed-loop real-time model (1) was used to exemplify validation based on emergent model behavior, i.e. not pre-specified or explicitly modeled, as compared with known physiology and pathophysiology. Model output such as pressure-volume loops, pressure and flow velocity traces through valves and in major vessels were compared with results from clinical invasive monitoring and echocardiography in normal physiology as well as in systolic/diastolic left/right heart failure and valve regurgitation/stenosis.

Results: The model output showed realistic pressure- volume-loops, iso-volumetric contraction/relaxation Wiggers diagram. Left ventricular (red), ascending aortic (dark red), right ventricular (yellow), pulmonary arterial (orange), left atrial (brown) and right atrial (blue) pressures. Curve shapes and pressures correspond well to established normal physiology. timing, arterial pressure traces and wave transport as well as valve flow velocity profiles in mitral and aortic stenosis, aortic and tricuspid regurgitation.

Discussion/Conclusion: We propose a multi-modal validation process including both external clinical measurements and emergent model behavior as the most effective and reliable method when securing

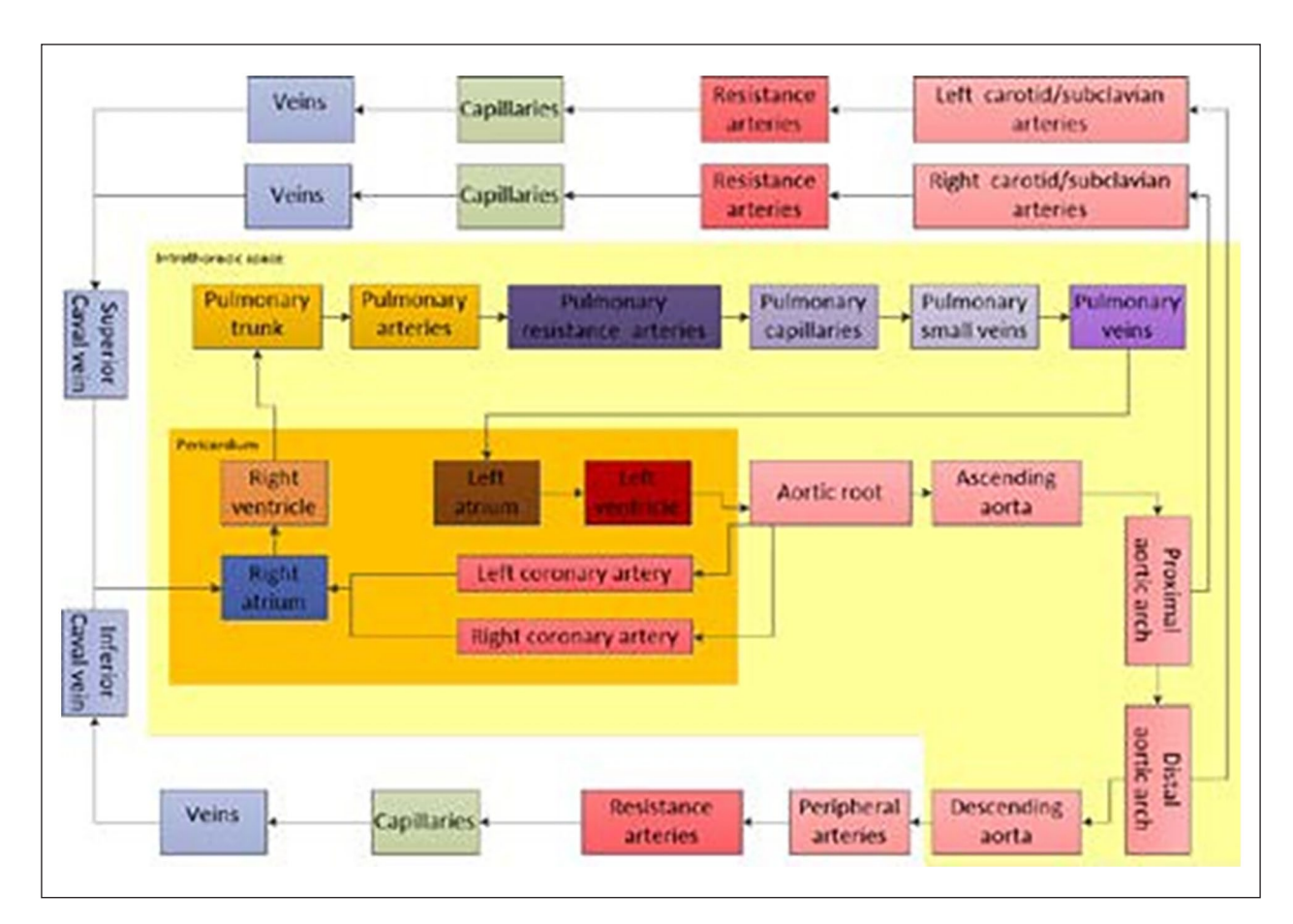


Figure 1. Overview of Aplysia cardiovascular model compartments.

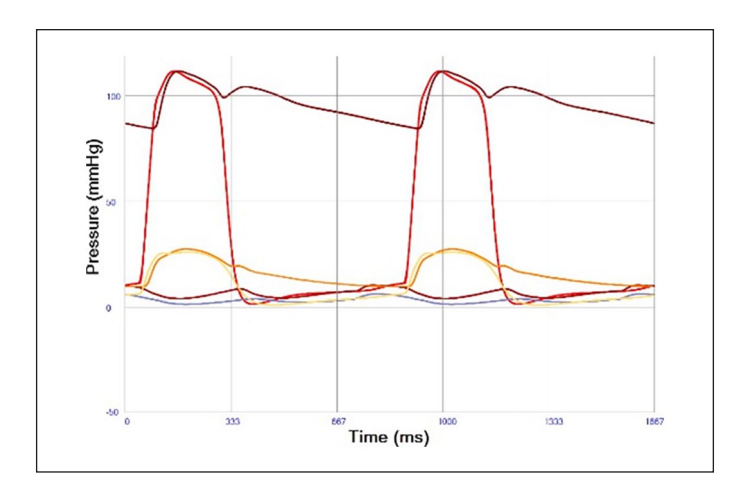


Figure 2. Valve timing and flows. Left panel shows timing of cardiac phases in normal adult physiology. Right panel shows aortic (red), pulmonary (yellow), mitral (brown) and tricuspid (blue) valve flows. Curve shapes and timing correspond well to established normal physiology.

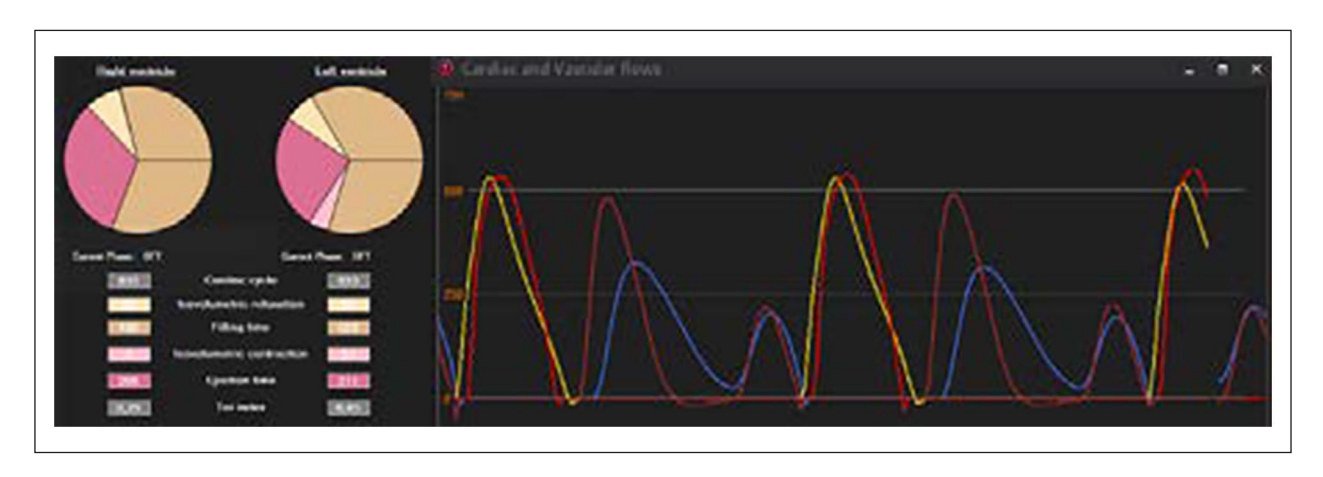


Figure 3. Valve timing and flows. Left panel shows timing of cardiac phases in normal adult physiology. Right panel shows aortic (red), pulmonary (yellow), mitral (brown) and tricuspid (blue) valve flows. Curve shapes and timing correspond well to established normal physiology.

relevance of 0-D computational cardiovascular and respiratory physiology models.

References

Broome M, Maksuti E, Bjallmark A, Frenckner B, Janerot-Sjoberg B. Closed-loop real-time simulation model of hemodynamics and oxygen transport in the cardiovascular system. Biomed Eng Online. 2013;12:69.

Acknowledgements

This work was supported by grant No. 20180265 from the Swedish Heart-Lung Foundation.

HIGH-RESOLVING VAD SIMULATIONS: CONRIBUTION OF FLOW IN FRONT SIDE CHAMBER ON HAEMOLYSIS

Vincenz Crone¹, Florian Voigt¹, Benjamin Torner², Hendrik Wurm¹

Introduction: The shortage of donor hearts has led to the use of ventricular assist devices (VADs) as a treatment for severe heart failure. In VADs, a highly complex flow field with non-physiological flow conditions has been associated with the occurrence of haemolysis. However, the direct relation between the flow field and the haemolysis is often vague in the literature and requires further investigation. Computational fluid dynamics (CFD) can be utilised to investigate these non-physiological flow conditions and predict the occurrence of haemolysis, a key factor in the pre-clinical development of VADs. To gain a deeper understanding of secondary and turbulent flow structures, high-resolution CFD simulations, such as Large Eddy Simulations (LES), are a suitable method. The modified index of haemolysis (MIH) is utilised to evaluate haemolysis in experimental and numerical contexts. The numerical MIH is linked to the equivalent (shear) stress $\tau \tau_{ss}$, the exposure time tt, and empirical constants, with shear stresses frequently associated with turbulent flows. The objective of this study is to establish a correlation between flow structures and the occurrence of haemolysis in the front side chamber of the VAD by using high-resolution LES.

Methods: In this study, VAD simulations of the HeartMate 3 were investigated by utilising the LES WALE model in CFX (ANSYS Inc., Canonsburg, PA) with a hexahedral mesh containing approximately 77 million elements and maintaining a RMS courant number below 1. The verification parameters,

¹Institute of Turbomachinery, University of Rostock, Germany;

²Department of Cardiac Surgery, Medical University of Vienna, Austria

including the LES Index of Quality, Kolmogorov length, turbulent kinetic energy (TKE) spectrum and the Power-Loss-Analysis (PLA), were all maintained within the limits specified in the literature for LES [1,2]. The validation of the VAD simulation was performed by utilising PTV measurements from [3] and the H-Q-Curve from [4]. The numerical MIH calculation was validated for three distinct operating points, with experimental results from [5]. Five different empirical constants for the MIH calculation, obtained from the literature, were tested and compared with the results of [5]. Finally, a "typical" operating point was investigated in greater detail to analyse the relationship between haemolysis and the flow field in the side chamber. To achieve this, the volume integral of the MIH in different regions of the pump was calculated to identify the most influential regions for haemolysis in the VAD. Furthermore, the volume integral of dissipation was calculated. The results of MIH and dissipation were compared and correlated. Additionally, unsteady flow patterns were analysed.

Results: The optimal alignment of the five evaluated MIH empirical constants was observed in the constants proposed by Fraser et al. [6], which demonstrated the strongest concordance with the findings from experiments [5]. It is important to note that the MIH values vary considerably depending on the region of the pump. The front side chambers of the pump have been found to cause high level of haemolysis with approx. % of the overall haemolysis.

The results correlate with the results of the dissipation analysis. It was therefore essential to investigate dissipation as a consequence of turbulence.

Flow structures have been identified in various parts of the HeartMate 3 causing turbulence and dissipation.

The findings demonstrated that the Taylor vortex was the predominant flow phenomenon within the axial gap of the front side chamber, resulting in increased wall shear stresses and consequent haemolysis.

Discussion: In order to conduct a study of the complex flow phenomena in the VAD, it is advantageous to utilise a highly turbulence-resolving Large Eddy Simulation (LES). With this method further parts of the VAD have to be investigated for a better understanding.

References

- Fröhlich: Large Eddy Simulation turbulenter Strömungen, 1st ed. Wiesbaden: Teubner, 2006
- 2. Torner et al., Int J Numer Method Biomed Eng, 3: e3431
- 3. Thamsen et al., ASAIO J., 60: 173-182, 2020
- 4. Belkin et al., J Card Fail., 28: 845-862, 2022
- 5. Bourque et al., ASAIO J., 62: 375-383, 2016
- 6. Fraser et al., J Biomech Eng., 134: 8, 2012

MIXED MATRIX MEMBRANES, CELLULOSE ACETATE/ SILICA/METAL ORGANIC FRAMEWORK, FOR PROTEIN-BOUND UREMIC TOXINS REMOVAL IN THE ARTIFICIAL KIDNEY

João Dionísio¹, Miguel Pereira da Silva², Tiago Ferreira³, Ricardo Pereira⁴, Miguel Minhalma⁵, Moisés Pinto⁶, Maria Norberta de Pinho⁷

¹Chemical Engineering Department/CeFEMA, Instituto Superior Técnico, Universidade de Lisboa, Portugal; ²Chemical Engineering Department/CeFEMA, Instituto Superior Técnico, Universidade de Lisboa, Portugal; ³Chemical Engineering Department/CeFEMA, Instituto Superior Técnico, Universidade de Lisboa, Portugal; ⁴Department of Bioengineering/Associate Laboratory i4HB, Instituto Superior Técnico, Universidade de Lisboa, Portugal; ⁵Instituto Superior de Engenharia de Lisboa/CeFEMA, Portugal; ⁵Chemical EngineeringDepartment/CERENA, Instituto Superior Técnico, Universidade de Lisboa, Portugal; ¹Chemical Engineering Department/CeFEMA, Instituto Superior Técnico, Universidade de Lisboa, Portugal; ¹Chemical Engineering Department/CeFEMA, Instituto Superior Técnico, Universidade de Lisboa, Portugal;

Introduction: Adsorption therapies have emerged in hemodialysis as an innovative approach for removing protein-bound uremic toxins (PBUTs). The present work addresses the enhancement of the adsorption capacity of hemodialysis membranes through the incorporation of Metal-Organic Frameworks (MOFs) in a cellulose acetate (CA)/silica (SiO2) matrix.

Methods: The membranes were synthesized by coupling the phase inversion technique with the sol-gel method in acidic conditions that assure the covalent bonding of the silica to the CA structure [1]. Two types of MOFs, UiO-66 and UiO-66-NH2, are synthesized and characterized. Its dispersion in the membrane casting solutions yields two sets of membranes, CA/SiO2/UiO-66 [2] and CA/ SiO2/UiO-66-NH2. The MOF concentration in the casting solution ranges from 0.5% to 2.5%

Results: All the membranes were characterized by the hydraulic permeability, molecular weight cut-off and rejection coefficients to p-cresyl sulfate (pCS), bovine serum albumin (BSA) and pCS+BSA solutions. The membranes with UiO-66-NH2 exhibited lower values of hydraulic permeability ranging from 5.1 to 8.2 kg m-2 h-1 bar-1 and molecular weight cut-off of 4.6 kDa when compared to the membranes with UiO-66 that have hydraulic permeability ranging from 12.1 to 30.0 kg m-2 h-1 bar-1 and molecular weight cut-off ranging from 7 to 16 kDa. For feed model solutions of 100 ppm pCS and 35 g L-1 BSA, simulating a hemodialysis session, membranes without MOF showed pCS rejection coefficients of 24.8% and 30.4%. Incorporating MOFs significantly improved permeation performance, with rejection coefficients to pCS of 0.2% for the CA22/SiO2/UiO-66 membrane with 1.5% of MOF and 2.6% for the CA22/SiO2/UiO-66-NH2 membrane with 2% of MOF. The removal capacity of pCS bound to BSA is 99.8% for the CA22/SiO2/UiO-66 membrane with 1.5% of MOF, and 95.9% for the CA22/SiO2/UiO- 66-NH2 membrane with 2% of MOF.

Discussion: The incorporation of UiO-66 and UiO-66-NH2 in mixed matrix membranes leads to the preferential adsorptive character of pCS bound to BSA, and envisages their potential application for PBUTs removal in hemodialysis.

References

- 1. Mendes et al, Carbohydr Polym, 189:342-351, 2018.
- 2. Guerreiro et al, Desalination, 565:116860, 2023.

Acknowledgements

All authors acknowledge financial support through UIDB/04540/2020 (CeFEMA, LaPMET), UIDB/04028/2020 (CERENA) and Associate Laboratory i4HB as FCT R&D Unit grants. T. Ferreira, M. Pinto and M. N. de Pinho acknowledge financial support through EU Project 101130006 BioMembrOS. M. P. da Silva acknowledge financial support through 2023.03206.BD FCT PhD studentship grant.

Case presentation: We report a case of a 9-year-old girl with Streptococcus pyogenes bacteremia-mediated septic shock who was admitted to the intensive care unit. She had a 3-day history of fever, erythema polymorphe and chest pain. With the deterioration of symptoms, including dyspnea, severe hypoxia, hypotension and oliguria, she was diagnosed with pleural empyema. Drainage of 1.5L of pus was performed, supportive treatment (fluid resuscitation, antibiotic therapy, mechanical ventilation, vasopressin, norepinephrine, and dobutamine) was applied for four days. The patient developed signs of irreversible shock. Due to the severe systemic inflammatory reaction, she developed myocarditis and stage 2 acute kidney injury. With the approval of the patient's family continuous veno-venous hemodiafiltration was implemented using an oXiris hemofilter to enhance the clearance of cytokines and endotoxins (2). The therapeutic dose of 30ml/kg/h was applied. blood flow was gradually increased up to 100ml/min, ultrafiltration 160ml/hour according to hematocrit and lactate level. This blood purification protocol was continued for 72 h using three filters which were changed every 24h. The inflammatory biomarkers and doses of vasopressors rapidly declined after first 10 hours and AKI recovered by 48hours. Considering dialysis, the dose of vancomycin was adjusted to 10 mg/kg/times each 12 h, and the dose of meropenem to 17.5 mg/kg/ times each 12 h. The patient was weaned off mechanical ventilation after 20 days and transferred to the general ward several days later with a total hospitalization duration of 40 days. Three months later, full recovery was notified.

Conclusion: Significant improvement in hemodynamic measures, decreased need of vasoactive drug dosage, reduced lactate level and infection measures is associated with oXiris-hemofiltration treatment in patients with sepsis or septic shock.

References

- Bauer M, et al, Mortality in sepsis and septic shock in Europe, North America and Australia between 2009 and 2019- results from a systematic review and meta- analysis. Crit Care. 2020 May 19;24(1):239
- Siew et al Outcomes of Extracorporeal Blood Purification with OXiris® Membrane in Critically III Patients: A Systematic Review and Meta-Analysis. J. Crit. Care 2024, 83, 154844.

TOWARDS BIOARTIFICIAL LUNG DEVELOPMENT – OPTIMIZATION AND INDIVIDUALIZATION USING 3D PRINTING

Sebastian V. Jansen^{1,6}, John Linkhorst², Michael Pflaum^{3,4,5}, Gerrit Sitarz^{3,4}, Kai Barbian¹, Lukas Hirschwald², Florian Neuhaus², Ulrich Steinseifer¹, Matthias Wessling^{2,6}, Arjang Ruhparwar^{3,4,5}, Bettina Wiegmann^{3,4,5,6}

¹Department of Cardiovascular Engineering, Institute of Applied Medical Engineering at the RWTH Aachen University, Germany; ²Chemical Process Engineering and Institute of Process Engineering, RWTH Aachen University, Germany; ³Department of Cardiothoracic, Transplantation and Vascular Surgery, Hannover Medical School, Germany; ⁴NIFE − Lower Saxony Centre for Biomedical Technology, Implant Research and Development, Germany; ⁵DZL − German Centre for Lung Research, Hannover Germany; ⁶Member of the DFG priority program SPP 2014, Germany

Objective: Extracorporeal hollow fiber membrane (HFM) oxygenators, currently in clinical use for supporting blood gas exchange of patients suffering from a severe lung disease, are afflicted with several limitations, excluding their use as long-term or destination therapy. Irregular blood flow patterns and synthetic foreign blood-contacting surfaces

"WHEN THE EXCEPTION BREAKS THE RULES: HEMOFILTRATION OXIRIS REVERSES EMPYEMA INDUCED SEPTIC SHOCK IN A CHILD: A CASE REPORT"

Aleksandra Canevska-Taneska, Irena Rambabova -Bushljetik, Vladimir Pushevski, Nikola Gjorgjievski, Petar Dejanov, Lada Trajceska

University Clinic of Nephrology; Medical Faculty, Ss Cyril and Methodius University, Republic of North Macedonia,

Introduction: Septic shock results in multiorgan dysfunction and high mortality(1). This is a report on a septic child with cytokine storm and acute kidney injury treated with oXiris hemofilter

provoke blood clot formation and proinflammatory reactions, device occlusion and failure, requiring frequent and risky device replacement. A novel generation of oxygenators based on triply periodic minimal surfaces (TPMS) could provide non-detrimental blood flow, while seeding all blood- contacting surfaces with an anti-thrombogenic and anti-inflammatory endothelial cell (EC) monolayer may prevent thrombus formation. Additive manufacturing could enable tailor-made implantable oxygenators, for individual patients. In our study, feasibility was assessed via computational fluid dynamics (CFD) of a TPMS- based prototype, featuring shape and size of a rat lung and compared with same-sized HFM oxygenators. Biocompatibility assays were done for identifying 3D-printable materials eligible for manufacturing endothelialized prototypes.

Methods: Computer tomography data obtained from a rat lung was used to model a TPMS oxygenator. CFD models simulated 3 x 2 x 2 unit cells of TPMS and HFM. O2 and CO2 gas transfer rates were modeled using Hormes' approach evaluating different membrane thicknesses (10, 100, 400 μ m) and at different flow rates (60 to 140 ml/min) under DIN ISO 7199 conditions.

Materials intended for 3D printing of membranes (MAP-PDMS, PDMS-coated FlexaGrey, PorePro and xPDMS) were checked for O2 permeability and tested for extract cytotoxicity on ECs using the WST8-assay. Thrombocyte binding affinity was tested with BCECF-stained human platelets. EC adhesion on fibronectin coated materials was assessed by calcein-am staining and activation status of pro-thrombogenic and pro-inflammatory genes was determined by qRT-PCR. EC confluence and *de novo* basement matrix generation were detected using immuno-fluorescence for CDH5 and Collagen-IV.

Results: CFD predicted uniform blood flow without stagnation in TPMS oxygenators, with only slightly elevated velocities around its ports. When compared to HFM superior O2 transfer rate at any assessed flow rate was found, when TPMS membranes were made from 10 μm thick silicone (PDMS). PDMS-coated FlexaGrey and xPDMS possessed excellent O2 permeability, passed biocompatibility and thrombocyte adhesion tests and enabled the cultivation of a non-activated, interconnected and confluent EC monolayer, on a self-synthesized basement matrix.

Discussion: These findings support the feasibility of an endothelialized, patient-specific, and implantable TPMS-based oxygenator, which could finally overcome the current clinical limitations in providing long-term support for patients with end- stage lung disease.

TARGETING IMMUNOTHROMBOSIS IN SEPSIS WITH EXTRACORPOREAL BLOOD ADSORBTION

<u>Vladislav Semak</u>¹, Tanja Eichhorn¹, Marwa Mostageer¹, Ivan Bessonov², Viktoria Weber¹

¹Department for Biomedical Research, University for Continuing Education Krems, 3500 Krems, Austria; ²Efferon International GmbH, Eßlinger Straße 13, 78532 Tuttlingen, Germany

Introduction: Sepsis and septic shock are life-threatening conditions characterised by dysregulated immune responses, including cytokine storm and immunothrombosis. Efferon LPS is a single-use cartridge filled with an adsorbent designed for extracorporeal blood purification [1]. The porous polymeric adsorbent selectively binds two different molecular targets: cytokines and middle-sized proteins (via intrinsic porosity) and lipopolysaccharides (LPS; via surface-immobilized ligand). Building on our previous research that demonstrated the effectiveness of heparin- functionalized adsorbents in eliminating platelet factor 4 (PF4), histones, and high-mobility group box 1 protein (HMGB1) [2], this in vitro study mainly aims to evaluate whether Efferon LPS is also efficient in removing these mediators of immunothrombosis.

Methods: The blood compatibility and adsorption efficacy of Efferon LPS were assessed using an in vitro hemoadsorption model. Key experiments included the depletion of mediators of immunothrombosis, such as PF4, histones/nucleosomes, and HMGB1, with levels quantified preand post-adsorption using ELISA and Western blot. The adhesion of activated platelets on the surface of the adsorbent beads was evaluated using scanning electron microscopy (SEM) and confocal laser scanning microscopy (CLSM), while platelet-derived extracellular vesicles (EVs) were quantified by flow cytometry (FC) and nanoparticle tracking analysis (NTA). The oxidized-to-native albumin ratio was also measured as a marker of oxidative stress using high-performance liquid chromatography (HPLC).

Results: Preliminary data focused on the capacity of Efferon LPS to deplete PF4, histones, and HMGB1, as well as its impact on platelet activation and EV capture. Our results will provide insights into how the Efferon LPS adsorbent mitigates immunothrombosis and oxidative stress in sepsis.

Discussion: Previous generations of anti-cytokine hemoadsorption cartridges have yielded controversial results in treating sepsis [3]. A possible explanation could be their inability to remove the primary sepsis trigger, the LPS molecule. Efferon LPS represents an advancement in blood purification technologies due to its ability to adsorb both, cytokines and LPS. This study investigates how this type of adsorbent can influence immunomodulation by examining its effects on the levels of PF4, histones, HMGB1, oxidised albumin, and platelet activation.

References

- Rey, S.; Kulabukhov, V. M.; Popov, A.; Nikitina, O.; Berdnikov, G.; Magomedov, M.; Kim, T.; Masolitin, S.; Ignatenko, O.; Krotenko, N.; Marysheva, A.; Chaus, N.; Ohinko, L.; Mendibaev, M.; Chumachenko, A.; Pisarev, V. Hemoperfusion Using the LPS-selective Mesoporous Polymeric Adsorbent in Septic Shock: a Multicenter Randomized Clinical Trial. Shock 2023, 59 (6), 846–854. https://doi.org/10.1097/ shk.0000000000002121.
- Ebeyer-Masotta, M.; Eichhorn, T.; Weiss, R.; Semak, V.; Lauková, L.; Fischer, M.B.; Weber, V. Heparin- Functionalized Adsorbents Eliminate Central Effectors of Immunothrombosis, including Platelet Factor 4, High-Mobility Group Box 1 Protein and Histones. *Int. J. Mol. Sci.* 2022, *23*, 1823. https://doi.org/10.3390/ijms23031823
- Becker, S.; Lang, H.; Clara Vollmer Barbosa; Tian, Z.; Melk, A.; Bernhard. Efficacy of CytoSorb®: A Systematic Review and Meta-Analysis. 2023, 27 (1). https://doi.org/10.1186/s13054-023-04492-9.

IN-HOUSE HEMODIALYZER VISUAL SCORE ASSESSMENT TOOL

Nelly Mesas¹, <u>Miquel Gomez-Umbert</u>¹, Isabel Ondoño-Montaner² Carolina Palomar-Ceballos², M.Mar Martinez-Nebreda², Francisco Maduell^{1,2}

¹Laboratori Experimental de Nefrologia i Trasplantament (LENIT), Fundació Recerca Clínic-Institut d'Investigacions Biomèdiques August Pi

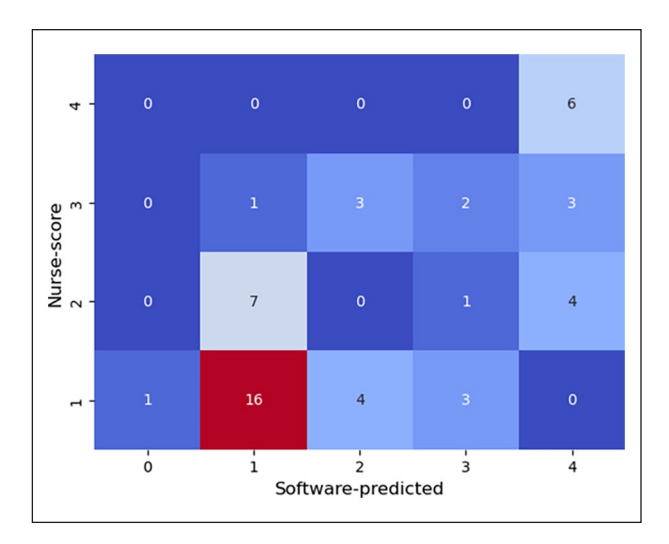


Figure 1. Heatmap of the software predicted vs. nurse reported values.

i Sunyer (IDIBAPS), Barcelona, Spain; ²Nephrology Department, Hospital Clinic de Barcelona, Spain

Introduction: The hemodialysis procedure forces the contact between blood and an endogenous material constituting the capillary at the hemodialyzer. To relate anticoagulation dose with membrane clotting and underperformance [1], a subjective assessment of dialyzer appearance score between 0-4 (0;clean, 1;25%, 2;50%, 3;75%, 4;100% fiber clogging) is stated by the nursing staff at the end of the session [2,3]. However, this subjective measurement might be highly influenced by the observer criteria. Herein we explore the potential of image processing software to objectively assess this score.

Methods: This exploratory study included 51 post-treatment hemodialyzer pictures obtained by a conventional mobile-phone camera. Images were processed by an in-house developed software, which detected the potential clogged fibers to total available pixel ratio, thus assigning the score value. In addition, the nursery staff value was also recorded for comparison.

Results: Figure 1 depicts the count heatmap for our software predicted value and the nursing staff criteria. A strong significant correlation (Spearman's Rho=0.962, p<0.001) was found. However, a moderated classification performance was obtained as a substantial quantity of predicted values did not match nursing staff criteria, only achieving 47% of images a satisfactory classification (Fisher's Exact test=33.633, p<0.001). Moreover, the software predicted values tended to overestimate moderately-clogged fibers (30% of analyzed cases).

Discussion: This is the first attempt to validate a software tool to quantify hemodialysis membrane clogging status at the end of the treatment. Our in-house developed image processing algorithm allowed us to explore the potential of an easy-to-implement and objective tool aimed at assessing the dialyzer appearance score, usually carried out by the nursing staff and therefore affected by observer bias.

The obtained results suggest the need of an improvement in the proposed model as well as a tailored classification criteria that would open a wide range of applications as further developments would be able to integrate the automated score obtention to the patient session database and foster elaborated AI generated predictive models.

References

- 1. Vanommeslaeghe, F. et al. Sci. Rep. 12, 1-10 (2022).
- 2. Fazendeiro Matos, J. et al. Hemodial. Int. 24, 61–70 (2020).
- 3. Puerta, M. et al. *J. Nephrol.* (2025).

Acknowledgements

We would like to thank all the nursing staff as well as the patients for their commitment and dedication with the current project.

A NOVEL FLOW THROUGH IN-VITRO PIPELINE FOR HEMOCOMPATIBILITY TESTING OF ARTIFICIAL KIDNEY MEMBRANES

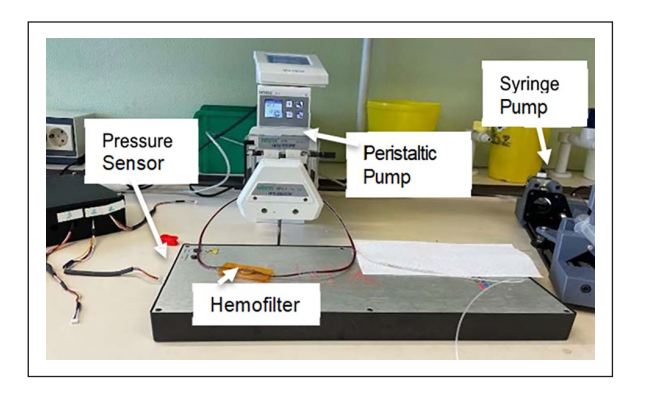
Tugrul Irmak¹, Tadeo Valdez¹, Jeroen Vollenbroek^{1,2}, Karin G.F. Gerritsen¹

¹Department of Nephrology, University Medical Centre Utrecht, Utrecht, The Netherlands; ²BIOS Lab on a Chip Group, MESA + Institute, University of Twente, Hallenweg 15, 7522 NH Enschede, The Netherlands

Introduction: An implantable artificial kidney (AK) aims to replace dialysis and act as a bridge to transplantation, but achieving sufficient filtration rates (~15 ml/min) over three years requires exceptional hemocompatibility. Protein fouling and coagulation are major barriers to long-term implantation, necessitating highly hemocompatible membranes with hydrophilic coatings[1]. The chemical composition and application method of these coatings significantly impact membrane performance, requiring rapid optimization and feedback. We present a novel in-vitro test pipeline to evaluate membrane coatings under controlled closed-loop blood flow, measuring real-time permeability during blood contact and tracking time-to-clot under near-physiological conditions to predict in-vivo performance. Typical sources of clotting are blood/air interface and changes in tubing dimensions (shear). This pipeline has no blood/air interface and a constant shear (tunable between 1-3 Pa) throughout the whole device.

Methods: A mini hemofilter device was 3D printed (200um internal blood channel) to house an aluminum oxide membrane, with one set bare and another coated with a PE coating to increase hemocompatibility. The hemofilter was designed to limit shear stress to 1 Pa to reduce platelet activation. Tygon medical tubing (50 cm) was press-fitted to the hemofilter, and two PE tubings were connected—one to a pressure sensor and the other to a syringe pump. The system volume was 1.2 ml. The syringe pump maintained 100 mmHg pressure and offset fluid loss via PID control, allowing additional real time permeability tracking. A mean flow rate of 1.5 ml/min was circulated with a peristaltic pump, with occlusion calibrated using custom setup to minimize hemolysis.

Results:



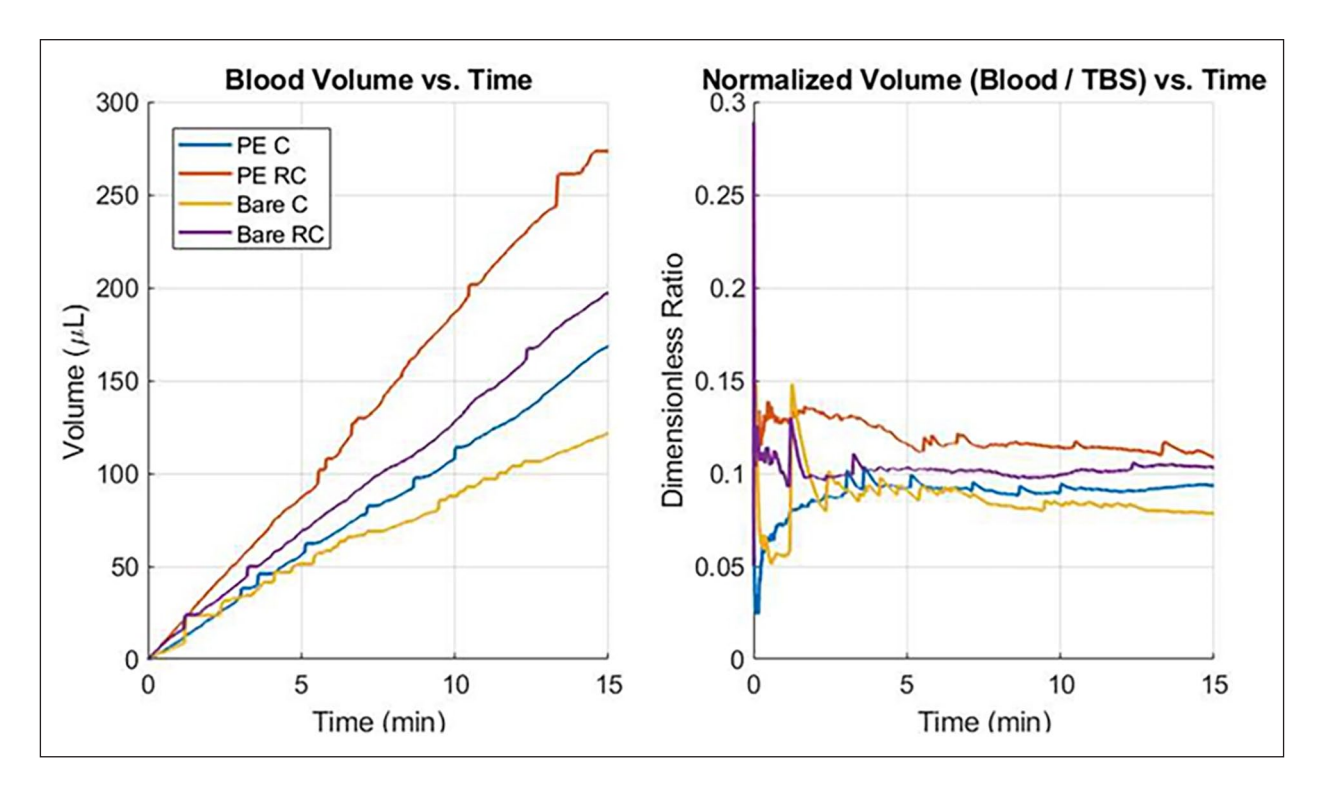


Figure 1. (Left) Permeate volume for polyelectrolyte coated (PE) and bare membrane shown for recalcified (RC) and citrated blood (C). (Right) permeate volume normalized to TBS (buffer) output expected in that time.

Discussion: Our setup reveals a direct and local measure of blood compatibility for hemofiltration membranes, that is the membrane permeability. In this the figures illustrate that the coated membrane maintained permeability for a longer length of time, prior to system clot. The differences however are not large, with about factor 10 drop in permeability, due to fouling compared to buffer, meaning the PE coating needs to be further optimized.

Permeability is obtained in real time and is arguably the most critical parameter for an artificial kidney. However, other parameters such as platelet activation markers, SEM imaging of the membranes after blood contact and selectivity changes were also obtained. Lastly, for the first time, we show the concurrent use of a syringe pump to control hydrostatic pressure and a peristaltic pump to maintain shear without hemolysis. This is an important milestone for better translation of in-vitro blood compatibility testing to the in-vivo situation.

References

1. Jaffer & Weitz, Acta Biomaterialia, 94:2-10, 2019.

Acknowledgements

This project was funded by European Innovation Council (project name: KIDNEW), ACX grants and NXTGEN Hightech

VA-ECMO CIRCUIT COMPONENT DECISION MATTERS: INVESTIGATING THE IMPACT OF CANNULA SIZE ON ECMO COMPONENTS AND HEMODYNAMICS IN AN IN-SILICO CLINICAL TRIAL

Lars Fischer¹, Jan-Niklas Thiel¹, Christopher Blum¹, Ulrich Steinseifer¹, Ifan Yen², Po-Lin Hsu², Michael Neidlin¹ **Introduction:** VA-ECMO is a complex critical care therapy associated with high mortality partially related to complications in device-patient interaction [1]. The blood damaging potential is highly influenced by the ECMO circuit's configuration [2]. This study investigates the impact of cannula size and pump choice on patient hemodynamics and device performance in an in-silico clinical trial.

Methods: Our in-silico clinical trial consists of a cardiovascular model, ECMO component models and clinical data of 30 VA-ECMO patient states [3]. ECMO components were modelled based on in- vitro and or in-silico data [4]. The system of differential equations was solved to evaluate device performance (hydraulic and hemocompatibility metrics) and patient hemodynamics, based on user-defined ECMO components, connection schemes, and fitted patient parameters. Three rotary blood pumps—Getinge Rotaflow, Deltastream DP3, and LivaNova Revolution—were included and tested with two cannula configurations: 19 Fr and 15 Fr for the small configuration, and 29 Fr and 23 Fr for the large configuration, for the drainage cannula and return cannula sizes, respectively. A total of 180 virtual patient states were evaluated.

Results: Figure 1 A shows the pumps' operation conditions and reveals that for each patient state, elevated pump pressures were observed with the small cannula configuration, with differences increasing up to two-fold at higher flow rates. B shows the respective pump speed distributions. Increased and broader distributed rotary speeds are required to maintain flow rates for smaller cannula configurations. C depicts the blood damage distribution of the pumps and cannulas. Pumps' hemolysis levels increase up to threefold with smaller cannulas, while the cannulas' contribution to the circuit's hemolytic potential remains negligible in comparison to the pump.

Discussion: Our in-silico clinical trial revealed up to a threefold increase in pump-induced blood damage with small cannula configurations, requiring higher rotary speeds, while the cannulas themselves had negligible impact, highlighting the importance of low ECMO circuit resistance.

¹Department of Cardiovascular Engineering, Institute of Applied Medical Engineering, MedicalFaculty, RWTH Aachen University; ²magAssist Co., Ltd., Suzhou, China

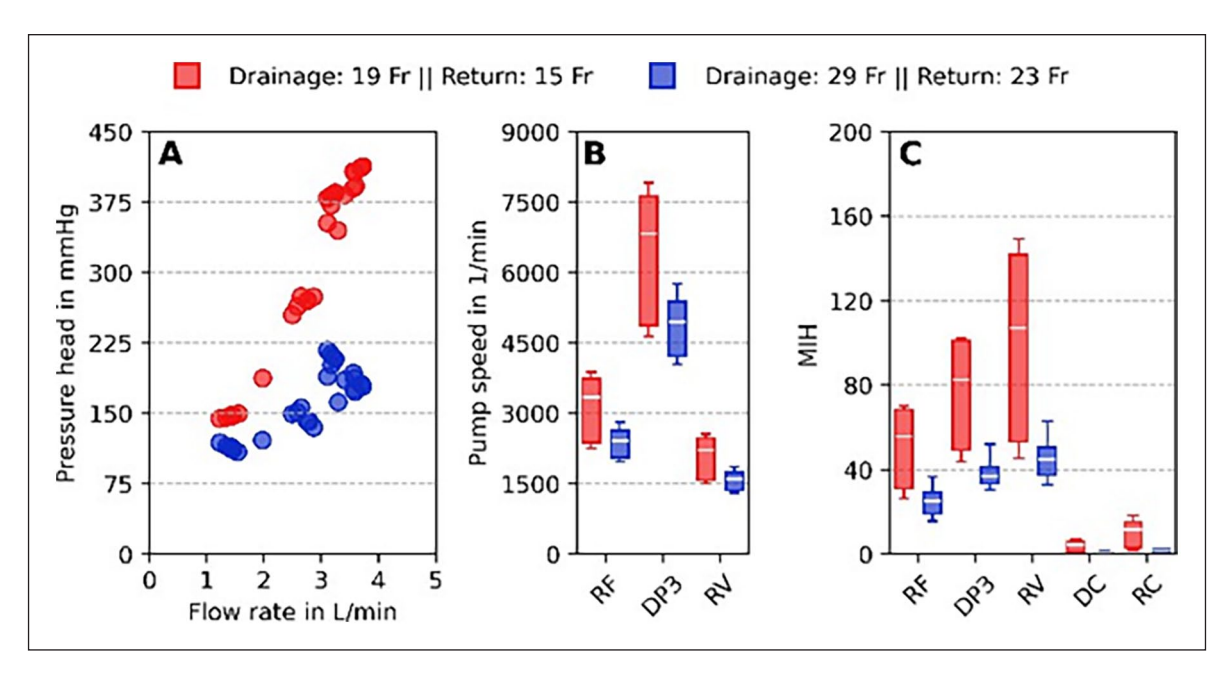


Figure 1. Subplot of device metrics. RF, DP3, RV, DC, and RC stand for Rotaflow, DP3, Revolution, drainage cannula, and return cannula, respectively. A) Pumps' operation conditions. B) Boxplots of the pumps' rotary speed. C) Boxplot of pump's numerical hemolysis prediction in form of modified index of hemolysis (MIH).

References

- 1. Makhoul et al., 2021, Artificial Organs, doi.org/10.1111/aor.14006
- 2. Blum et al., 2024, Critical Care, doi.org//10.1186/s13054-024-05121-9
- Thiel et al., 2025, Computers in Biology and Medicine, doi. org/10.1016/j.compbiomed.2025.109668.
- Blum et al., 2023, Computers in Biology and Medicine, 10.1016/j. compbiomed.2023.107772.

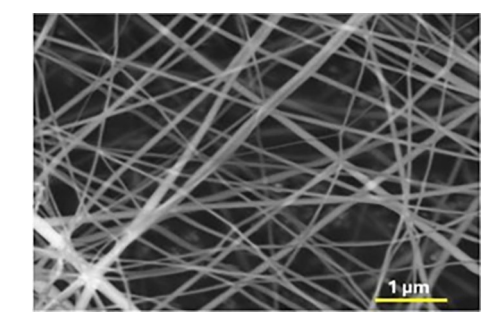


Figure 1. PVDF non-woven microstructure (magnification x50 000).

ELECTROSPUN PVDF NANOFIBERS: A PROMISING APPROACH FOR SOFT TISSUE REGENERATION

Anna Marszałek¹, Dominika Wójtowicz¹, Anna Ścisłowska-Czarnecka², Ewa Stodolak-Zych¹

¹Department of Biomaterials and Composites, AGH University of Krakow, Poland; ²Institute of Applied Sciences, University School of Physical Education in Krakow, Poland;

Introduction: Loss of soft tissue, such as the stomach or intestine, is a common problem in clinical medicine after resection for tumour removal [1]. Stable polymeric fibre materials are a promising choice for stimulating tissues that function under harsh environmental conditions (low or high pH). Such materials can be used as extracellular substrates or scaffolds to enable proliferation and differentiation of cells in damaged tissue [2]. However, there are several important conditions: the material has to present interconnected porosity to allow tissue integration and vascularisation; it must encourage cell adhesion, differentiation and proliferation through appropriate surface chemical properties and finally, it must be biocompatible [3]. The aim of this study was to obtain electrodeposited fibre membranes based on the stable polymer polyvinylidene (PVDF). Mechanical properties, i.e. breaking strength and durability at low pH conditions, were investigated. The physicochemical properties of the membrane materials and their porosity and microstructure were checked. The biocompatibility of the membranes in the presence of human fibroblasts was confirmed and their metabolic activity in terms of collagen secretion was investigated.

Methods: The polyvinylidene fluoride (PVDF, Sigma-Aldrich, Mw~275 kDa) solution was prepared using system of solvents: dimethylformamide (DMF, POCH) and acetone (Ac, Sigma-Aldrich). An electrospinning machine able to stabilize humidity and temperature was used to obtain the fibers.

Microstructure of the fibrous materials was observed with scanning electron microscope (Apreo 2 SEM, ThermoFisher Scientific). Wettability was measured using a goniometer (DSA 25, KRÜSS). Porosity was determined by gravimetric method. The nonwovens were subjected to a static tensile test (RetroLine ZwickRoell). Biocompatibility was tested using the BJ fibroblasts line. Viability and cytotoxicity were tested after 3 and 7 days of incubation of cells with the materials.

Results: Based on SEM images, fibers were measured and their average thickness was found around 120 nm.

Non-wovens were highly porous, with porosity above 90%.

The obtained material was highly hydrophobic (contact angle above 100°) and had high surface free energy, consisting mainly of disperse component. During the tensile testing, the material elongated up to 75% in elastic range and no further plastic deformation was observed before destruction. Tensile strength value of Rm=7,75 MPa was measured. Studied material showed biocompatibility in *in vitro* conditions.

Discussion: PVDF is a polymer from which a stable solution can be obtained, allowing to produce nanofibers using electrospinning method. In effect, highly porous, hydrophobic substrates can be effectively

produced. PVDF non-woven proved to be a brittle material with high tensile strength – however, small range of elastic deformation may limit its applications to tissues not subjected to high deformations. The material is biocompatible, with high porosity promoting cells growth. The results of study indicate that the tested material has the potential to

be used as a substrate to promote soft tissue regeneration.

References

- 1. X. Li et al, Sci. Transl. Med., 11: 490, 2019
- 2. K. Nathani et al, J Drug Deliv Sci Technol, 94: 105503, 2024
- 3. D. R. Marques et al, J Biomed Mater Res, 105:8: 2581-2591, 2017

Acknowledgements

Research project supported by program "Excellence Initiative – Research University" for the AGH University of Krakow (ID 4204).

EVALUATION OF MATERIALS FOR A SOFT ARTIFICAL VENTRICLE

Nienke S. Reitsma¹, Maziar Arfaee², Johannes T. B. Overvelde³

¹Autonomous Matter Department, AMOLF, The Netherlands; ²Department of Cardiothoracic Surgery, Erasmus MC, The Netherlands; ³Autonomous Matter Department, AMOLF, The Netherlands

Introduction: Soft robotics is gaining traction in the medical field with applications ranging from wearable assistive devices [1] to total artificial hearts (TAH) [2]. We are developing the LIMO (Less In, More Out) TAH, aimed as a compact device with an efficient fluidic transmission system [3]. The design consists of a cylindrical ventricle surrounded by pouch motors. These pouch motors are soft actuators made by sealing two materials together, forming an airtight chamber [4]. As the pouches inflate, they displace volume within the ventricle, pumping out blood. Different than a membrane pump, the primary pumping force results from the circumferential shrinkage of the ventricle, caused by the inextensibility of the material. Our previous work demonstrated that the ratio of input to output volume can exceed 1, enabling a compact design. In this study, we build upon these findings by conducting in vitro experiments using a single-sided mock circulatory loop (MCL) to evaluate different materials with the aim to evaluate performance.

Methods: The design is fabricated by heat-sealing layers of thermoplastic polyurethane (TPU) using a customized 3D printer. After sealing, 3D-printed TPU air inlets and valve holders with mechanical valves are



Figure 1. Design and experimental setup. (A) Prototype made from transparent TPU, mechanical valves, and yellow TPU holder. (B) Mock circulatory loop with the transparent design during systole, showing inflated pouch motors.

placed. Multiple material configurations are tested including nylon-coated TPU, transparent pure TPU, and a combination of both. A prototype made entirely of the transparent TPU is shown in Fig. 1A.

The designs are assessed in a MCL (Fig. 1B) consisting of two chambers representing preload and afterload, connected by a manually adjustable resistance. Pressure in both chambers, as well as inflow and outflow, is recorded throughout the experiments. The opening and closing of the valves are monitored using cameras. The pouch motors are pneumatically actuated through a driveline that connects them to either a pressure regulator or a vacuum, enabling controlled inflation and deflation. Key performance metrics, including stroke volume, heart rate, and cardiac output are calculated. This setup enables testing under both pulmonary and systemic conditions, both of which are examined in this study.

Results: Preliminary results show a cardiac output of 6.1 L/min under pulmonary conditions for the transparent TPU design, 6.8 L/min for the nylon- coated TPU design, and 5.1 L/min for the design using both materials. The pulmonary conditions included an afterload of approximately 33/5 mmHg, a preload of 5 mmHg, and a heart rate of 56 beats per minute. Additional testing will assess the performance of these designs under various conditions including systemic.

Discussion: Initial results suggest that the choice of material has a notable impact on the performance of the LIMO ventricle. However, additional experiments are needed to assess whether this effect persists under varying experimental conditions.

References

- P. H. Nguyen and W. Zhang, 'Design and computational modeling of fabric soft pneumatic actuators for wearable assistive devices', Scientific reports, vol. 10, no. 1, p. 9638, 2020.
- L. G. Guex et al., 'Increased longevity and pumping performance of an injection molded soft total artificial heart', Soft robotics, vol. 8, no. 5, pp. 588–593, 2021.
- M. Arfaee, L. C. van Laake, S. Zou, C. Bording, J. Kluin, and J. T. B. Overvelde, "A soft fluidic transmission system enabling a compact total artificial heart," unpublished.

 R. Niiyama, D. Rus, and S. Kim, 'Pouch motors: Printable/inflatable soft actuators for robotics', in 2014 IEEE International Conference on Robotics and Automation (ICRA), 2014, pp. 6332–6337.

PRODUCTION OF OUTSIDE-IN FILTRATION HOLLOW FIBERS FOR A COMBINED LUNG AND KIDNEY SUPPORT DEVICE FOR PRETERM BABIES

L. Romano¹, D. Ramada¹, N. Rochow², D.J.M. Van Galen³, J. Arens³, O.E.M. ter Beek¹ D. Stamatialis¹ on behalf of the ArtPlac Research Consortium⁴

¹Faculty of Science and Technology, Advanced Organ Bioengineering and Therapeutics (AOT), University of Twente, Enschede; ²Department of Neonatology, Klinikum Nurnberg, Nuremberg, German; ³Faculty of Engineering Technologies, Department of Biomechanical Engineering, Engineering Organ Support Technologies, University of Twente, Enschede, the Netherlands; ⁴HORIZON-EIC-2022-PATHFINDEROPEN-01, Grant agreement ID: 101099596

Introduction: Reducing newborn mortality, particularly in pre-mature infants (born \leq 37 weeks) with lung and kidney complications, remains critical [1]. Current solutions like mechanical ventilation and artificial organ support systems often fail this vulnerable population due to high blood priming volume and separate vascular access requirements. To address this, we are developing an artificial placenta device (ArtPlac), designed to connect to the umbilical vessels, mimicking the natural placenta in utero [2] [Fig.1].

ArtPlac integrates oxygenator and dialysis hollow fibers (HF) in one fiber bundle, working in Outside- in flow (OIF) mode. In this configuration, blood flows around the fibers, while oxygen or dialysate fluid flows inside the lumen of the fibers [3] [Fig.1].

Methods: OIF-HF were prepared using a polymer solution with different ratios of polyethersulfone, polyvinyl-pyrrolidone and N-methylpyrrolidone, by dry-wet spinning set-up via solvent/nonsolvent exchange. The HFs

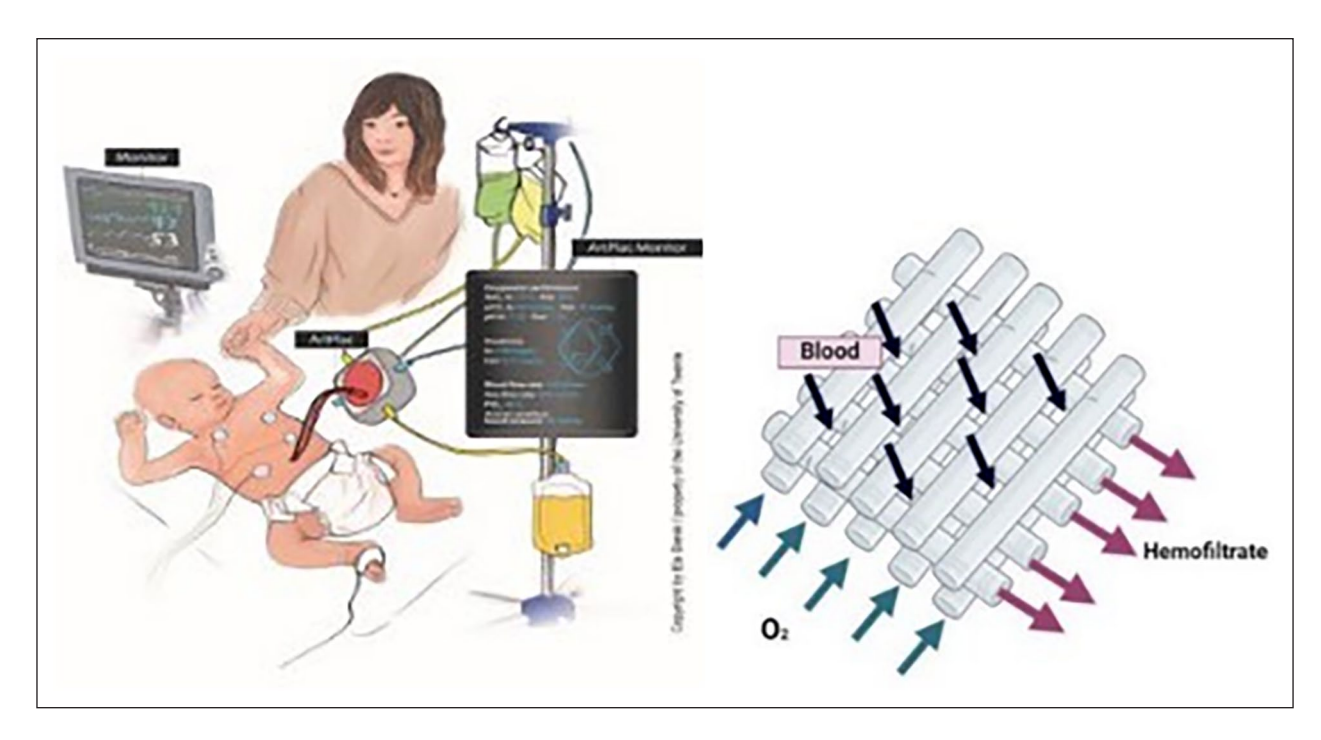


Figure 1. ArtPlac – one device attached to the umbilical cord, combining lung and kidney support (Left), Right: configuration of hollow fiber mats.

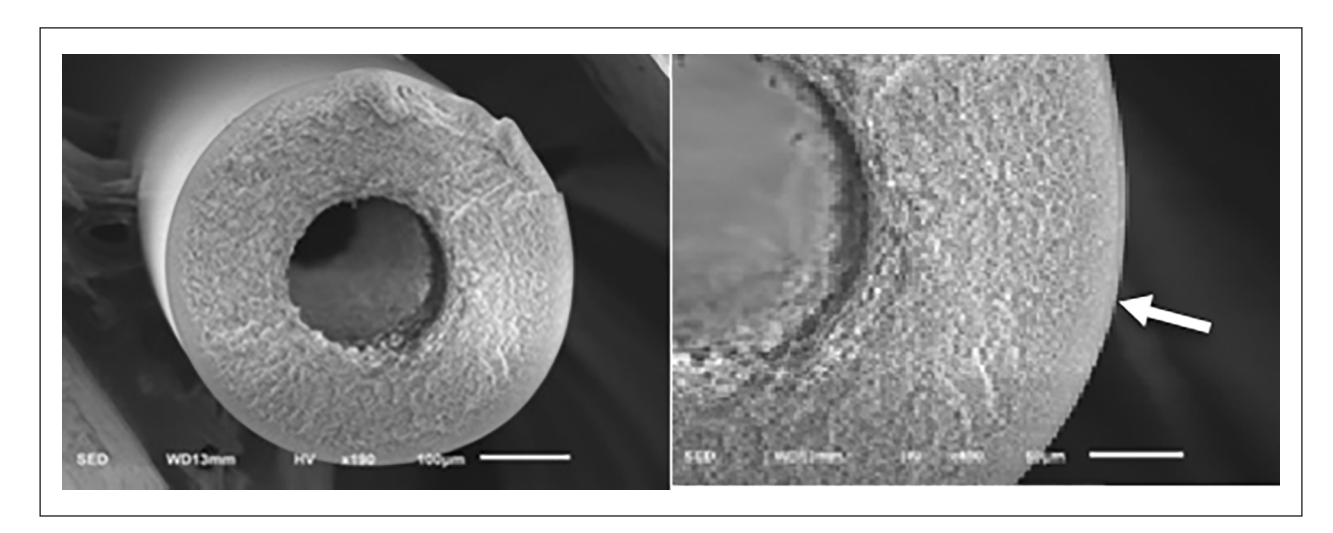


Figure 2. SEM images of the produced OIF-HF. The arrow indicates the outer selective layer.

were fabricated via large spinning set-up with collecting spool and compared to Micro- PES10TF commercial fibers (3M Membrana- Ger- many). The HFs were soaked in glycerol for 24h and then air-dried. Scanning Electron Microscopy (SEM) was employed for fiber morphology characterization.

Results and Discussion: Figure 2 presents typical SEM images of HF for OIF, with sponge-like pores, an outer selective blood contacting layer, and an inner porous layer in contact with the dialysis fluid. The fibers' ultra- filtration coefficient is 11 mL/(m²·h·mmHg). Table 1 compares the mechanical properties of the OIF-HF to MicroPES10TF. Glycerol enhances the elasticity of the produced OIF-HF by increasing elongation before break. Further studies are underway to assemble the HF to the Artplac device and to investigate the removal of uremic toxins from human plasma and full blood.

Table 1. Mechanical properties of the HF.

Hollow fibers	Young's modulus (MPa)	Max. force before break (MPa)	Max. elongation before break (%)
OIF-HF	59 ± 17	2 ± 0.1	3 ± 0.4
OIF-HF (gly)	27 ± 3	2 ± 0.1	23 ± 6
MicroPES10TF	46 ± 5	3 ± 0.5	26 ± 8

References

- 1. Howson, C. P. et al., Reprod Health 10, S1,2013
- 2. Niels Rochow et al., J Artif Organs, 36 (6): 377-391,2013
- 3. S.S. Dukhin et al., J Memb Sci, 464: 173-178, 2014

Acknowledgements

This project is funded by the European Union's Horizon Europe research and innovation programme (EIC Pathfinder) under grant agreement Nº 101099596.

DIRECT CARDIAC COMPRESSION DEVICE OPTIMIZATION THROUGH HEART COMPLIANCE SIMULATIONS

Kristóf Sárosi, Patrick Jenny

Institute of Fluid Dynamics, Department of Mechanical and Process Engineering, ETH Zürich, Switzerland

Introduction: Optimizing direct cardiac compression (DCC) devices poses challenges due to their complex interaction with heart tissue. As DCC devices drive the flow in the circulation with compressing the heart, their optimization requires information on the mechanical properties and behavior of the tissue. Currently, computationally expensive finite element models (FEM) or experiments provide the only framework for device optimization.

Methods: We propose a lumped parameter model (LPM) that characterizes the heart through compliances. Unlike existing 0D models, ours employs a general compliance model, eliminating the need for predefined time-varying pressure [1], compliance [2] parameters, or coupling with higher- dimensional models [3]. We introduce a predefined actuation displacement boundary condition, which our compliance model translates into a source term to generate pressure and flow in the circulation.

Considering a simple relation between the volume change in the ventricles and the pressure inside them (p), and displacement of the patches (ω), we define the following model: from an FEM model [3] with experimental data, using data-driven approaches.

$$\frac{dV_1}{dt} = II \frac{dp}{dt} Ir \frac{dp}{dt} II \frac{d\omega}{dt}$$

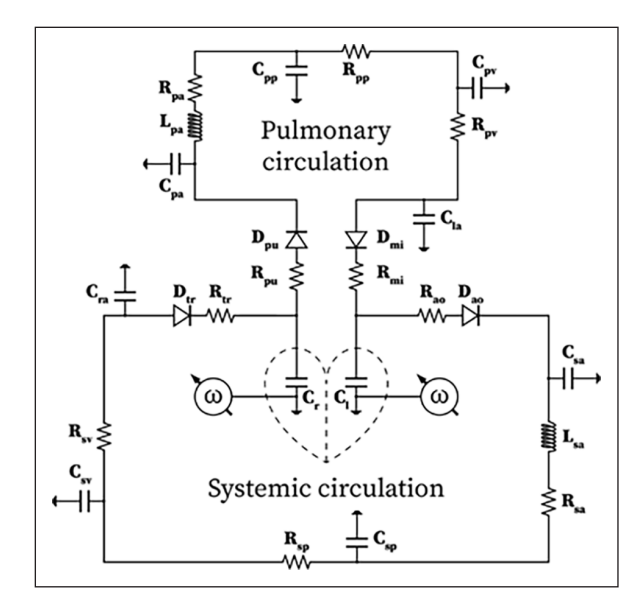


Figure 1. Lumped parameter model using a compliance-based displacement-driven approach.

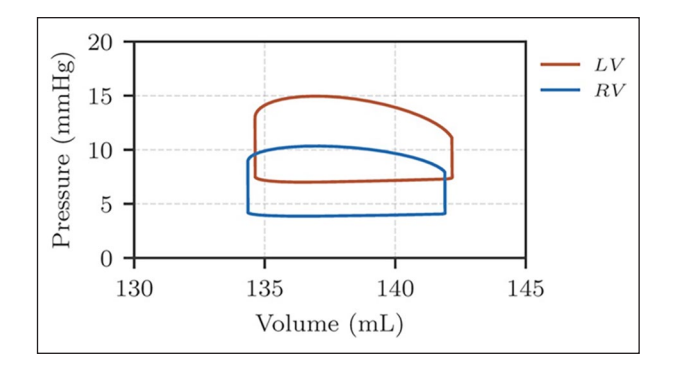


Figure 2. Simulated pressure-volume curves using constant heart compliances. The results are in agreement with DCC device publications [4].

However, obtaining a robust ventricular compliance model is challenging due to limited heart compliance data and the interactions with the DCC device. We address this by combining results

Results: Our model can produce similar results to already existing 0D models. Figure 2 shows results in agreement with pre-clinical DCC studies [4] without coupling the LPM with higher dimensional models or using time-varying parameters. Our approach also highlights the sensitivity of models that rely on time-varying parameters. Our framework offers detailed insights into pressure, flow rate, volume, and valve states throughout the circulatory system. Using optimization algorithms in combination with our compliance model, we can optimize the DCC device developed in our lab.

Discussion: This compliance-based lumped parameter approach provides a powerful tool for optimizing DCC devices for improved patient outcomes. Characterizing the heart through compliances provides a novel approach for 0D models and understanding the macro-mechanical properties of the heart alike.

References

- Milišić V, Quarteroni A. ESAIM: Mathematical Modelling and Numerical Analysis. 38(4):613-632, 2004.
- 2. Ursino M., Am J Physiol., 275(5): 1733-44, 1998.
- 3. Kummer et al., Cardiovasc Eng Tech, 13: 764–782, 2022.
- Hord, E.C, et al.: Preclinical Proof-of-Concept of a Minimally Invasive Direct Cardiac Compression Device for Pediatric Heart Support, Cardiovasc Eng Tech, 15:147–158, 2024.

A NOVEL DIRECT CARDIAC COMPRESSION DEVICE FOR SHORT-TERM MECHANICAL CIRCULATION SUPPORT

Kristóf Sárosi¹, Thomas Kummer¹, Stijn Vandenberghe², Stefanos Demertzis², Patrick Jenny¹

¹Institute of Fluid Dynamics, Department of Mechanical and Process Engineering, ETH Zürich, Switzerland; ²Faculty of Biomedical Sciences, Università della Svizzera italiana, Switzerland

Introduction: Patients requiring short-term ventricular assistance have limited options. While resuscitation, organ perfusion, bridge-to-decision, and cardiac recovery do not necessarily require blood-contacting support, all current devices are invasive and interact with the blood-stream. Direct cardiac compression (DCC) devices offer a potential solution by providing mechanical circulatory support (MCS) without contact with the blood stream [1].



Figure 1. DCC patch device. The patches are in direct contact with the heart and are actuated through the driveline.

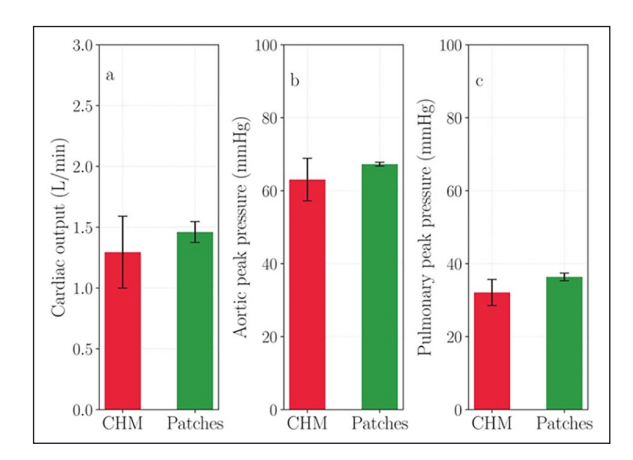


Figure 2. Main indicators of performance: CO, MAP, and mean pulmonary artery pressure.

There is no single MCS or DCC solution solving every problem of patients with heart failure or cardiac arrest [2]. We created an accessible DCC device concentrating on emergency scenarios and short-term circulatory support [3].

Methods: This proof-of-concept study compares a novel DCC patch system for short-term MCS to cardiac hand massage (CHM) using an ex vivo cardiac arrest ovine heart model. Performance is evaluated by assessing pressure, flow rate, and valve functionality, as well as any damage to the tissue.

The DCC patch device consists of two patches, shaped like the cups of a hand, a driveline, and a vacuum line. Figure 1 shows the DCC patch device on a porcine model. The patches are in direct contact with the epicardium, compressing directly on the ventricles. The shape of the two patches is different as the LV patch has less curvature than the RV patch. This design difference should help in balancing the pressure in the LV and RV, a feature that is unmatched by other DCC devices [4].

Results: The DCC patch system demonstrates comparable performance to the standard CHM technique. In Figure 2, the system achieves 1.5 L/ min cardiac output (CO) and a mean aortic pressure (MAP) of 55 mmHg. Despite direct epicardial compression, the DCC patch system maintains effective valve function.

Discussion: This ex vivo proof-of-concept study demonstrates that the DCC patch system achieves comparable performance to CHM, supporting previous in vitro findings [3]. The results suggest the potential for this

novel DCC patch system to be applied across a range of short-term mechanical circulatory support scenarios, potentially replacing CHM.

References

- Anstadt MP, Anstadt GL, Lowe JE: Direct mechanical ventricular actuation: A review. Resuscitation, 21:7–23, 1991
- Callan P, Dimarakis I: Mechanical circulatory support: an overview, 85–102, 2020
- Sárosi K, et al.: Demonstration of a mechanical external biventricular assist device for resuscitative thoracotomy, 2024
- Hord, E.C, et al.: Preclinical Proof-of-Concept of a Minimally Invasive Direct Cardiac Compression Device for Pediatric Heart Support, Cardiovasc Eng Tech, 15:147–158, 2024

ENHANCING BLOOD COMPATIBILITY THROUGH SURFACE ENGINEERING: A SYSTEMATIC REVIEW

Marlene Schadow ¹, Johanna C. Clauser ¹

Department of Cardiovascular Engineering, Institute of Applied Medical Engineering, RWTH Aachen University, University Hospital Aachen; Germany

Introduction: Poor hemocompatibility of artificial materials is still a bottleneck in medical engineering. A current approach is the micro-structuring of substrate surfaces to reduce platelet adhesion as an initialization of thrombus formation. Although the advantage has already been demonstrated [1-12], the underlying mechanism is still not fully understood. The aim of this review is to provide an overview of studies that been carried out to date and the methods used for in vitro testing and quantification of hemocompatibility.

Methods: PubMed and Google Scholar were searched for original articles in English-language journals with the following keywords: *structure*, topograph*, *pattern* in combination with: surface and *adhesion. 43 papers were found and analyzed with the help of the Al research assistant Elicit (https://elicit.com/) for the prompts: dimension microstructure, structural shapes, material, adhesion, static or dynamic, wettability. If no answer was found for 3 or more categories, the articles were excluded after manual confirmation. 21 papers resulted, 14 of which focus on the adhesion of blood platelets.

Results: The modification of artificial surfaces to influence the adhesion behavior of cells is also known in other areas, whereby the areas of application are characterized by different methodologies. When investigating the survival rate of bacteria, for example, the vitality is determined after several days of incubation [13-15]. For the ingrowth of implants, the morphology of the cells after days/weeks of incubation is often used to determine whether the surface structuring has an effect [16,17].

In studies of adhesion of blood platelets, 75% used the area of deposition as the key criteria, although vitality and morphology were also included in some cases. The studies that measured metabolic activity, which is a standard test to measure the vitality of cells, were the only ones to show a drop in hemocompatibility in the modified samples compared to unstructured samples [18,19].

Discussion: The systematic review of existing work can help in the planning of future studies and thus save costs and time. For the current approach of micro- structuring substrate surfaces to reduce platelet adhesion, the underlying mechanism is still not fully understood. The standard methods of in vitro testing and quantification of the hemocompatibility could be determined in this review. To assess the influencing factors of surface structuring, a systematic study must be performed.

References

- Chen et. al. 2009. Colloids and Surfaces, 71,275–281.
- 2. Clauser et. al. 2014. Journal of Biomaterials Science, 25, 504–518.

- 3. Honglei et. al. 2009. small, 2144-2148.
- 4. Huang et. al. 2012. Biomaterials, 33, 8213-8220.
- Khorasani et. al. 2003. Journal of Applied Polymer Science, 2042–2047.
- 6. Minelli et. al. 2008. Journal of nanobiotechnology 6, 3.
- 7. Park et. al. 2000. Clinical Oral Implant Reserch, 530–539.
- Pham et. al. 2016. Colloids and surfaces. B, Biointerfaces 145, 502–509.
- 9. Yang et. al. 2010. Colloids and Surfaces, 309–313.
- Yui et.al. 1986. JOURNAL OF BIOMEDICAL MATERIALS RESEARCH, 20, 929–943.
- Zhao et. al. 2013. Chemical communications (Cambridge, England), 80, 9191–9193.
- 12. Zhou et. al. 2008. JNanoR 2, 129-136.
- 13. Efremov et. al. 2013. Biomaterials 34, 7, 1757–1763.
- Hsu et. al. 2013. Applied and environmental microbiology, 79, 2703–2712.
- 15. Jafar et. al. 2015. RSC advances 5, 56, 44953-44959.
- 16. Di Mundo et. al. 2011. Langmuir: the ACS journal of surfaces and colloids 27, 8, 4914–4921
- 17. Ranella et. al. 2010. Acta Biomaterialia, 6, 2711–2720.

Acknowledgements

This work is funded by DFG (Project: 490779571).

DIFFERENCES IN COMPLEMENT PRE-ACTIVATION IN PIG AND HUMAN AFTER BLOOD DONATION

Maike Scönborn¹, Ilona Mager¹, Sofie Hardt¹, Ulrich Steinseifer¹, Johanna C. Clauser¹

¹. Department of Cardiovascular Engineering, Institute of Applied Medical Engineering, University Hospital RWTH Aachen University, Germany

Introduction: The hemocompatibility of medical devices that come into contact with blood is a major challenge in development and approval. Thrombogenicity tests, which are usually performed in animal studies, raise ethical concerns, are costly and often inefficient. This highlights the need for standardized in vitro methods to assess thrombogenicity at an early stage. Blood from pig abattoirs offers an ethically acceptable alternative to human donor blood, but its suitability is questioned due to possible pre-activation during the slaughter process and species-related differences in blood composition.

In this study, hemocompatibility parameters according to DIN EN ISO 10993-4 were investigated in both porcine and human blood. By focusing on species-specific differences, particularly in complement pre-activation, we aim to assess the feasibility of using porcine blood for standardized in vitro thrombogenicity assays.

Methods: Porcine blood was collected directly at the slaughterhouse after a cut in the jugular vein of the animals. Blood from one animal was separated in two blood bottles and immediately anticoagulated with 2000 IU/L enoxaparin (Clexane) and sodium citrate, (3.13 %, ratio 1:10) respectively. Human blood was collected at the Medical Center of the RWTH Aachen University (EK 23-092) and divided into two separate portions anticoagulated as the porcine blood.

After arrival at the lab, blood, blood gas analysis, thromboelastometry, fluorescence activated cell sorting with CD61, CD62P, CD45 markers and impedance aggregometry, were measured in whole blood from both species. Plasma samples were frozen at -80 °C for further ELISA analysis. The ELISA test comprises the analysis of plasma parameters including serotonin, adrenalin, cortisol, PMN Elastase, soluble C5b-9, C3a, and thrombin-antithrombin-complex.

Results: The analyses include all parameters described in DIN EN ISO 10993-4: Hematology, complement activity, platelet activation and

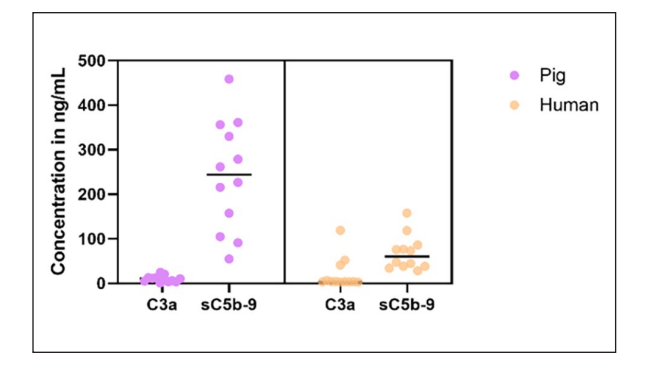


Figure 1. C3a and sC5b-9 concentrations of pig and human blood anticoagulated with enoxaparin.

coagulation. In hematology, the initial values for both species were within the normal range, but showed significant differences. Platelet activation showed pre- activated but still functional platelets in pig blood. With regard to complement activity, the concentration of the activated C3a fragment was low in both species, while SC5b-9 levels were increased. Significantly higher values were found in porcine blood (Figure 1).

For coagulation, measurements showed that the maximum clot firmness and the thrombin- antithrombin complex values were significantly higher in pig blood than in human blood.

Discussion: The results show that although coagulation has already been initiated in slaughterhouse blood, it is still functional for further tests. Of particular importance are the significantly increased sC5b-9 values in pig blood, which indicate increased terminal complement activation. Future material tests will investigate whether pig blood still reacts to materials due to the already partially completed coagulation. Taking species-specific differences into account and using the various markers can help to assess the biocompatibility of materials more precisely and optimise the development of medical devices.

Acknowledgements

This work was supported by the Flow Cytometry Facility, a core facility of the Interdisciplinary Center for Clinical Research (IZKF) Aachen within the Faculty of Medicine at RWTH Aachen University. We thank Dr. Doris Keller for blood withdrawal and all volunteers who donated blood.

THE EMBOLESS® VENOUS CHAMBER EXTENSIVELY REDUCE AIR CONTAMINATION PASSING INTO HD PATIENTS' BLOOD

Introduction: Hemodialysis (HD) is a life sustaining treatment for patients with end-stage renal failure, and ongoing efforts aim to enhance both its efficiency and safety. In terms of safety, the precautionary principle has been applied. The quality of the water used in dialysis and the biocompatibility of dialysis filters has been significantly improved, while prevention of air contamination of the bloodline lacks behind. Dialysis machines are equipped with air detectors that shall trigger alarms if larger amounts of air enter the venous side.

However, air bubbles larger than 500 μ m diameter can bypass these detectors without activating alarms. Air is foreign to the bloodstream and contains inert gases, which can cause severe complications such as emboli and tissue damage, confirmed by case reports and autopsy studies. No data exist of the air volumes contaminating the blood during regular HD and difference in air elimination.

The objective of this interventional clinical study was to ascertain whether the elimination of air entering the patients can be more efficacious.

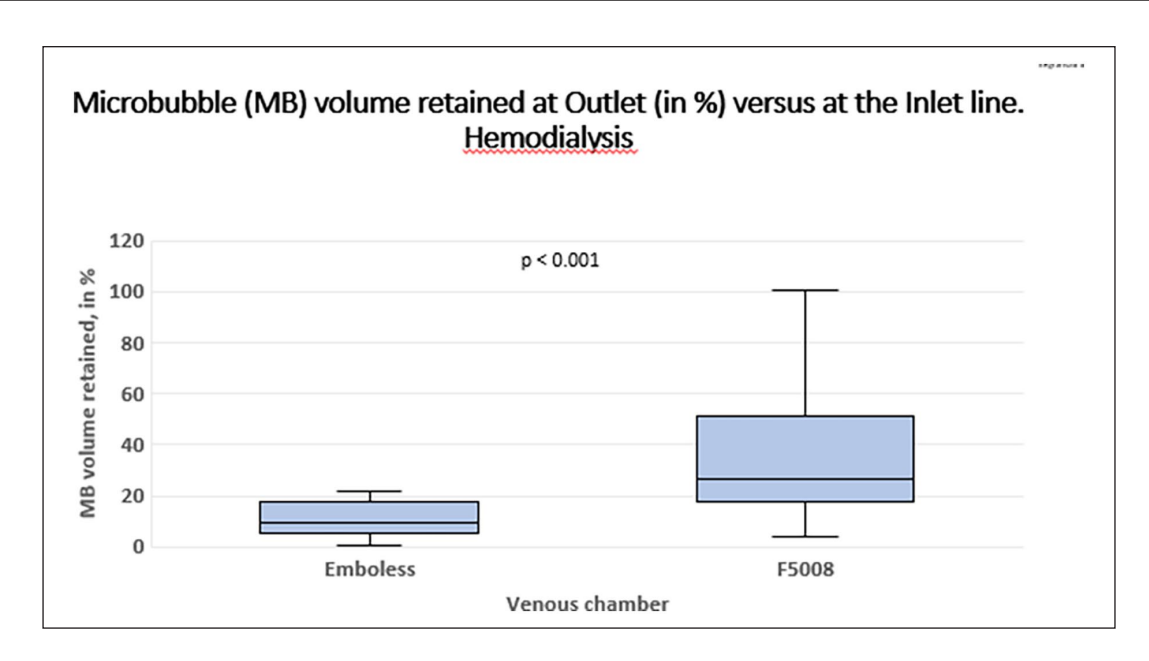


Figure 1.

Methods: Twenty chronic HD patients participated in a randomized crossover study comparing the Emboless® and F5008 venous chambers. Each patient underwent four dialysis sessions divided into two paired series, resulting in 80 analysed sessions. The same dialyzers, blood pump speeds, HD settings, and ultrafiltration parameters were used within each pair. The cumulative volumes of air bubbles (>20 μm in diameter) were measured at the inlet and outlet line of each venous chamber using an adapted ultrasound device (BCC200, GAMPT). The measurement duration was 30 minutes, extended if fewer than 1000 detections were recorded at the Inlet. The percentage of air volume passing through the venous chamber and reaching the patient was calculated (Mann-Whitney U- test).

Results: The median air Inlet volume of 80 dialyses was 20.5 mL (IQR 12.2–38.4 mL), with no significant difference in air inflow between the two venous chambers. The median (IQR) proportion of volumes of air leakage passing to the patient was lower with the Emboless® (8.7%) compared to the F5008 chamber (25.9%, p<0.001, Fig. 1).

Discussion: The Emboless® venous chamber is the preferred choice for minimizing potentially harmful air contamination during hemodialysis. Air leakage to patients was reduced to one-third when using the Emboless® compared to the F5008 venous chamber, making it a safer option for clinical use.

Acknowledgements

This work was supported by grants from VINNOVA, Sweden, MedTech4Health, and the patient Society for Kidney Diseases, Västerbottten, Sweden.

NEW MEMBRANES FOR HEMODIALYSIS BASED ON BLENDS OF POLYETHERSULFONE (PES) WITH POLYETHYLENE OXIDE - POLYETHERSULFONE (PEO-PES) COPOLYMER

Malgorzata Tasior¹, Oliver Gronwald², Odyl ter Beek¹, Dimitrios Stamatialis ¹

¹Advanced Organ bioengineering and Therapeutics, Faculty of Science and Technology, TechMed Centre, University of Twente, The Netherlands; ²Performance Materials, Research Ultrason, BASF SE, Germany Introduction: End Stage Kidney Disease patients are commonly receiving dialysis therapy. During this therapy, patient's blood is filtered using a hollow fiber (HF) membrane-based dialyzer, to remove uremic toxins present in the blood [1]. Often these HF are made from hydrophobic polymers, such as polyethersulfone (PES), and hydrophilic polymer additives, such as polyvinylpyrrolidone (PVP) [2]. It has been shown that PVP can be eluted from HF during dialysis, leading to decreased hemocompatibility of the filters [3,4]. To achieve extended dialysis and, therefore, increased toxin removal [5], there is a need for fibers that do not release hydrophilic additive throughout the dialysis therapy session. It has been shown by other researchers [6,7] and our group [8] that alternative polymers are a promising solution. Here, we investigate the application of copolymer PEO-PES as hydrophilic additive in HF dialysis membranes. We hypothesize that this copolymer will result in high flux membranes with low hydrophilic additive leakage during prolonged therapy, leading to increased dialysis efficiency.

Methods: The polymer dopes consisted of PES and a PEO- PES, dissolved in N-Methyl-2-pyrrolidone (NMP). To fabricate HF membranes, wet spinning using liquid induced phase separation was applied. Various spinning conditions were investigated. The produced membranes were washed and air dried at room temperature. Scanning electron microscopy (SEM) was used to investigate their morphology. Clean water flux measurements were performed for all HF membranes to determine their ultrafiltration coefficient (KUF). For selected membranes, we investigated the albumin transport properties.

Results - **Discussion:** Figure 1 presents typical SEM image of a HF obtained by blending PES and PEO-PES (PES/PEO-PES). The fibers have finger-like macrovoid structure with selective layer on the fiber lumen. Inner diameter of the fibers is $271\pm12~\mu m$ and wall thickness is $88\pm16~\mu m$. The obtained dimensions are higher than commercial fibers that usually have 180 to 200 μm inner diameter and 35 to 50 μm wall thickness. PES/PEO-PES fibers have KUF $=50\pm9~m L/(m^2*h*mmHg)$ and protein sieving coefficient (SC) of 0.15 \pm 0.05. Similar values can be found for commercial fibers in high flux range.

Future studies will focus on investigating toxin removal from human plasma as well as long term membrane stability / hydrophilic additive elution.

References

- 1. Bello et al, Nat Rev Nephrol, 18:378-395, 2022
- 2. Yang et al, J of Memb Sci, 326: 322-331, 2009.

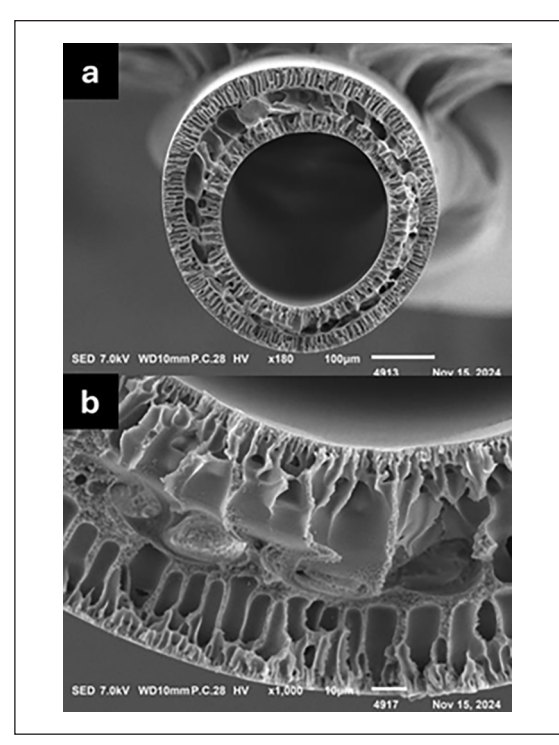


Figure 1. Cross-section of PES/PEO-PES fiber: a) whole fiber, x180, b) fiber wall, x1000.

- 3. Namekawa et al, J Artif Organs, 15:185-192, 2012
- 4. Sato et al, Bioch and Biophy Rep, 28:101140, 2021
- 5. Davenport, Pediatr Nephrol, 30:2053–2060, 2015
- 6. Ying et al, J of Memb Sci, 695:122457, 2024
- 7. Helmecke et al, J of Memb Sci, 689: 122050, 2024
- 8. Ter Beek et al, J of Mem Sc, 604: 118068, 2020

Acknowledgements

This work was financially supported by BASF.

This work was based on initial studies done by Floris Pel, as Capita Selecta at the University of Twente.

EXPANDABLE PERCUTANEOUS MICRO-AXIAL FLOW BLOOD PUMPS: TECHNIQUES FOR ACCURATE HYDRAULIC PERFORMANCE MEASUREMENT

The author list goes here ("Authors" style) Thomas George Logan 1 , Tingting Wu 1,2 , Mengjie Liu 1 , Xuhui Hua 1 , Ifan Yen 1 , Jamshid H. Karimov 1 , Po-Lin Hsu 1,2 , Chiahao Hsu 1

¹magAssist Co., Ltd., Suzhou, China; ²Artificial Organs Technology Lab, School of Mechanical and Electrical Engineering, Soochow University, Suzhou, China

Introduction: NyokAssist[™] is a commercially developed transvalvular micro-axial flow blood pump optimized for supporting patients during high-risk PCI [1]. The pump folds down to 9 Fr diameter during insertion and self-expands in the descending aorta into 24 Fr diameter, working in parallel with native cardiac function. Accurate pump hydraulic performance measurements are critical for design improvement, care delivery and quality control, and is the subject of this study.

Methods: Measuring static and dynamic hydraulic performance is relatively straightforward for conventional rigid VADs as they can easily be



Figure 1. NyokAssist™ pVAD foldable pump structure, 9Fr folded insertion state (top) and 24Fr expanded operation state (bottom).

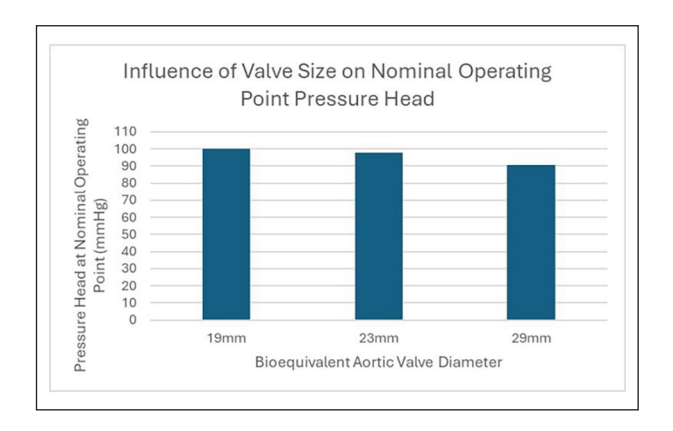


Figure 2. Impact of valve diameter when an early pump design is tested for operated in conjunction a bioequivalent aortic valve.

connected to fixed tubing either directly in the case of extracorporeal VADs (Centrimag, MoyoAssist, etc.), or via trivial adaptors (Heart Mate 3, etc., or Impella series). For expandable VADs, making representative connections is much more difficult because the connections impact on the performance of the pump, for example by influencing the blade tip clearance or shape of the flow path, or causing leakage flows in the measurement equipment. Device connections were carefully designed to enable accurate testing, both to minimize external force impact on pumps and to test application performance through bioequivalent valves (19-29 mm). Recommended configurations and tolerance requirements will be presented.

Results: Prototypes for an early expandable pVAD were tested. Results showed that fixture dimension changes in the order of $20\mu m$ had a significant impact on measured pressures. Figure 2 shows when testing the catheter sets with bioequivalent valves, the sizing of the valve itself resulted in a 10% influence on the measured pressure, emphasizing the importance of standard conditions when comparing alternative pumps. Valve dimensions and contact position between the pump have effects on both pump hydraulic and hemolysis performance.

Discussion: Measurement methods that properly represent operating conditions within patients are critical for the accurate characterization of expandable pVADs. Considerations for proper testing methodology are design-dependent and should be developed according to the specific technology architecture and performance.

References

 R. Wang et al, J American College of Cardiology, 84 (18_Supplement) B213, 2024.

Acknowledgements

This work is sponsored by magAssist Co., Ltd.